ANALYTICA CHIMICA ACTA

International monthly devoted to all branches of analytical chemistry
Revue mensuelle internationale consacrée à tous les domaines de la chimie analytique
Internationale Monatsschrift für alle Gebiete der analytischen Chemie

Editors

PHILIP W. WEST *(Baton Rouge, La., U.S.A.)*

A. M. G. MACDONALD *(Birmingham, Great Britain)*

Editorial Advisers

R. G. BATES, *Gainesville, Fla.*
R. BELCHER, *Birmingham*
F. BURRIEL-MARTÍ, *Madrid*
G. CHARLOT, *Paris*
E. A. M. F. DAHMEN, *Enschede*
G. DEN BOEF, *Amsterdam*
C. DUVAL, *Paris*
G. DUYCKAERTS, *Liège*
D. DYRSSEN, *Göteborg*
P. J. ELVING, *Ann Arbor, Mich.*
W. T. ELWELL, *Birmingham*
H. FLASCHKA, *Atlanta, Ga.*
G. G. GUILBAULT, *New Orleans, La.*
J. HOSTE, *Ghent*
H. M. N. H. IRVING, *Leeds*
M. JEAN, *Paris*
R. S. JUVET, JR., *Tempe, Ariz.*
M. T. KELLEY, *Oak Ridge, Tenn.*
O. G. KOCH, *Neunkirchen/Saar*
H. MALISSA, *Vienna*
J. MITCHELL, JR., *Wilmington, Del.*
D. MONNIER, *Geneva*
G. H. MORRISON, *Ithaca, N.Y.*
E. PUNGOR, *Budapest*
J. W. ROBINSON, *Baton Rouge, La.*
Y. RUSCONI, *Geneva*
J. RUŽIČKA, *Copenhagen*
D. E. RYAN, *Halifax, N.S.*
E. B. SANDELL, *Minneapolis, Minn.*
G. K. SCHWEITZER, *Knoxville, Tenn.*
S. SIGGIA, *Amherst, Mass.*
A. A. SMALES, *Harwell*
W. I. STEPHEN, *Birmingham*
N. TANAKA, *Sendai*
A. WALSH, *Melbourne*
H. WEISZ, *Freiburg i. Br.*
YU. A. ZOLOTOV, *Moscow*

ELSEVIER SCIENTIFIC PUBLISHING COMPANY
AMSTERDAM

Anal. Chim. Acta, Vol. 68, No. 2, 253–496, February 1974
Published monthly
Completing Volume 68

Publication Schedule for 1974

Vol. **68**, No. **1**	January 1974	
Vol. **68**, No. **2**	February 1974	**(completing Vol. 68)**
Vol. **69**, No. **1**	March 1974	
Vol. **69**, No. **2**	April 1974	**(completing Vol. 69)**
Vol. **70**, No. **1**	May 1974	
Vol. **70**, No. **2**	June 1974	**(completing Vol. 70)**
Vol. **71**, No. **1**	July 1974	
Vol. **71**, No. **2**	August 1974	**(completing Vol. 71)**
Vol. **72**, No. **1**	September 1974	
Vol. **72**, No. **2**	October 1974	**(completing Vol. 72)**
Vol. **73**, No. **1**	November 1974	
Vol. **73**, No. **2**	December 1974	**(completing Vol. 73)**

Subscription price: Dfl. 492.00 plus Dfl. 36.00 postage. Subscribers in the U.S.A. and Canada receive their copies by airmail. Additional charges for airmail to other countries are available on request. For advertising rates apply to the publishers.

GENERAL INFORMATION

Languages

Papers will be published in English, French or German.

Submission of papers

Papers should be sent to:

PROF. PHILIP W. WEST,
Coates Chemical Laboratories,
College of Chemistry and Physics,
Louisiana State University,
Baton Rouge 3,
La. 70803 (U.S.A.)

or to:

DR. A. M. G. MACDONALD,
Department of Chemistry,
The University,
P.O. Box 363
Birmingham B15 2TT (Great Britain)

Reprints

Fifty reprints will be supplied free of charge. Additional reprints (minimum 100) can be ordered at quoted prices. They must be ordered on order forms which are sent together with the proofs.

© ELSEVIER SCIENTIFIC PUBLISHING COMPANY, 1974

All rights reserved. No part of this publication may be reproduced, stored in a retrieval system, or transmitted, in any form or by any means, electronic, mechanical, photocopying, recording, or otherwise, without permission in writing from the publisher.

PRINTED IN THE NETHERLANDS

vous avez au moins 2500000 bonnes raisons de lire La Recherche

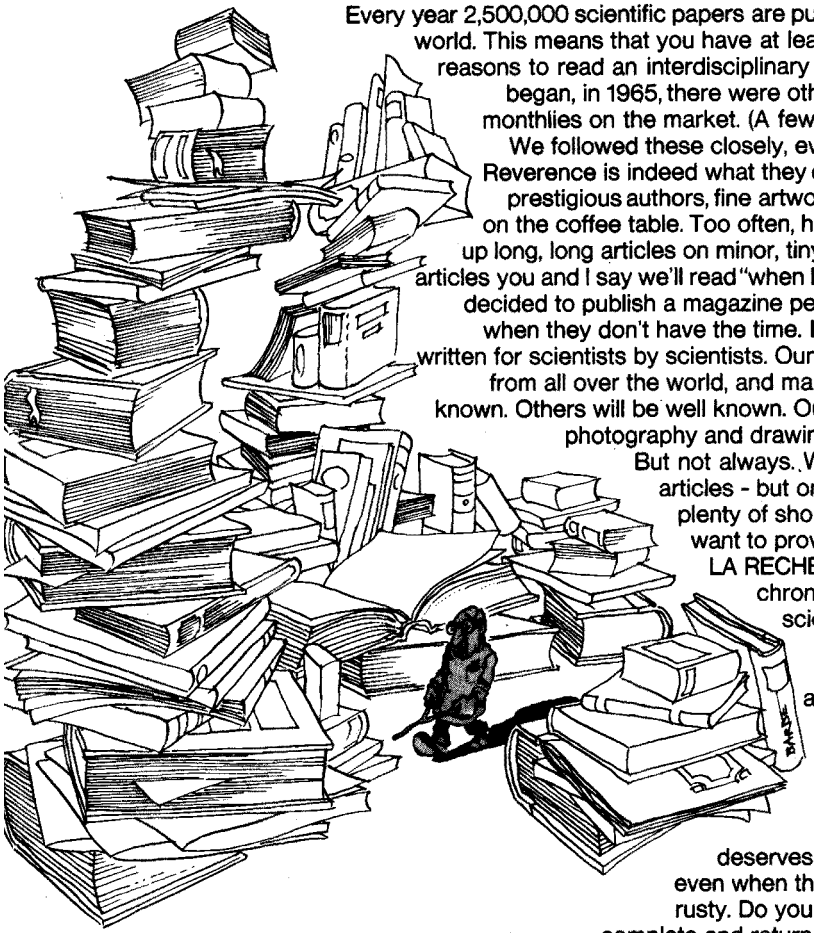

Every year 2,500,000 scientific papers are published all over the world. This means that you have at least 2,500,000 good reasons to read an interdisciplinary monthly. When we began, in 1965, there were other interdisciplinary monthlies on the market. (A few of these still exist). We followed these closely, even with reverence. Reverence is indeed what they deserve. They have prestigious authors, fine artwork: They look good on the coffee table. Too often, however, they serve up long, long articles on minor, tiny subjects. Just the articles you and I say we'll read "when I have the time". We decided to publish a magazine people will read even when they don't have the time. LA RECHERCHE is written for scientists by scientists. Our contributors come from all over the world, and many of them are well known. Others will be well known. Our artwork includes photography and drawings. Mostly serious. But not always. We have some long articles - but on major topics. And plenty of short articles. What we want to provide every month in LA RECHERCHE is a running chronicle of international scientific news across the board, from biochemistry to astronomy. Readers in 78 countries seem to think that we give them just that and that LA RECHERCHE deserves thorough reading... even when their French is a little rusty. Do you want to try it? Just complete and return the coupon below. Be our guest.

Special offer

Name _____

Address _____

_____

Mail to LA RECHERCHE, 4, place de l'Odéon, 75006 Paris, France.

HACH

I wish to receive the next 3 issues of LA RECHERCHE on a trial basis. If interested, I'll settle your invoice on receipt of the third issue and benefit from the special subscription rate of fl. 45 instead of the usual fl.60 for a year's volume of 11 issues. Otherwise I'll keep the 3 issues received at no charge to me.

Progress in Medicinal Chemistry, 9

Edited by **G. P. ELLIS**, University of Wales, Cardiff, Wales,
and **G. B. WEST**, North East Londen Polytechnic, Dagenham, Essex, U.K.

1973. 354 pages. Clothbound ed.: Dfl.70.00 (about US$26.90)
Paperback ed. (in two vols.): Dfl.50.00 (about US$19.20)

The policy of the editors of Progress in Medicinal Chemistry is to publish reviews written by chemists, biochemists, pharmacologists, microbiologists, pharmacists, clinicians and other specialists.
In this way, the many different points of view of all who are concerned with the discovery, development and study of new drugs will be presented.

CONTENTS:
Naturally-occurring Antitumour Agents (K. Jewers, A. H. Manchanda and Mrs. H. M. Rose). Chromone-2- and -3-carboxylic Acids and their Derivatives (G. P. Ellis and G. Barker). 4-Oxopyranoazoles and 4-Oxopyranoazines (M. A. Khan). Isotope Techniques in the Study of Drug Metabolism (Y. Kobayashi and D. V. Maudsley). The Pharmacotherapy of Parkinsonism (R. M. Pinder). Adrenochrome and Related Compounds (R. A. Heacock and W. S. Powell).

north-holland P.O. BOX 211 AMSTERDAM THE NETHERLANDS

1180 NH

Sole distributors for the U.S.A. and Canada
American Elsevier Publishing Company, Inc., 52 Vanderbilt Avenue, New York, N.Y. 10017

DATA: MIRRORS OF SCIENCE

by R. HOUWINK

Wassenaar, The Netherlands

6 × 9″, ix + 213 pages, Illustrated
1970, US$9.50, ISBN 0-444-00068-2

"... a treasure trove of interesting facts concerning the entire field of science-broadly interpreted. The intent is to put these data into a more common context through the use of aptly chosen analogies and comparisons ... filled with fascinating tangential pieces of information: for example, the number of years that have elapsed since the earth solidified is equal to the number of people on earth, which is equal to the number of cells in a man's brain, which is equal to the number of heartbeats in a man's life ... Houwink has managed to evolve examples that stick in the memory with the tenacity of sheep burrs ... ideally suited to browsing, and if made required reading for anyone presenting any of the sciences to students at any level (the book) could have a revolutionary effect on all contemporary classroom exercises." — D. Allan Bromley, **American Scientist**

Of interest to: Scientists in all disciplines and at all levels; all laymen interested in the world in which they live.

Contents: Why this Book? Compiler's Note. Acknowledgments. Data and Images. Mathematics and Fundamental Physics. The Building Blocks: Atoms and Molecules. Space. Our Planet. The Source of Everything: Energy. Perception. The Biological World. Man and Science. Technical Flashes. The Hydroworld. Military. Sport and Games. Surprises for the Great. Bibliography. Units. Index.

Orders for this title may be placed with the publisher or with your regular bookseller

ELSEVIER PUBLISHING COMPANY

NEW YORK - LONDON - AMSTERDAM

618EV

The Analysis of Organic Materials
An International Series of Monographs

Number 4

Chemical Analysis of Organometallic Compounds Volume 1

T. R. Crompton

December 1973, x + 258 pp., £5.80
0.12.197301.8

This book (the first of three volumes) deals with the compounds of lithium, sodium, potassium, copper, silver, gold, beryllium, magnesium, calcium, zinc, cadmium, mercury, boron, gallium and thallium. Each chapter provides a complete review of all aspects of the organocompounds of the element in question, together with critical comments on the relative importance, merits and demerits of the methods of analysis applicable.

Number 5

The Determination of Nitro and Related Functions

Y. A. Gawargious

December 1973, viii + 154 pp., £3.50
0.12.277950.9

This monograph offers detailed systematic information on the determination of a variety of nitrogen-containing functions that are of common occurrence in organic compounds and are important in research and industry. These include the nitro, nitroso, azo, azide, nitrate, nitramine, azoxy, oxime, diazonium and amine oxide groups.

Academic Press
London and New York
A Subsidiary of
Harcourt Brace Jovanovich, Publishers

24-28 Oval Road, London NW1, England
111 Fifth Avenue, New York, NY 10003, USA

608 V

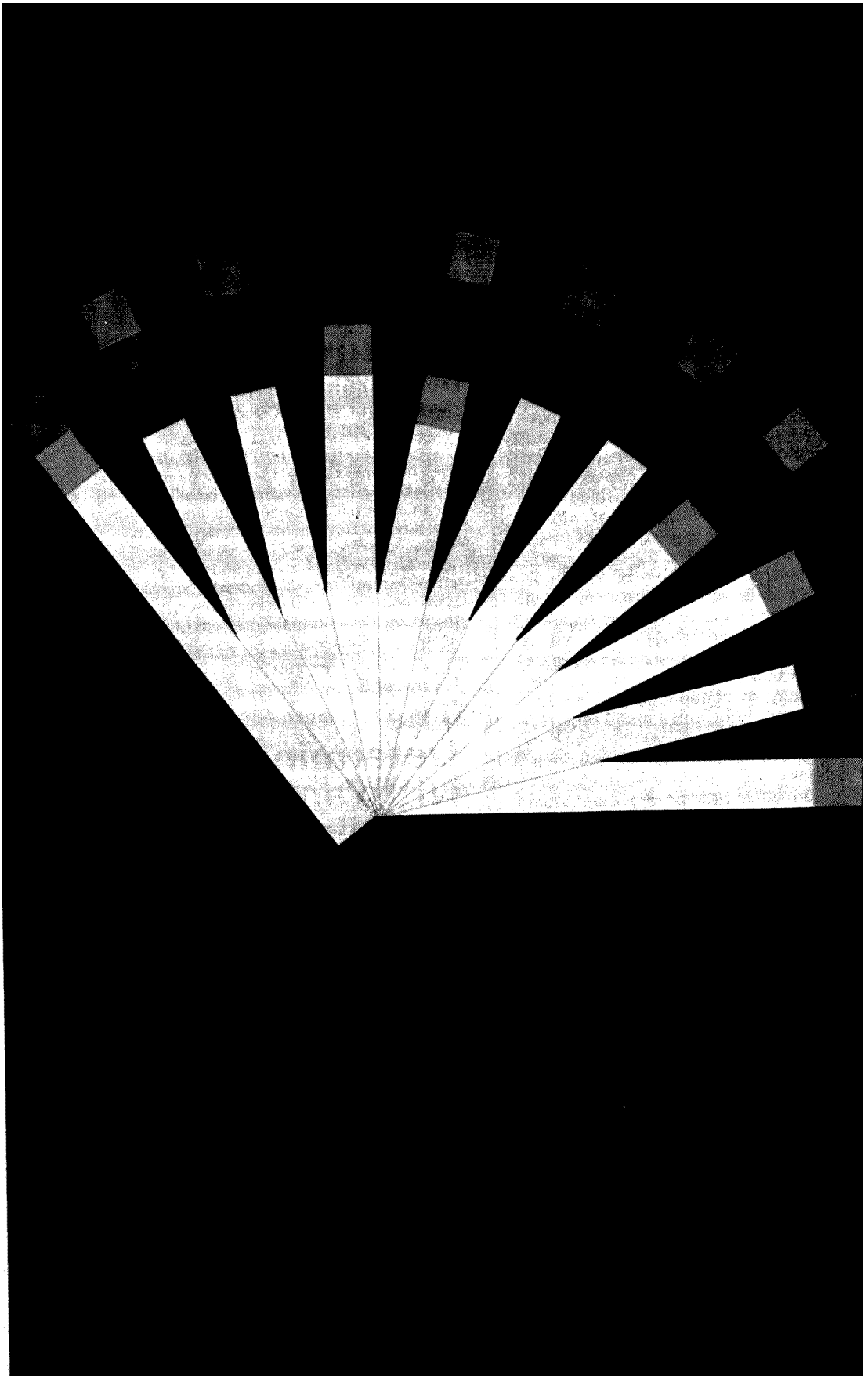

Analytica Chimica Acta, 68 (1974) 253–266

© Elsevier Scientific Publishing Company, Amsterdam – Printed in The Netherlands

STUDY OF THE BEHAVIOUR OF SOLID-STATE MEMBRANE ELECTRODES*

PART II. ROLE OF ADSORPTION OF FLUORIDE IONS ON FLUORIDE ION-SELECTIVE ELECTRODE AND DETERMINATION OF SOLUBILITY OF THE MEMBRANE

J. BUFFLE, N. PARTHASARATHY and W. HAERDI

Department of Inorganic and Analytical Chemistry, University of Geneva (Switzerland)

(Received 27th June 1973)

In Part I of this series[1], it was shown that the factors limiting the use of chloride electrode in the low concentration range were the solubility of the silver chloride membrane, and, in some cases, the interference of ions of the supporting electrolyte if the concentration of the latter is very high, and the chloride impurities which may be present in the electrolyte. On the other hand the results obtained with fluoride electrode seem to indicate that the last two factors mentioned above are more important than the first. These factors have been cited by several authors without having been rigorously verified[2–4]. The object of this work was to try to identify precisely the role of the solubility of the electrode membrane in the case of the fluoride electrode.

EXPERIMENTAL

The apparatus used for the potentiometric study with solid electrodes, the reagents and experimental conditions have already been described in Part I of the series[1]. As before, various experiments were performed in order to compute the deviation of the relation $E = f(\log c_F^a)$ from the Nernst equation, in the low concentration range, where c_F^a is the added fluoride concentration in the solution. This deviation, denoted by Δc_F, was calculated by using the values of the standard potential E' and the slope s of the electrode. These values were obtained by carrying out linear regression analysis in the region of high fluoride concentrations.

The measurements were carried out at $25° \pm 0.1°$ in different media and with two different electrodes, namely the Orion fluoride electrode No. 94-09 A and the Beckman combination electrode No. 39650. The electrode surfaces were never polished.

Neutron activation of lanthanum(III) was carried out in the Federal Institute for Nuclear Research, Würenlingen (Switzerland) with a neutron flux of $4\text{–}6 \cdot 10^{12}$ n cm^{-2} s^{-1}. The γ-spectra were recorded on an Intertechnique SA-40 400-channel γ-spectrometer.

* This paper is dedicated to Professor D. Monnier on the occasion of his 70th birthday.

Calculations were made with the Hewlett-Packard 9100 A and Geneva University computer CDC 3800.

THE IMPORTANCE OF VARIOUS FACTORS IN THE SENSITIVITY LIMIT OF THE FLUORIDE ELECTRODE

Role of hydroxide ions

Preliminary experiments showed that the curve $E = f(\log c_F^a)$ is not modified in the pH range 4 to 7; thus, hydroxide ions do not play an important role even at low fluoride concentrations, which is in agreement with the results of Frant and Ross[5]. The stability of various fluoride and hydroxide compounds of lanthanum(III)[6,7] (Table I) support this conclusion.

TABLE I

LOGARITHMS OF STABILITY CONSTANTS OF VARIOUS LANTHANUM(III) HYDROXIDE AND FLUORIDE COMPOUNDS AT 25°[a]

Fluoride compounds		
$\log K_{sp} = -19$	(I varied)	$\log K_{sp} = -17.7$
$\log \beta_1 = 3.3$	($I = 3M$ $LiClO_4$)	$\log \beta_1 = 2.67$ ($I = 1$ M $NaClO_4$)
$\log \beta^*_{12} = -9.98$	($I = 3M$ $LiClO_4$)	
$\log \beta^*_{95} = -71.4$	($I = 3M$ $LiClO_4$)	

[a] K_{sp} = solubility product, $\beta_1 = [LaL^{2-}]/[La^{3+}][L^-]$, and $\beta^*_{nm} = [La_mL_n^{3m-n}][H^+]^n/[La^{3+}]^m$, where $L^- = F^-$ or OH^-.

From the values given, it can be easily verified that, under the conditions used (pH 5.5), the complexes such as La_2OH^{5+} and $La_5(OH)_9^{6+}$ do not exist. The same reasoning applies for LaF^{2+} and $LaOH^{2+}$ if the concentration of fluoride or hydroxide is less than 10^{-5} M, which is the region of interest in this case. Finally, the solubility products of freshly precipitated LaF_3 and $La(OH)_3$ are fairly close to each other. If one takes into account the fact that the departure from linearity of the curve $E = f(\log c_F^a)$ occurs around $c_F^a = 5 \cdot 10^{-6}$ M (*i.e.* for $c_F^a/[OH^-] = 10^3$), and the solubility product of the electrode crystal is much lower than that of the amorphous powder[2,8], then it seems unlikely that the deviation can be attributed to hydroxide ions.

An attempt was made to verify these considerations experimentally by running i.r. spectra for freshly precipitated lanthanum fluoride at different pH values. However, no hydroxide band in the hydroxide finger-print region (800–4000 cm^{-1}) was observed, either with these samples or with pure lanthanum hydroxide.

Effect of interferences and fluoride impurities on the electrode response

The effect of these two factors would be adequate to explain why Δc_F is independent of c_F^a in a given set of measurements, as was observed[1]. However, the primary sources of interferences or impurities arise from the supporting electrolyte or the buffering agent.

From Tables II and III, it can be seen that Δc_F does not vary with

TABLE II

EXPERIMENTAL CONDITIONS USED TO VERIFY THE EFFECT OF IMPURITIES OR INTERFERENCES

(The three sets of measurements were performed with the Beckman electrode at 25°)

Experiment no	*Background electrolyte*	*Buffer*	*Measured E' (mV)*	*Measured value of s (mV)*
I	$NaNO_3$, 1*M*	CH_3COONa, 0.3*M* pH = 5.5	-193.5 ± 1.2	-60.1 ± 0.3
II	$NaNO_3$, 0.1*M*	none pH = 5.5	-195.2 ± 5.4	-59.0 ± 1.2
III	none	$CH_3COOONa$, 0.1 *M* pH = 5.5	-194.0 ± 1.8	-58.0 ± 0.4

TABLE III

RELATIONSHIP BETWEEN Δc_F AND c_F^a FOR VARIOUS CONCENTRATIONS OF BACKGROUND ELECTROLYTE AND BUFFER

Experiment I		*Experiment II*		*Experiment III*	
c_F^a *(M)*	Δc_F *(M)*	c_F^a *(M)*	Δc_F *(M)*	c_F^a *(M)*	Δc_F *(M)*
$1.5 \cdot 10^{-6}$	$1.6 \cdot 10^{-7}$	$4.0 \cdot 10^{-6}$	$1.1 \cdot 10^{-7}$	$1.5 \cdot 10^{-6}$	$2.7 \cdot 10^{-7}$
$8.0 \cdot 10^{-7}$	$1.9 \cdot 10^{-7}$	$8.0 \cdot 10^{-7}$	$4.0 \cdot 10^{-7}$	$8.0 \cdot 10^{-7}$	$3.1 \cdot 10^{-7}$
$6.0 \cdot 10^{-7}$	$1.2 \cdot 10^{-7}$	$6.0 \cdot 10^{-7}$	$2.1 \cdot 10^{-7}$	$6.0 \cdot 10^{-7}$	$2.1 \cdot 10^{-7}$
$5.0 \cdot 10^{-7}$	$1.6 \cdot 10^{-7}$	$3.0 \cdot 10^{-7}$	$2.1 \cdot 10^{-7}$	$4.0 \cdot 10^{-7}$	$1.7 \cdot 10^{-7}$
$4.0 \cdot 10^{-7}$	$1.5 \cdot 10^{-7}$	$1.0 \cdot 10^{-7}$	$2.0 \cdot 10^{-7}$	$3.0 \cdot 10^{-7}$	$1.6 \cdot 10^{-7}$
$3.0 \cdot 10^{-7}$	$1.3 \cdot 10^{-7}$			$1.5 \cdot 10^{-7}$	$2.0 \cdot 10^{-7}$
$1.5 \cdot 10^{-7}$	$2.6 \cdot 10^{-7}$			$1.0 \cdot 10^{-7}$	$2.2 \cdot 10^{-7}$
$1.0 \cdot 10^{-7}$	$2.0 \cdot 10^{-7}$				
$6.0 \cdot 10^{-8}$	$2.4 \cdot 10^{-7}$				
$1.0 \cdot 10^{-8}$	$2.8 \cdot 10^{-7}$				

the concentration of background electrolyte. Thus it seems that the effect of these two factors is not sufficient to interpret correctly the behaviour of the fluoride electrode in dilute solutions.

Role of the solubility of the electrode membrane

As Δc_F varies very little with c_F^a, irrespective of experimental conditions, the solubility of the electrode membrane does not seem to be a highly significant factor in the value of Δc_F. This is confirmed by the fact that Δc_F does not vary with the concentration of acetate between 0 and 0.3 *M*, although under these conditions the degree of complexation calculated from the stability constants of lanthanum(III) with acetate ($\log \beta_1 = 1.56$, $\log \beta_2 = 2.48$, $\log \beta_3 = 2.98$, $\log \beta_4 = 2.95$)[6] varies from 1 to $10^{1.73}$ at pH 5.5, *i.e.* the solubility of the lanthanum fluoride crystal should increase by a factor of 3.6.

In order to confirm that the solubility of the crystal plays a minor role in Δc_F values, an attempt was made to determine the order of magnitude of the solubility of the LaF_3 crystal. This was done by determining the lanthanum(III)

ion in fluoride solutions at low concentrations, once the electrode had attained equilibrium. The experiments were carried out in $5 \cdot 10^{-3}$ M lithium nitrate as background electrolyte and in the absence of acetate. The solutions were divided into two portions, and in one, known quantities of lanthanum nitrate solutions ranging from $4 \cdot 10^{-8}$ to $7 \cdot 10^{-8}$ M were added. These solutions were evaporated to 5 ml, transferred to the quartz cells used for neutron activation, evaporated to dryness under low pressure, and then left in an oven at 400° for 2 h to remove all traces of water. The samples were then cooled to room temperature and sealed before irradiation with a neutron flux of $4\text{–}6 \cdot 10^{12}$ n cm^{-2} s^{-1} for 120 h. The lanthanum(III) was determined by means of the 1.6 MeV peak obtained from the disintegration reaction of ^{140}La (half-life = 40.2 h) (Fig. 1a). The quartz cell and the lithium nitrate used contained impurities of sodium and potassium which hampered the determination of lanthanum(III) in the sample immediately after activation. However, after a decay time of 120 h, lanthanum-(III) could be determined without separation; at this time, the measured half-life was 40.19 h (Fig. 1b), which corresponds quite well with the half-life of lanthanum(III).

In this way, the concentrations of lanthanum(III), c_{La}, were determined after the electrode had been equilibrated in solutions containing different concentrations of fluoride. The results are given in Table IV. The accuracy of these results is limited by the difficulty in preparing the sample. However, it can be

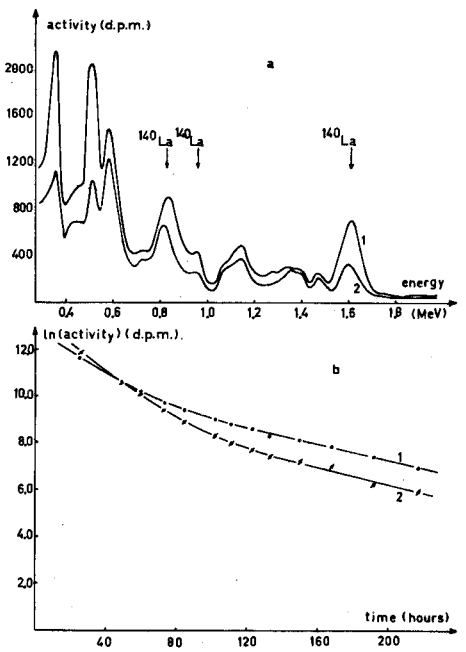

Fig. 1. Examples of the spectra (a) and of the radioactive decay curves (b) obtained for lanthanum-(III) by neutron activation at a flux of $4\text{–}6 \cdot 10^{12}$ n cm^{-2} s^{-1} for 120 h. These curves correspond to the sample under investigation (curves 2) and the same sample with a known quantity of lanthanum added (curves 1). The quantities of lanthanum were found to be $3.8 \cdot 10^{-8}$ g and $1.1 \cdot 10^{-7}$ g.

TABLE IV

VALUES OF c_{La} OBTAINED BY NEUTRON ACTIVATION ANALYSIS, FOR VARIOUS VALUES OF c_F^a

(c_F is the value of fluoride concentration computed from the value of the corresponding measured potential and from the Nernst equation, assuming that the effect of interfering ions is negligible)

c_F^a (M)	c_F (M)	Δc_F (M)	c_{La} (M)
$1.50 \cdot 10^{-7}$	$2.13 \cdot 10^{-7}$	$6.3 \cdot 10^{-8}$	$5.4 \cdot 10^{-8}$
$1.00 \cdot 10^{-7}$	$1.52 \cdot 10^{-7}$	$5.2 \cdot 10^{-8}$	$9.1 \cdot 10^{-9}$
$5.00 \cdot 10^{-8}$	$9.79 \cdot 10^{-8}$	$4.8 \cdot 10^{-8}$	$2.7 \cdot 10^{-8}$
$3.00 \cdot 10^{-8}$	$9.40 \cdot 10^{-8}$	$6.4 \cdot 10^{-8}$	$2.5 \cdot 10^{-8}$
$1.50 \cdot 10^{-8}$	$7.70 \cdot 10^{-8}$	$6.2 \cdot 10^{-8}$	$5.3 \cdot 10^{-9}$

seen that, under these conditions, the order of magnitude of the solubility is about $2\text{–}3 \cdot 10^{-8}$ M.

EFFECT OF ADSORPTION OF FLUORIDE IONS

Several authors[9] have mentioned that fluoride ions can be adsorbed on container walls; in order to obtain reproducible results, freshly prepared solutions must be used in the low concentration range[1]. However, the effect of adsorption or desorption on the walls of the container would not explain the observed results, because of their good reproducibility. Moreover, for measurements in very dilute solutions, carefully washed beakers, which had not been used for measuring concentrated solutions of fluoride, were used.

On the other hand, the behaviour of the fluoride electrode can be explained if one assumes that the fluoride ions may be adsorbed on the electrode surface. Such an assumption has been made by Ross[10] in discussing the behaviour of the sulfide electrode.

Theory

In the general case, the electrode crystal has the composition $A_{z_M}M_{z_A}$ where A is the anion, M the cation, and z_A and z_M are their number of charges. It is assumed that, when the electrode crystal is immersed in a solution containing A^{-z_A} ions, these ions can be adsorbed at the crystal surface. If this adsorption follows the Langmuir-type isotherm, in dilute solutions, then[11]:

$$\theta/(1-\theta) = (c_A/55.5) \exp(-\Delta\bar{G}^A_{ads}/RT) \qquad (1)$$

where θ is the fraction of surface covered ($1 \geqslant \theta \geqslant 0$), and c_A is the concentration of ion A^{-z_A} in the solution. $\Delta\bar{G}^A_{ads}$ is the standard electrochemical free energy of adsorption of A^{-z_A} ions; it is composed of two terms, namely the chemical term ϕ and the electrical one: $-z_A F\psi$, where ψ is the potential difference between the bulk solution and the plane of closest approach determined by the radius of hydrated A^{-z_A} ions (see Fig. 2). In eqn. (1), the term $\exp(-\Delta\bar{G}^A_{ads}/RT)/55.5$ is identical with the equilibrium constant for adsorption, K_L.

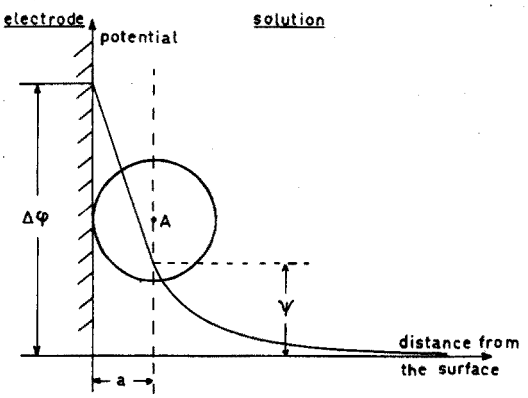

Fig. 2. Schematic potential gradient curve at the crystal solution interface: a = distance of closest approach; $\Delta\varphi$ = total potential difference between the crystal and the solution.

Equation 1 shows that, even if $\psi \cong 0$, which can be the case when the ionic strength of the solution is high, the possibility of adsorption cannot be neglected because of the chemical term ϕ which may at times be greater than the electrical term $-z_A F\psi$[12].

Such a process of adsorption might offer an explanation for the phenomenon of "memory" observed with certain electrodes whose response seems to be influenced by their previous history. If θ_0 is the fraction of surface covered for an electrode which is in equilibrium with a preconditioning solution of concentration c_A^0, then we can write

$$\theta_0 = K_L c_A^0/(1+K_L c_A^0) \tag{2}$$

If this electrode is immersed into another solution containing concentration c_A^a of the added test ion, in such a way that the surface concentration at the interface can be assumed to remain unchanged during the transfer, then two processes are likely to occur in the second solution: first, the dissolution (or crystallization) process causes an increase (or decrease) in the concentration of A^{-z_A}, c_A^d; secondly, desorption (or adsorption) of ions at the surface yields a new value for the fraction of total area covered, θ, and leads to an increase (or decrease), c_A^θ, in the concentration of A^{-z_A} ions.

Hence the total concentration of A in the second solution is given by:

$$c_A = c_A^a + c_A^i + c_A^d + c_A^\theta \tag{3}$$

where c_A^i is an additional concentration term representing the possible impurities of ion A^{-z_A} in the solution.

c_A^θ is given by:

$$c_A^\theta = (\theta - \theta_0)(S\Gamma/V) \tag{4}$$

where S is the surface area of the electrode, Γ is the surface concentration of A^{-z_A} ion, for $\theta = 1$, V is the volume of the solution, and

$$\theta = K_L c_A/(1+K_L c_A) \tag{5}$$

The value of c_A^d is given by (see eqns. 3 and 4, ref. 1):

$$c_A^d = \frac{z_M}{z_A} \cdot \frac{K_{sp}^{1/z_A}}{\gamma_M^{z_A} \cdot \gamma_A^{z_M}} \cdot \frac{1}{c_A^{z_M/z_A}} \tag{6}$$

By substituting the terms given above for θ_0, θ, c_A^θ, and c_A^d, in eqn. 3, we obtain:

$$c_A = c_A^a + c_A^i + \frac{z_M}{z_A} \cdot \frac{K_{sp}^{1/z_A}}{\gamma_M^{z_A} \cdot \gamma_A^{z_M}} \cdot \frac{1}{c_A^{z_M/z_A}} + \left[\frac{K_L c_A^0}{1+K_L c_A^0} - \frac{K_L c_A}{1+K_L c_A} \right] \cdot \frac{S\Gamma}{V} \tag{7}$$

It should be borne in mind that, strictly speaking, c_A^0 depends both on the phenomenon of adsorption and solubility. However, if c_A^0 is sufficiently high ($c_A^0 > 10^{-5}$ M for the fluoride electrode), the c_A^0 value can be assumed equal to the concentration of the added ion in the solution used for preconditioning the electrode.

The measured potential is given by:

$$\begin{aligned} E &= E' + s \log(c_A + Kc_E) \\ &= E' + s \log(c_T) \end{aligned} \tag{8}$$

where Kc_E is the term representing interfering ions in the background electrolyte[1]. As the measurement of E allows only c_T to be evaluated, eqn. (7) becomes:

$$\Delta c_A = c_T - c_A^a = c_A^i + Kc_E + \frac{z_M}{z_A} \cdot \frac{K_{sp}^{1/z_A}}{\gamma_A^{z_M} \cdot \gamma_M^{z_A}} \cdot \frac{1}{(c_T - Kc_E)^{z_M/z_A}} + \left[\frac{K_L(c_T^0 - Kc_E)}{1+K_L(c_T^0 - Kc_E)} - \frac{K_L(c_T - Kc_E)}{1+K_L(c_T - Kc_E)} \right] \cdot \frac{S\Gamma}{V} \tag{9}$$

where c_T^0 is calculated from the measured potential of the solution in which the electrode is preconditioned.

It is apparent from eqn. (9) that if $c_T^0 \gg c_T$, and if the solubility is small compared to the adsorption process, then:

$$\Delta c_A = c_A^i + Kc_E + \frac{K_L(c_T^0 - Kc_E)}{1+K_L(c_T^0 - Kc_E)} \cdot \frac{S\Gamma}{V}$$

Thus Δc_A is independent of c_A. Moreover, if the number of sites for adsorption is large, c_A^i and Kc_E can be small with respect to the third term, and Δc_A may become independent of the background electrolyte concentration.

Adsorption of fluoride on lanthanum fluoride powder

The possibility of adsorption of fluoride at the solution–solid interface was verified by adding different quantities of lanthanum fluoride powder to a solution of fluoride of concentration $c_F^a = 10^{-4}$ M, and measuring the corresponding potential with the Beckman combination fluoride electrode. As the surface area of the powder was much greater than that of the electrode, adsorption on the latter can be considered negligible, compared to the adsorption on the powder. It was possible to carry out experiments at concentrations of c_F^a in the range (10^{-5}–10^{-4} M) where the electrode response is of the Nernstian type.

If the potential *versus* time is recorded as soon as the lanthanum fluoride powder is added to the solution, then the profile of the curve is as shown in Fig. 3a (curve 1). (In some cases, a maximum is not observed, and a plateau

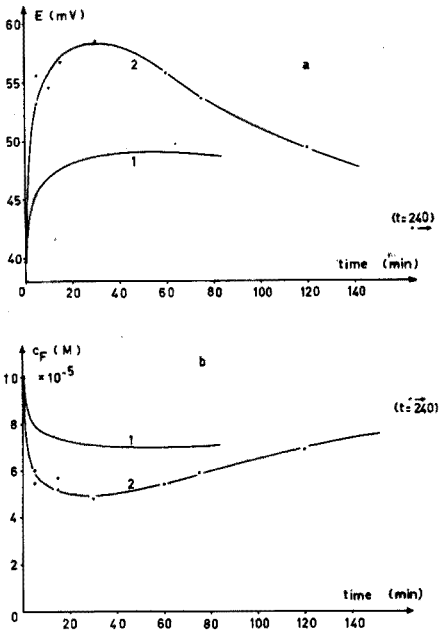

Fig. 3. The variation of potential of fluoride electrode (a) and corresponding concentration (b) calculated from the former, as a function of time, after adding 40 mg of LaF_3 in 40 ml of 10^{-4} *M* fluoride solution. Curves 1, potential recorded in the presence of the powder. Curves 2, potential measured after centrifuging the solution. Electrolyte, 1 *M* $NaNO_3$; buffering agent, 0.3 *M* CH_3COONa; pH = 5.5; $T = 25 \pm 0.1°$.

is obtained). If the concentration of fluoride at different points of the curve is calculated from the Nernst equation, a curve such as that shown in Fig. 3b curve 1) is obtained.

The above experiment was repeated by adding lanthanum fluoride powder to the fluoride solution without immersion of the electrode, and standing for different lengths of time. Then these solutions were centrifuged and the concentration of fluoride in the solution was measured with the electrode (see Fig. 3, curves 2). It can be seen that the maximum (minimum) observed with centrifuged solutions is more pronounced than when the powder is added with the electrode immersed. This is probably due to an interaction between the powder and the electrode. Despite this interaction, in both cases, the potential change corresponds to a decrease in concentration of fluoride ion.

In order to ensure that this variation was not due to the dissolution of lanthanum(III) ions, experiments were carried out by adding lanthanum(III) in the concentration range 10^{-7}–10^{-4} *M* to a 10^{-5} *M* solution of fluoride. There was no variation in the electrode potential, thus indicating the absence of interference from lanthanum(III) under these conditions. Thus, the variation in potential observed in Fig. 3a is due to a decrease in fluoride concentration and can be attributed to the adsorption of fluoride on lanthanum fluoride powder. The increase in concentration in the later parts of the curves is probably due to slow dissolution of the powder. In the following experiments, the same conditions as

for curves 1 (Figs. 3a and 3b) were used to investigate the influence of different parameters on the adsorption.

It should be stressed that, although the form of these curves is reproducible, the error in the measurement of concentration from one experiment to another is fairly large. This is because when lanthanum fluoride is added to the solution, it becomes semi-colloidal and its surface area is difficult to control. For this reason, eqn. (7) cannot be rigorously verified from the values of equilibrium potential obtained.

However, the surface area S of the powder in the suspension increases with its weight P. Hence from eqn. (7) it is apparent that Δc_F should become more negative when P is large and V is small. This was verified by measuring the change in concentration as a function of P and V (Fig. 4) and using the same experimental conditions in the various series of measurements (in particular, temperature and rate of stirring). In Fig. 4, Δc_F^{max} is the value of Δc which corresponds to the maximum of $E = f(t)$ or the equilibrium potential if no maximum is obtained.

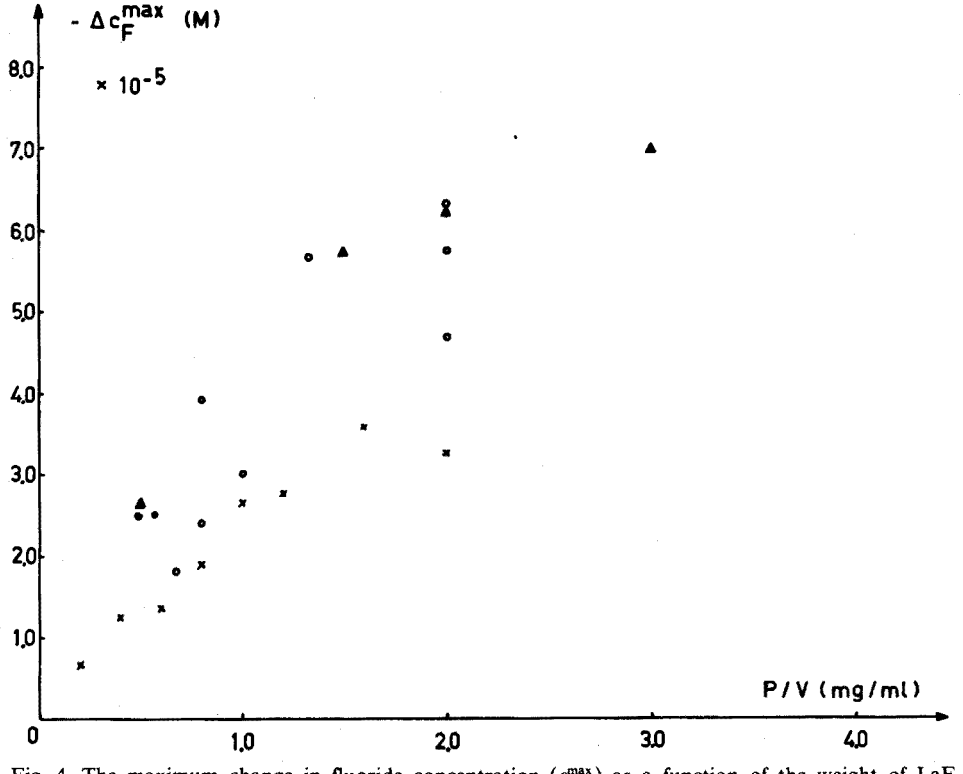

Fig. 4. The maximum change in fluoride concentration (c_F^{max}) as a function of the weight of LaF_3 added (P), and the volume of the solution (V): (▲) V constant at 20 ml, P varied; (×) V constant at 50 ml, P varied; (○) P constant at 40 mg, V varied. Electrolyte, 1 M $NaNO_3$; buffering agent, 0.3 M CH_3COONa; T, 25±0.1°.

Adsorption of fluoride on the electrode surface

In order to verify if the process of adsorption occurs also at electrode surface, Δc_F was determined by keeping c_F^a constant and varying c_F^0 (Fig. 5, curve a). In these experiments, the Orion fluoride electrode was first equilibrated in solution, with concentration c_F^0, and then it was quickly rinsed with demineralized water, dried with tissue paper and then dipped into the fluoride solution

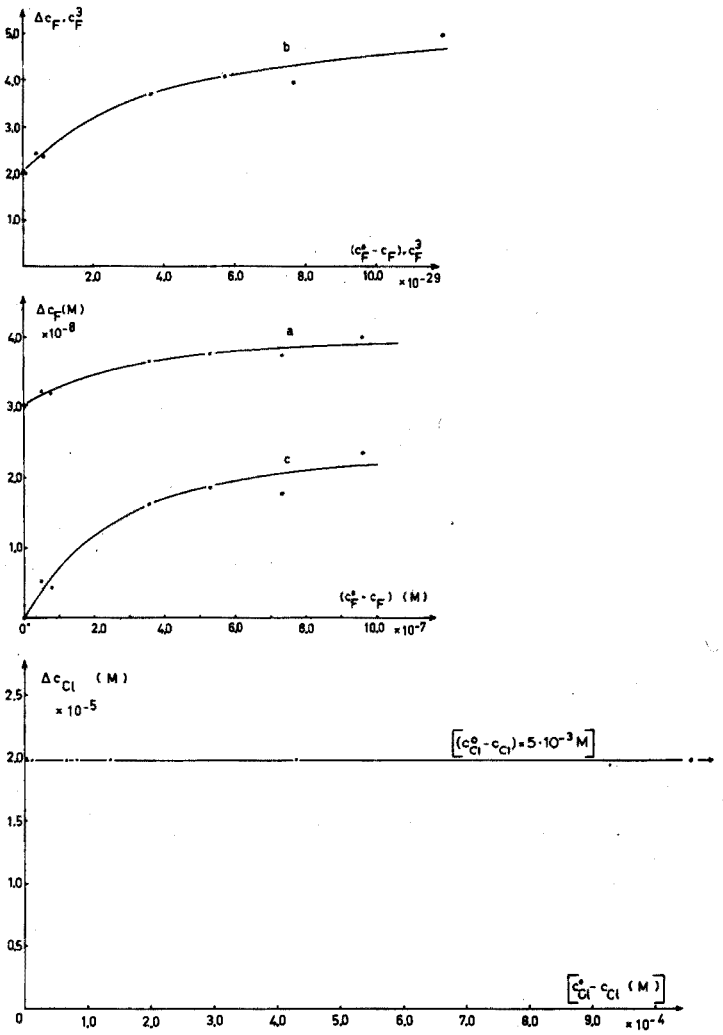

Fig. 5. The relation between Δc_F and c_F^0 (curve a), $\Delta c_F(c_F)^3$ and $(c_F^0 - c_F)(c_F)^3$ (curve b), and $(\Delta c_F - K_{SP}/c_F^3)$ and c_F^0 (curve c). Results obtained with the Orion electrode in 10^{-2} M $NaNO_3$ without acetate buffer. $T = 25 \pm 0.1°$. In curve c, the points are experimentally measured values and the continuous curve was calculated from the values of K_L and $S\Gamma$ obtained as indicated in the text. In all these measurements, c_F^a was kept constant at 10^{-8} M.

Fig. 6. Relation between Δc_{Cl} and $c_{Cl}^0 - c_{Cl}$ obtained with Beckman chloride electrode No. 39604 in KNO_3 at $25 \pm 0.1°$. c_{Cl}^a was kept constant at 10^{-5} M.

of concentration c_F. It can be seen that Δc_F increases with c_F^0 and a curve with the profile of an adsorption isotherm is obtained. For comparison, in the case of chloride electrode, Δc_{Cl} is independent of c_{Cl}^0 (Fig. 6), which confirms that phenomenon of adsorption is absent in this case[1].

If one supposes that, under experimental conditions used, (*i.e.* 10^{-2} *M* sodium nitrate without buffer), $Kc_E = 0$ and $c_A^i = 0$, then, from eqn. (9) one obtains the following:

$$\Delta c_F (c_F)^3 = 3K'_{sp} + \frac{K_L S\Gamma}{V}\left[\frac{(c_F^0 - c_F)(c_F)^3}{1 + K_L(c_F^0 + c_F) + K_L^2 c_F^0 c_F}\right] \tag{10}$$

where $K'_{sp} = K_{sp}/\gamma_F^3 \gamma_{La}$. This equation makes it possible to determine K'_{sp} by extrapolating the curve $\Delta c_F (c_F)^3 = f[(c_F^0 - c_F)(c_F)^3]$ (Fig. 5b), to $[(c_F^0 - c_F)(c_F)^3] = 0$. Extrapolation is facilitated by the fact that the curve becomes linear when $(c_F^0 + c_F) \to 0$. The value of K'_{sp} so obtained was $6.7 \cdot 10^{-31}$. This value of K'_{sp} was used with eqn. (9) and values of $\Delta c_F = f(c_F^0)$ to obtain the best estimates of K_L and $S\Gamma$, by means of a computer program MINUITS, programmed by the calculation centre at CERN (Geneva). This program finds the values of the parameters K_L and $S\Gamma$ which minimize the function H:

$$H = \sum_i \left[c_{F,i} - c_F^a - \frac{3K_{sp}}{\gamma_F^3 \gamma_{La}} \cdot \frac{1}{(c_{F,i}^3)} - \left(\frac{K_L c_{A,i}^0}{1 + K_L c_{A,i}^0} - \frac{K_L c_{A,i}}{1 + K_L c_{A,i}}\right)\frac{S\Gamma}{V}\right]$$

This method gave values for K_L and $S\Gamma$ of $(3.9 \pm 1) \cdot 10^6\ M^{-1}$ and $(6.8 \pm 2.7) \cdot 10^{-10}$, respectively. As the macroscopic surface area of the electrode was 0.8 cm^2, Γ could be evaluated as $\leqslant 0.064$ ion $Å^{-2}$, a value which seems quite reasonable. These computations were verified by another computer program (MALIK), programmed by the Centre Cantonal d'Informatique, University of Geneva. These values were used to plot curve c of Fig. 5.

SOLUBILITY OF THE CRYSTAL IN DIFFERENT MEDIA

The experiment used to establish curve A of Fig. 5 was repeated with the Orion electrode first in the absence of background electrolyte and buffer (Fig. 7a), and then in their presence (Fig. 7b). In the first case, it is impossible to say whether adsorption occurs or not at the electrode surface, owing to the imprecision in the measurements, probably caused by the absence of background electrolyte. In the second case, the estimated values of $S\Gamma$ and K_L are $2 \cdot 10^{-9}$ and $2 \cdot 10^4$, respectively, on assuming $Kc_E = c_F^i = 0$.

From Fig. 7a, despite the scattered points, it can be seen that extrapolation for $(c_F^0 - c_F) \to 0$ gives a value of $(3 \pm 0.5) \cdot 10^{-8}$ for Δc_F, which is in accordance with the value of $3.0 \cdot 10^{-8}$ found with 10^{-2} *M* sodium nitrate. Moreover, this value is in good agreement with the order of magnitude obtained by determining lanthanum(III) after equilibration of the electrode crystal in $5 \cdot 10^{-3}$ *M* lithium nitrate solution (see above).

In the case of Fig. 7b, extrapolation of the curve $\Delta c_F (c_F)^3$ versus $(c_F^0 - c_F)(c_F)^3$ (Fig. 8a) made it possible to calculate K'_{sp}, which was found to be $2.0 \cdot 10^{-28}$. This value, which is greater than that obtained in the presence of 10^{-2} *M* sodium nitrate or in the absence of background electrolyte, can be

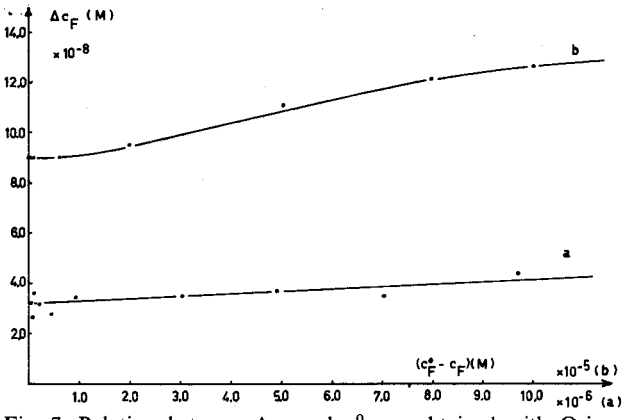

Fig. 7. Relation between Δc_F and $c_F^0 - c_F$ obtained with Orion electrode at $25 \pm 0.1°$. (a) Without electrolyte or buffer; c_F^a was kept constant at 10^{-8} *M*. (b) With electrolyte, 1 *M* $NaNO_3$; 0.3 *M* CH_3COONa; c_F^a was kept constant at 10^{-7} *M*.

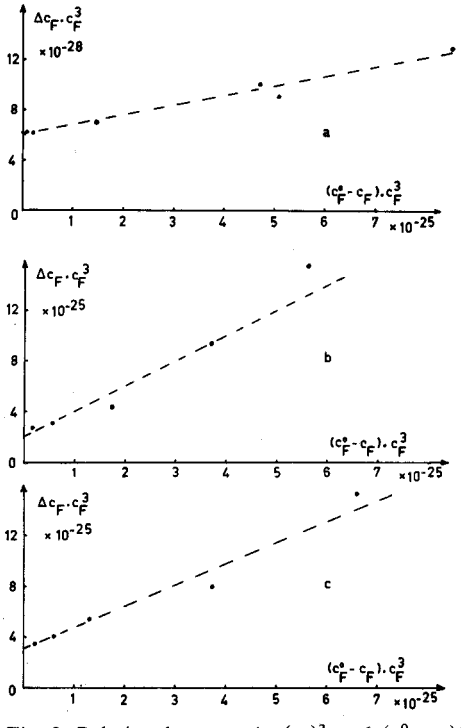

Fig. 8. Relation between $\Delta c_F(c_F)^3$ and $(c_F^0 - c_F)(c_F)^3$ obtained with the Orion electrode at $25 \pm 0.1°$. (a) Electrolyte, 1 *M* $NaNO_3$; 0.3 *M* CH_3COONa; $c_F^a = 10^{-7}$ *M*. (b) Electrolyte, 1 *M* KNO_3 0.15 *M* $K_2C_2O_4$; no acetate; c_F^a varied. (c) No electrolyte or acetate; 0.15 *M* $K_2C_2O_4$; c_F^a varied. The curves b and c were calculated directly from the calibration curve in oxalate medium, the value of c_F^0 being equal to the preceding c_F.

explained in various ways: (a) as a decrease in the activity coefficients of lanthanum(III) and fluoride, because of an increase in ionic strength; (b) by complexation of lanthanum(III) with acetate ($\alpha_{La} = 10^{1.73}$, see above); (c) the presence of impurities or interference in the electrolyte. The precision of the measurements does not allow these three factors to be distinguished. It should, however, be noted that if the value of α_{La} is taken into account to correct K'_{sp} then one obtains the value $K'_{sp} = 3.7 \cdot 10^{-30}$.

Finally, an attempt to study the effect of complexation was made by determining the solubility product of the Orion electrode crystal in the presence of 0.15 *M* oxalate and 1 *M* potassium nitrate (Fig. 8b) and also without the nitrate (Fig. 8c). The values of K'_{sp} obtained were $7 \cdot 10^{-26}$ and $1 \cdot 10^{-25}$, respectively. These show that K'_{sp} varies very little with ionic strength, whereas complexation plays an important role. From the stability constants of the complexes given in the literature[6] ($\log \beta_1 = 4.3$, $\log \beta_2 = 7.9$, $\log \beta_3 = 10.3$), the degree of complexation of lanthanum(III) was calculated as $10^{7.8}$ at pH 5.5. The solubility products corrected for this value were found to be: $K'_{sp} = 1.1 \cdot 10^{-33}$ in the presence of 1 *M* potassium nitrate, $K'_{sp} = 1.6 \cdot 10^{-33}$ in the absence of electrolyte. These values are lower than those obtained in the absence of complexing agent. This may be due to the fact that the values of the stability constants are not exactly correct under the experimental conditions used. Another possible explanation of this result could be that despite the steady potential observed during these measurements, the system does not reach thermodynamic equilibrium. Recent studies with the complexing agent EDTA support this view.

Conclusion

It seems reasonable to say that the solubility product of the Orion lanthanum fluoride electrode crystal is probably of the order of 10^{-30} or less. A similar order of magnitude for the solubility products was obtained with the Beckman combination electrode. These values are slightly lower than those cited by Frant and Ross[5] (10^{-29}) and much lower than those given by Butler[2] (10^{-23}). These differences in values are most probably due to the adsorption effects observed in this work. It should be emphasized that, according to the present results, the process of adsorption, rather than solubility of the crystal, determines the lower limit of detection of the electrode.

We wish to thank Mr. R. Morel (Section de Mathématiques, University of Geneva) for his advice on the use of MINUITS program. We also thank both Orion Research, Inc, and Beckman Instruments, Inc, for providing the electrodes.

SUMMARY

The phenomena limiting the sensitivity of the fluoride-selective electrode are described. Although the interference of electrolyte ions or fluoride impurities can play a part in this lower detection limit, it seems that the adsorption of fluoride ions at the membrane–solution interface and the solubility of the electrode crystal are the two principal parameters. The solubility of the electrode crystal under different conditions was estimated.

RÉSUMÉ

On a étudié les phénomènes qui limitent la sensibilité de l'électrode sélective au fluorure. Bien que l'interférence des ions de l'électrolyte ou les impuretés de fluorure puissent jouer un rôle dans cette limite de sensibilité, il semble que l'adsorption des ions F^- à l'interface membrane–solution et la solubilité du cristal soient les deux principaux paramètres importants. Cette solubilité a été déterminée dans différentes conditions.

ZUSAMMENFASSUNG

Die Faktoren, die die Empfindlichkeit der fluoridselektiven Elektrode begrenzen, werden beschrieben. Wenn auch die Störung durch Elektrolytionen oder Fluoridverunreinigungen bei dieser Nachweisgrenze eine Rolle spielen kann, scheinen die Adsorption von Fluoridionen an der Grenzfläche zwischen Membran und Lösung und die Löslichkeit des Elektrodenkristalls die beiden wesentlichen Ursachen zu sein. Die Löslichkeit des Elektrodenkristalls unter verschiedenen Bedingungen wurde ermittelt.

REFERENCES

1 N. Parthasarathy, J. Buffle and D. Monnier, *Anal. Chim. Acta*, 68 (1974) 185.
2 J. N. Butler, in R. A. Durst (Ed.), *Ion-Selective Electrodes*, NBS Special Publication No. 314, 1969, Ch. 5, p. 159.
3 E. Messmer, *Anal. Chem.*, 40 (1968) 443.
4 E. W. Baumann, *Anal. Chim. Acta*, 54 (1971) 189.
5 M. Frant and J. W. Ross, *Science*, 154 (1966) 1553.
6 L. G. Sillen and A. E. Martell, *Stability Constants*, Special Publication No. 17, The Chemical Society, London, 1964, pp. 43, 365; L. G. Sillen and A. E. Martell, *Stability Constants*, Special Publication No. 25, The chemical Society, London, 1971, p. 247.
7 T. Eriksson and G. Johansson, *Anal. Chim. Acta*, 52 (1970) 465.
8 J. W. Ross, in R. A. Durst (Ed.), *Ion-Selective Electrodes*, NBS Special Publication No. 314, Ch. 12, 1969, p. 417.
9 See R. Durst and B. T. Duhart, *Anal. Chem.*, 42 (1970) 1002.
10 J. W. Ross, in R. A. Durst (Ed.), *Ion-Selective Electrodes*, NBS Special Publication No. 314, Ch. 12, 1969, p. 435.
11 E. Gileadi, *Electrosorption*, Plenum Press, New York, 1967, p. 24; B. E. Conway, *Theory and Principles of Electrode Processes*, Ronald Press, New York, 1965, p. 33.
12 W. Stumm, G. P. Huang and S. R. Jenkins, *Croat. Chem. Acta*, 42 (1970) 223.

Analytica Chimica Acta, 68 (1974) 267–275

© Elsevier Scientific Publishing Company, Amsterdam – Printed in The Netherlands

ÉTUDE DU MÉCANISME DE L'OXYDATION PERBORIQUE DE L'INDOLE EN PRÉSENCE DE TRACES DIMÉTHYLE-O,O-DICHLOROVINYLE PHOSPHATE (DDVP)★

PARTIE I. ÉTAT DU DDVP EN SOLUTION ISOPROPANOLIQUE

M. MARCANTONATOS et L. GENOUD

Département de Chimie Minérale et de Chimie Analytique de l'Université de Genève (Suisse)

(Reçu le 7 septembre 1973)

Parmi les plus sensibles des méthodes physicochimiques de dosage de traces d'esters phosphoriques inhibiteurs de la cholinestérase, figurent les techniques cinétiques fluorimétriques[1-3]. Leur principe est une variante à la réaction chromogénique de Schoenemann[4] et consiste à oxyder l'indole en leucoindigo fluorescent dans un mélange eau –isopropanol, par du perborate et en présence de faibles quantités d'ester, suivant[1-3]:

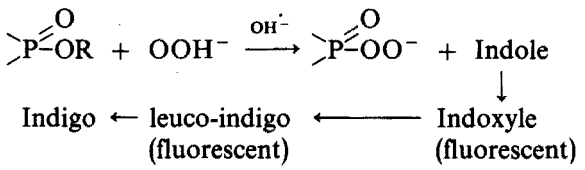

Dans la partie I du présent travail, nous étudions par spectrophotométrie u.v. l'état d'un de ces esters, à savoir du diméthyle-O, O-dichlorovinyle phosphate (DDVP), en solution diluée dans l'isopropanol.

La partie II est consacrée à l'étude cinétique de son hydrolyse et perhydrolyse basiques dans isopropanol–eau (32 + 68) et à l'influence de l'acétone sur leurs mécanismes.

Enfin, dans la partie III nous étudions le mécanisme de la réaction fluorogénique de l'oxydation de l'indole par du perborate en présence de traces de DDVP.

PARTIE EXPÉRIMENTALE

Solutions de DDVP (Ciba-Geigy) à diverses concentrations dans l'isopropanol puriss (Fluka).

Spectrophotomètre Pye-Unicam SP 8000 B; cuves en quartz $l = 1$ cm. Solutions thermostatisées à 20°.

AUTO-ASSOCIATION DU DDVP DANS L'ISOPROPANOL

Les déterminations spectrophotométriques nous ont permis de la mettre en

★ Cette publication est dédiée au Professeur D. Monnier, à l'occasion de son 70ème anniversaire.

évidence, même au sein de solutions diluées. Elle traduit les effets de concentration caractérisés par des légers déplacements des maximums de bandes d'absorption $-\lambda_{max}$205 et 212 nm pour $5 \cdot 10^{-5}$ et $3.2 \cdot 10^{-4}$ M de DDVP respectivement—et surtout par des écarts à la loi de Beer. Celle-ci, comme le montre la Fig. 1, se trouve bien vérifiée jusqu'à $6 \cdot 10^{-5}$ M[r (coefficient de corrélation linéaire) = 0.996, pour $D_{212} = f(DDVP)$], montrant ainsi la quasi prédominance d'une seule espèce probablement monomère, mais elle cesse d'être valable pour des concentrations supérieures.

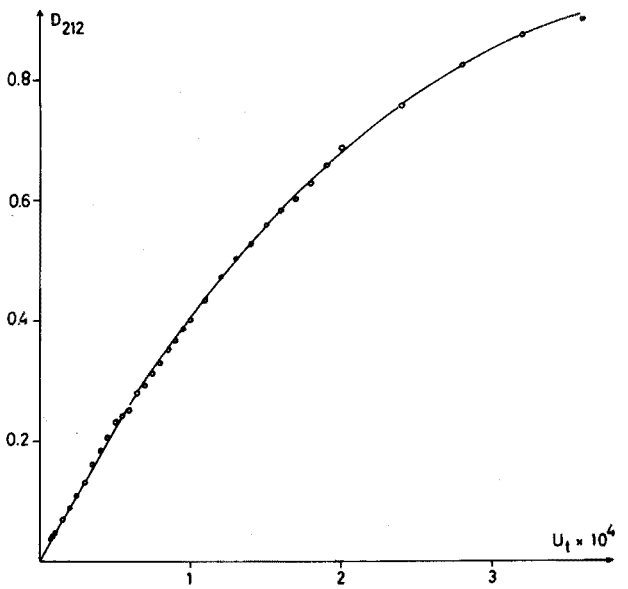

Fig. 1. Variation de la densité optique à 212 nm avec la concentration de DDVP (l = 1 cm; T = 20°).

Tétramérisation

Pour étudier cette auto-association, nous avons premièrement supposé la formation prédominante d'un seul i-mère U_i du DDVP selon:

$$iU \rightleftharpoons U_i \; ; \qquad \beta_{i0} = [U_i] u^{-i} \tag{1}$$

où U = monomère, u = sa concentration libre à l'équilibre, $[U_i]$ = concentration du i-mère et β_{i0} = constante de formation de U_i, et contrôler, pour le domaine de déviations à la linéarité de $D_{212} = f([DDVP])$, l'applicabilité de la relation (2)

$$\ln[U_i] = \ln \beta_{i0} + i \ln u \tag{2}$$

Pour ce faire, nous avons:

(i) évalué graphiquement ε_{10} et ε_{i0}/i (voir Fig. 2) à l'aide de l'expression (3) et les conditions (4)

$$D_\lambda U_t^{-1} l^{-1} = E = \varepsilon_{10}(1-\xi) + i^{-1} \varepsilon_{i0} \xi \tag{3}$$

$$\lim_{U_t \to 0} E = f(U_t) = \varepsilon_{10} ; \quad \lim_{U_t^{-1} \to 0} E = f(U_t^{-1}) = \varepsilon_{i0}/i ; \quad \lim_{U_t^{-1} \to 0} E^{-1} = i/\varepsilon_{i0} \tag{4}$$

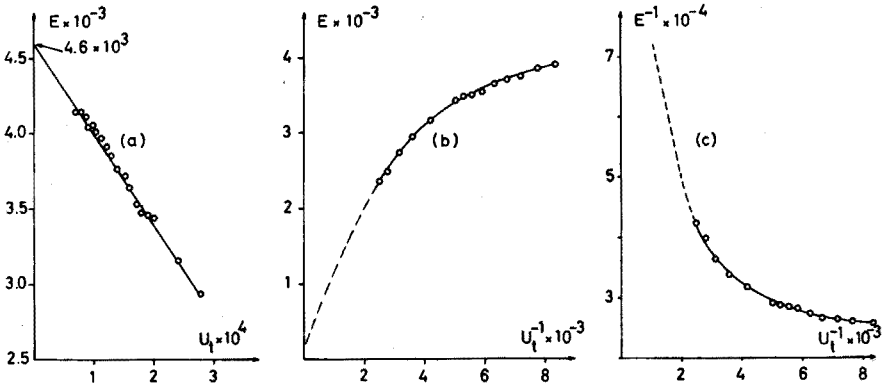

Fig. 2. Détermination graphique de ε_{10} et ε_{i0}/i.

où U_t = concentration totale du DDVP et l = épaisseur de la solution;

(ii) calculé la fraction ξ de U_t combinée à U_i, par la relation (5)

$$\xi = (E-\varepsilon_{10})(i^{-1}\varepsilon_{i0}-\varepsilon_{10})^{-1} \tag{5}$$

et

(iii) pris l'expression (2) sous la forme (6)

$$\ln \xi U_t = \ln i\beta_{i0} + i \ln(1-\xi)U_t \tag{6}$$

Toutefois, si la détermination de ε_{10} par $D=f(U_t)$ pour $U_t < 6\cdot 10^{-5}$ (voir Fig. 1) et par lim $U_t \to 0$ $E(U_t)$ (voir Fig. 2a) est relativement aisée, l'évaluation graphique de ε_{i0}/i ne peut être que hazardeuse, car les données $E(C_t^{-1})$ et E^{-1} (C_t^{-1}) sont très éloignées de la limite considérée (voir Fig. 2, b et c).

Aussi, pour contrôler la validité de l'expression (6), des valeurs de ε_{i0}/i comprises entre 80 et 1000 ont été choisies pour le calcul de ξ selon la relation (5). La Figure 3 montre que, dans tous les cas, la linéarité de l'expression (6) n'est pas vérifiée. Par contre, i varie très approximativement de 2 à $\geqslant 4$.

Ces premiers résultats, quoiqu'approximatifs, indiquent que le DDVP, essentiellement sous forme monomère pour $U_t < 5\cdot 10^{-6}$, s'auto-associe par étapes successives pour des concentrations supérieures.

Or, pour les équilibres de la forme:

$$2U \rightleftharpoons U_2 + U \rightleftharpoons U_3 \ldots \tag{7}$$

leur résolution spectrophotométrique peut en principe s'effectuer à l'aide de la relation (8)

$$D_\lambda l^{-1} = \sum_1^I \varepsilon_{10}[U_i] = \sum_1^I \varepsilon_{i0}\beta_{i0}u^i \tag{8}$$

Cependant, comme l'expression (8) contient $2I-1$ paramètres inconnus, sa solution pour $I > 3$ par les seules données D, U_t est difficile; seuls les cas où $\varepsilon_{10} = \varepsilon_{20} = \varepsilon_{30} = \ldots$ peuvent être traités d'une manière satisfaisante[5a].

Pour contrôler l'hypothèse d'une tétramérisation du DDVP dans la zone de concentrations U_t utilisées, nous avons procédé de la façon suivante.

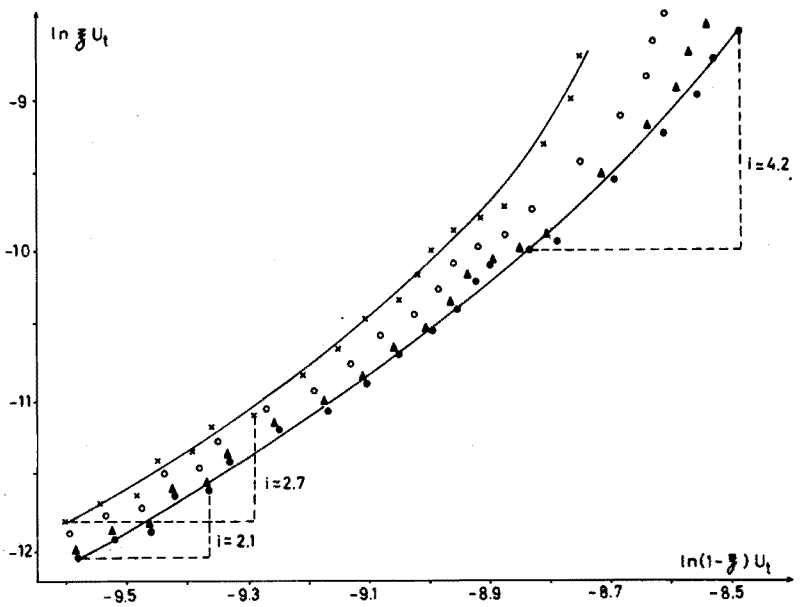

Fig. 3. Ln ξU_t en fonction de $\ln(1-\xi)U_t$. $\varepsilon_{i0}/i = 80(\bullet)$, $300(\blacktriangle)$, $540(\circ)$ et $1000(\times)$.

Soient U_t, u et u_i les concentrations respectivement totale du DDVP, libre et celle combinée au i-mère U_i. Soient encore $[U_i]$ la concentration de ce dernier à l'équilibre et ξ_i la fraction de U_t combinée à U_i:

$$U_t = \sum_0^4 i[U_i] = \sum_0^4 i\beta_{i0} u^i \tag{9}$$

$$[U_i] = i^{-1} u_i \tag{10}$$

$$u_i = \xi_i U_t \tag{11}$$

La densité optique D_λ par épaisseur de solution l à la longueur d'onde d'absorption des espèces U_i est donnée par:

$$D_\lambda l^{-1} = \sum_1^4 \varepsilon_{i0}[U_i] = \sum_1^4 i^{-1}\varepsilon_{i0} u_i = \varepsilon_{10} u + U_t \sum_2^4 e_{i0}\xi_i \tag{12}$$

et

$$E = D_\lambda l^{-1} U_t^{-1} = \varepsilon_{10} u U_t^{-1} + \sum_2^4 e_{i0}\xi_i = \varepsilon_{10} u U_t^{-1} + e_{20} \sum_2^4 e_{i0} e_{20}^{-1}\xi_i \tag{13}$$

où $e_{i0} = \varepsilon_{i0}/i$. Si:

(iv) $e_{i0}/e_{20} = 1$ (14)

$$\lim_{U_t \to 0} E = \varepsilon_{10} \; ; \; U_t \to u \; ; \; \xi_i \to 0 \tag{15}$$

$$\lim_{U_t^{-1}} E = e_{20} \; ; \; \sum_2^4 e_{i0} e_{20}^{-1}\xi_i \to 1 \tag{16}$$

(v) $e_{i0}/e_{20} \neq 1$

l'expression (15) reste toujours valable, mais

$$\lim_{U_t^{-1}\to 0} E \neq e_{20} \; ; \; \sum_2^4 e_{i0} e_{20}^{-1} \xi_i \not\to 1 \tag{17}$$

Par les relations (9), (10), (11), (13) et avec (14) valable:

$$u = U_t - \sum_2^4 u_i = \left(1 - \sum_2^4 \xi_i\right) U_t \tag{18}$$

$$E = \varepsilon_{10}\left(1 - \sum_2^4 \xi_i\right) + e_{20} \sum_2^4 \xi_i \tag{19}$$

$$\sum_2^4 \xi_i = (E - \varepsilon_{10})/(e_{20} - \varepsilon_{10}) = S \tag{20}$$

et les relations (9), (18) et (20) donnent:

$$U_t = \sum_0^4 i\beta_{i0}[(1-S)U_t]^i = \sum_0^4 i\beta_{i0} u^i \tag{21}$$

Si $e_{i0}/e_{20} \approx 1$, l'utilisation de l'expression (20) fournit des sommes, soit S', de fractions de U_t combinées aux U_i et des concentrations libres de U, soit $(1-S')U_t$, approximatives; les constantes, également approximatives, vb_{i0} et $(v+1)b_{v+1,0}$ pouvant être obtenues par l'intersection et la pente limite de

$$F_v = f((1-S')U_t) \quad \text{(ref. 5b)}$$

$$F_v = U_t[(1-S')U_t]^{-v} - \sum_1^{v-1} ib_{i0}[(1-S')U_t]^{i-v}$$

$$= vb_{v0} + (v+1)b_{v+1,0}[(1-S')U_t] + \sum_{v+2}^{I} ib_{i0}[(1-S')U_t]^{i-v} \tag{22}$$

$$(v = 2, 3; \quad U_t = \sum_0^4 ib_{i0}[(1-S')U_t])$$

D'autre part, on peut calculer des densités optiques D'_λ par:

$$D'_\lambda/l = \varepsilon_{10}[(1-S')U_t] + \sum_2^4 i e_{i0} b_{i0}[(1-S')U_t]^i$$

$$= \varepsilon_{10}[(1-S')U_t] + e_{20} \sum_2^4 e_{i0} e_{20}^{-1} ib_{i0}[(1-S')U_t]^i \tag{23}$$

et la condition (24):

$$(D-D')/l = \sum_1^4 \varepsilon_{i0}\beta_{i0}u^i - \varepsilon_{10}[(1-S')U_t] + e_{20}\sum_2^4 e_{i0}e_{20}^{-1} ib_{i0}[(1-S')U_t]^i$$

$$= \varepsilon_{10}[u - (1-S')U_t] + \sum_2^4 \varepsilon_{i0}\beta_{i0}u^i - e_{20}\sum_2^4 e_{i0}e_{20}^{-1} ib_{i0}[(1-S')U_t]^i = 0 \tag{24}$$

impliquant que:

$$u = (1-S')U_t \tag{25}$$

et

$$\varepsilon_{20}\beta_{20} = 2e_{20}b_{20}; \; \varepsilon_{30}\beta_{30} = 3e_{20}(e_{30}/e_{20})b_{30}; \; \varepsilon_{40}\beta_{40} = 4e_{20}(e_{40}/e_{20})b_{40} \tag{26}$$

permet d'obtenir u, de déterminer les β_{i0} par un procédé graphique analogue à l'expression (22) (voir l'expression (21)) et de calculer les ε_{i0} au moyen de relations (26).

Pour contrôler l'hypothèse de tétramérisation et obtenir les valeurs de β_{i0} et ε_{i0} des i-mères du DDVP, nous avons:

(a) déterminé graphiquement ε_{10}, pris $e_{20}=540$, calculé S' à l'aide de l'expression (20) et évalué graphiquement les b_{i0} à l'aide de l'expression (22);

(b) introduit les données obtenues dans (23) et calculé $D'l^{-1}$ en prenant $e_{30}e_{20}^{-1}=1.5$ et $e_{40}e_{20}^{-1}=2$;

(c) recalculé S' en donnant à e_{20} des valeurs différentes et réajusté les b_{i0} jusqu'à ce que les valeurs de D'/l calculées satisfassent la relation (24);

(d) utilisé les u obtenues par la condition (25) pour exprimer $F_v=f(u)$ et déterminer graphiquement les β_{i0}, et

(e) évalué les ε_{i0} à l'aide des expressions (26).

RÉSULTATS

Avec $\varepsilon_{10}=4.48\cdot10^3$ ($\varepsilon_{10}=4.37\cdot10^3$ par $D=f(U_t)$, $U_t\leqslant 6\cdot10^{-5}$ et $\varepsilon_{10}=4.59\cdot10^3$ par la relation (4)), $e_{20}=5.4\cdot10^2$ et S' calculée par l'expression (20), l'analyse graphique des données F_v, $(1-S')U_t$ selon l'expression (22) (voir Fig. 4), donne:

$$b_{20}=3.3\cdot10^2\ ;\ b_{30}=3.7\cdot10^6\ ;\ b_{40}=1.5\cdot10^{10}\ ,$$

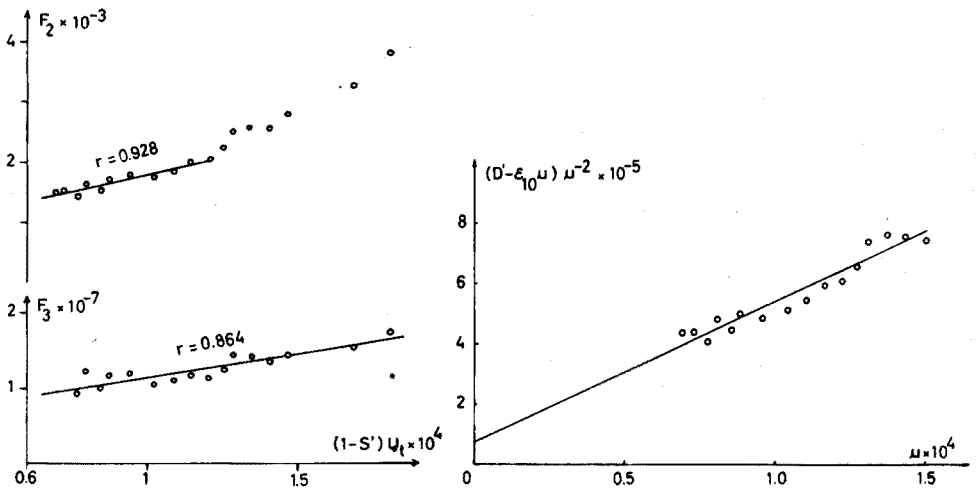

Fig. 4. Détermination graphique des b_{i0} selon l'expression (22).

Fig. 5. Détermination graphique de ε_{20} et ε_{30} selon l'expression (29); (—): $7.64\times10^4+4.62\times10^9\,u$, $r=0.958$.

et la condition $(D-D'_1)/l\simeq 0$ (voir Tableau I; D'_1 calculée à l'aide de la relation 23) est trouvée atteinte pour:

$$\varepsilon_{10}=4.48\cdot10^3\ ;e_{20}=3.3\cdot10^2\ ;\ e_{30}e_{20}^{-1}=1.5;\ \ e_{40}e_{20}^{-1}=2;$$
$$2b_{20}=3.3\cdot10^2\ ;\ 3b_{30}=3.7\cdot10^6\ ;\ 4b_{40}=4\cdot10^{10} \qquad (27)$$

TABLEAU I

VALEURS EXPÉRIMENTALES (D) ET CALCULÉES (D'_1 ET D'_2) DE DENSITÉ OPTIQUE À 212 nm
($l = 1$ cm)

$U_t \times 10^4$ [a] ($mol\ l^{-1}$)	D			$\bar{D} - D'_1$ [b]	$\bar{D} - D'_2 = \Delta$	$\Delta \cdot 100/\bar{D}$ (%)
0.08	0.028	0.038	0.037	0.0001	0.0001	+0.29
0.09	0.040	0.047	0.040	−0.0001	−0.0001	−0.24
0.1	0.044	0.044	0.045	0	0	—
0.15	0.063	0.070	0.067	0	0	—
0.2	0.087	0.085	0.092	0.0001	0	—
0.25	0.100	0.108	0.112	0.0003	0.0002	+0.18
0.3	0.125	0.133	0.135	0.0002	0.0001	+0.08
0.35	0.154	0.162	0.167	−0.0004	0.0005	+0.31
0.4	0.182	0.178	0.174	0	0.0002	+0.11
0.45	0.205	0.207	0.200	−0.0005	0.0006	+0.29
0.5	0.238	0.230	0.232	−0.0012	0.0011	+0.47
0.55	0.240	0.241	0.240	0	0.0002	+0.08
0.6	0.245	0.255	0.250	0.0009	0.0006	+0.24
0.7	0.290	0.290		0.0009	0.0006	+0.21
0.75	0.310	0.310		0.0004	0.0005	+0.16
0.8	0.328	0.330		0.0009	0.0005	+0.15
0.85	0.350	0.350		0.0006	0.0002	+0.06
0.9	0.360	0.365		0.0011	0.0006	+0.16
0.95	0.385	0.385		0.0007	0.0003	+0.08
1.0	0.397	0.400		0.0011	0.0006	+0.15
1.1	0.432	0.432		0.0011	0.0006	+0.14
1.2	0.468	0.470		0.0005	0.0001	−0.02
1.3	0.500	0.500		0.0002	−0.0002	−0.04
1.4	0.525	0.530		0.0004	−0.0001	−0.02
1.5	0.552	0.565		−0.0002	−0.0006	−0.11
1.6	0.580	0.585		0	−0.0003	−0.05
1.7	0.600	0.600		0.0009	0.0007	+0.12
1.8	0.625	0.630		0.0003	0.0003	+0.05
1.9	0.655	0.660		−0.001	−0.0007	−0.11
2.0	0.690	0.685		−0.0027	−0.0024	−0.35
2.4	0.755	0.760		−0.0015	−0.0004	−0.05
2.8	0.820	0.825		−0.001	0.0006	+0.07
3.2	0.875	0.870		0.0021	0.0046	+0.53
3.6	0.900	0.900		0.0113	0.0141	+1.6
4.0	0.940	0.940		0.016	0.0196	+2.1

[a] U_t = concentration totale de DDVP. [b] $\bar{D}$ = moyenne des D; D'_1 : calculée par l'expression (23) et avec les valeurs de l'expression (27); D'_2 : calculée par l'expression (8) et avec les valeurs de l'expression (30).

Les valeurs suivantes pour les β_{i0} :

$$\beta_{20} = 3.5 \cdot 10^2 \ ; \ \beta_{30} = 1.62 \cdot 10^6 \ ; \ \beta_{40} = 1.05 \cdot 10^{10} \qquad (28)$$

sont obtenues par le traitement des données F_v, u (u, tirées de la condition (24)) et celles pour les ε_{i0} :

$$\varepsilon_{20} = 3.11 \cdot 10^2 \ ; \ \varepsilon_{30} = 1.13 \cdot 10^3 \ ; \ \varepsilon_{40} = 2.51 \cdot 10^3$$

par les expressions (26) et à l'aide de valeurs (27) et (28).

Enfin (voir Fig. 5):

$$\varepsilon_{20} = 2.18 \cdot 10^2 \; ; \; \varepsilon_{30} = 2.85 \cdot 10^3$$

sont tirées de:

$$(D' - \varepsilon_{10}\, u)u^{-2} = \varepsilon_{20}\beta_{20} + \varepsilon_{30}\beta_{30}\, u + \varepsilon_{40}\beta_{40}u^2 \tag{29}$$

et un meilleur ajustement (voir $(D - D'_2)l^{-1}$, Tableau I; D'_2 calculée à l'aide de l'expression 8) est atteint avec:

$$\beta_{20} = 3.5 \cdot 10^2 \; ; \; \beta_{30} = 1.58 \cdot 10^6 \; ; \; \beta_{40} = 1.02 \cdot 10^{10} \; ;$$
$$\varepsilon_{10} = 4.48 \cdot 10^3 \; ; \; \varepsilon_{20} = 3.16 \cdot 10^2 \; ; \; \varepsilon_{30} = 1 \cdot 10^3 \; ; \; \varepsilon_{40} = 2.2 \cdot 10^3 \tag{30}$$

RÉSUMÉ

Des solutions diluées du diméthyl-O,O-dichlorovinyle phosphate dans l'isopropanol sont étudiées spectrophotométriquement dans l'u.v. et montrent, pour des concentrations $> 5 \cdot 10^{-5}$ M, des déviations appréciables à la loi de Beer. Le traitement quantitatif des données indique une tétramérisation successive. Une méthode d'extrapolation combinée à des ajustements à la courbe expérimentale, utilisant les valeurs de densité optique et les concentrations totales, est élaborée pour la détermination des constantes de formation β_{i0} et des coefficients d'extinction molaire ε_{i0} du di-, tri- et tetramère. Les valeurs trouvées sont: $\beta_{20} = 3.5 \cdot 10^2$. $\beta_{30} = 1.6 \cdot 10^6$, $\beta_{40} = 1.0 \cdot 10^{10}$, $\varepsilon_{10} = 4.5 \cdot 10^3$, $\varepsilon_{20} = 3.2 \cdot 10^2$, $\varepsilon_{30} = 1 \cdot 10^3$, $\varepsilon_{40} = 2{\cdot}2 \cdot 10^3$.

SUMMARY

Dilute solutions of O,O-dimethyl-2,2-dichlorovinyl phosphate (DDVP) in isopropanol were investigated spectrophotometrically in the u.v. region and were found to show appreciable deviations from Beer's law for concentrations above $5 \cdot 10^{-5}$ M. Quantitative treatment of data indicates successive tetramerization. A method based on extrapolation coupled with curve fitting, which uses absorbance and total concentration values, was developed for the evaluation of formation constants β_{i0} and molar absorptivities ε_{i0} of the di, tri-, and tetramer. Values found are: $\beta_{20} = 3.5 \cdot 10^2$, $\beta_{30} = 1.6 \cdot 10^6$, $\beta_{40} = 1.0 \cdot 10^{10}$, $\varepsilon_{10} = 4.5 \cdot 10^3$, $\varepsilon_{20} = 3.2 \cdot 10^2$, $\varepsilon_{30} = 1 \cdot 10^3$, $\varepsilon_{40} = 2.2 \cdot 10^3$.

ZUSAMMENFASSUNG

Verdünnte Lösungen von O,O-Dimethyl-2,2-dichlorovinyl-phosphat(DDVP) in Isopropanol wurden spektrophotometrisch im u.v.-Bereich untersucht. Bei Konzentrationen oberhalb $5 \cdot 10^{-5}$ M traten merkliche Abweichungen vom Beerschen Gesetz auf. Die quantitative Auswertung der Ergebnisse weist auf nacheinander folgende Tetramerisierung hin. Eine Methode, die auf einer Extrapolation in Verbindung mit einer Kurvenangleichung beruht und bei der die Extinktions- und Gesamtkonzentrationswerte verwendet werden, wurde für die Berechnung der Bildungskonstanten β_{i0} und molaren Extinktionskoeffizienten ε_{i0} des Dimeren, Trimeren und Tetrameren entwickelt. Die gefundenen Werte sind: $\beta_{20} = 3.5 \cdot 10^2$, $\beta_{30} = 1.6 \cdot 10^6$, $\beta_{40} = 1.0 \cdot 10^{10}$, $\varepsilon_{10} = 4.5 \cdot 10^3$, $\varepsilon_{20} = 3.2 \cdot 10^2$, $\varepsilon_{30} = 1 \cdot 10^3$, $\varepsilon_{40} = 2.2 \cdot 10^3$.

BIBLIOGRAPHIE

1 B. Gehauf et J. Goldenson, *Anal. Chem.*, 29 (1957) 276.
2 B. Gehauf, J. Epstein, G. B. Wilson, B. Witten, S. Sass, V. E. Bauer et W. H. C. Rueggeberg, *Anal. Chem.*, 29 (1957) 278.
3 G. G. Guilbault et G. J. Lubrano, *Anal. Chim. Acta*, 43 (1968) 253.
4 R. B. Schoenemann, PB 119887 (1944), Office of Publication Board, U.S. Dept. of Commerce.
5 F. J. C. Rossotti et H. Rossotti, *The Determination of Stability Constants*, McGraw-Hill, London, 1961. (a) p. 338, (b) p. 329.

Analytica Chimica Acta, 68 (1974) 277–287

© Elsevier Scientific Publishing Company, Amsterdam – Printed in The Netherlands

ÉTUDE DU MÉCANISME DE L'OXYDATION PERBORIQUE DE L'INDOLE EN PRÉSENCE DE TRACES DE DIMÉTHYLE-O,O-DICHLOROVINYLE PHOSPHATE (DDVP)*

PARTIE II. CINÉTIQUE DE SCISSION PERHYDROLYTIQUE DU DDVP ET ACTION CATALYTIQUE DE L'ACÉTONE

M. MARCANTONATOS et L. GENOUD

Département de Chimie Minérale et de Chimie Analytique de l'Université de Genève (Suisse)

(Reçu le 7 septembre 1973)

Il est bien connu[1] que l'hydrolyse alcaline des phosphates de vinyle se fait par attaque sur l'atome de phosphore et départ du reste vinylique:

$$(RO)_2P(O)OC=C\lesssim \xrightarrow{OH^-} (RO)_2P(O)OH + {}^-O-C=C\lesssim \qquad (1)$$

la vitesse dépendant des substituants du phosphore et augmentant avec le caractère électrophile de ceux-ci.

D'autre part, selon différents auteurs[2-4], l'action de l'ion perhydroxyle sur les esters phosphoriques conduit à des intermédiaires perhydroxylés:

$$(RO)_2P(O)OR' + OOH^- \xrightarrow{OH^-} (RO)_2P(O)OO^- \qquad (2)$$

qui, en présence d'un réactif approprié, l'oxydent[3-4] en composé coloré ou fluorescent:

$$(RO)_2P(O)OO^- + \text{réactif} \rightarrow \text{comp. coloré (fluorescent)} \qquad (3)$$

Il a été constaté[5-6] que la sensibilité de la réaction (3) est considérablement augmentée par des faibles concentrations d'acétone. L'action de celle-ci reste encore mal connue, mais il est supposé qu'elle forme un complexe[7] avec l'ion perhydroxyle réagissant avec l'ester phosphorique plus rapidement que O_2H^-.

Le but de cette partie du travail est d'apporter, par l'étude cinétique de la scission perhydrolytique du DDVP, une contribution à la connaissance du mécanisme de la perhydrolyse des esters phosphoriques et du rôle de l'acétone dans cette réaction.

PARTIE EXPÉRIMENTALE

Réactifs et appareillage

Dimethyle-O,O-dichlorovinyl phosphate (DDVP), Ciba-Geigy; isopropanol puriss., Fluka; acétone *pro analysi*, Merck; perborate de sodium, Fischer Scientific; eau tridistillée.

* Cette publication est dediée au Professeur D. Monnier à l'occasion de son 70ème anniversaire.

Spectrophotomètre Pye Unicam SP 8000 B; cuves en quartz $l = 1$ et 0.5 cm; pH-mètre Beckman Century 55; solutions thermostatisées à 20°.

Hydrolyse et perhydrolyse du DDVP

Des courbes de l'évolution en fonction du temps de la densité optique mesurée à 210 nm par rapport à un blanc (à la même concentration de perborate que la solution étudiée) ont été enregistrées à 20° pour deux séries de solutions de concentrations variables de perborate dans l'isopropanol–eau (32 + 68), l'une renfermant du DDVP à la concentration de $1.4 \cdot 10^{-4}$ *M*, l'autre à $2.5 \cdot 10^{-4}$ *M*. Le pH de ces solutions a été contrôlé et le Tableau I montre que celles-ci sont bien tamponnées.

TABLEAU I

pH DES SOLUTIONS DE DDVP DANS L'ISOPROPANOL–EAU Á DIFFÉRENTES CONCENTRATIONS DE PERBORATE

$[P] \times 10^{3a}$ (mol l^{-1})	5.2	7.02	10.4	11.7
pH	11.00	11.06	11.06	11.08

[a] [P] = concentration de perborate.

RÉSULTATS

Dans les Figs. 1–4, nous représentons, à titre d'exemple, quelques évolutions $D = f(t)$ et les résultats de leur analyse. Le Tableau II comprend, d'autre part, les caractéristiques des diverses réactions et les valeurs de constantes observées de vitesse.

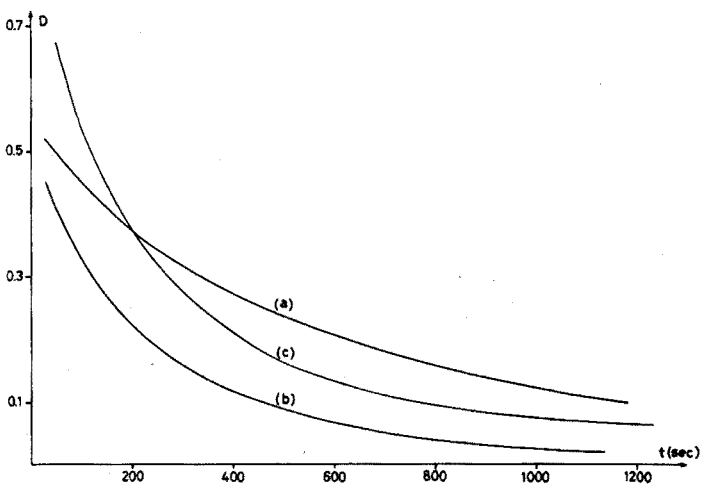

Fig. 1. Variation de la densité optique D (210 nm) en fonction du temps t. $l = 0.5$ cm; $T = 20°$. [DDVP]/[P] (M/M): (a) $1.4 \cdot 10^{-4}/5.2 \cdot 10^{-3}$; (b) $1.4 \cdot 10^{-4}/7.02 \cdot 10^{-3}$; (c) $2.5 \cdot 10^{-4}/1.17 \cdot 10^{-2}$.

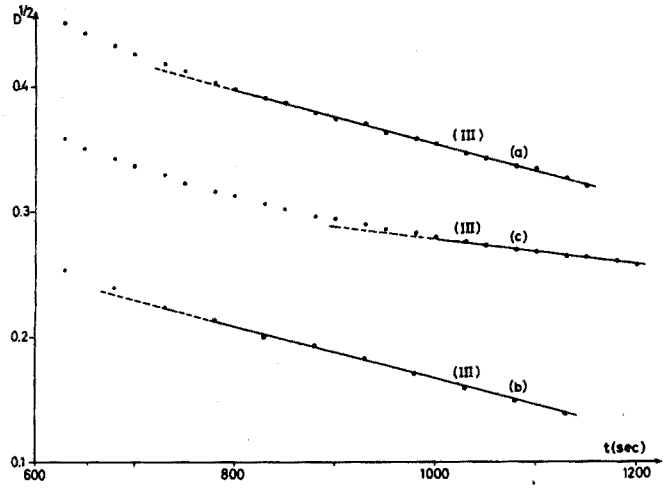

Fig. 2. $D^{\frac{1}{2}} = f(t)$. $l = 0.5$ cm; $T = 20°$. [DDVP]/[P] (M/M): (a) $1.4 \cdot 10^{-4}/5.2 \cdot 10^{-3}$; (b) $1.4 \cdot 10^{-4}/7.02 \cdot 10^{-3}$; (c) $2.5 \cdot 10^{-4}/1.17 \cdot 10^{-2}$. (III): $D^{\frac{1}{2}} = D^{\frac{1}{2}}_{U_2(0)} - k^{III}_{\frac{1}{2}} t$.

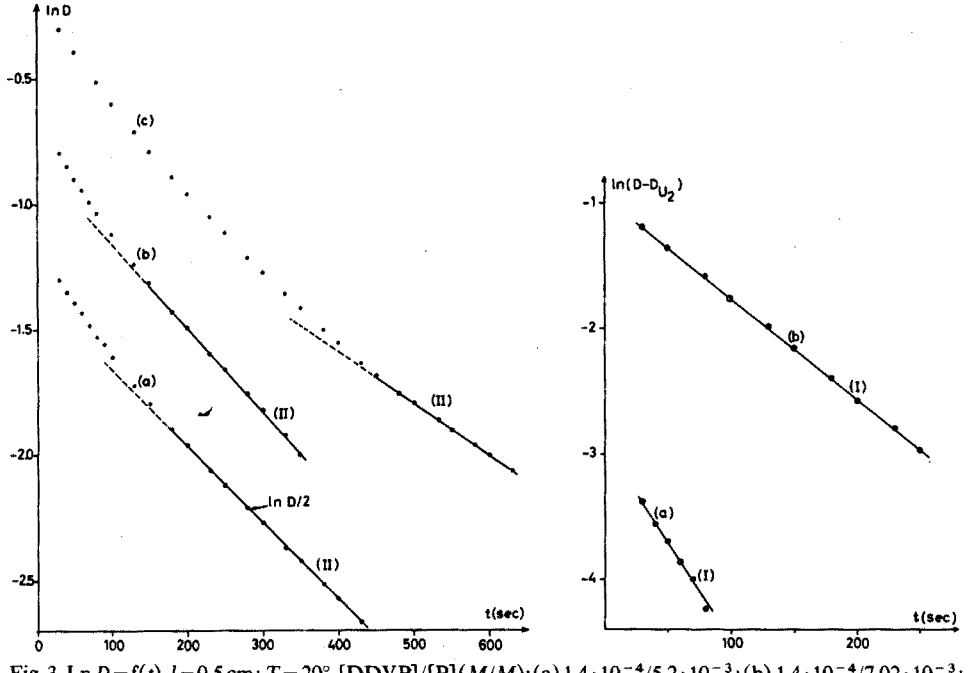

Fig. 3. Ln $D = f(t)$. $l = 0.5$ cm; $T = 20°$. [DDVP]/[P] (M/M): (a) $1.4 \cdot 10^{-4}/5.2 \cdot 10^{-3}$; (b) $1.4 \cdot 10^{-4}/7.02 \cdot 10^{-3}$; (c) $2.5 \cdot 10^{-4}/1.17 \cdot 10^{-2}$. (II): Ln $D = \ln D_{U_2} = \ln D_{U_2(0)} - k^{II}_1 t$.

Fig. 4. Ln $(D\text{-}D^{II}) = f(t)$. $l = 0.5$ cm; $T = 20°$. [DDVP]/[P] (M/M): (a) $1.4 \cdot 10^{-4}/5.2 \cdot 10^{-3}$; (b) $2.5 \cdot 10^{-4}/1.17 \cdot 10^{-2}$. (I): Ln $D_u = \text{Ln}(D\text{-}D_{U_2}) = \text{Ln } D_{U(0)} - k^{I}_1 t$.

On remarque que les lois cinétiques régissant la scission de l'ester se modifient avec le temps. Ainsi, l'ordre de l'évolution de la densité optique qui, à partir de 800 s environ, est de $\frac{1}{2}$ (Fig. 2), a une valeur supérieure pour des temps inférieurs. Pendant cette période ($t<600$ s), la cinétique est relativement complexe et l'analyse des données D, t montre qu'elle est composée de deux réactions du 1er ordre intervenant simultanément (Fig. 3 et 4) et dont la plus lente (Fig. 3) évolue vers l'ordre fractionnaire.

TABLEAU II

CARACTÉRISTIQUES DES RÉACTIONS ET VALEURS DE $k_{obs.}$

([DDVP] = $2.5\cdot10^{-4}$ M)

$[P]\times10^{3}$ [a]	$[P]/[DDVP]$	$k_1^{II}\times10^{3}$	r	$k_1^{I}\times10^{3}$	r	$k_{\frac{1}{2}}^{III}\times10^{5}$	r
		$n=1$; éq. (16)[b]		$n=1$; éq. (17)[b]		$n=\frac{1}{2}$; éq. (24)[b]	
5.2	20.8	1.01	0.9994	3.93	0.9993	5.13	0.9986
7.02	28.08	1.26	0.9994	5.21	0.9993	6.04	0.9974
10.4	41.6	1.86	0.9994	7.29	0.9999	8.9	0.9999
11.7	46.8	2.05	0.9995	8.11	0.9999	9.4	0.9999

[a] [P]: concentration de perborate.
[b] n: ordre de réaction; éq.: équation (numérotation).

Pour la série de solutions renfermant du DDVP à la concentration $1.4\cdot10^{-4}$ M, seule la cinétique pour $[P]=5.2\cdot10^{-3}$ M et en partie celle pour $[P]=7.02\cdot10^{-3}$ M, ont pu être analysées avec précision. Pour $[P]>7\cdot10^{-3}$ M, la décomposition trop rapide de la forme monomère (voir les schémas 4), la plus active, limite trop le nombre des données D, t (voir Fig. 4a) et l'évaluation de k_1^{I} n'est pas précise. De plus, dans ces conditions, les valeurs de D à la fin de l'évolution sont trop faibles et ne permettent pas la détermination de $k_{\frac{1}{2}}^{III}$.

Proposition de mécanismes

Nos résultats conduisent à proposer les schémas réactionnels suivants:

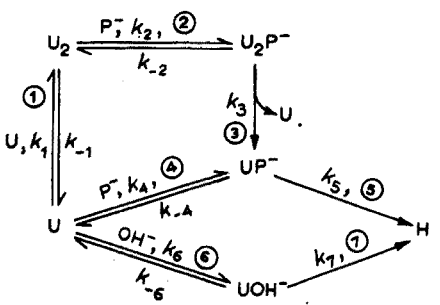

(4)

où U, U_2, H et P^-: sont respectivement monomère, dimère, produit de l'hydrolyse, du DDVP et ion perhydroxyle.

Ces schémas sont proposés avec l'hypothèse qui le trimère et le tétramère (voir partie I) n'y interviennent pas; il est supposé que le changement du milieu

isopropanolique par l'adjonction d'eau (voir conditions ci-dessus) déplace fortement les équilibres vers les formes simples du DDVP.

Conformément au schéma (4), nous avons pour expression de la vitesse V:

$$V = d[H]/dt = -d[U]/dt - d[U_2]/dt = k_5[UP^-] + k_7[UOH^-] \quad (5)$$

Dans l'hypothèse (du régime stationnaire):

$$d[UP^-]/dt = 0,\ d[UOH^-]/dt = 0,\ d[U_2P^-]/dt = 0 \quad (6)$$

$$[UP^-] = (k_4[U][P^-] + k_3[U_2P^-])(k_{-4} + k_5)^{-1} \quad (7)$$

$$[UOH^-] = k_6[U][OH^-](k_{-6} + k_7)^{-1} \quad (8)$$

$$[U_2P^-] = k_2[U_2][P^-](k_{-2} + k_3)^{-1} \quad (9)$$

et si,

$$k_{-4} \gg k_5,\ k_{-6} \gg k_7,\ k_{-2} \gg k_3 \quad (10)$$

$$-(d[U]/dt) - (d[U_2]/dt) = k_1^{I}[U] + k_1^{II}[U_2] \quad (11)$$

où

$$k_1^{I} = k_4 k_5 k_{-4}^{-1}[P^-] + k' \quad (12)$$

$$k' = k_6 k_7 k_{-6}^{-1}[OH^-] \quad (13)$$

$$k_1^{II} = k_3 k_5 k_2 (k_{-4} k_{-2})^{-1}[P^-] \quad (14)$$

Avec les intégrées:

$$[U] = [U]_0 e^{-k_1^{I} t} \text{ et } [U_2] = [U_2]_0 e^{-k_1^{II} t}$$

$$D_U = D_{U(0)} e^{-k_1^{I} t} \text{ et } D_{U_2} = D_{U_2(0)} e^{-k_1^{II} t}$$

$$\ln D = \ln(D_U + D_{U_2}) = \ln(D_{U(0)} e^{-k_1^{I} t} + D_{U_2(0)} e^{-k_1^{II} t}) \quad (15)$$

et en admettant que le monomère U est beaucoup plus actif que U_2, il vient, après un certain temps de réaction, que (voir tableau III, dernière colonne) $[U_2] \gg [U_1]$ et

$$\ln D = \ln D_{U_2(0)} - k_1^{II} t \quad (16)$$

expression dont les branches (II) de la Fig. 3 sont représentatives. La soustraction de D, des ordonnées D_{U_2} conduit d'autre part à:

$$\ln (D - D_{U_2}) = \ln D_U = \ln D_{U(0)} - k_1^{I} t \quad (17)$$

dont les représentations graphiques sont les droites (I) de la Fig. 4.

Remarquons que la validité de l'expression (16) ne saurait se maintenir que durant un certain temps seulement. En effet, lorsque $[U] \simeq 0$ et à cause de l'étape (3), l'approximation $d[U]/dt = 0$ est probablement satisfaite et

$$k_{-1}[U_2] + k_{-4}[UP^-] + k_{-6}[UOH^-]$$
$$= k_4[U][P^-] + k_3[U_2P^-] + k_1[U]^2 + k_6[U][OH^-] \quad (18)$$

On peut, de plus, admettre que dans ces conditions:

$$k_{-1}[U_2] \gg k_{-4}[UP^-],\ k_{-1}[U_2] \gg k_{-6}[UOH^-] \quad (19)$$

et, en outre:

$$k_4[U][P^-] \gg k_3[U_2P^-] \tag{20}$$

ce qui réduit la relation (18) en:

$$k_1[U]^2 + k_4[U][P^-] + k_6[U][OH^-] - k_{-1}[U_2] = 0 \tag{21}$$

D'après les relations (4), (7), (8), (10) et (20), nous avons:

$$d[H]/dt = k_5[UP^-] + k_7[UOH^-]$$
$$= (k_4 k_5 k_{-4}^{-1}[P^-] + k_6 k_7 k_{-6}^{-1}[OH^-])[U] = M[U]$$

et l'expression (21) s'écrit:

$$k_1 M^{-2}(d[H]/dt)^2 + NM^{-1}(d[H]/dt) - k_{-1}[U_2] = 0 \tag{22}$$

où

$$N = k_4[P^-] + k_6[OH^-]$$

d'où,

$$d[H]/dt = [-NM^{-1} + (N^2M^{-2} + 4k_1M^{-2} + 4k_1M^{-2}k_{-1}[U_2])^{\frac{1}{2}}](2k_1M^{-2})^{-1}$$
$$= -\tfrac{1}{2}NMk_1^{-1} + [(\tfrac{1}{2}NMk_1^{-1})^2 + k_{-1}k_1^{-1}M^2[U_2]]^{\frac{1}{2}} = -\underbrace{d[U]/dt}_{0} - d[U_2]/dt$$

Si $k_1 \gg NM$, nous avons:

$$-d[U_2]/dt = MK^{\frac{1}{2}}[U_2]^{\frac{1}{2}};\quad K = k_{-1}k_1^{-1} \tag{23}$$
$$-(\varepsilon_{U_2} l)^{-1}(dD_{U_2}/dt) = MK^{\frac{1}{2}}(\varepsilon_{U_2} l)^{-\frac{1}{2}} D_{U_2}^{\frac{1}{2}}$$
$$-dD_{U_2}/dt = M(K\varepsilon_{U_2} l)^{\frac{1}{2}} D_{U_2}^{\frac{1}{2}} = QD_{U_2}^{\frac{1}{2}}$$

et

$$D_{U_2}^{\frac{1}{2}} = D_{U_2(O)}^{\frac{1}{2}} - k_{\frac{1}{2}}^{III} t \tag{24}$$

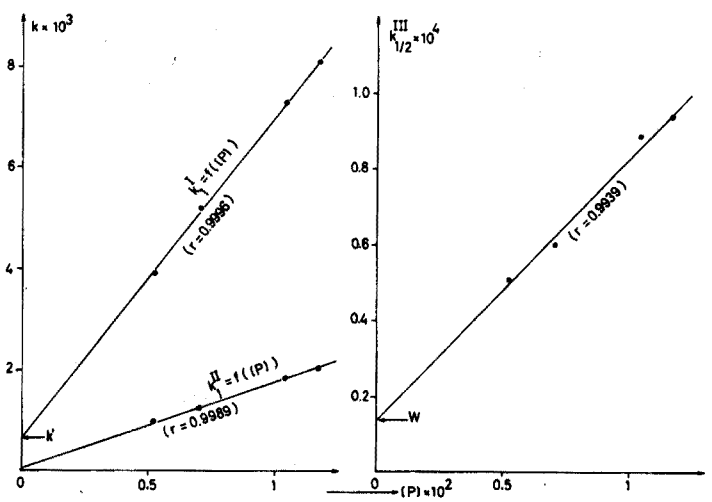

Fig. 5. Variation de k_1', k_1'', $k_{\frac{1}{2}}^{III}$ en fonction de [P], la concentration de perborate; [DDVP] = $2.5 \cdot 10^{-4}$ *M*.

où

$$k_{\frac{1}{2}}^{III} = \tfrac{1}{2}Q = \underbrace{\tfrac{1}{2}k_4 k_5 k_{-4}^{-1}(K\varepsilon_{U_2} l)^{\frac{1}{2}}}_{Z}[P^-] + \underbrace{\tfrac{1}{2}k_6 k_7 k_{-6}^{-1}(K\varepsilon_{U_2} l)^{\frac{1}{2}}}_{W}[OH^-] \qquad (25)$$

les représentations graphiques de l'expression (24) étant les branches (III) de la Fig. 2.

Dans la Fig. 5, nous représentons la variation de diverses constantes k en fonction de la concentration de perborate; on remarque que les expressions (12), (14) et (25) sont bien vérifiées.

TABLEAU III

VALEURS CALCULÉES DE $D_{U(0)}e^{-k_1^I t}$ ET $D_{U_2(0)}e^{-k_1^{II} t}$ POUR QUELQUES TEMPS t DE L'ÉVOLUTION $D = f(t)$

$[P] \times 10^3$ (mol l^{-1})	t (s)	D observée	$D_{U(0)}e^{-k_1^I t} + D_{U_2(0)}e^{-k_1^{II} t}$ calculée
5.2	300	0.568	$8.86 \cdot 10^{-2} + 4.76 \cdot 10^{-1}$
	660	0.351	$2.15 \cdot 10^{-2} + 3.27 \cdot 10^{-1}$
7.02	270	0.505	$1.41 \cdot 10^{-1} + 3.43 \cdot 10^{-1}$
	630	0.260	$2.16 \cdot 10^{-2} + 2.18 \cdot 10^{-1}$
10.4	50	0.726	$2.62 \cdot 10^{-1} + 4.64 \cdot 10^{-1}$
	300	0.329	$4.24 \cdot 10^{-2} + 2.91 \cdot 10^{-1}$
11.7	30	0.737	$3.04 \cdot 10^{-1} + 4.34 \cdot 10^{-1}$
	200	0.382	$7.64 \cdot 10^{-2} + 3.06 \cdot 10^{-1}$
	Intervalle de validité de l'expression (16)		
5.2	900	0.263	$8.38 \cdot 10^{-3} + 2.59 \cdot 10^{-1}$
	1740	0.112	$3.09 \cdot 10^{-4} + 1.11 \cdot 10^{-1}$
7.02	1110	0.121	$1.77 \cdot 10^{-3} + 1.19 \cdot 10^{-1}$
	1590	0,065	$1.45 \cdot 10^{-4} + 6.50 \cdot 10^{-2}$
10.4	500	0.203	$9.86 \cdot 10^{-3} + 2.01 \cdot 10^{-1}$
	700	0.139	$2.29 \cdot 10^{-4} + 1.38 \cdot 10^{-1}$
11.7	480	0.178	$7.89 \cdot 10^{-3} + 1.72 \cdot 10^{-1}$
	600	0.135	$2.98 \cdot 10^{-3} + 1.35 \cdot 10^{-1}$

TABLEAU IV

CONSTANTES DE VITESSE, $k_{1(A)}^{II}$, $k_{1(A)}^{I}$ ET $k_{\frac{1}{2}(A)}^{III}$ POUR DIFFÉRENTES CONCENTRATIONS D'ACÉTONE

([DDVP] = $2.5 \cdot 10^{-4}$ mol l^{-1}; [P] = $1.04 \cdot 10^{-2}$ mol l^{-1})

[Acetone] (mol l^{-1})	$k_{1(A)}^{II}$	r	$k_{1(A)}^{I}$	r	$k_{\frac{1}{2}(A)}^{III}$	r
$1.25 \cdot 10^{-4}$	$1.46 \cdot 10^{-3}$	0.9983	$5.70 \cdot 10^{-3}$	0.9998	$1.06 \cdot 10^{-4}$	0.999
$2.5 \cdot 10^{-4}$	$1.34 \cdot 10^{-3}$	0.9985	$6.3 \cdot 10^{-3}$	0.9999	$1.12 \cdot 10^{-4}$	0.9973
$5.0 \cdot 10^{-4}$	$1.36 \cdot 10^{-3}$	0.9989	$5.7 \cdot 10^{-3}$	0.9999	$9.35 \cdot 10^{-5}$	0.999
$6.25 \cdot 10^{-4}$	$1.31 \cdot 10^{-3}$	0.9969	$5.92 \cdot 10^{-3}$	0.9998	$1.05 \cdot 10^{-4}$	0.9949
$1.0 \cdot 10^{-3}$	$1.68 \cdot 10^{-3}$	0.9995	$7.32 \cdot 10^{-3}$	0.9999	$8.58 \cdot 10^{-5}$	0.9959
$1.25 \cdot 10^{-3}$	$2.51 \cdot 10^{-3}$	0.9997	$8.20 \cdot 10^{-3}$	0.9991	$1.39 \cdot 10^{-4}$	0.9986
$2.0 \cdot 10^{-3}$	$2.50 \cdot 10^{-3}$	0.9984	$8.45 \cdot 10^{-3}$	0.9997	—	—
$2.5 \cdot 10^{-3}$	$3.32 \cdot 10^{-3}$	0.9997	$1.09 \cdot 10^{-2}$	0.9996	$1.14 \cdot 10^{-4}$	0.9974

Influence de l'acétone

Les lois cinétiques régissant la scission du DDVP ne sont pas modifiées par la présence d'acétone. Par contre, son rôle catalytique est mis en évidence et traduit par les modifications observées aux valeurs des constantes k_1^{II}, k_1^{I} et k_2^{III} (voir tableau IV). On note, en effet, qu'avec une augmentation de la concentration en acétone, leurs valeurs diminuent, puis elles croissent (Fig. 6).

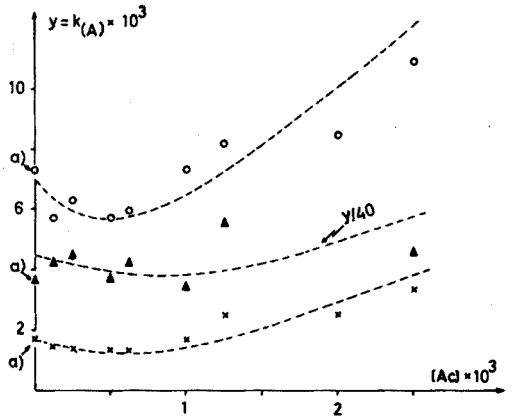

Fig. 6. Variation of $k_{1(A)}^{I}$ (O), $k_{2(A)}^{III}$ (▲), et $k_{1(A)}^{II}$ (X), en fonction de la concentration en acétone. (a): Valeurs calculées a l'aide des expressions (12), (14) et (25) (Voir Fig. 5).

Théoriquement, on peut considérer l'intervention de l'acétone soit:
(i) à l'étape 5 du processus (4)

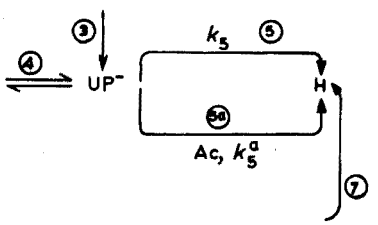

(26)

où Ac = acétone

(ii) avant l'action de P^- et OH^-

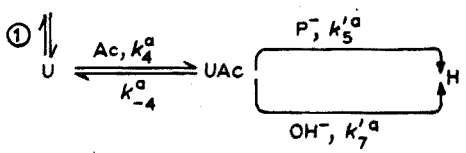

(27)

ou bien, envisager la possibilité d'une association:

$$Ac + P^- \rightleftharpoons AcP^-;\ \beta_{AcP} = [AcP^-]([Ac][P^-])^{-1} \qquad (28)$$

susceptible soit:

(iii) d'intervenir à l'étape 4

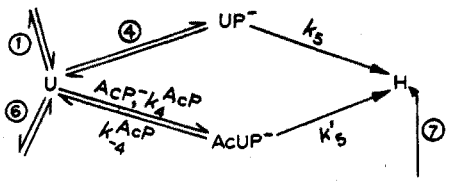

(29)

(iv) d'affecter le processus (27) ou

(v) d'influer sur le mécanisme (26).

Cette dernière supposition (v) et (26) avec l'étape 5a concurrencée par la réaction (28), semblent les plus probables, car ils rendent mieux compte des résultats obtenus et notamment de la particularité de variation des constantes $k^{II}_{1(A)}$, $k^{I}_{1(A)}$ et $k^{III}_{\frac{1}{2}(A)}$ avec la concentration de l'acétone.

En effet, d'après processus (26):

$$V_a = d[H]/dt = -(d[U]/dt) - (d[U_2]/dt) = (k_5 + k^a_5[Ac])[UP^-] + k_7[UOH^-] \tag{30}$$

d'où, par les expressions (6), (7), (8), (9) et (10) et avec:

$$[UP^-] = (k_4[U][P^-] + k_3[U_2P^-])(k_{-4} + k^a_5[Ac])^{-1} \tag{31}$$

$$V_a = \underbrace{[k_6k_7k_{-6}^{-1}[OH^-] + (k_4k_5[P^-] + k_4k^a_5[Ac][P^-])(k_{-4} + k^a_5[Ac])^{-1}]}_{k^{I}_{1(A)}}[U]$$
$$+ \underbrace{[(k_3k_5k_2[P^-] + k_3k_2k^a_5[Ac][P^-])(k_{-4}k_{-2} + k_{-2}k^a_5[Ac])^{-1}]}_{k^{II}_{1(A)}}[U_2] \tag{32}$$

Par ailleurs, dans les conditions aboutissant à l'expression (18) et avec les relations (19), (20), (30) et (31), l'équation (22) prend la forme:

$$k_1M'^{-2}(d[H]/dt)^2 + NM'^{-1}(d[H]/dt) - k_{-1}[U_2] = 0 \tag{33}$$

où

$$M' = [(k_5 + k^a_5[Ac])k_4[P^-](k_{-4} + k^a_5[Ac])^{-1} + k_6k_7k_{-6}^{-1}[OH^-]$$

et l'expression de la constante $k^{III}_{\frac{1}{2}}$ (voir l'équation 25) devient:

$$k^{III}_{\frac{1}{2}(A)} = \tfrac{1}{2}(k_4k_5[P^-] + k_4k^a_5[Ac][P^-])(k_{-4} + k^a_5[Ac])^{-1}(K\varepsilon_{U_2}l)^{\frac{1}{2}} +$$
$$\tfrac{1}{2}\, k_6k_7k_{-6}^{-1}(K\varepsilon_{U_2}l)^{\frac{1}{2}}[OH^-] \tag{34}$$

Remarquons que, sans les hypothèses (28) et (v), les fonctions $k^{I}_{1(A)}$, $k^{II}_{1(A)}$ et $k^{III}_{\frac{1}{2}(A)}$ (voir les expressions 32 et 34) ne se vérifient pas; elles devaient, en effet, suivant les valeurs respectives de termes constants dans leurs expressions, soit croître, soit décroître, ou bien, dans l'hypothèse que le terme cinétique catalytique $k^a_5[Ac]$ est négligeable devant k_{-4}, augmenter linéairement avec [Ac].

Par contre, avec le processus (28) et (v), les expressions pour les constantes $k_{(A)}$ peuvent être prises sous les formes:

$$k^{I}_{1(A)} = k' + (k_4k_5[P^-] + k_4k^a_5\beta^{-1}_{AcP}\gamma[Ac]_t)(k_{-4} + k^a_5(1-\gamma)[Ac]_t)^{-1} \tag{35}$$

$$k^{II}_{1(A)} = (k_3k_5k_2[P^-]$$
$$+ k_3k_2k^a_5\beta^{-1}_{AcP}\gamma[Ac]_t)(k_{-4}k_{-2} + k_{-2}k^a_5(1-\gamma)[Ac]_t)^{-1} \tag{36}$$

$$k^{III}_{\frac{1}{2}(A)} = \tfrac{1}{2}[(k_4k_5[P^-]$$
$$+ k_4k^a_5\beta^{-1}_{AcP}\gamma[Ac]_t)(k_{-4} + k^a_5(1-\gamma)[Ac]_t)^{-1} + k'](K\varepsilon_{U_2}l)^{\frac{1}{2}} \tag{37}$$

(où $[Ac]_t$ = concentration totale de Ac et γ = fraction de $[Ac]_t$ combinée à AcP^-) lesquelles rendent bien compte de l'allure des courbes de la Fig. 6.

En effet, si l'association AcP^- est peu stable, γ reste petit pour de faibles concentrations d'acétone et les $k_{1(A)}$ diminuent. Pour des concentrations $[Ac]_t$ élevées, γ augmente et à partir d'une certaine valeur de celui-ci, les fonctions $k_{1(A)}$ croissent, les coordonnées de leur minimum dépendant des valeurs de constantes figurant aux numérateur et dénominatuer des expressions (35), (36) et (37).

D'autre part, d'après les expressions (35), (36) et (37):

$$\lim_{[Ac]_t \to 0} k^{I}_{1(A)} = k' + k_4 k_5 k_{-4}^{-1}[P^-]; \quad \lim_{[Ac]_t \to 0} k^{II}_{1(A)} = k^{II}_1 [P]^-;$$

$$\lim_{[Ac]_t \to 0} k^{III}_{\frac{1}{2}(A)} = Z[P^-] + W \qquad \text{(voir expression (25))}$$

et la Fig. 6 montrent que ces conditions limites sont assez bien vérifiées. D'autres considérations résultant d'une analyse de schémas réactionnels (27) et (29), montrent que les hypothèses (ii) et (iii), ne sont pas vérifiées ce qui, en conclusion, nous amène à proposer le mécanisme suivant:

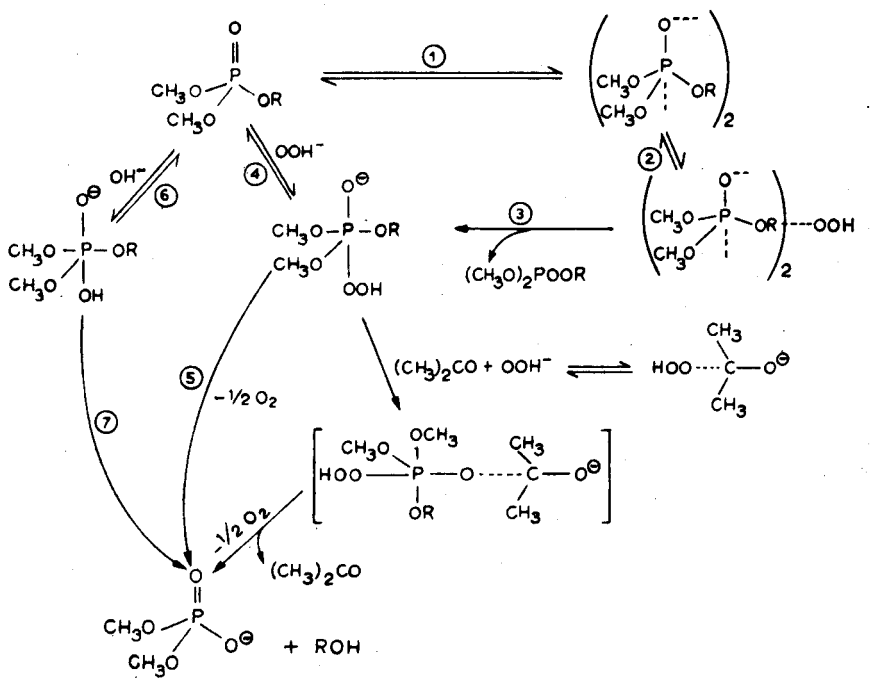

RÉSUMÉ

La scission perhydrolytique du diméthyle-O,O-dichlorovinyle phosphate (DDVP) est étudiée dans isopropanol–eau (32+68) et trouvée régie par deux réactions simultanées du premier ordre se dégénérant avec le temps en ordre fractionnaire. Il peut être montré que ces cinétiques complexes sont dûes à la

présence de la forme dimère du DDVP. L'influence de l'acétane sur ces réactions est recherchée et les résultats sont en accord avec l'hypothèse de formation d'un complexe entre l'acétone et l'ion perhydroxyle. Des mécanismes de réaction sont proposés.

SUMMARY

The scission of O,O-dimethyl-2,2-dichlorovinyl phosphate (DDVP) by perhydroxy ions in isopropanol–water (32+68) was found to be expressed by two initially simultaneous first-order reactions which degenerate with time to fractional order. It can be shown that these complex kinetics are due to the presence mainly of the dimer form of DDVP. The influence of acetone on these reactions was investigated and results are in agreement with the assumption of complex formation between acetone and the perhydroxy ion. Reaction mechanisms are proposed.

ZUSAMMENFASSUNG

Die Spaltung von O,O-Dimethyl-2,2-dichlorvinyl-phosphat (DDVP) durch Perhydroxy-Ionen in Isopropanol-Wasser (32+68) verläuft anfänglich nach zwei simultanen Reaktionen erster Ordnung, welche mit der Zeit in eine gebrochene Ordnung übergehen. Es kann gezeigt werden, dass diese komplexe Kinetik auf die Gegenwart hauptsächlich der dimeren Form von DDVP zurückzuführen ist. Der Einfluss von Aceton auf diese Reaktionen wurde untersucht; die Ergebnisse stimmen mit der Annahme einer Komplexbildung zwischen Aceton und den Perhydroxy-Ionen überein. Reaktionsmechanismen werden vorgeschlagen.

BIBLIOGRAPHIE

1 M. Schuler, *Chimia*, 21 (1967) 342.
2 J. Epstein, M. M. Demek et D. H. Rosenblatt, *J. Org. Chem.*, 21 (1956) 796.
3 D. N. Kramer et R. M. Gamson, *Anal. Chem.*, 29 (1957) 21A.
4 G. G. Guilbault et G. J. Lubrano, *Anal. Chim. Acta*, 43 (1968) 253.
5 B. Gehauf et J. Goldenson, *Anal. Chem.*, 29 (1957) 276.
6 B. Gehauf, J. Epstein, G. B. Wilson, B. Witten, S. Sass, V. E. Bauer et W. H. C. Rueggeberg, *Anal. Chem.*, 29 (1957) 278.
7 D. N. Kramer dans E. Crabtree et E. Poziomek, *Chemistry of Schoenemann Reaction* (a review), Edgewood Arsenal Special Publication, 1966, p. 18.

Analytica Chimica Acta, 68 (1974) 289–295
© Elsevier Scientific Publishing Company, Amsterdam – Printed in The Netherlands

ÉTUDE DU MÉCANISME DE L'OXYDATION PERBORIQUE DE L'INDOLE EN PRÉSENCE DE TRACES DE DIMÉTHYLE-O,O-DICHLOROVINYLE PHOSPHATE (DDVP)*

PARTIE III. CINÉTIQUE DE LA RÉACTION FLUOROGÉNIQUE ET LE RÔLE DE L'ACÉTONE

L. GENOUD et M. MARCANTONATOS

Département de Chimie Minérale et de Chimie Analytique de l'Université de Genève (Suisse)

(Reçu le 7 septembre 1973)

Dans les parties I et II de ce travail[1], nous avons étudié l'auto-association du diméthyle-O,O-dichlorovinyle-2,2-phosphate (DDVP), la cinétique de sa scission hydro- et perhydrolytique, et l'influence de l'acétone sur leurs vitesses.

Le but de la présente partie est la recherche du mécanisme de la réaction fluorogénique de l'oxydation de l'indole par le perborate, en présence de traces de DDVP et d'acétone.

Il est admis[2–4] que cette réaction a lieu de la façon suivante:

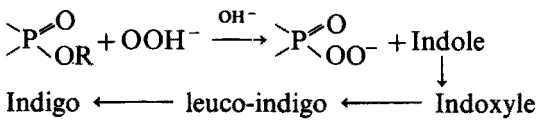

(1)

mais le rôle que joue l'acétone dans celle-ci ou dans sa variante chromogénique (réaction de Schönemann) n'est, à notre connaissance, pas encore entièrement élucidé.

PARTIE EXPÉRIMENTALE

Reactifs et appareillage

Diméthyle-O,O-dichlorovinyle phosphate (DDVP), Ciba-Geigy; isopropanol puriss. et indole puriss., Fluka A.G.; acétone *pro analysi*, Merck; perborate de sodium, Fischer Scientific (certified); eau tridistillée. Spectrofluorimètre Zeiss ZFM4C; cuves de quartz $l = 1$ cm.

Déterminations fluorimétriques

Les intensités d'émission F à 480 nm (maximum de la bande de fluorescence) (exc.: 365 nm), d'une série de solutions (isopropanol–eau, 32+68) renfermant du DDVP, du perborate, de l'acétone et de l'indole aux concentrations respectivement de $1.375 \cdot 10^{-6}$ M, $1.3 \cdot 10^{-2}$ M, variable et $3.41 \cdot 10^{-4}$ M, ont été enregistrées en

* Cette publication est dediée au Professeur D. Monnier, à l'occasion de son 70ème anniversaire.

fonction du temps (temp.=25°). F atteint rapidement une valeur maximale, puis décroît par suite de la transformation du leuco-indigo en indigo non fluorescent (voir le processus 1 et Fig. 1). Les valeurs maximales de la fluoresence (F_{max}) corrigées par rapport aux blancs correspondants (négligeables dans nos conditions de mesure), sont représentées en fonction de la concentration de l'acétone dans la Fig. 3A.

PROPOSITION DE MÉCANISMES

Dans leur étude de mise au point de methodes de dosage de traces de certains nervins (R(R'O)(PO)F) par la réaction de Schönemann, Gehauf *et al.*[2,3] constatent que la sensibilité de la réaction indicatrice augmente d'une façon marquée en présence de faibles quantités d'acétone; ce même effet se produit dans la réaction fluorescente (1).

Pour expliquer le rôle de l'acétone, Kramer[5] suppose la formation d'un complexe entre cette dernière et l'ion perhydroxyle, capable de réagir avec l'ester phosphorique plus rapidement que l'ion perhydroxyle. Des résultats, cependant, obtenus dernièrement par les présents auteurs[1], montrent que, si l'hypothèse de formation d'un complexe "acétone–perhydroxyle" se trouve en effet vérifiée, l'association "acétone–perhydroxyle" ne saurait toutefois réagir directement avec l'ester.

Par ailleurs, une réaction directe entre le complexe en question et l'ester devait, avec un accroissement de la concentration en acétone, se traduire par une augmentation de l'intensité de la coloration ou de la fluorescence. Or, nos déterminations d'émission lumineuse montrent qu'avec une augmentation de la concentration en acétone, l'intensité de fluorescence croît puis décroît (Fig. 1).

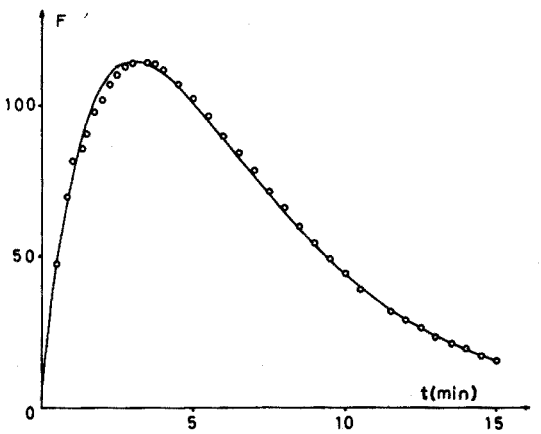

Fig. 1. Variation de l'intensité de fluorescence F en fonction du temps: (○), valeurs expérimentales; (–), courbe calculée par l'équation (19).

Ce mode de variation de l'intensité de fluorescence maximale en fonction de la concentration totale de l'acétone $[Ac]_t$, ne pourrait se traduire que si l'on considère comme étape initiale dans la transformation en indigo de l'indole, l'oxydation de ce dernier, non seulement par le le perphosphonate, mais également par l'intermédiaire actif $AcUP^-$ (Voir schéma 2).

En effet, d'après les mécanismes (2) et (2')[1] que nous proposons, et où l'on

ne tient pas compte du dimère de DDVP ([DDVP] = $1.375 \cdot 10^{-6}$ M; voir aussi partie I):

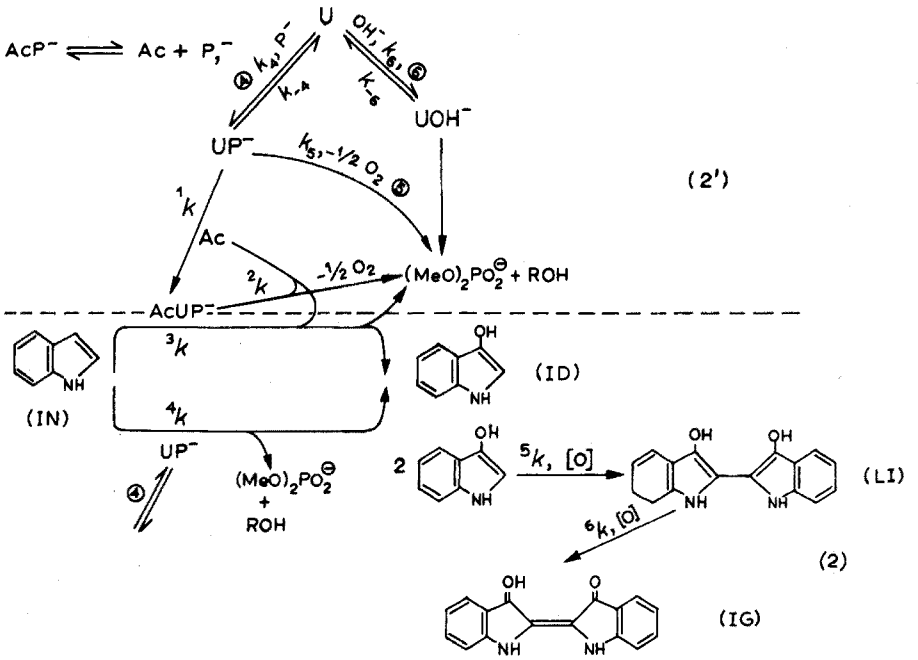

où U = DDVP

$P^- = OOH^-$

$AcP^- =$ 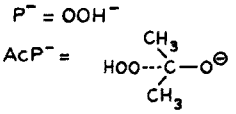

$UOH^- =$ 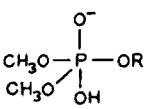

$UP^- =$ 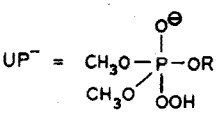

$AcUP^- =$ 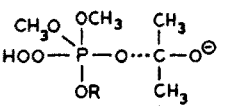

les vitesses de formation de l'indigo(IG), du leuco-indigo (LI), de l'indoxyle (ID), de l'intermédiaire ($AcUP^-$) et du perphosphonate (UP^-), sont données (en admettant que l'étape LI→IG fait intervenir l'oxygène dissous) par:

$$d[IG]/dt = {}^6k[LI][O] = {}^6k'[LI] \tag{3}$$

$$d[LI]/dt = \tfrac{1}{2}{}^5k[ID]^2[O] - {}^6k[LI][O] = \tfrac{1}{2}{}^5k'[ID]^2 - {}^6k'[LI] \tag{4}$$

$$d[ID]/dt = {}^4k[IN][UP^-] + {}^3k[IN][AcUP^-] - \tfrac{1}{2}{}^5k'[ID]^2 \tag{5}$$

$$d[AcUP^-]/dt = {}^1k[UP^-][Ac] - ({}^2k[AcUP^-] + {}^3k[IN][AcUP^-]) \tag{6}$$

$$d[UP^-]/dt = k_4[U][P^-] - (k_{-4}[UP^-] + k_5[UP^-] + {}^1k[UP^-][Ac]) \tag{7}$$

En outre, avec l'hypothèse

$$d[AcUP^-]/dt = 0; \quad d[UP^-]/dt = 0 \tag{8}$$

$$d[ID]/dt = 0 \tag{9}$$

$$[AcUP^-] = {}^1k[UP^-][Ac]({}^2k + {}^3k[IN])^{-1} \tag{10}$$

$$[UP^-] = k_4[U][P^-](k_4 + k_5 + {}^1k[Ac])^{-1} \tag{11}$$

$$[ID] = [2({}^4k[IN][UP^-] + {}^3k[IN][AcUP^-])^5k^{-1}]^{\frac{1}{5}}$$
$$= [2({}^4k[IN][UP^-] + [{}^3k\,{}^1k[IN][UP^-][Ac]]({}^2k + {}^3k[IN])^{-1})^5k^{-1}]^{\frac{1}{5}}$$

et comme $[IN] \gg [U]$:

$$[ID] = [2({}^4k'[UP^-] + [{}^3k'k_1[UP][Ac]({}^2k + {}^3k')^{-1}]^5k^{-1}]^{\frac{1}{5}} \tag{12}$$

où

$${}^4k' = {}^4k[IN];\ {}^3k' = {}^3k[IN] \tag{13}$$

et l'expression (4) pour la vitesse de formation du leuco-indigo (LI) devient:

$$d[LI]/dt = {}^4k'[UP^-] + ({}^1k\,{}^3k'[UP^-][Ac])({}^2k + {}^3k')^{-1} - {}^6k'[LI]$$
$$= {}^4k'[UP^-] + k^*[UP^-][Ac] - {}^6k'[LI] \tag{14}$$

où $k^* = {}^1k\,{}^3k'({}^2k + {}^3k')^{-1}$ (15)

La forme de $F = f(t)$

D'après la schéma (2'), on déduit:

$$-d[U]/dt = k_6[OH^-] - k_{-6}[UOH^-] + k_4[U][P^-] - k_{-4}[UP^-]$$

et si, outre les conditions (8), $d[UOH^-]/dt = 0$ est satisfaite, l'expression pour la vitesse de réaction de U devient (voir aussi partie II):

$$-[dU]/dt = [k_6k_7k_{-6}^{-1}[OH^-] + (k_4k_5[P^-] + k_4\,{}^1k[Ac][P^-])(k_{-4} + {}^1k[Ac])^{-1}]U =$$
$$= k_A[U] \tag{16}$$

($[Ac]$ et $[P^-] \simeq$ constantes).

D'autre part, d'après l'expression (11):

$$[UP^-] = {}^1k_a^*[U]$$

et d'après l'expression (14):

$$d[LI]/dt = k^{**}[U] - {}^6k'[LI] \tag{17}$$

où $k^{**} = {}^4k' \cdot {}^1k_a^*$,

et les relations (16), (17) et (3) donnent:

$$[LI] = k^{**}[U]_0({}^6k' - k_A)^{-1}(e^{-k_At} - e^{-{}^6k't}) \tag{18}$$

où $[U]_0$ = concentration initiale de U.

De plus, au maximum de $F = f(t)$:

$$\varphi_{LI}^{-1}(dF/dt) = k^{**}[U]_{max} - \varphi_{LI}^{-1}\,{}^6k'F_{max} = 0$$

où $F = \varphi_{LI}[LI]$; φ_{LI} = rendement quantique apparent de LI, et l'expression (18) prend la forme:

$$F = [U]_0\left[\frac{[U]_{max}}{F_{max}}\left(1 - \frac{k_A}{{}^6k'}\right)\right]^{-1}(e^{-k_At} - e^{-{}^6k't}) \tag{19}$$

L'analyse des données ln F et t vers la fin de la cinétique $F = f(t)$ permet

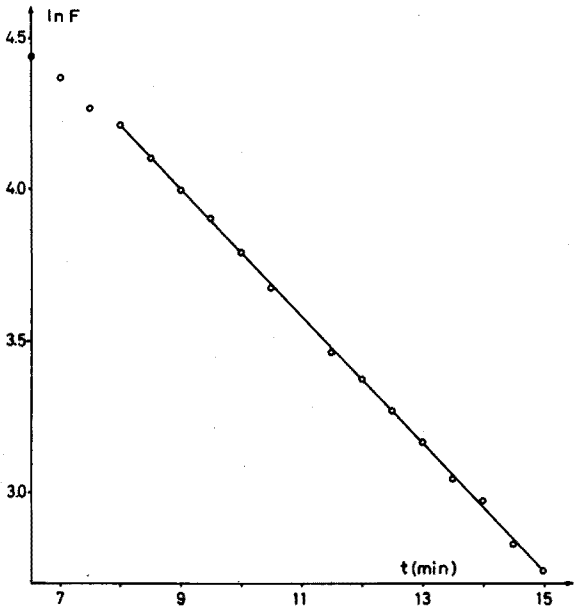

Fig. 2. ln F en fonction du temps.

d'obtenir (voir Fig. 2) la valeur approximative ${}^{6}k' \simeq 0.21$ min^{-1}; k_A et $[U]_{max}$ sont ensuite obtenus par ittération.

La Figure 1 montre que la courbe calculée à l'aide de l'équation (19) et avec ${}^{6}k' = 0.225$, $k_A = 0.44$, $[U]_0 = 1.375 \cdot 10^{-6}$ M, $F_{max} = 114.2$, $[U]_{max} = 3.451 \cdot 10^{-7}$ M, est en bon accord avec les résultats expérimentaux.

La forme probable de $F_{max} = f([Ac]_t)$

Les valeurs maximales de l'intensité de fluorescence (F_{max}), exprimées en fonction de la concentration totale de l'acétone dans la Fig. 3A, correspondent à la condition

$$(\partial F/\partial t)_{[U]_0,[P]_0,[IN]_0,[Ac]_t} = 0$$

où $[U]_0$, $[IN]_0$, $[P]_0$ sont les concentrations initiales de DDVP, indole et perborate: et (voir l'expression (14)):

$$dF_{LI}/dt = \varphi_{LI}({}^{4}k'[UP^-] + k^*[UP^-][Ac] - \varphi_{LI}^{-1}{}^{6}k' F_{LI}) = 0 \quad (20)$$

et

$$F_{max} = {}^{4}K[UP^-] + K^*[UP^-][Ac] \quad (21)$$

D'autre part, en admettant la formation d'un complexe "acétone–perhydroxyle" AcP^- (voir schéma (2')), la concentration combinée de P^- soit $[P^-]_c$, au tempts t_m du maximum de la courbe cinétique $F = f(t)$, est donnée par:

$$[P^-]_c = [UP^-] + [AcP^-] + [AcUP^-] \simeq [UP^-] + [AcP^-] \quad (22)$$

et

$$F_{max} \simeq {}^{4}K([P^-]_c - \gamma[Ac]_t) + K^*([P^-]_c - \gamma[Ac]_t)(1-\gamma)[Ac]_t \quad (23)$$

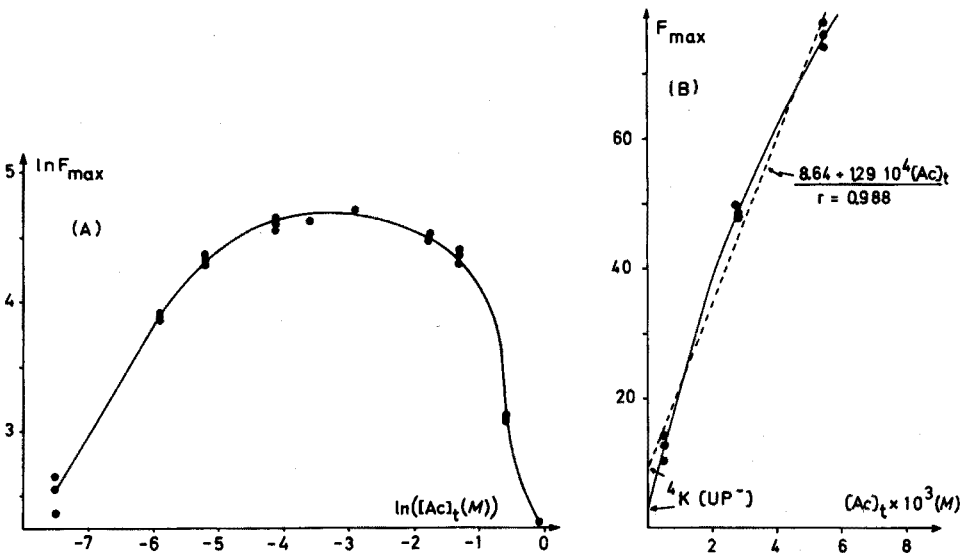

Fig. 3. (A) Variation de l'intensité maximale de la fluorescence (F_{max}) avec la concentration totale de l'acétone $[Ac]_t$; $[U]_0 = 1.375 \cdot 10^{-6}$ M, $[IN]_0 = 3.41 \cdot 10^{-4}$ M, $[P]_0 = 1.3 \cdot 10^{-2}$ M, $[Ac]_t$: $5.45 \cdot 10^{-4}$ à 1.09 M; $T = 25°$; $l = 1$ cm. (B) Détermination approximative de ${}^4K[UP^-]$ et $K^*[UP^-]$.

où γ = fraction de $[Ac]_t$ combinée à AcP^-.

Ainsi, lorsque:

(i) $[Ac]_t \to 0$; $\gamma \to 0$; $[P^-]_c \to [UP^-]$,

$$F_{max} \approx {}^4K[UP^-] + {}^*K[UP^-][Ac]_t \qquad (24)$$

(ii) $[Ac]_t \gg [P]_0$,

$$[P^-]_c \to [AcP^-] = \gamma[Ac]_t,\ F_{max} \to 0$$

Notons que la relation approximative (24) est en assez bon accord avec les données expérimentales (Fig. 3B). De plus, la comparaison des ordonnées à l'origine (Fig. 3B) avec les pentes fournit ${}^*K \approx 4 \cdot 10^3 \cdot {}^4K$ où (voir l'équations (20), (15), et (13)):

$${}^3k\,{}^4k^{-1} \approx 4 \cdot 10^3 ({}^2k + {}^3k')\,{}^1k^{-1}$$

indiquant ainsi, du fait que certainement $({}^2k + {}^3k')\,{}^1k^{-1} \gg 10^{-3}$ ($AcUP^-$, fugace), une oxydation de l'indole par l'intermédiaire "acétone–perphosphonate" beaucoup plus active que par UP^-.

Enfin, $[Ac]_t/[P]_t = 1.09/1.3 \cdot 10^{-2}$ (Fig. 3A; point: $\ln[Ac]_t = -0.0862$) n'est pas suffisant pour annuler F_{max} ($F_{max} = 10$), ce qui est en accord avec l'hypothèse déjà avancée dans la partie II de ce travail, à savoir que le complexe "acétone–OOH^-" serait peu stable.

RÉSUMÉ

Une étude est effectuée sur le rôle des traces de diméthyle-O,O-dichlorovinyle

phosphate (DDVP) et l'action de l'acétone dans la réaction fluorogénique de l'oxydation de l'indole par l'ion perborate. A partir des cinétiques $F=f(t)$ et des données F_{max}, $[Ac]_t$ où F est l'intensité de la fluorescence, F_{max} sa valeur maximale et $[Ac]_t$ la concentration totale d'acétone et à partir de résultats antérieurs[1], des relations sont dérivées permettant: (a) d'obtenir une expression mathématique pour $F=f(t)$ en accord avec les résultats expérimentaux; (b) de proposer une interprétation de la variation de F_{max} en fonction de $[Ac]_t$; (c) d'apporter des preuves en faveur d'une oxydation plus énergique de l'indole par l'intermédiaire "acétone–perphosphonate" que par le perphosphonate seul; et (d) d'avoir des preuves cinétiques supplémentaires en faveur de la formation d'un complexe "acétone–ion perhydroxyle"[1,2].

SUMMARY

The action of traces of O,O-dimethyl-2,2-dichlorovinyl phosphate (DDVP) and the function of acetone in the fluorogenic reaction of the oxidation of indole by perborate, were investigated. From data on kinetics and fluorescence intensity, and from previous results, it is shown that: (a) a mathematical form can be derived for the variation of fluorescence with time, consistent with the experimental data; (b) the variation of maximal fluorescence as a function of the acetone concentration can be interpreted. Evidence is presented that an intermediate "acetone–perphosphonate" complex is a much more active oxidant for indole than perphosphonate alone; additional kinetic evidence supports the formation of an "acetone–perhydroxy ion" complex.

ZUSAMMENFASSUNG

Die Wirkung von Spuren von O,O-Dimethyl-2,2-dichlorvinyl-phosphat (DDVP) und die Funktion von Aceton bei der fluoreszenzerzeugenden Reaktion der Oxidation von Indol durch Perborat wurden untersucht. Mit den Daten der Kinetik und der Fluoreszenzintensität sowie mit früheren Ergebnissen wird gezeigt, dass (a) ein mathematischer Ausdruck für die Variation der Fluoreszenz mit der Zeit abgeleitet werden kann, der mit den experimentellen Ergebnissen übereinstimmt, (b) die Variation der maximalen Fluoreszenz als eine Funktion der Acetonkonzentration vollständig interpretiert werden kann. Es wird belegt, dass ein intermediärer "Aceton–Perphosphonat"-Komplex ein viel wirksameres Oxidationsmittel für Indol ist als Perphosphonat allein; zusätzliche kinetische Ergebnisse weisen auf die Bildung eines "Aceton–Perhydroxyion"-Komplexes hin.

BIBLIOGRAPHIE

1 M. Marcantonatos et L. Genoud, *Anal. Chim. Acta*, 68 (1974) 267, 277.
2 B. Gehauf et J. Goldenson, *Anal. Chem.*, 29 (1957) 276.
3 B. Gehauf, J. Epstein, G. B. Wilson, B. Witten, S. Sass, V. E. Bauer et W. H. C. Rueggeberg, *Anal. Chem.*, 29 (1957) 278.
4 G. G. Guilbault et G. J. Lubrano, *Anal. Chim. Acta*, 43 (1968) 253.
5 D. N. Kramer, dans E. Crabtree et E. Poziomek (Eds.), *Chemistry of Schönemann Reaction* (a review), Edgewood Arsenal Publication, 1966, p. 18.

Analytica Chimica Acta, 68 (1974) 297–304

© Elsevier Scientific Publishing Company, Amsterdam – Printed in The Netherlands

MOLECULAR EMISSION CAVITY ANALYSIS—A NEW FLAME ANALYTICAL TECHNIQUE*

PART II. THE DETERMINATION OF SELENIUM AND TELLURIUM

R. BELCHER, T. KOUIMTZIS** and A. TOWNSHEND

Department of Chemistry, The University of Birmingham, PO Box 363, Birmingham B15 2TT (England)

(Received 24th July, 1973)

In Part I[1] of this series, a new flame device that enabled small samples to be analysed in cool flames was described. In particular, the determination of sulphur by measurement of S_2 emission was discussed. It was also indicated that it is possible to determine various other elements, many of which can be determined only with difficulty, by means of conventional nebulization into a cool flame. Typical examples of such elements are selenium and tellurium: aspiration of an aqueous solution of a selenium compound into a hydrogen–nitrogen diffusion flame or a hydrogen–

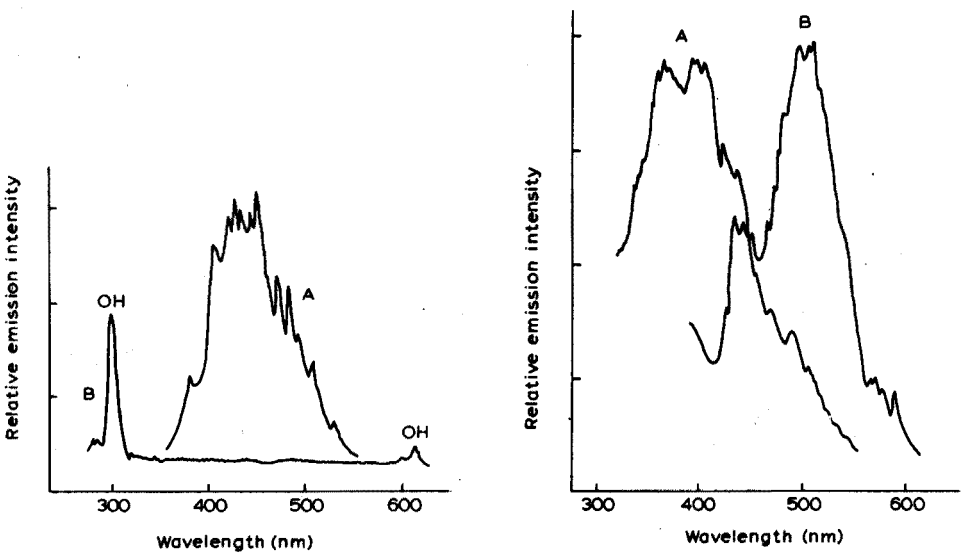

Fig. 1. (A), Spectrum obtained from SeO_2 by MECA with a hydrogen–nitrogen flame; (B) Flame background.

Fig. 2. Tellurium spectra obtained from TeO_2: (A) blue emission above cavity, (B) green emission inside cavity, for a flame composed of 5 l N_2 min^{-1}, 5 l air min^{-1} air and 4 l H_2 min^{-1}.

* This paper is dedicated to Professor D. Monnier on the occasion of his 70th birthday.

** Present address: Department of Chemistry, University of Thessaloniki, Greece.

nitrogen–air flame gives no emission attributable to a selenium species, and aspiration of an aqueous tellurium solution into a hydrogen–nitrogen flame gives only a faint blue emission.

When selenium powder was placed in the specially designed cavity of the MECA instrument[1] and a hydrogen–nitrogen flame was used, a weak blue emission was observed. The intensity of the emission was greatly enhanced when air was also introduced into the flame. Selenium compounds such as selenium dioxide and sodium selenate gave the same emission spectrum (Fig. 1), very similar to that obtained by previous workers[2–4]. Telluric acid gave rise to a green emission from the cavity, with a faint blue emission in the hydrogen–nitrogen–air flame above the cavity. The spectra of both emissions are shown in Fig. 2. The spectrum of the green emission resembled that obtained previously[5], which was described as possibly due to the Te_2 and/or TeO species.

DETERMINATION OF SELENIUM

Optimization of Flame Conditions

The addition of air to the hydrogen–nitrogen flame had a similar effect on selenium emission (Fig. 3) as on sulphur[1]. The enhanced emission at higher air

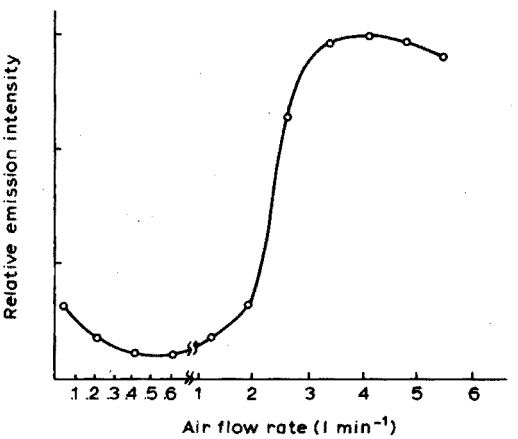

Fig. 3. Effect of air added to a flame of hydrogen (4 l min^{-1}) diluted with nitrogen (5 l min^{-1}) on emission from selenous acid at 411 nm.

content is not due solely to increased temperature, because maximal emission intensity occurred[6] at a cavity temperature of about 315°, which was readily achieved without air in the flame gases. It should be noted that selenium dioxide sublimes at 315° whereas selenium volatilizes at 688°. Thus it would appear that the oxygen promotes the formation of (or at least resists the reduction of) readily volatile selenium dioxide, which is subsequently converted to the emitting species within the cavity.

The position of the cavity in the flame was fairly critical. Under the flame conditions used, the most intense emission was obtained with the orifice of the cavity 23 mm above the centre of the burner.

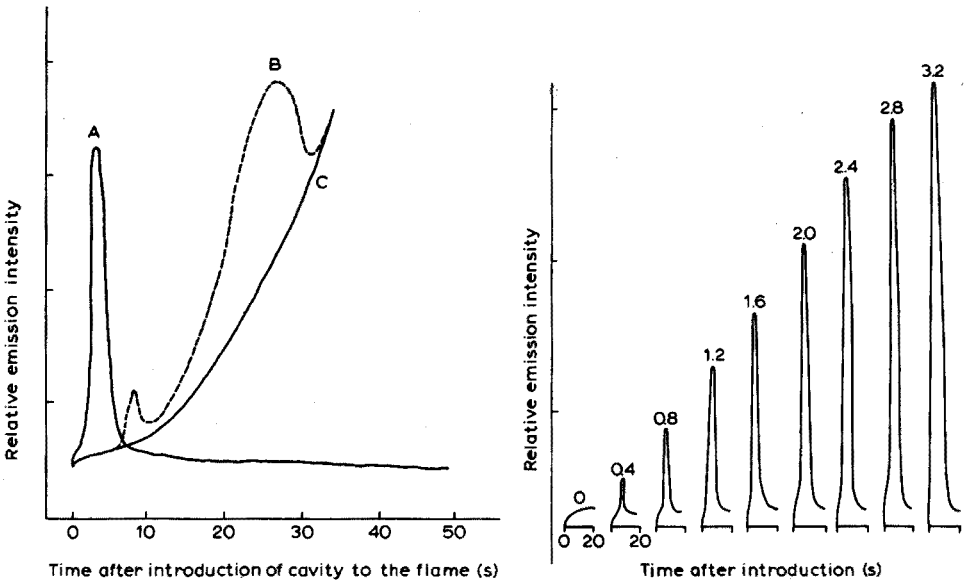

Fig. 4. Effect of time of exposure to optimal hydrogen–nitrogen–air flame on emission of: (A) 1 μg of selenium (as selenous acid) at 411 nm; (B) 10 μg of tellurium (as telluric acid) at 500 nm; (C) incandescent background from cavity at 500 nm.

Fig. 5. Emission response from various amounts of selenium (as selenous acid) in the optimal hydrogen–nitrogen–air flame. Numbers indicate μg of Se.

The change in emission intensity, measured at 411 nm, with time for a sample of selenium dioxide in the cavity is shown in Fig. 4. The response for various amounts of selenium dioxide is shown in Fig. 5. A plot of peak height *versus* amount of selenium added as selenium dioxide was linear for 0.4–3.0 μg of selenium. For larger amounts of selenium, the calibration graph flattened off, possibly because of self-absorption. Less than 0.4 μg of selenium gave no response. The standard deviation for the determination of 2.0 μg of selenium (as SeO_2) was 0.1 μg (7 results).

Interferences

The emission–time response from various organic and inorganic selenium compounds varied with the constitution of the compound, in a similar way to the response from sulphur compounds[1]. Thus, separate calibration graphs are necessary for each selenium compound introduced into the cavity.

After four or five selenium determinations in the same cavity, the inner surface of the cavity becomes black and shiny. If the cavity is pretreated by running several samples of selenium so that this type of surface is achieved, the determination of selenium becomes reproducible. Acidic test solutions attack this pretreated surface and make the determinations less reproducible. The effect of acids may be alleviated by adjusting the pH of the test solution to above 8 with ammonia. An excess of ammonia does not affect the emission intensity of aqueous selenium dioxide solutions. Similarly ammonium fluoride, nitrate and chloride do not interfere in amounts 10-fold by weight compared to the weight of selenium. Tellurium, sulphur,

arsenic and phosphorus can be tolerated when present in amounts up to 40 times the weight of selenium. Metal ions delay the appearance of the emission from selenite or selenate ions, in a similar way to their effect on sulphate ions[1].

Elimination of interferences

When this investigation was carried out, some of the devices reported previously[1] for removing interference effects, such as selective volatilization, had not been investigated fully. Thus, in order to eliminate the interference effects arising from the varying volatilities of different selenium species, and from other elements that interfere spectrally, methods of separating and isolating selenium before the application of MECA were studied.

Where the effect is a general effect of an organic matrix, and is not due to specific interfering elements, the samples may be burned in an oxygen flask, and the resulting solution measured directly by MECA, aqueous selenium dioxide solutions being used as standards. This relatively rapid technique was used successfully to determine very small quantities (0.02 and 0.04%) of selenium in shampoo formulations and also to determine percentage amounts of selenium in organo-selenium compounds (Table I); the carbon and hydrogen analyses for these compounds are also given together with selenium determinations carried out by atomic absorption spectrophotometry. Table I also shows that organo-selenium compounds containing arsenic or bismuth can be analysed by the MECA technique without separating selenium from those elements. When other metal ions are present in commensurate amounts, this technique may not be applicable.

If such interfering species are present, selenium must be selectively removed from the sample solution. The most effective way of separating selenium from inorganic interferences was found to be by reduction to elemental selenium and filtration through a very fine filter paper. By use of suitably small filtration equipment,

TABLE I

DETERMINATION OF SELENIUM IN ORGANOSELENIUM COMPOUNDS

Compound		*C* (%)	*H* (%)	*Se* (%)[a]		
				A	*B*	*C*
$(C_6H_5)_2SeCl_2$	calc.	47.2	3.3		26	
	found	47.1	3.5	26	25	27.5
$As(SeC(=Se)N(C_2H_5)_2)_3$	calc.	22.5	3.8		59	
	found	21.9	3.9	57	57	57
$As(SeC(=Se)N(CH_2C_6H_5)_2)_3$	calc.	46.1	3.6		40	
	found	46.4	3.9	39	38	41
$As(SeC(=Se)N(CH_2C(CH_3)_3)_2)_3$	calc.	33.5	5.6		49	
	found	33.2	5.8	48	48	49
$Bi(SeC(=Se)N(C_2H_5)_2)_3$	calc.	19.3	3.2		51	
	found	19.5	3.5	48	49	50
$O_2N–C_6H_4–SeCN$	calc.	37.0	1.8		35	
	found	36.7	1.7	34	35	33

[a] A: O_2 flask, direct injection. B: O_2 flask, precipitation. C: atomic absorption.

as little as 0.3 μg of selenium can be quantitatively collected. If a cellulose-based filter (e.g. Millipore VMWP, 0.2-μm pore size) is used for filtration, it may be burned in an oxygen flask and a few μl of the resulting solution injected directly into the cavity.

Filtration through a fine glass-fibre filter, which quantitatively retains particles greater than 1 μm in diameter, gives an equally efficient collection of selenium, with the advantage that the non-combustible filter can be inserted into the cavity and the selenium emission measured directly. The use of normal paper in the cavity results in a green emission when the cavity is placed in the flame, whereas the glass fibre gives no emission. Asbestos paper was also investigated, but in the cavity it gave appreciable emission from elements such as sodium.

The efficiency of the selenium precipitation–collection method was checked by analysing the organo-selenium compounds by this method after oxygen flask combustion. Table I shows that there is no significant difference between these results and those obtained by direct injection of the solution from the oxygen flask combustion, which indicates that recovery is quantitative. Filtration takes about 30 min. The precipitation technique was also applied to the determination of selenium in the mixture of selenium and sulphur sometimes known as 'selenium sulphide'. A sample reported as containing 41.0–42.5% Se was found to contain 44.6% Se. Similarly, synthetic solutions of trace selenium in concentrated sulphuric acid (5 ml) were analysed; the results are given in Table II.

TABLE II

DETERMINATION OF SELENIUM IN CONCENTRATED SULPHURIC ACID

μg Se ml^{-1}				
	taken	0.40	0.60	0.80
	found	0.36	0.61	0.74
		0.42	0.66	0.81

The methods devised are readily applicable to other types of sample. It should be possible to determine selenium in sulphur after nitric acid dissolution, or in mineral samples after acid digestion and distillation from hydrobromic acid.

DETERMINATION OF TELLURIUM

Like selenium, tellurium emission is more intense when a reasonable amount of air is added to the flame. As the cavity heats up, two peaks occur when the emission from telluric acid is measured at 500 nm (Fig. 4)[6]. The first peak, which occurs at a cavity temperature of *ca.* 500°, could arise from the volatilization of tellurium dioxide, which is reported to occur at 450°. This peak is much smaller than the second peak, and does not allow less than 10 μg of tellurium to be determined. The second peak occurs at a cavity temperature of *ca.* 780°, and is superimposed on the incandescent emission of the cavity, which is increasing rapidly at this stage[6]. Measurement of this peak therefore requires that the background emission be taken into account. If this is done, as little as 1 μg of tellurium can be determined.

DISCUSSION

The determination of selenium by most flame techniques is relatively insensitive. Atomic absorption, with a conventional nebulization system, has a maximal sensitivity of only 0.5 μg ml^{-1} for 1% absorption of the 196.0-nm selenium line, with triple-pass optics[7]. Moreover, the determination is subject to numerous interferences from other elements[7,8]. The use of a nitrogen-separated nitrous oxide–acetylene flame doubles the sensitivity, and might eliminate many of the interferences[9]. The carbon rod atomizer provides a sensitivity for selenium of 32 pg for 1% absorption and is free of interference from many metals[10].

An indirect method has been published in which selenium is converted to naphtho-(2-3-*d*)-2-seleno-1,3-diazole, and extracted as its palladium(II) complex into chloroform[11]; the palladium is determined by atomic absorption spectrometry. The method is more than an order of magnitude more sensitive than direct atomic absorption; interfering metals are removed by ion exchange.

The equipment used for MECA measurements in this investigation was not designed to achieve high sensitivity. It is believed that a more suitable optical detection system will give greater sensitivies than those reported here. Under the present conditions, however, more than 0.4 μg of selenium or 1 μg of tellurium can be readily determined.

EXPERIMENTAL

The spectroscopic equipment and experimental technique used were the same as described previously[1]. A stainless steel cavity with an aperture diameter of 5 mm and a volume of 45 μl was used throughout.

Reagents

Standard selenium solution (1000 p.p.m.): Dissolve exactly 1 g of elemental selenium powder in 5 ml concentrated nitric acid, and dilute to 1 l with water. Add ammonia solution to give pH 8 before dilution is completed.

All tellurium experiments were carried out with an aqueous 2000-p.p.m. solution of telluric acid.

Determination of selenium in organo-selenium compounds

Burn the accurately weighed sample (2–5 mg) in a 250-ml oxygen flask containing 7 ml of water. After dissolving the combustion gases, make the solution ammoniacal with a few drops of concentrated ammonia liquor. Make up the volume to exactly 10 ml (or 2 ml for less than 0.2 mg of selenium), evaporating the solution if necessary.

If interfering elements are absent, inject exactly 5 μl of the solution from a syringe onto the interior surface of a warm cavity. After exactly 1 min, during which all the water evaporates, place the cavity in the flame, and measure the maximal emission intensity, as described previously[1]. Determine the amount of selenium present by reference to a calibration graph prepared by measuring the emission from exactly 1, 2, 3, and 4 μl of stock selenium solution under the same conditions (Fig. 5).

If interfering elements are present, take an aliquot of the 10-ml solution, containing 0.4–4 μg of selenium, dilute if necessary, and mix with concentrated hydrochloric acid so that the acidity exceeds 6 *M*. Add 2–3 drops of 10% hydroxylammonium chloride solution, or bubble sulphur dioxide for 15 min. Heat at 70° for a few min. Filter the hot suspension through a glass-fibre filter disc (2–4 mm diam.; Whatman GF/C) supported on an asbestos sheet disc in a Millipore filtration apparatus. Wash the precipitate with a few ml of 9 *M* hydrochloric acid followed by hot water. Dry the filter paper in a desiccator over silica gel and transfer to the cavity so that it fits the contour of the cavity, with the selenium deposit towards the aperture. Measure the selenium emission as above, and determine the amount of selenium present by reference to a calibration graph prepared by measuring the emission of 1, 2, 3 and 4 μg of selenium taken through the precipitation procedure, and filtered onto the glass fibre paper. The calibration must be done with selenium on the paper because of the slightly different peak intensities obtained with and without the paper. This could arise from the changed thermal contact between sample and cavity surface and the light reflection from the white paper.

Determination of selenium in shampoo formulations or in 'selenium sulphide'

Carry out an oxygen flask combustion on an amount of sample containing 0.6–8 mg of selenium. Dissolve the evolved gases in 5–7 ml of water, and make up to 10 ml with water. Inject exactly 5 μl of this solution into the cavity, and proceed as described above, for interfering elements absent.

Determination of selenium in sulphuric acid

Dilute a volume of concentrated sulphuric acid containing less than 4 μg of selenium with twice the volume of water. Add to this solution one third of the volume of concentrated hydrochloric acid, and 0.5 ml of 10% tartaric acid solution to prevent precipitation of antimony. Pass sulphur dioxide for 15 min and continue as described above with the precipitation, filtration and determination of selenium.

The authors thank Mr. S. Bogdanski for recording the tellurium spectra. They also thank Fisons Pharmaceuticals Ltd. for the provision of synthetic shampoo samples, and the Inorganic Chemistry Department, University of Thessaloniki and Dr. E. R. Clark, University of Aston in Birmingham, for provision of the organoselenium compounds. Th. Kouimtzis thanks the Greek Ministry of National Economy for the award of a research scholarship.

SUMMARY

The determination of 0.4–4 μg of selenium by molecular emission cavity analysis is described. Selenium in organic compounds is determined after oxygen flask combustion. Metal ion interferences are eliminated by reduction of selenium to the element, filtration onto a glass-fibre paper, and direct incorporation of the filter into the cavity. Applications to the determination of selenium in inorganic and organic compounds are described. The determination of μg-amounts of tellurium is also outlined.

RÉSUMÉ

Une méthode est décrite pour le dosage du sélénium (0.4–4 μg) par analyse d'émission moléculaire. Le sélénium dans des composés organiques est dosé après combustion dans l'oxygène. Les interférences métalliques sont éliminées par réduction du sélénium à l'état élémentaire, filtration sur fibre de verre et incorporation directe du filtre dans la cavité pour l'émission moléculaire. On décrit des applications de ce dosage de sélénium dans des composés inorganiques et organiques. Le dosage de microquantités de tellure est également mentionné.

ZUSAMMENFASSUNG

Die Bestimmung von 0.4–4 μg Selen durch Molekülemissionsanalyse unter Verwendung eines Hohlraums wird beschrieben. Selen in organischen Verbindungen wird nach Verbrennung in einem Sauerstoffkolben bestimmt. Störungen durch Metallionen werden vermieden, indem das Selen zum Element reduziert, auf Glasfaserpapier abfiltriert und das Filter direkt in den Hohlraum gegeben wird. Anwendungen auf die Bestimmung von Selen in anorganischen und organischen Verbindungen werden beschrieben. Die Bestimmung von μg-Mengen Tellur wird ebenfalls dargelegt.

REFERENCES

1 R. Belcher, S. Bogdanski and A. Townshend, *Anal. Chim. Acta*, 67 (1973) 1.
2 Mitika Miyanisi, *Sci. Pap. Inst. Phys. Chem. Res., Tokyo*, 37 (1940) 955.
3 G. Salet, *Ann. Chim. Phys.*, 28 (1873) 5.
4 H. J. Emeleus and H. L. Riley, *Proc. Royal. Soc., London*, 140A (1933) 378.
5 R. M. Dagnall, B. Fleet and T. H. Risby, *Talanta*, 18 (1971) 155.
6 S. Bogdanski, Ph.D. thesis, Birmingham University, 1973.
7 C. S. Rann and A. N. Hambly, *Anal. Chim. Acta*, 32 (1965) 346.
8 C. L. Chakrabarti, *Anal. Chim. Acta*, 42 (1968) 379.
9 G. F. Kirkbright and L. Ranson, *Anal. Chem.*, 43 (1971) 1238.
10 R. B. Baird, S. Pourian and S. M. Gabriel, *Anal. Chem.*, 44 (1972) 1887.
11 H. K. Y. Lau and P. F. Lott, *Talanta*, 18 (1971) 303.

Analytica Chimica Acta, 68 (1974) 305–309

© Elsevier Scientific Publishing Company, Amsterdam – Printed in The Netherlands

ATOMIC-ABSORPTION SPECTROMETRIC DETERMINATION OF COPPER, LEAD, CADMIUM AND MANGANESE IN PULP AND PAPER BY THE DIRECT-ATOMIZATION TECHNIQUE*

F. J. LANGMYHR, Y. THOMASSEN and A. MASSOUMI**
Department of Chemistry, University of Oslo, Oslo 3 (Norway)
(Received 15th July 1973)

A knowledge of the content of the trace metals in pulp and paper is of importance to many users, *e.g.* the food and photographic industries. Methods for trace metal determinations in pulp and paper are normally based on tedious and time-consuming ashing and/or separation/preconcentration steps; other disadvantages are that appreciable amounts of contaminants may be introduced from the reagents added or may be taken up from the ambient atmosphere.

The present paper describes the application of the furnace technique of atomic-absorption spectrometry to the determination of copper, lead, cadmium and manganese in a sample of pulp and four types of paper.

In a matrix of cellulose the trace metals are probably found in or attached to the fibers. After the ashing step—which takes place in the absence of oxygen—the metal compounds are evenly dispersed in a carbon matrix, this distribution is ideal for the subsequent atomisation.

Nothing was found in the literature on the analysis of pulp and paper by the present technique.

EXPERIMENTAL

Apparatus

A Perkin-Elmer 303 atomic-absorption spectrophotometer equipped with a deuterium lamp for background correction was used. The high-frequency induction-heated graphite furnace has been described elsewhere[1]. The signals were detected with a two-channel recorder: one of the channels plotted the peak (in percent absorption), and the other was connected to equipment that transformed the signals into absorbance and recorded the integrated peak area.

Weighings were made with a microbalance.

Reagents

Standard solutions were prepared from high-purity metals, and the acids employed were of Suprapur quality (Merck). The furnace was purged with argon of purity 99.99% (by volume).

---

* This paper is dedicated to Professor D. Monnier on the occasion of his 70th birthday.

** On leave from Department of Chemistry, Pahlavi University, Shiraz, Iran.

Standard solutions

Separate primary standard solutions of lead and copper were prepared by dissolving 1 g of metal in a small excess of nitric acid. After dissolution, 5.0 ml of sulfuric acid were added to the copper solution, and the solution was evaporated to dense white fumes and finally diluted to 1 l. To the lead solution, sulfuric acid was added during the final dilution step, 50 ml of 0.5-p.p.m. lead solution containing 0.5 ml of acid.

The cadmium and manganese solutions (1000 p.p.m.) were prepared by dissolving 1 g of the metals in 50 ml of sulfuric acid (1+9).

The concentrations of the standard solutions employed in the analyses were: copper, 10 p.p.m.; lead, 0.5 p.p.m.; cadmium, 10 p.p.b.; manganese, 10 p.p.m. These solutions should always be freshly prepared, because on standing the concentrations decreased by adsorption of metal on the glass.

In accordance with previous observations[2,3], a loss of cadmium from neutral or nearly neutral solutions in contact with syringes was experienced. This error was avoided by adding sulfuric acid to all standard solutions during the final dilution step to a pH of about 1.

Samples and sampling

Some of the metals found in pulp originate from the raw materials; others, such as copper and iron, are likely to be taken up during the production process.

The samples were: pulp for photographic purposes (Borregaard Industries Ltd., Norway), letterhead paper (Hamang Paper Mill, Norway), chromatographic paper (Whatman No. 1), filter paper (Schleicher & Schüll No. 589[3]), and greaseproof paper (Drammen Paper Mills, Norway). The samples were stored in contact with air, and were not dried before analysis.

From the sheets to be analyzed, 5.5-mm diameter disks were cut from various parts by means of an ordinary office puncher (the cutting edges of the puncher were cleaned by washing with acetone and water). For each sample, the average mass of one disk was found by weighing 10 disks, and samples for analysis were later taken by simply counting a suitable number of disks. For the five types of samples analyzed, the average mass ($\bar{x}$) of one disk, the standard deviation (s) and relative standard deviation (s_r) from weighing 10 disks separately were found to be: pulp: $\bar{x}=19.11$ mg, $s=0.81$ mg, $s_r=4.2\%$; letterhead paper: $\bar{x}=1.618$ mg, $s=0.040$ mg, $s_r=2.5\%$; chromatographic paper: $\bar{x}=1.990$ mg, $s=0.030$ mg, $s_r=1.5\%$; filter paper: $\bar{x}=1.918$ mg, $s=0.050$ mg, $s_r=2.6\%$; greaseproof paper: $\bar{x}=0.936$ mg, $s=0.035$ mg, $s_r=3.7\%$.

Procedure

Before the start of the measurements, the hollow-cathode and deuterium lamps were heated for about 1 h. The measurements were made at the following wavelengths: copper, 216.5 and 324.7 nm; lead, 283.3 nm; cadmium, 228.8 nm; and manganese, 279.5 and 403.1 nm. The flow of argon was adjusted to 6 ml s^{-1}, and 1–20 mg of paper (*i.e.* 1–10 disks) were put in a small tantalum scoop and placed in the middle of the graphite tube by means of a specially constructed adjustable inserting device (a commercial type is produced by Perkin-Elmer). The furnace was moved into its preadjusted position. Standard solutions were added

to the paper by means of a syringe, the liquid being added through the radial opening of the furnace.

The drying, ashing and atomization procedures were as follows. For lead, 60-s drying at 40 V (80°), and 60-s ashing at 80 V (300°) was followed by 30-s atomization at 260 V (1900°); for cadmium, the same procedure was followed, except that atomizations were carried out at 200 V (1500°). For copper the drying at 40 V and ashing at 80 V were maintained but a 30-s ashing step at 100 V (460°) was introduced followed by atomization at 260 V. For manganese, drying was performed at 40 V, ashing at 80 V and atomizations at 220 V (1600°). When atomizations were made at voltages below 260 V, the graphite tube was cleaned by heating for 60 s at maximum voltage.

The standard addition curves were drawn by averaging the values from duplicate measurements of the paper without and with two additions of standard solution.

Blanks were run for the empty furnace.

In addition to a determination of the total content of copper, it was also of interest to know the amounts extractable by water. The present samples were extracted as specified in British Standard 1133, Appendix K (Method for the determination of total water-soluble extract), and the contents of copper and manganese were determined by the conventional flame techniques (the amounts of lead and cadmium were below the detection limits of this method).

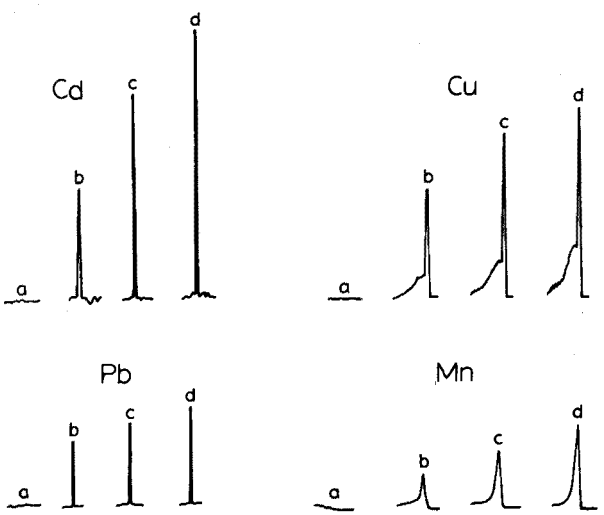

Fig. 1. Typical signals obtained from samples of letterhead paper. For all metals, *a* represents the blank signal from the empty furnace. For cadmium, *b* shows the signal from 6 sample disks, *c* and *d* from 6 disks + 10 and 20 μl, respectively, of 10-p.p.b. cadmium standard solution. For copper, *b* gives the signal from 3 sample disks, *c* and *d* from 3 disks + 5 and 10 μl, respectively, of 10-p.p.m. copper standard solution. For lead, *b* shows the signal from 5 sample disks, *c* and *d* from 5 disks + 10 and 20 μl, respectively, of 0.5-p.p.m. lead standard solution. For manganese, *b* represents the signal from 3 sample disks, *c* and *d* from 3 disks + 2.5 and 5 μl, respectively, of 10-p.p.m. manganese standard solution.

RESULTS

Figure 1 shows typical signals obtained from the letterhead paper. The very sharp peaks of lead and cadmium permitted these metals to be determined by measuring peak heights. At the relatively low maximum temperature of the present furnace (*ca.* 1950°), copper and manganese exhibited broader peaks which required integration*.

The precision was calculated from replicate analyses of the pulp and the letterhead paper; the data on precision are given in Table I. Table II shows

TABLE I

DATA ON THE PRECISION OF THE DIRECT-ATOMIZATION METHODS

Sample	*Metal*	*Content*	*No. of analyses*	*No. of disks taken per analysis*	*Relative standard deviation (%)*	
					Calcd. from peak height	*Calcd. from peak area*
Pulp	Copper	42 p.p.b.	9	1	—	28
	Copper	22 p.p.m.	10	5	—	8.5
Letterhead paper	Lead	4.9 p.p.m.	10	2	16	—
	Cadmium	14 p.p.b.	10	6	45	37
	Manganese	4.6 p.p.m.	10	3	—	28

TABLE II

ANALYTICAL RESULTS FOR COPPER, LEAD, CADMIUM AND MANGANESE

(A = results obtained by direct atomization in the furnace. B = results obtained by atomization of the water extract in a conventional flame).

Sample	*Copper (p.p.m.)*		*Lead (p.p.m.)*	*Cadmium (p.p.b.)*	*Manganese (p.p.m.)*	
	A	*B*	*A*	*A*	*A*	*B*
Pulp	0.042[a]	<0.05	0.26	<0.3	1.5	<0.05
Letterhead paper	22	1.6	4.9	14	4.6	0.15
Chromatographic paper	2.5	0.26	0.17	1.9	0.29	<0.05
Filter paper	1.4	0.18	0.31	2.0	0.15	<0.05
Greaseproof paper	46	1.9	0.64	7.7	2.7	<0.05

[a] The pulp was measured at the wavelength 324.7 nm, and the other samples in column A at the less sensitive line at 216.5 nm.

* When some samples of the letterhead paper were atomized in the Perkin-Elmer heated graphite atomizer Model 70, the signals recorded for copper and manganese at the higher temperatures of this furnace were as sharp as those shown in Fig. 1 for lead and cadmium.

the analytical results. It should be noted that the results given in Table II represent the total content, *i.e.* they include the contribution from any fillers, whiteners, binders and other materials added to the pulp.

Attempts were made also to determine the total contents of copper and manganese by ashing 5 or 10 g of sample in a platinum dish, decomposing the residue by evaporation with hydrofluoric and sulfuric or perchloric acid, dissolving the salts in water and determining the amounts by atomization in a conventional flame. However, high blank values and poor precision made the results less dependable.

The present direct-atomization method is simple, rapid and sensitive, no reagents are added to the samples, and the sample amounts required are only in the range 1–20 mg. The method is probably applicable to the determination of a large number of other metals in pulp and paper.

SUMMARY

The direct-atomization technique of atomic absorption spectrometry was applied to the determination of copper, lead, cadmium and manganese in a sample of pulp and four types of paper. Samples of 1–20 mg were ashed and atomized in a graphite furnace, the determinations being based on the standard addition technique. The method is simple, rapid and sensitive, and no reagents are added to the samples.

RÉSUMÉ

La technique d'atomisation directe de la spectrophotométrie par absorption atomique est appliquée au dosage du cuivre, du plomb, du cadmium et du manganèse dans un échantillon de pulpe et de quatre types de papier. Des échantillons de 1 à 20 mg sont incinérés et atomisés dans un four de graphite; ces dosages sont basés sur la technique de l'étalon interne. Cette méthode est simple, rapide et sensible; aucun réactif n'est ajouté aux échantillons.

ZUSAMMENFASSUNG

Kupfer, Blei, Cadmium und Mangan wurden in einer Probe von Papierbrei und vier Sorten Papier durch Atomabsorptions spektrometrie nach dem Verfahren der direkten Atomisierung bestimmt. Proben von 1–20 mg wurden in einem Graphitofen verascht und atomisiert, wobei die Bestimmungen nach der Standard-Zumischmethode erfolgten. Das Verfahren ist einfach, schnell und empfindlich, und zu den Proben werden keine Reagenzien hinzugegeben.

REFERENCES

1 F. J. Langmyhr and Y. Thomassen, *Z. Anal. Chem.*, 264 (1973) 122.
2 R. D. Reeves, B. M. Patel, C. J. Molnar and J. D. Winefordner, *Anal. Chem.*, 45 (1973) 246.
3 B. M. Patel, R. D. Reeves, R. F. Browner, C. J. Molnar and J. D. Winefordner, *Appl. Spectrosc.*, 27 (1973) 171.

Analytica Chimica Acta, 68 (1974) 311–316
© Elsevier Scientific Publishing Company, Amsterdam – Printed in The Netherlands

THERMOMETRIC AND CONDUCTOMETRIC OBSERVATION OF COPPER(II)-CATALYZED REACTIONS IN THE CATALYTIC–KINETIC DIFFERENCE METHOD*

DETERMINATION OF MICROGRAM AMOUNTS OF COPPER(II)

SIEGBERT PANTEL and HERBERT WEISZ

Lehrstuhl für Analytische Chemie, Chemisches Laboratorium der Universität, 78-Freiburg i.Br. (Germany)

(Received 10th August 1973)

Analytical methods based on catalyzed reactions are of considerable importance in trace analysis because of their high sensitivity and, in many cases, because of their very distinct selectivity, the latter being especially true of enzymatic methods. Difference methods are very well known in analytical chemistry, for instance in photometry or in polarography, their special advantage being the possible partial compensation of errors. It therefore seemed obvious to combine the two methods.

The principle of the catalytic–kinetic difference method has already been discussed in detail[1]. Two vessels, each containing the same amount of a reaction mixture A+B of a catalyzable reaction are thermostated. To one of them a known concentration $[K]_1$ of the catalyst is added, whereas to the other one is added simultaneously the unknown concentration $[K]_2$ of the catalyst to be determined. This means that the two systems differ only in their catalyst concentration (Fig. 1). Whatever poperty of the system is used to indicate the course of reaction, *e.g.* absorbance or potential, the difference between the two measured values must of course be zero initially; both systems are absolutely equal at the start. Then, because of the different catalyst concentrations in the systems, the differences of the measured effects increase to a maximum; at the end, after the reactions in the two vessels have been completed, a process which might take a very long time, the difference is again zero. From the change in

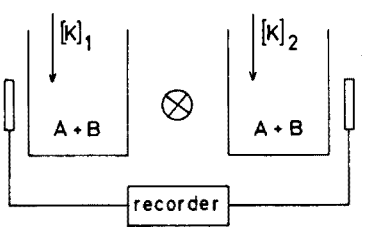

Fig. 1. Schematic representation of the catalytic–kinetic difference method, with photometric observation of the reaction $A+B \overset{K}{\rightarrow} X+Y$.

* This paper is dedicated to Professor D. Monnier on the occasion of his 70th birthday.

the difference of the measured quantity with time, it should be possible to deduce from a plotted graph, be it from the size of the maximum, from the area or from the inclination of the curve, something about the ratio between the two catalyst concentrations. Since one is known, it is now possible to determine the unknown one.

The application of this method to the copper-catalyzed reduction of iron(III) with thiosulfate and to the *l*-cystine-catalyzed reduction of iodine with sodium azide has already been discussed in detail[1]; the course of reaction was followed potentiometrically and photometrically. The latter method has likewise been used in the determination of microgram amounts of silver by means of the silver-catalyzed oxidation of leucomalachite green with peroxydisulfate in the presence of 2,2′-bipyridine as activator[2].

In the present paper, it will be shown that the course of the reactions in the difference method may also be followed by thermometry and conductometry.

EXPERIMENTAL

The essential measuring device used consists of a Wheatstone bridge, two resistors being replaced by special detectors (depending, of course, on the method used). The bridge signal is transmitted to a recorder via an operational amplifier. The circuit diagram of this device is given in Fig. 2. For the conductometric method two tall-form 50-ml beakers were used as measuring cells; in the thermometric device two 50-ml Dewar vessels were used.

The two identical measuring cells were mounted in a hollow aluminium block connected to a rotary thermostat ($22.5 \pm 0.3°$); both reaction systems were mixed simultaneously by a double-spindled stirring motor. The reactions were started simultaneously by use of a suitable double-starting pipette as already described[1].

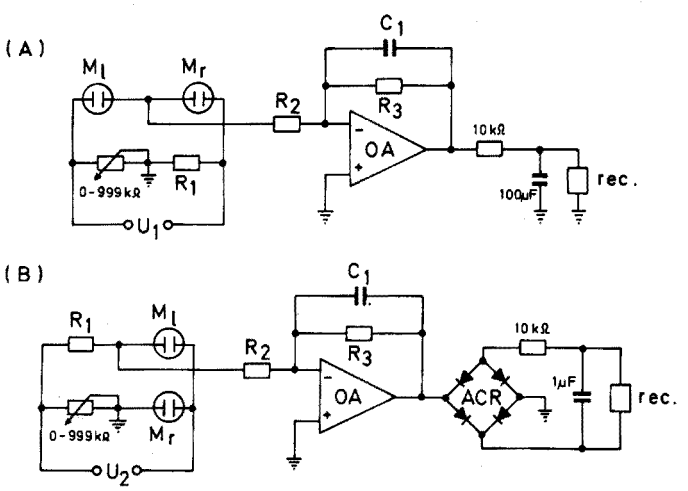

Fig. 2. Measuring circuit for (A) d.c., thermometry and biamperometry; (B) a.c., conductometry. OA, Philbrick-Nexus Q 200; ACR, ITT/SEL B 30 C 300-1 rec., compensating strip chart recorder Servogor RE 541.

DETERMINATION OF COPPER(II) IN THE MICROGRAM RANGE BY A CATALYTIC–THERMOMETRIC DIFFERENCE METHOD

The copper(II)-catalyzed autodecomposition of hydrogen peroxide[3,4] in ammoniacal medium is a strongly exothermic reaction. Therefore it may be observed thermometrically.

Measuring device

See Fig. 2 A. $U_1 = 1.35$ V, $R_1 = 68$ kohms, $R_2 = 10$ kohms, $R_3 = 1$ Mohm, $C_1 = 0.01$ μF. M_1 and M_r, thermistors Siemens K 17 or ITT/SEL F 15, 100 kohms/20° with identical physical properties.

Procedure

Into each of the two Dewar vessels, add 5 ml of 2 *M* aqueous ammonia solution and 2 ml of hydrogen peroxide solution (5 mg H_2O_2 ml^{-1}) and make up to 27 ml with distilled water.

Both solutions are well stirred and thermostated for 10 min. Start the reactions by simultaneous addition of 3 ml of standard solution of copper (6 μg Cu ml^{-1} as copper acetate) to the left vessel and of 3 ml of neutralized copper sample solution (6–23 μg Cu ml^{-1}) to the right vessel by use of the above-mentioned starting pipette.

RESULTS

Figure 3 shows a recorder plot obtained in this way for the differences between a standard solution of copper(II) (18 μg/30 ml) and a sample solution of copper(II) containing 65 μg/30 ml. At the beginning of the reaction, the thermometric difference curve shows a linear dependence on time; therefore the inclination may be used for the evaluation.

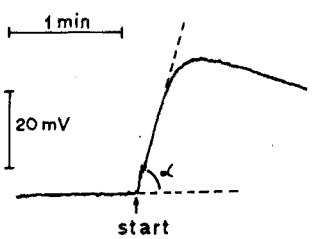

Fig. 3. Recorder plot for catalytic–thermometric observation in the difference method.

With a number of known copper concentrations in the right cell and, of course, always the same standard concentration in the left cell, a calibration graph was prepared. Figure 4 shows that a linear relationship was found, when tan α was plotted against the square of the copper concentration. Because of this relation, only a rather limited range of unknown copper concentrations can be determined, but a very reasonable degree of accuracy can be achieved (see Table I).

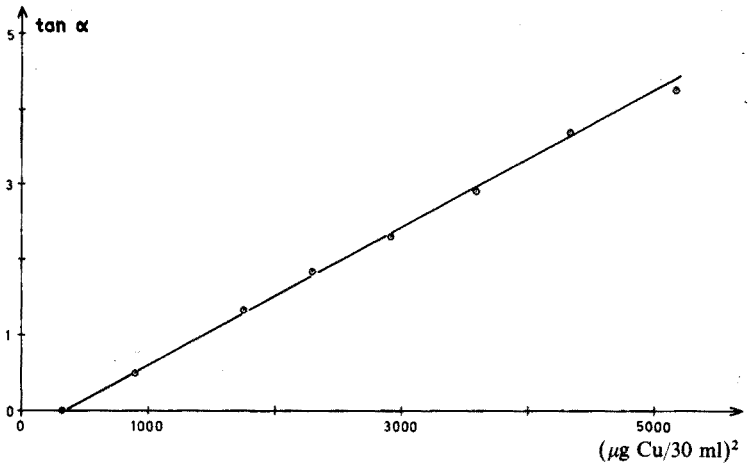

Fig. 4. Calibration graph for the determination of copper(II) by catalytic–thermometric observation in the difference method.

TABLE I

DETERMINATION OF COPPER(II) BY THE CATALYTIC–THERMOMETRIC DIFFERENCE METHOD

(Results given as μg Cu/30 ml)

Given	20.0	24.0	27.0	33.0	39.0	54.0	60.0	69.0
Found	20.6	23.9	25.7	33.6	39.5	54.4	60.0	67.2
Error	+0.6	−0.1	−1.3	+0.6	+0.5	+0.4	0.0	−1.8

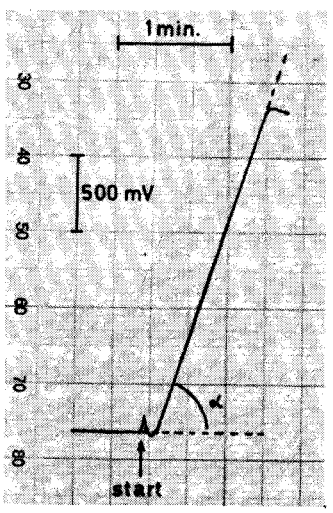

Fig. 5. Recorder plot for catalytic–conductometric observation in the difference method.

DETERMINATION OF COPPER(II) BY A CATALYTIC–CONDUCTOMETRIC DIFFERENCE METHOD

The oxidation of thiosulfate with hydrogen peroxide in acidic solution[5] is also copper-catalyzed. The conductivity of this system increases as a result of the oxidation of thiosulfate to sulfate[6]. Therefore it is possible to follow the course of the reaction conductometrically. Figure 5 represents a typical curve obtained in this way for the differences between a standard solution of copper(II) containing 10 μg/30 ml and a sample solution containing 100 μg/30 ml. In this case a linear calibration curve is obtained when tan α is plotted directly against the catalyst concentration. This means that a better determination range is available compared with the method described above. The calibration curves obtained were of the same type as that shown in Fig. 4, being linear over the range 10–100 μg Cu/30 ml with tan α values varying from 0 to 3.

Measuring device

See Fig. 2 B. $U_2 = 2$ V/50 cycles s^{-1} $R_1 = 500$ ohms, $R_2 = 100$ kohms, $R_3 = 1$ *M*ohm. M_1 and M_r, conductivity electrodes for dipping in, type L 201/L 21 (Pusl, München) with identical physical properties.

Procedure

Into each of the two beakers add 1 ml of 2 *M* acetic acid and 1 ml of 0.1 *M* sodium thiosulfate; then to the left one, add 10 μg of copper(II) as copper acetate and to the right one add 3 ml of the neutralized sample solution containing 4–40 μg Cu ml^{-1} and make up to 27 ml with distilled water. Stir both solutions well and thermostat for 10 min. Start the catalyzed reactions by simultaneous addition of 3 ml of hydrogen peroxide solution containing 10 mg H_2O_2 ml^{-1} from the starting pipette.

RESULTS

Some results for the determination of copper(II) in this way are given in Table II.

Because hydrogen peroxide can be oxidized as well as reduced[7], the change in its concentration can be followed biamperometrically. This was tried with the same apparatus (Fig. 2 A; $U_1 = 60$ mV, $R_1 = 10$ kohms, $R_2 = R_3 = 100$ kohms, $C_1 = 0.01$ μF; M_1 and M_r, double platinum electrodes for dead-stop titrations,

TABLE II

DETERMINATION OF COPPER(II) BY THE CATALYTIC–CONDUCTOMETRIC DIFFERENCE METHOD

(Results given as μg Cu/30 ml)

Given	12.0	21.0	30.0	45.0	60.0	75.0	90.0	99.0
Found	12.2	21.5	29.5	44.0	60.0	75.0	89.0	97.0
Error	+0.2	+0.5	−0.5	−1.0	0.0	0.0	−1.0	−2.0

type Pt 020 (Schott u. Gen. Mainz). Unfortunately, here, as in the thermometric observation, a linear relationship was found between tan α and the square of the copper concentrations; the range of determination was thus too small for practical applications.

SUMMARY

The course of reactions in the catalytic–kinetic difference method, previously described, can also be followed by conductometry and thermometry. The copper-catalyzed decomposition of hydrogen peroxide can be followed by thermometry, and the copper-catalyzed oxidation of thiosulfate with hydrogen peroxide by conductometry. Both reactions can be used for the determination of microgram amounts of copper(II).

RÉSUMÉ

La conductométrie et la thermométrie ont permis de suivre le cours de réactions par la méthode de différence catalytique cinétique précédemment décrite. La décomposition du péroxyde d'hydrogène, catalysée par le cuivre, peut être suivie par thermométrie, et l'oxydation du thiosulfate par le péroxyde d'hydrogène, catalysée par le cuivre, par conductométrie. Ces deux réactions peuvent être utilisées pour le dosage de microquantités de cuivre(II).

ZUSAMMENFASSUNG

Es wird gezeigt, dass der Reaktionsablauf bei der bereits beschriebenen katalytisch–kinetischen Differenz-Methode auch konduktometrisch und thermometrisch verfolgt werden kann. Die durch Kupfer katalysierte Selbstzersetzung von Wasserstoffperoxid (Thermometrie) und die ebenfalls durch Kupfer katalysierte Oxydation von Thiosulfat mit Wasserstoffperoxid (Konduktometrie) werden beide zur Bestimmung von Kupfer(II) im Mikrogramm-Bereich verwendet.

REFERENCES

1 H. Weisz and H. Ludwig, *Anal. Chim. Acta*, 55 (1971) 303.
2 H. Weisz and S. Pantel, Unpublished studies, Freiburg, 1972.
3 A. V. Kiss and E. Lederer, *Rec. Trav. Chim. Pays-Bas*, 46 (1927) 453.
4 L. A. Nikolaev, *Vestn. Mosk. Univ.*, 2 (1946) 105; *Chem. Abstr.*, 42 (1948) 3653 b.
5 V. A. Litvinenko, *Ukr. Khem. Zh.*, 32 (1966) 1338; *Chem. Abstr.*, 66 (1967) 119228; *Ukr. Khem. Zh.*, 35 (1969) 311; *Chem. Abstr.*, 70 (1969) 118519; *Radiokhimiya*, 11 (1969) 74; *Chem. Abstr.*, 71 (1969) 25058.
6 K. B. Yatsimirskii, *Kinetic Methods of Analysis*, Pergamon Press, Oxford, 1966, p. 83.
7 K. G. Stone and H. G. Scholten, *Anal. Chem.*, 24 (1952) 671.

Analytica Chimica Acta, 68 (1974) 317–322

© Elsevier Scientific Publishing Company, Amsterdam – Printed in The Netherlands

DETERMINATION OF TRACE CONCENTRATIONS OF CITRATE IN AQUEOUS SYSTEMS*

ROBERTA MAE BUSTIN** and PHILIP W. WEST***

Environmental Science Institute, Chemistry Department, Louisiana State University, Baton Rouge, La. 70803 (U.S.A.)

(Received 5th August 1973)

Citrate forms complexes in solution above a pH of about 6 with metals such as aluminum, chromium, iron, manganese, or zinc. Thus, it is likely that metal citrate complexes are present in natural waters. The behavior of these complexed species is quite different from that of the individual ions acting alone. It is highly possible that these citrate complexes play a significant role in the quality of water. Glooshenko and Moore[1] reported that citrate, used as a replacement for phosphate in detergents, caused a proliferation of algal growth in highly polluted water. They postulated that the stimulation of growth was due to the formation of chelates with metals which would be toxic to algae if left free in solution. An alternative explanation is that citrate makes essential trace elements nutritionally available to the algae by forming complexes with these metals. It has been proposed[2] that citrate may play an important role in the phenomenon of the Florida red tide by forming a complex with iron(III) and thus allowing it to be utilized metabolically by *Gymnodinium breve*, the organism responsible for the occurrence of the red tide.

Citrates and citric acid are prevalent in the natural environment. Citrus fruits and pineapples are natural sources of citric acid. Citrate is an important constituent of the soils in citrus groves and is eventually washed from the soil into surrounding waters. Citric acid is also widely used in industrial processes. It is included in many food, beverage, and medicinal preparations and is important in the manufacturing of mirrors, in engraving, and in the dyeing industry. It finds wide use as a rust inhibitor. Certain esters of citric acid are used as plasticizers and other citrates are important in the blueprint industry. Citrates have also gained publicity as builders in detergents. Citric acid plays an important role in body metabolism. It is one of the components of the series of reactions generally referred to as the Krebs cycle or citric acid cycle, a mechanism which is important in respiration in living cells. Citric acid is a common metabolite and is present in certain body fluids. Blood serum contains about 25 mg l^{-1} and about 0.5 g per day is excreted in the urine[3]. Aue *et al.*[4] report that citric acid can be present at fairly high levels in effluents from sewage treatment plants. These examples indicate the widespread distribution of citric acid and point to the likelihood of its presence, at least in low concentrations, in many lakes and streams.

* This paper is dedicated to Professor D. Monnier on the occasion of his 70th birthday.

** On leave from Arkansas College, Batesville, Arkansas.

*** To whom correspondence should be addressed.

Numerous methods exist for the determination of citrate and citric acid. Many of them were originally proposed for biological studies. The most widely used methods are the pentabromoacetone method proposed in 1897 by Stahre[5] and modifications of this procedure[6–11]. Although these methods are quite selective, the procedures are laborious and the sensitivities are not great enough for determinations of trace quantities of citrate. Other oxidation methods have been described[12,13], but they also suffer from lack of sensitivity. A color reaction of citrate with acetic anhydride and pyridine was utilized by Furth and Herrman[14], and their method was later modified by Saffran and Denstedt[15]. Thunberg[16] developed a method involving the bleaching of methylene blue by citric acid; a similar test is based on the bleaching effect of citrate on molybdenum blue[17]. The formation of iron(III) citrate has been the basis of at least two tests[18,19]. Lack of sensitivity limits these procedures from being adapted for use in water quality studies. Many of the methods also suffer from interferences by other hydroxy acids or heavy metals. Liquid chromatography has been successfully used to separate citric acid from other components in solution[20–23], and gas chromatography is being used widely in the separation and determination of citric acid[4,24–28]. These techniques are superior to previous methods in both sensitivity and selectivity.

Because trace concentrations must be determined in water quality studies, sensitivity was an important consideration in choosing a technique for the present study. Owing to its inherent sensitivity, spectrofluorimetry seemed promising. In a study of enzymatic reactions involving acetyl coenzyme A in aldol condensations, Calvo *et al.*[29] showed that a fluorescent compound resulted from the reaction of citric acid with resorcinol and that a fluorimetric assay could be run to determine the amount of citric acid present. Guyon and Marks[30] used the quenching effect of citrate on the fluorescence of a tungstate–flavanol complex to develop a fluorimetric test capable of detecting 0.2 μg of citrate. Tartrate, oxalate, and iodide were reported to interfere. Thus, it was desirable to develop a test having the sensitivity which can be achieved in fluorimetry but not suffering from the normal interferences. It was found that citrate and citric acid could be converted into ammonium citrazinate[31] which exhibits a blue fluorescence. This is the basis of the method described in this paper.

EXPERIMENTAL

Reagents and solutions

Citrate solution. A stock solution containing 10 mg of citrate per ml was prepared by dissolving 1.555 g of trisodium citrate (analytical reagent grade) in water and diluting to 100 ml. This solution was prepared daily and was used to make standard citrate solutions.

Sodium metaperiodate solution. A 5% (w/w) solution was prepared by dissolving 5 g of sodium metaperiodate (analytical reagent grade) in 95 g of water.

Solutions for study of interferences. Stock solutions having a concentration of 10 mg ml^{-1} were used.

Other reagents. Thionyl chloride, ammonia liquor, hydrochloric acid and sulfuric acid (analytical reagent grade).

Apparatus

An Aminco-Bowman spectrophotofluorimeter equipped with an optical unit, a photomultiplier microphotometer, and a power supply was used. A 10-mm quartz cell was used to hold the sample.

Recommended procedure

Pipet 0.5 ml of sample solution into a microcasserole and add 0.1 ml of 2 *M* hydrochloric acid. Evaporate the solution to dryness on a hot plate. Cool, add 0.3 ml of thionyl chloride, and again evaporate to dryness. Add 0.4 ml of concentrated ammonia solution, and boil until about 2 drops of liquid remain. After allowing the casserole to cool, add 0.3 ml of concentrated sulfuric acid, and heat the solution for 2 min at a temperature sufficiently high to cause evolution of sulfur trioxide vapors. Wash the solution into a 5-ml volumetric flask; add concentrated ammonia solution to bring the pH to at least 9; and dilute to the mark with deionized water. After 10 min, measure the fluorescence intensity at 430 nm, using an excitation source of 340 nm.

If the procedure is being used for samples which contain tartrate, 0.1 ml of 5% sodium metaperiodate solution should be added before the initial evaporation to dryness.

Calibration curve

Standard citrate solutions were prepared by appropriate dilutions of a 10 mg ml^{-1} stock solution. The recommended procedure was repeated for each solution, and a value of the fluorescence intensity was obtained. The calibration curve is shown in Fig. 1. After the value of the blank has been subtracted, the curve is linear in the concentration range 0.01–10 μg ml^{-1}.

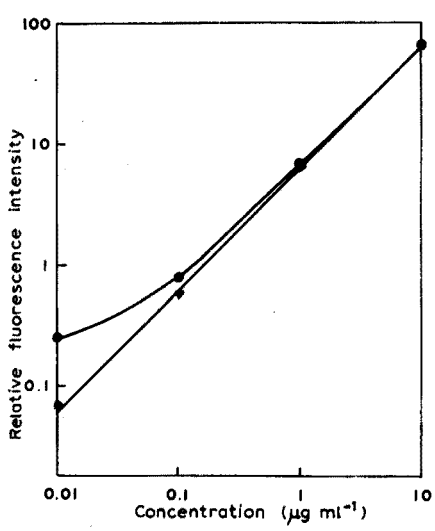

Fig. 1. Calibration curve: (▼) blank subtracted; (●) blank not subtracted.

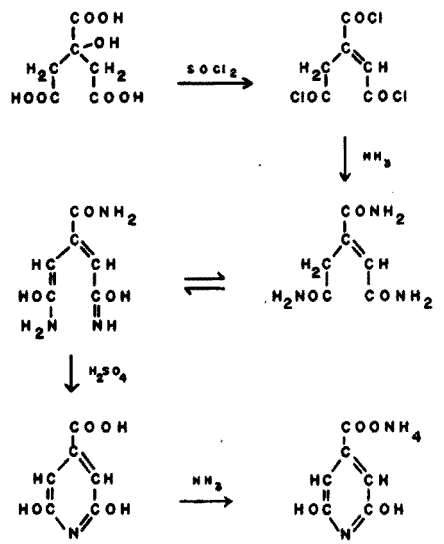

Fig. 2. Reaction scheme.

RESULTS AND DISCUSSION

Investigations employing a spot test of Feigl[31] showed that citrate could be converted into a fluorescent product. The conversion takes place through a series of steps shown in Fig. 2. The citrate is converted to citric acid, and the solution is evaporated to dryness. The solid citric acid is then treated with thionyl chloride to form the acid chloride of aconitic acid. Boiling with ammonia converts the acid chloride into the triamide. Upon heating with sulfuric acid, ammonia is given off; the ring closes, and the acid amide group on the middle carbon is saponified. The product is 2,6-dihydroxyisonicotinic acid or citrazinic acid, whose ammonium salt forms a colorless solution which exhibits a bright blue fluorescence.

The excitation and fluorescence spectra were obtained. The excitation maximum occurred at 340 nm, and the emission wavelength for maximum fluorescence was 430 nm. The optimal amount of each reagent was found by keeping all conditions constant except the variable being studied and determining the amount of that particular reagent necessary to give maximum fluorescence.

The rate of development of fluorescence and the stability of the product were studied. Three separate trials indicated that the intensity of the fluorescent product had reached its expected value by the time a reading could be taken and that it remained constant for about 2 h. Figure 3 is a graphical representation showing the stability of the fluorescent product.

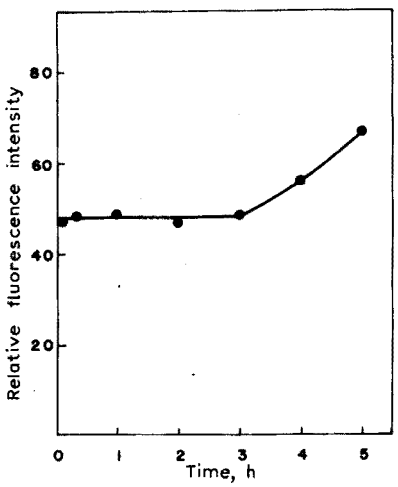

Fig. 3. Stability of product.

The initial addition of acid serves two functions. It demasks metal citrate complexes potentially present and forms citric acid from the citrate ion. For most samples, 0.1 ml of acid is a large excess; however, the excess of acid is driven off in the initial heating and does not affect subsequent reactions. The elimination of the tartrate interference is due to the oxidation of the tartaric acid by periodate. This reaction is characteristic of compounds containing two or more –OH or =O groups attached to adjacent carbon atoms. Because citric acid does not have this structure, it is not affected by the periodate. Although oxalate could be tolerated

in this procedure, it does interfere in many citrate determinations and could be eliminated by the use of periodate.

A wide range for the method is possible by means of adjustments of instrumental sensitivity. The best working range is 0.1–10 μg ml^{-1}. However, the limit of detection was found to be 0.01 μg ml^{-1}, and samples with concentrations as low as 0.001 μg ml^{-1} can usually be differentiated from the blank. Although samples in the concentration range below 0.1 μg ml^{-1} can be determined, the values of the fluorescence intensity for such samples are close together and do not differ markedly from the blank value. Hence, when samples are being run in this concentration range, extreme care should be exercised in both the experimental work and the interpretation of results.

All glassware used throughout the determination must be scrupulously clean. It can be boiled in concentrated nitric acid but should not be cleaned with chromic acid. Aluminum foil, Saran wrap, or polyethylene stoppers should be used instead of cork or rubber stoppers. Foreign material present in the solution can change both the nature and intensity of the fluorescence and give erroneous results.

The method described here does not suffer from the normal interferences. The sensitivity is adequate for water quality work, and the procedure could easily be adapted for use in biological studies.

We wish to acknowledge partial support for this research from the National Science Foundation (grant no. GI 35114 X).

SUMMARY

A fluorimetric method for the determination of citrate is described. Through a series of reactions, citrate is converted into citrazinic acid. The ammonium salt of this compound exhibits a fluorescence maximum at 430 nm when an excitation source of 340 nm is used. The method does not suffer from the normal interferences. The limit of detection is 0.01 μg ml^{-}, and the best working range is 0.1–10 μg ml^{-1}.

RÉSUMÉ

On décrit une méthode fluorimétrique pour le dosage des citrates. Après une série de réactions, le citrate est transformé en acide citrazinique. Le sel d'ammonium de ce composé présente une fluorescence maximum à 430 nm, lorsqu'une source d'excitation de 340 nm est utilisée. La méthode ne souffre pas des interférences normales. La limite de détection est de 0.01 μg ml^{-1}; le domaine d'utilisation le plus favorable va de 0.1 à 10 μg ml^{-1}.

ZUSAMMENFASSUNG

Es wird eine fluorimetrische Methode für die Bestimmung von Citrat beschrieben. Mit Hilfe einer Reihe von Reaktionen wird Citrat in Citrazinsäure umgewandelt. Das Ammoniumsalz dieser Verbindung zeigt ein Fluoreszenzmaximum bei 430 nm, wenn eine Anregungsquelle von 340 nm verwendet wird. Die Methode leidet nicht an den normalen Störungen. Die Nachweisgrenze ist 0.01 μg ml^{-1} und der beste Arbeitsbereich 0.1–10 μg ml^{-1}.

REFERENCES

1 W. A. Glooshenko and J. E. Moore, *American Chemical Society National Meeting*, Washington, D.C., Sept. 1971.
2 P. W. West and R. Bustin, *Environ. Lett.*, 3 (1972) 247.
3 D. A. Shirley, *Organic Chemistry*, Holt, Rinehart and Winston, New York, 1964.
4 W. A. Aue, C. R. Hastings, K. O. Gerhardt, J. O. Pierce, H. H. Hill and R. F. Moseman, *J. Chromatogr.*, 72 (1972) 259.
5 H. Stahre, *Z. Anal. Chem.*, 36 (1897) 195.
6 R. Kunz, *Arch. Chem. Mikrosk.*, 7 (1914) 285.
7 G. W. Pucher, C. C. Sherman and H. B. Vickery, *J. Biol. Chem.*, 113 (1936) 235.
8 A. S. Goldberg and A. R. Bernheim, *J. Biol. Chem.*, 156 (1944) 33.
9 S. Natelson, J. B. Pincus and J. K. Lugovoy, *J. Biol. Chem.*, 170 (1947) 597.
10 C. A. Hargreaves, M. D. Abrahams and H. B. Vickery, *Anal. Chem.*, 23 (1951) 467.
11 P. J. Elving and R. E. Van Atta, *Anal. Chem.*, 26 (1954) 295.
12 H. Backstrom, *Z. Anal. Chem.*, 123 (1942) 96.
13 H. T. Gordon, *Anal. Chem.*, 23 (1951) 1853.
14 O. Furth and H. Herrman, *Biochem. Z.*, 280 (1935) 448.
15 M. Saffran and O. F. Denstedt, *J. Biol. Chem.*, 175 (1948) 849.
16 T. Thunberg, *Biochem. Z.*, 206 (1929) 109.
17 R. M. Matulis and J. C. Guyon, *Anal. Chem.*, 36 (1964) 118.
18 A. S. Williams, R. H. Müller and J. B. Niederl, *Mikrochemie*, 3 (1931) 269.
19 R. D. Tiwari and U. C. Pande, *Microchem. J.*, 14 (1969) 138.
20 F. A. Isherwood, *Biochem. J.*, 40 (1946) 688.
21 V. Zbinovsky and R. H. Burris, *Anal. Chem.*, 26 (1954) 208.
22 G. A. Harlow and D. H. Morman, *Anal. Chem.*, 36 (1964) 2438.
23 K. W. Stahl, G. Schafer and W. Lamprecht, *J. Chromatogr. Sci.*, 10 (1972) 95.
24 C. W. Gehrke and D. F. Goerlitz, *Anal. Chem.*, 35 (1963) 76.
25 H. H. Luke, T. E. Freeman and L. B. Kier, *Anal. Chem.*, 35 (1963) 1916.
26 F. L. Estes and R. C. Bachman, *Anal. Chem.*, 38 (1966) 1178.
27 M. A. Harmon and H. W. Doelle, *J. Chromatogr.*, 42 (1969) 157.
28 E. C. Horning and M. G. Horning, *J. Chromatogr. Sci.*, 9 (1971) 129.
29 J. M. Calvo, J. C. Bartholomew and B. I. Stieglitz, *Anal. Biochem.*, 28 (1969) 164.
30 J. C. Guyon and J. Y. Marks, *Mikrochim. Acta*, (1969) 731.
31 F. Feigl, *Spot Tests in Organic Analysis*, 6th ed., Elsevier Publishing Co., New York, 1960.

Analytica Chimica Acta, 68 (1974) 323–330

© Elsevier Scientific Publishing Company, Amsterdam – Printed in The Netherlands

DOSAGE TITRIMÉTRIQUE DU TRIBUTYLPHOSPHATE, DE LA DI-n-HEXYLSULFOXYDE ET DE L'OXYDE DE TRI-n-BUTYLPHOSPHINE PAR LES ACIDES DE LEWIS AVEC REPÉRAGE VISUEL DU TERME*

G. ROLAND et G. DUYCKAERTS

Laboratoire de Chimie Analytique, Université de Liège au Sart Tilman, B-4000 Liège (Belgique)

(Reçu le 20 juillet 1973)

Les titrages en milieu non aqueux des fonctions organiques par les acides de Lewis ont suscité peu de travaux. À notre connaissance, les seules recherches effectuées dans ce domaine concernent principalement les titrages des fonctions azotées[1–8] et oxygénées[1,2,6,9–11]. En général, les solutions titrées ou titrantes sont préparées par dissolution d'un dérivé chloré ou bromé de l'aluminium, de l'étain(IV), du titane(IV) ou de l'antimoine(V) dans un solvant anhydre (chlorure d'acétyle, chlorure de benzyle, chlorobenzène, chlorure de thionyle, 1,2 dichloroéthane...) et le terme du titrage est déterminé soit visuellement[1,3,4,7] par l'intermédiaire d'un indicateur, soit par les méthodes physico-chimiques classiques (conductométrie[1,2,5,8], potentiométrie[2,7] lorsque les solvants sont suffisamment conducteurs ou encore par titrages haute fréquence[6], spectrophotométrie[10] ou thermométrie[11]).

Nous avons essayé d'appliquer cette méthode de dosage pour titrer quelques bases organiques fréquemment utilisées en extraction liquide–liquide en portant notre attention tout spécialement sur le tributylphosphate (TBP), sur la di-n-hexylsulfoxyde (DH_xSO) et sur l'oxyde de tri-n-butylphosphine (TBPO) en repérant le terme visuellement.

CONDITIONS EXPÉRIMENTALES

Le 1,2-dichloroéthane (p.a.) a été séché par ébullition à reflux sur P_2O_5 pendant plusieurs jours et a été distillé avant l'emploi.

Le TBP, $SnCl_4$ et $TiCl_4$ anhydres ont été obtenus comme précédemment[12,13].

La di-n-hexylsulfoxyde a été préparée par synthèse puis purifiée par recristallisation fractionnée dans un mélange cyclohexane–benzène.

Le TBPO a été préparé par synthèse puis distillé sous vide avant l'emploi.

Le tétrabromure d'étain a été préparé par synthèse directe puis distillé sous vide à plusieurs reprises.

Les spectres visibles ont été enregistrés par un spectrophotomètre Cary 17; la concentration en indicateur étant choisie de telle façon que l'absorbance de l'indicateur (dans la zone visible du spectre) soit comprise entre 1 et 1.5 pour un trajet optique de 1 cm.

---

* Cette publication est dédiée au Professeur D. Monnier, à l'occasion de son 70ème anniversaire.

Les titrages ont été effectués à l'aide d'une burette à piston plongeant directement dans les ballons jaugés contenant les solutions à titrer.

RÉSULTATS EXPÉRIMENTAUX

Nous avons utilisé deux indicateurs, le vert de malachite et le crystal violet qui, en solution dans le 1,2-dichloroéthane, présentent une bande d'absorption intense dont le maximum se situe respectivement à 625 et 590 nm.

Lors de l'addition des acides de Lewis étudiés, on observe une diminution progressive de l'absorbance de la bande de l'indicateur et l'apparition d'une nouvelle bande d'absorption caractéristique de la forme complexée de l'indicateur dont le maximum se situe vers 430 nm. Le comportement du violet de crystal est cependant plus complexe: au fur et à mesure que l'on ajoute les acides de Lewis à la solution de base (et bien avant le terme), l'indicateur, violet au départ, devient progressivement bleu (bande d'absorption à 645 nm). Avant le terme cette coloration s'atténue et l'indicateur vire au jaune au terme. Sur la Fig. 1 nous avons porté, en fonction de la concentration en $SnCl_4$, les rapports $A^{645nm}/A^{590nm}_{réf.}$ et $A^{590nm}/A^{590nm}_{réf.}$ où A^{645nm}, A^{590nm} et $A^{590nm}_{réf.}$ représentant respectivement les absorbances mesurées à 645 et 590 nm et l'absorbance de l'indicateur à 590 nm en l'absence d'acide de Lewis. Cette évolution du spectre du violet de crystal a également été observée lors de titrages acide–base de Brønsted en milieu non aqueux[14]. Du point de vue pratique, cette modification est sans grande importance mais si on veut suivre le titrage spectrophotométriquement il est nécessaire d'effectuer les mesures à 645 nm.

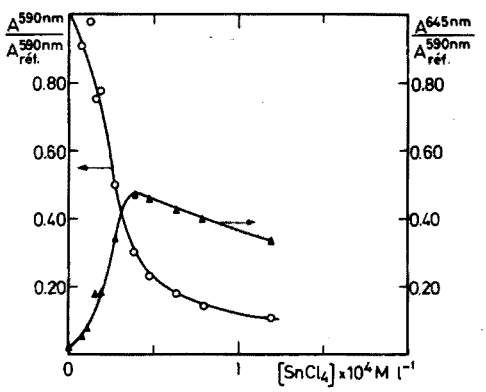

Fig. 1. Evolution du rapport d'intensité des bandes d'absorption du crystal violet en fonction de la concentration en $SnCl_4$.

Dosage du TBP

Pour chaque série d'expériences, nous avons maintenu les concentrations en TBP et en indicateur constantes et nous avons fait varier la concentration en acide en supposant que le terme du titrage corresponde à un rapport stoechiométrique [base]/[acide] égal à 2.00. Les Fig. 2 et 3 représentent les variations des absorbances de l'indicateur en fonction du degré d'avancement du titrage (x) pour différentes concentrations en TBP. On peut constater que le vert de malachite donne lieu à

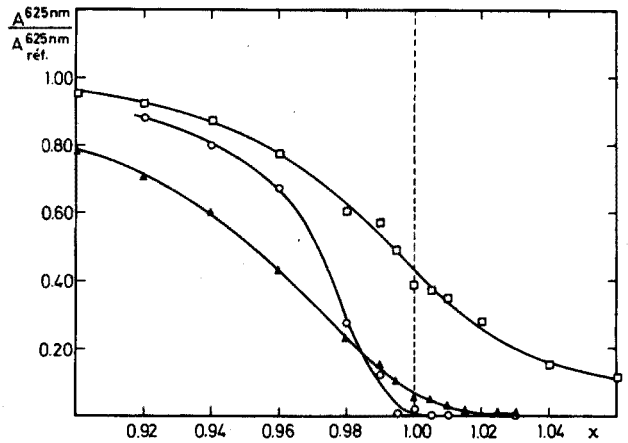

Fig. 2. Variation de l'absorbance du vert de malachite en fonction du degré d'avancement du titrage du TBP par $SnCl_4$. (□) $[TBP]_t = 0.020$ mol l^{-1}; (▲) $[TBP]_t = 0.100$ mol l^{-1}; (○) $[TBP]_t = 0.500$ mol l^{-1}.

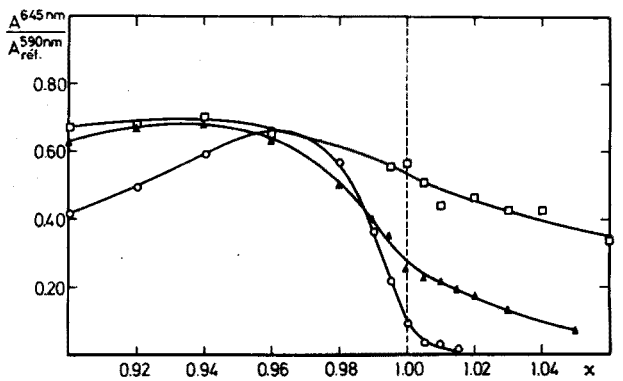

Fig. 3. Variation de l'absorbance de la bande d'absorption du crystal violet située à 645 nm en fonction du degré d'avancement du titrage du TBP par $SnCl_4$. (□, ▲, ○) Voir Fig. 2.

des variations de coloration beaucoup plus nettes que le crystal violet et son virage au terme est presque total pour des concentrations en $[TBP]_t \simeq 0.1$ *M*. Pour des solutions plus diluées ($[TBP]_t \simeq 0.02$ *M*), les variations de coloration des deux indicateurs ne sont pas nettes et rendent le dosage imprécis.

Si pour les deux indicateurs utilisés nous comparons les résultats réels et trouvés pour une série de dix dosages (Tableau I) nous obtenons des écarts généralement inférieurs à 1% relatif mais affectés d'une légère erreur systématique qui provient probablement de l'estimation visuelle du terme du titrage. Cette erreur pourrait être éliminée par étalonnage de la solution titrante de tetrachlorure d'étain par une solution de TBP de concentration voisine de celles que l'on se propose de doser.

Les titrages du TBP par une solution de $SnBr_4$ ou de $TiCl_4$ qui forment également des complexes de stoechiométrie 2:1 très stables avec le TBP[12,13] n'ont donné que des résultats médiocres:

TABLEAU I

DOSAGE DU TBP

Indicateur: vert de malachite						*Indicateur: crystal violet*					
$[(TBP)_2SnCl_4]$ au terme:						*$[(TBP)_2SnCl_4]$ au terme:*					
0.05 M		*0.3 M*		*0.65 M*		*0.05 M*		*0.25 M*		*0.6 M*	
mM TBP		*mM TBP*		*mM TBP*		*mM TBP*		*mM TBP*		*mM TBP*	
Vrai	*Trouvé*	*Vrai*	*Trouvé*	*Vrai*	*Trouvé*	*Vrai*	*Trouvé*	*Vrai*	*Trouvé*	*Vrai*	*Trouvé*
2.070	2.081	9.533	9.478	13.32	13.28	1.999	1.997	8.935	8.906	12.73	12.76
1.899	1.895	9.460	9.410	13.41	13.43	1.922	1.932	8.916	8.906	12.97	13.07
1.806	1.817	9.159	9.100	13.88	13.87	1.854	1.887	8.894	8.852	12.78	12.86
1.878	1.888	9.760	9.720	13.35	13.37	1.910	1.932	8.795	8.785	12.44	12.48
1.972	1.974	9.561	9.512	13.24	13.21	1.989	1.993	9.132	9.100	12.11	12.17
1.850	1.867	9.728	9.682	13.56	13.58	1.851	1.858	8.525	8.473	13.01	13.08
1.826	1.834	9.009	8.930	13.35	13.32	1.842	1.870	9.261	9.307	12.97	13.03
1.917	1.921	9.512	9.427	13.06	12.98	1.858	1.883	9.200	9.197	12.76	12.86
1.838	1.863	9.434	9.376	13.55	13.58	1.898	1.924	8.970	8.927	12.92	13.03
1.967	1.981	9.222	9.172	13.30	13.26	2.004	2.026	9.324	9.296	13.25	13.32

1. avec $SnBr_4$, l'indicateur vire beaucoup trop tard et la variation de coloration au terme n'est pas nette;

2. avec $TiCl_4$, acide de Lewis beaucoup plus fort que $SnCl_4$ ou $SnBr_4$, on obtient des résultats affectés d'une erreur par excès qui peut atteindre 3 à 5% relatifs pour des concentrations en $[TBP]_t$ de l'ordre de 0.1 *M* mais qui tombe à 1% relatif pour des concentrations en $[TBP]_t$ de l'ordre de 0.5 *M*. Signalons également que l'indicateur est lentement détruit par $TiCl_4$ et que la coloration jaune des complexes TBP–$TiCl_4$ rend la détermination visuelle du terme plus difficile.

Les résultats obtenus par titrage semblent indiquer que les complexes de stoechiométrie 1:1 qui peuvent se former entre le TBP d'une part et $SnCl_4$ ou $TiCl_4$ d'autre part, ne sont pas assez stables pour interférer avec les indicateurs choisis.

Dosage de la di-n-hexylsulfoxyde

Les courbes représentant les variations d'extinction de l'indicateur en fonction du degré d'avancement du titrage sont représentées sur les Figs. 4 et 5. On peut constater que le virage de l'indicateur est plus net avec la di-n-hexylsulfoxyde qu'avec le TBP.

Les résultats des titrages obtenus pour différentes concentrations en DH_xSO figurent dans le Tableau II.

TABLEAU II

DOSAGE DE LA DI-n-HEXYLSULFOXYDE

(Indicateur: vert de malachite dans le 1,2-dichloroéthane.)

$[DH_xSO]_t$ au terme ($mol\ l^{-1}$)	*mM* DH_xSO	
	Réel	*Trouvé*
≃0.2	2.108	2.106
≃0.2	3.460	3.474
≃0.6	10.55	10.57
≃0.6	10.63	10.64
≃1	15.74	15.86
≃1	16.08	16.09

On peut constater que cette méthode de titrage s'avère exacte pour autant que la concentration en complexe au terme soit supérieure ou égale à 0.05 *M* car pour de plus faibles concentrations le terme n'est plus suffisamment net.

Dosage de l'oxyde de tri-n-butylphosphine

Sur la Fig. 6 nous avons porté les courbes de titrages du TBPO par $SnCl_4$ en présence de vert de malachite. On peut voir que le terme du titrage de cette base, plus forte que le TBP ou la DH_xSO, peut encore être repéré visuellement avec une exactitude satisfaisante pour des solutions diluées ($[TBPO]_t \simeq$ 0.02 *M*).

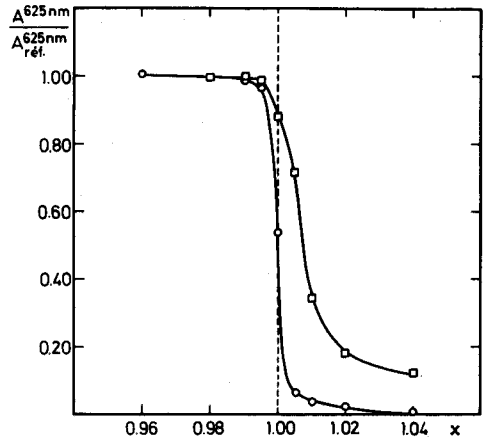

Fig. 4. Variation de l'absorbance du vert de malachite en fonction du degré d'avancement du titrage de la DH_xSO par $SnCl_4$. (○) $[DH_xSO]=0.100$ mol l^{-1}; (□) $[DH_xSO]=0.020$ mol l^{-1}

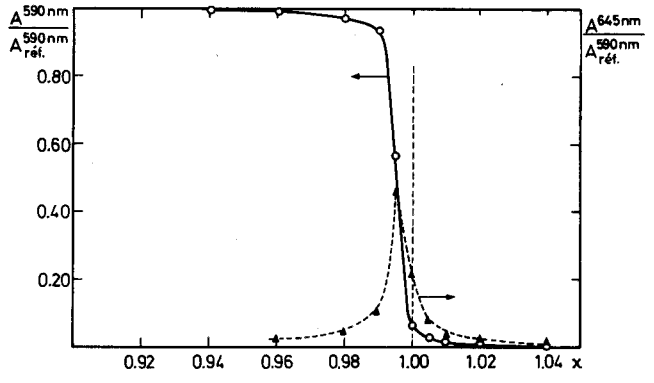

Fig. 5. Variation de l'absorbance des bandes d'absorption du crystal violet situées à 590 et 645 nm en fonction du degré d'avancement du titrage de la DH_xSO par $SnCl_4$. (○) $[DH_xSO]=0.100$ mol l^{-1}

L'erreur relative, de l'ordre du pour cent relatif pour des solutions diluées ($0.1 \leqslant [TBPO]_t \leqslant 0.5$ *M*), atteint 2–3% par excès lors du titrage de solutions plus concentrées. Par analogie avec les résultats obtenus par spectrométrie Raman pour le système TBP–$SnCl_4$[13], cette erreur peut être attribuée à la formation d'un complexe TBPO–$SnCl_4$ de stoechiométrie 1:1.

L'utilisation de chloroforme qui s'associe à la fonction →P=O par liaison hydrogène et qui diminue donc la constante de stabilité apparente des complexes permet de réduire l'erreur relative commise sur le titrage des solutions concentrées en TBPO mais de toute façon, et contrairement aux dosages du TBP et de la DH_xSO, il y a lieu de considérer le terme du titrage comme atteint dès le virage de l'indicateur au vert.

En conclusion, cette méthode de dosage expérimentée sur les bases précédentes devrait pouvoir s'appliquer de la même manière aux autres alkylphosphates, di-n-hexylsulfoxydes et oxydes de phosphine à condition cependant que la stabilité

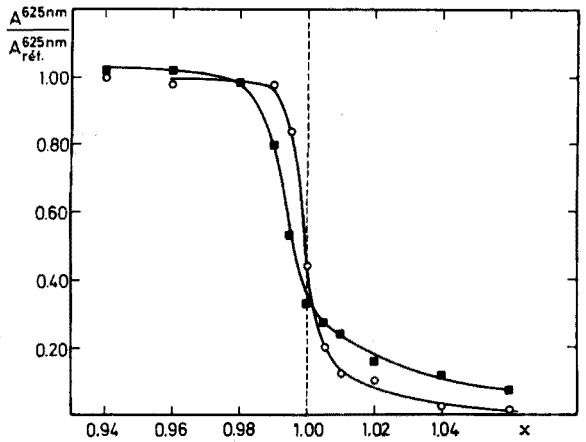

Fig. 6. Variation de l'absorbance du vert de malachite en fonction du degré d'avancement du titrage du TBPO par $SnCl_4$. (○) [TBPO] = 0.100 mol l^{-1}; (■) [TBPO] = 0.020 mol l^{-1}.

des complexes formés ne soit pas modifiée d'une manière appréciable par des effets stériques importants ou par la présence sur les chaînes alkyles d'atomes susceptibles de modifier fortement la basicité de la fonction titrée.

Nous remercions le Fonds National de la Recherche Scientifique et l'Institut Interuniversitaire des Sciences Nucléaires pour l'intérêt constant apporté à nos travaux et pour le soutien financier accordé à notre laboratoire.

RÉSUMÉ

Nous avons titré le tri-n-butylphosphate, la tri-n-butylphosphine oxyde et la di-n-hexylsulfoxyde par des solutions de $SnCl_4$, $SnBr_4$ et $TiCl_4$ en solution dans le 1,2-dichloroéthane anhydre en présence de vert de malachite ou de crystal violet. Les meilleurs résultats ont été obtenus en utilisant une solution titrante de $SnCl_4$ avec le vert de malachite comme indicateur. L'exactitude de la méthode est de l'ordre du 1–2% pour des concentrations en complexes au terme supérieures ou égales à 0.05 *M*.

SUMMARY

Tri-n-butylphosphate, tri-n-butylphosphine oxide and di-n-hexylsulfoxide were titrated with $SnCl_4$, $SnBr_4$ and $TiCl_4$ in anhydrous 1,2-dichloroethane with malachite green or crystal violet as indicator. Best results were obtained when $SnCl_4$ was used with malachite green as indicator. The accuracy of the method is about 1–2% for complex concentrations greater or equal to 0.05 *M* at the equivalence point.

ZUSAMMENFASSUNG

Tri-n-butylphosphat, Tri-n-butylphosphinoxyd und Di-n-hexylsulfoxyd wur-

den mit $SnCl_4$, $SnBr_4$ und $TiCl_4$ im wasserfreien 1,2-Dichloräthan mit dem Malachitgrün und dem Krystallviolett titriert. Die besten Ergebnisse wurden erzielt, wenn $SnCl_4$ mit dem Malachitgrün als Indicator benutzt wurde. Die Genauigkeit der Methode ist ungefähr ein Prozent für gleiche oder grössere als 0.05 *M* Komplex-konzentrationen auf dem Endpunkt.

BIBLIOGRAPHIE

1 E. B. Graber, L. E. D. Pease, Jr. et W. F. Luder, *Anal. Chem.*, 25 (1953) 581.
2 H. Spandau et E. Brunneck, *Z. Anorg. Allg. Chem.*, 278 (1955) 197.
3 R. C. Paul, S. S. Sandhu, J. Singh et G. Singh, *J. Indian Chem. Soc.*, 35 (1958) 869.
4 J. Singh, R. Paul et S. S. Sandhu, *Chem. Ind. (London)*, (1958) 622; *J. Chem. Soc.*, (1959) 845; *Anal. Chem.*, 31 (1959) 1495.
5 R. C. Paul, J. Kaur et S. S. Sandhu, *J. Indian Chem. Soc.*, 38 (1961) 93.
6 E. T. Hitchcock et P. J. Elving, *Anal. Chim. Acta*, 28 (1963) 301.
7 R. C. Paul, K. Raj et P. S. Singh, *J. Indian Chem. Soc.*, 44 (11) (1967) 920.
8 R. C. Paul, K. Raj et P. Sarvinder, *J. Indian Chem. Soc.*, 46 (1) (1969) 26.
9 R. E. Van Dyke et H. E. Crawford, *J. Amer. Chem. Soc.*, 71 (1949) 2694.
10 I. M. Kolthoff, D. Stocesova et T. S. Lee, *J. Amer. Chem. Soc.*, 75 (1953) 1834.
11 S. T. Zenchelsky, Y. Periale et J. C. Cobb, *Anal. Chem.*, 28 (1956) 67.
12 G. Roland, B. Gilbert et G. Duyckaerts, *Spectrochim. Acta*, 28A (1972) 835.
13 G. Roland, B. Gilbert, J. Decerf et G. Duyckaerts, *Spectrochim. Acta*, 29A (1973) 879.
14 E. Bishop (éditeur), *Indicators*, Pergamon Press, 1972, p. 183.

Analytica Chimica Acta, 68 (1974) 331–337

© Elsevier Scientific Publishing Company, Amsterdam – Printed in The Netherlands

ÉTUDE DE LA STABILITÉ CHIMIQUE ET MÉCANIQUE DES TUBES DE POMPES TECHNICON LORS DE L'EMPLOI DE SOLVANTS ORGANIQUES TRÈS AGRESSIFS (AMINES ET ÉTHERS)*

J. BOSSET et B. BLANC

Station Fédérale de Recherches Latières, 3097 Liebfeld-Bern

E. PLATTNER

Institut de Génie Chimique, École Polytechnique Fédérale, Lausanne (Suisse)

(Reçu le 31 juillet 1973)

En dépit de nombreuses améliorations, l'un des points les plus délicats des systèmes d'analyse automatique dits "à flux continu" reste toujours le dispositif de pompage. Ce "coeur" assure à lui seul le prélèvement de l'échantillon, la ou les dilution(s) nécessaire(s), l'introduction des réactifs et la circulation générale des fluides dans tout le système (bobines de mélange, de thermostatisation et de réaction, modules de dialyse, de filtration, de séparation, etc.), le passage au travers de la cuvette de mesure ("push–pull"), sans oublier encore l'importante segmentation (bulles) des échantillons. L'ensemble de ces opérations, qui représente souvent une perte de charge considérable, doit pourtant être très précis ($\pm 1\%$), rapide (cadence de 10^1 à 10^2 (analyses h^{-1})) et constant (pas ou très peu de dérive dans le temps, surtout avec une expansion d'échelle).

Ces quelques considérations conduisent à une conclusion impérative: les tubes de pompe utilisés doivent présenter une résistance chimique et une stabilité mécanique excellentes. Paradoxalement, vu le nombre important de publications analytiques traitant de l'automatisation au moyen de tels équipements, très peu d'entre elles abordent ce point de première importance. Quelques auteurs[1–3] cherchent à corriger mathématiquement la dérive des résultats obtenus au moyen d'ordinateurs. Cooke et Stockwell[4] étudient ce problème en travaillant avec de l'eau et des solutions eau/alcool (éthanol, n-propanol, isopropanol, à diverses concentrations) pour des tubes "standard" et "solvaflex". Davidson *et al.*[5] examinent le cas des tubes "acidflex" avec un acide concentré (l'acide sulfurique à 90%).

Types de tubes de pompe existants et domaines d'application

Pendant de nombreuses années, on ne trouvait sur le marché que trois types de tubes de pompe différents: les "standards" (PVC ou tygon), les "acidflex" et les "solvaflex". Récemment, Technicon vient de mettre sur le marché trois nouveaux types de tubes:

* Cette publication est dédiée au Professeur D. Monnier, à l'occasion de son 70ème anniversaire. Extrait d'une thèse de doctorat publiée prochainement sous la direction des Prof. Dr. B. Blanc et E. Plattner.

les nouveaux "standards" ("SMA flow-rated pump tubes");
les nouveaux "acidflex" (de couleur rouge, au lieu de noire);
les "silicones".

En se basant sur les spécifications données par le fabricant, il apparaît que le système de pompage péristaltique ne doit pas poser de problèmes particuliers en ce qui concerne[6]:

les alcools et les acides aliphatiques à chaînes relativement courtes;
les aldéhydes et les cétones ordinaires lorsqu'elles sont assez diluées;
les hydrocarbures aliphatiques et aromatiques, même nitrés ou chlorés;
les acides minéraux même concentrés;
les acides et les bases (organiques ou inorganiques) dilués et de manière générale toutes les solutions où l'eau joue le rôle déterminant.

Il n'est fait mention nulle part de deux classes de solvants particulièrement importants: les amines et les éthers. Parmi eux, deux représentants courants, la n-butylamine (BTA) et le tétrahydrofurane (THF), feront plus particulièrement l'objet de ce travail.

DISPOSITIF EXPÉRIMENTAL ET MODE OPÉRATOIRE*

Les différents tubes à essayer sont montés sur une pompe Technicon III selon la technique habituelle.

Afin de simuler des conditions de travail réelles (écrasement des tubes, charge de la pompe, etc.), les tubes de pompe à tester sont montés parallèlement à d'autres tubes "standards" qui assurent simultanément la circulation d'autres flux (air, eau). La température est celle du laboratoire, les variations étant inférieures à $\pm 1°$.

Le solvant (BTA ou THF) employé à 60% (v/v) (les 40% (v/v) restant sont de la soude 0.4 *M*) est placé dans un erlenmeyer de 200 ml, connecté à la pompe au moyen de tuyaux d'aspiration et de retour en téflon. Le système travaille en circuit fermé avec un minimum d'évaporation. Chaque heure, on mesure le débit de chacun des tubes en chronométrant le temps nécessaire pour remplir un ballon jaugé de 20 ml. Les solutions de BTA et de THF sont périodiquement renouvelées (indiqué par une petite flèche verticale descendante sur les graphiques).

Cette étude a été effectuée sur des tubes de débit Q et de diamètre d moyens, indiqués dans le Tableau I.

Les divers essais ont été poursuivis en principe jusqu'à destruction du tube de pompe (dissolution, rupture, obstruction, écrasement ou relâchement complet) repérée par une croix ($\times$) sur les Figures. Pour les tubes qui, au contraire, ont montré dès le début une bonne résistance à l'usure et au vieillissement tant chimique que mécanique, les tests ont été menés jusqu'à preuve de leur stabilité, c'est à dire au minimum sur 150 h de fonctionnement ininterrompu.

Les tuyaux ont tous été montés avec une tension moyenne (supports en position médiane). Après un certain nombre d'heures de fonctionnement ininterrompu (54 ou 77 h suivant les cas), ils ont été retendus d'un cran, afin

* Sauf indications spéciales, celles données par Cooke et Stockwell[4] sont valables.

TABLEAU I

TUBES UTILISÉS POUR CETTE ÉTUDE[a]

Matériau	*Type*	$Q(0)$ (ml min^{-1})[b]	*d (inch)*[c]
"Silicone"	Clair/clair	1.27	0.058
"Solvaflex"	Jaune/bleu	1.27	0.060
"Standard"	Jaune/jaune	1.15	0.056
"Acidflex noir"	Bleu/bleu	1.28	0.065
"Acidflex rouge"	Jaune/jaune	1.00	0.056

[a] Aimablement mis à disposition par Technicon International.
[b] $Q(0)$ = débit mesuré en début d'essai (première mesure).
[c] d = diamètre intérieur selon indications de Technicon.

de pouvoir estimer l'influence de la tension sur le débit (discontinuité représentée par une verticale sur les graphiques).

Remarque. Pour des raisons de sécurité, la pompe a été arrêtée pendant la première nuit d'utilisation de nouveaux tubes, c'est à dire après 4 h de fonctionnement. Les tuyaux, vidés de leur contenu, ont été maintenus sous tension, mais le couvercle assurant la pression a été enlevé.

RÉSULTATS ET DISCUSSION

Les temps de remplissage $T(t)$ mesurés en fonction de la durée de l'essai t(h) ont été convertis par ordinateur en:

$Q(t)$: le débit du tube de pompe (ml min^{-1}) au temps t(h).
$Q(t)/Q(0)$: le rapport de ce débit au débit initial ($t=0$) (sans dimension).

TABLEAU II

RÉSUMÉ DES OBSERVATIONS FAITES

Matériau	*Solvant*	*Durée vie (h)*	*Observations et remarques*
"Silicone"	Eau	$\geqslant 200$	Aucune modification significative de la couleur, de
"Standard"	Eau	$\geqslant 200$	l'élasticité ou de la forme des tubes, si ce n'est un
"Solvaflex"	Eau	$\geqslant 200$	léger aplatissement après un grand nombre d'heures de
"Acidflex"	Eau	$\geqslant 200$	travail.
"Silicone"	BTA	$\geqslant 200$	Aplatissement marqué, état lég. vitreux.
"Standard"	BTA	~ 175	Apparition d'une forte coloration jaune-brun,
"Solvaflex"	BTA	~ 50	perte d'élasticité, durcissement, écrasement.
"Acidflex"	BTA	25–30	Gonflement, lég. décoloration, ramollissement.
"Silicone"	THF	$\geqslant 200$	Pas de modifications significatives.
"Standard"	THF	~ 0	Dissolution totale en quelques minutes,
"Solvaflex"	THF	~ 0	aucune résistance chimique.
"Acidflex"	THF	~ 5	Gonflement, décoloration, ramollissement.

$d[Q(t)/Q(0)]/dt$: la dérivée de ce rapport par rapport au temps, caractérisant la variation horaire de ce débit (‰ par h).

Le rapport $Q(t)/Q(0)$ en fonction de t pouvant être considéré comme l'un des critères les plus significatifs de la qualité des divers tubes testés, les résultats obtenus sont présentés sous la forme de trois graphiques (Figs. 1–3) correspondant aux trois solvants proposés: l'eau, la n-butylamine et le tétrahydrofurane. Les valeurs de $Q(0)$ étant donnés dans le Tableau I, il est possible d'en déduire $Q(t)$; quant à la dérivée, elle est donnée par la pente des graphes.

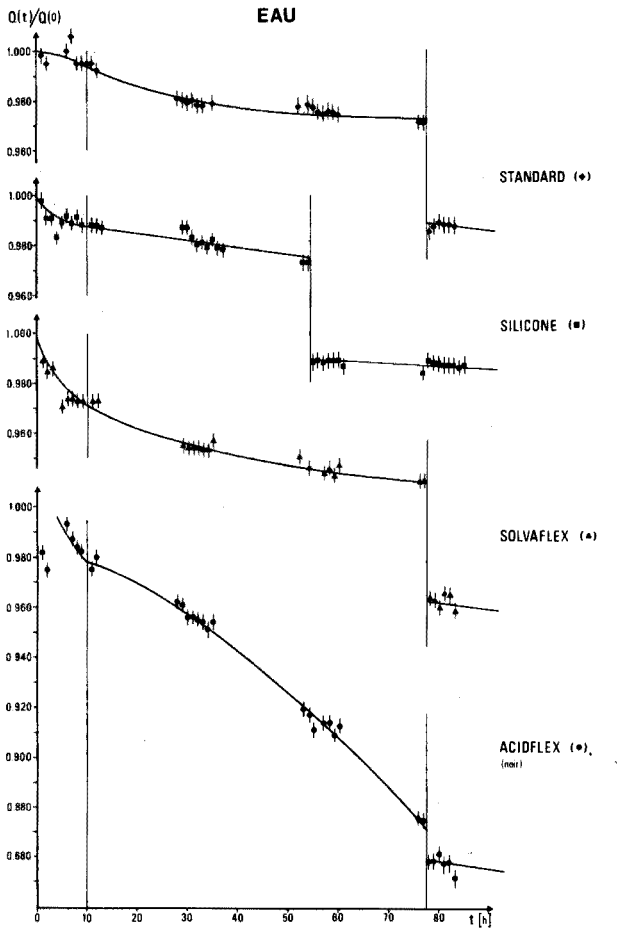

Fig. 1. Stabilité mécanique lors du pompage d'eau distillée.

Les échelles utilisées étant toujours les mêmes, le mode de représentation adopté permet de comparer directement le comportement des divers matériaux disponibles pour un solvant donné, et l'influence des divers solvants proposés sur un matériau donné. Pour une variation de débit de 1% (≙une graduation de l'axe des ordonnées), on lira en abscisse l'intervalle de temps maximum tolérable entre deux étalonnages successifs. Les domaines d'erreur indiqués sur

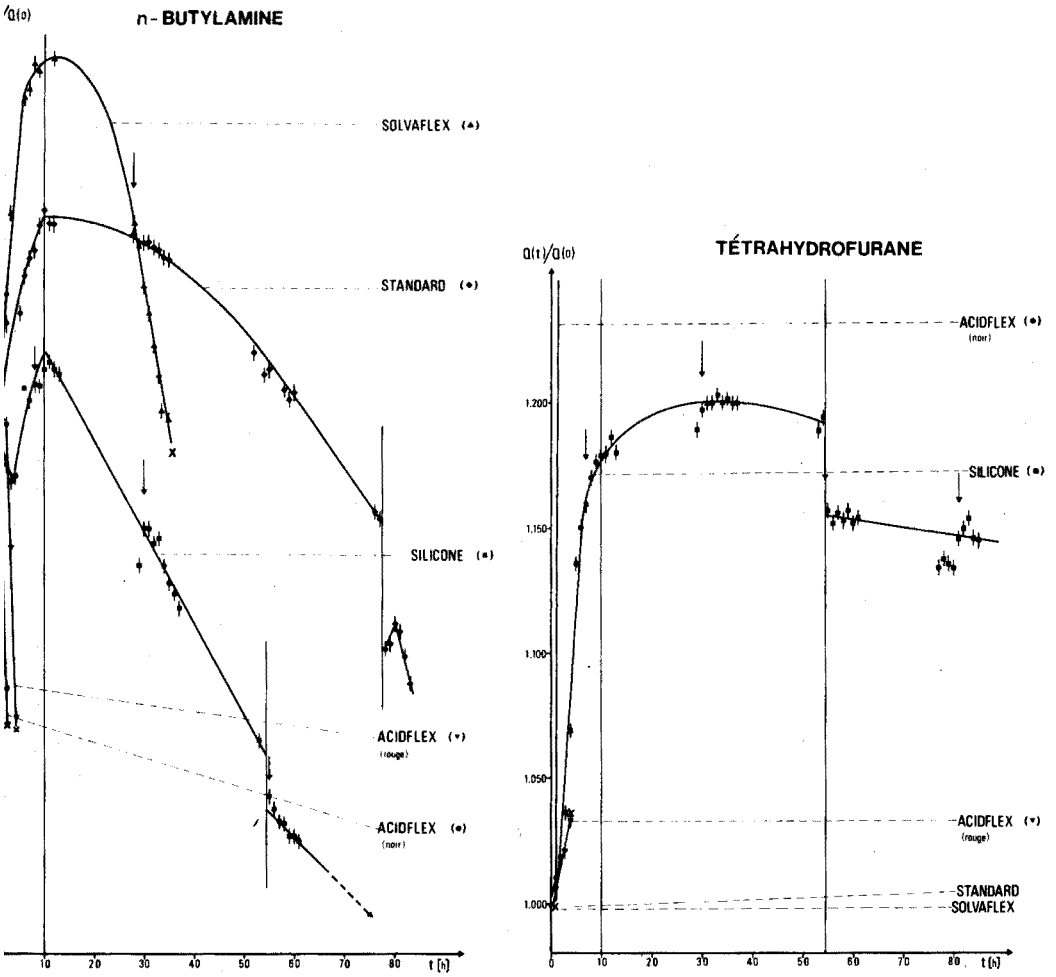

Fig. 2. Stabilité chimique et mécanique lors du pompage d'une solution de n-butylamine concentrée (60% v/v).

Fig. 3. Stabilité chimique et mécanique lors du pompage d'une solution de tétrahydrofurane concentrée (60% v/v).

les graphiques correspondent à $\pm 3^{\circ}/_{\circ\circ}$ pour $T(t)$. Les autres erreurs sont négligeables ou interviennent sur des valeurs constantes.

En complément, le Tableau II résume les observations faites sur les divers tubes à la fin des essais.

Conclusion

La résistance tant mécanique que chimique des divers tubes de pompe disponibles varie énormément avec le matériau et le solvant utilisés, comme l'indique le Tableau III.

On peut conclure que:

TABLEAU III

VARIATION TOTALE DE $Q(t)$ ENTRE $t=80^a$ ET $t=150$ POUR LES DIVERS TUBES DE POMPE DISPONIBLES

Solvant	*Silicone*	*Standard*	*Solvaflex*	*Acidflex*
Eau	7°/₀₀	0°/₀₀	32°/₀₀	59°/₀₀
BTA (60%)	100°/₀₀	234°/₀₀	—[b]	—[b]
THF (60%)	5°/₀₀	—[b]	—[b]	—[b]

[a] Le temps nécessaire pour stabiliser le tube est largement atteint. [b] Tube détruit.

avec l'eau, il n'y a pas d'attaque chimique du matériau. Seule la résistance mécanique à l'usure joue un rôle dans le choix de ce dernier. On retiendra donc le tube "standard", pour son prix également.

avec la n-butylamine et le tétrahydrofurane, les deux facteurs interviennent de manière conjuguée, limitant de façon beaucoup plus nette la durée de vie des tubes. On retiendra donc le tube "silicone".

Pour des concentrations encore plus élevées en n-butylamine et en tétrahydrofurane, les tubes en "silicone" sont encore acceptables, mais leur durée d'utilisation en est d'autant plus réduite.

RÉSUMÉ

La résistance à l'attaque chimique et à l'usure mécanique des "tubes" (tuyaux) de pompe Technicon a été étudiée lors de l'emploi de solutions aqueuses riches en solvants organiques hétéropolaires, tels la n-butylamine et le tétrahydrofurane. Les résultats des mesures de débit effectuées sur plus de 200 h avec des tubes en "tygon" (ou PVC), en "solvaflex", en "acidflex rouge", "acidflex noir" et en "silicone" indiquent que seul ce dernier matériau est acceptable pour les solvants précités. Avec les autres tubes, on arrive très rapidement à la dissolution, au relâchement complet ou à la rupture. Une comparaison effectuée dans les mêmes conditions avec de l'eau distillée permet d'apprécier l'importance respective de l'attaque chimique et de l'usure mécanique.

SUMMARY

The resistance of Technicon pump tubing to mechanical usage and chemical attack was studied for aqueous solutions rich in heteropolar organic solvents such as n-butylamine and tetrahydrofuran. The results of flow-rate measurements, over 200 h, with "tygon" (PVC), "solvaflex", "acidflex" (black/red) and "silicone" tubing indicate that only the last is acceptable for use with the above-mentioned solvents. With the other types of tubing there is rapid solubilization, deformation or rupture of the material. A comparison carried out under identical conditions with distilled water allows the respective importance of chemical attack and mechanical usage to be assessed.

ZUSAMMENFASSUNG

Es wurde die chemische und mechanische Beständigkeit von Schläuchen,

wie sie für Technicon Pumpen gebräuchlich sind, bei der Verwendung von konzentrierten wässerigen Lösungen heteropolarer organischer Lösungsmittel (n-Butylamin und Tetrahydrofuran) untersucht. Die Messung der Durchflussmessungen über mehr als 200 Stunden bei Schläuchen aus "Tygon" (PVC), "Solvaflex", "Acidflex rot", "Acidflex schwarz" und "Silikon" ergaben, dass einzig "Silikon"-Schläuche bei der Verwendung der oben erwähnten Lösungen eine brauchbare Lebensdauer aufweisen. Bei allen anderen Materialien erfolgte eine mehr oder weniger rasche Erweichung und Auflösung oder ein Zerreissen der Schläuche. Eine unter gleichen Bedingungen durchgeführte Untersuchung mit destilliertem Wasser als Lösungsmittel zeigte, welche Veränderungen durch chemische Einwirkungen und welche durch mechanische Beanspruchung und Alterung des Materials verursacht werden.

BIBLIOGRAPHIE

1 M. A. Blaivas and A. H. Mencz, *Automation in Analytical Chemistry: Technicon Symposium, 1966*, Vol. 1, Mediad Inc., New York, 1967, pp. 368–372; *Technicon Symposium, 1967*, Vol. 1, 1968, pp. 133–136.
2 H. E. Gould and A. Brooks, *Automation in Analytical Chemistry: Technicon Symposium, 1966*, Vol. 1, Mediad Inc., New York, 1967, pp. 378–382.
3 H. E. Gould, *Automation in Analytical Chemistry: Technicon Symposium, 1967*, Vol. 1, Mediad Inc., New York, 1968, pp. 141–146.
4 J. R. Cooke and P. B. Stockwell, *Lab. Pract.*, 20 (2) (1971) 125.
5 J. Davidson, J. Mathieson and A. W. Boyne, *Analyst*, 95 (1970) 181.
6 Technicon, *General Operating Instruction Manual*, Section M, p. 11.

Analytica Chimica Acta, 68 (1974) 339–362

© Elsevier Scientific Publishing Company, Amsterdam – Printed in The Netherlands

CHEMILUMINESCENCE IN ANALYTICAL CHEMISTRY

U. ISACSSON and G. WETTERMARK

Division of Physical Chemistry, The Royal Institute of Technology, 100 44 Stockholm 70 (Sweden)

(Received 2nd April 1973)

Chemiluminescence arises when a chemical reaction produces an electronically excited state which emits light as it returns to its ground state. Such reactions are common in biological systems where the phenomenon is called bioluminescence. In the latter part of the 19th century it was found that rather simple organic (non-biological) compounds could also give rise to chemiluminescence. Thus, Radziszewski[1] found that lophine (2,4,5-triphenylimidazole) emitted green light when it reacted with oxygen in alkaline solution. This discovery was published in the year 1877. Today many chemiluminescent systems are known, biological as well as non-biological, but, despite intensive studies the detailed mechanisms involved are largely unknown.

The quantum yield of chemiluminescence, *i.e.* the number of emitted photons divided by the number of reacting molecules, is often very low. The development of sensitive photomultipliers has made it possible to follow very weak luminescence[2,3], even when the quantum yield is as low as 10^{-15}. The possibility of measuring small amounts of light also means that sensitive analytical methods based on luminescence can be developed. By using reactions where the quantum yield is of the order 0.01–1, these analytical methods often attain exceedingly high sensitivities.

The phenomenon of chemiluminescence has been discussed in several review articles[2–6]. However, analytical applications have been dismissed in only a few words or not mentioned at all. One notable exception is measurements of air pollutants. Excellent review articles[7–9] have recently been published covering this area. There is also a long article by Bark and Wood[10] entitled *Photoluminescence and Chemiluminescence in Inorganic Analysis*; this is, however, almost completely devoted to analyses where fluorescence and phosphorescence techniques are employed.

The present review covers the general field of analytical methods based on the recording of chemiluminescence. It omits analysis carried out with the help of extracts from bioluminescent organisms.

ANALYSIS IN THE GAS PHASE

The development of chemiluminescent methods for determining components of a gas has largely originated from the great need for determining atmospheric pollutants. Although chemiluminescence analysis in general has engaged scientists for less than a decade, several methods are already in practical use. Some of

these reactions take place entirely in the gas phase and will now be described. (A gas mixture may also be analysed by means of a reagent in solution or adsorbed on a solid carrier. Such methods will be described later, *e.g.* for oxygen, ozone, chlorine and nerve gases.)

Sulphur compounds

Sulphur compounds are important atmospheric pollutants, especially sulphur dioxide. The development of a hydrogen-rich flame photometric detector[11,12] means that such substances can now be readily analysed. In this detector, a strong luminescence arises when volatile compounds of phosphorus or sulphur are present. The reaction in the flame is a reduction. In the case of sulphur dioxide and other sulphur compounds, electronically excited sulphur is formed[13,14].

$$SO_2 + 2H_2 \rightarrow S + 2H_2O$$
$$S + S \rightarrow S_2^*$$
$$S_2^* \rightarrow S_2 + h\nu \text{ (300–425 nm)}$$

With appropriate optical filters, it is possible to record a characteristic band at 394 ± 5 nm, and a selectivity for sulphur compounds (compared to non-sulphur compounds) of at least 10,000:1 can be reached[13]. The detector is said to be sensitive for p.p.b. quantities of phosphorus compounds and less than p.p.m. quantities of sulphur compounds[12] (p.p.b. = parts per 10^9). Chromatography can be used to separate various sulphur compounds occurring as pollutants, *e.g.* SO_2, H_2S, CH_3SH, CH_3–S–CH_3 and CS_2[13]. As mentioned above, the luminescence arises from the S_2 molecule, which is formed in an excited state when sulphur atoms recombine in the flame.

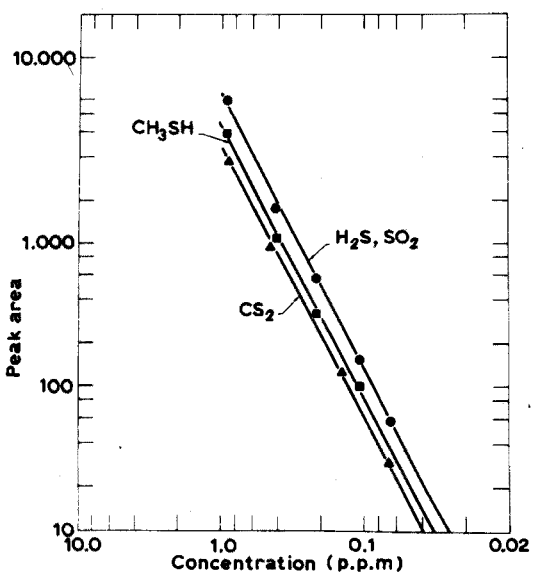

Fig. 1. Area response of the gas chromatographic–flame photometric detection to varying concentrations of some sulphur pollutants (from ref. 15).

The signal should thus be proportional to the square of the sulphur atom concentration. In experiments[15], log–log plots of peak size against concentration yielded a straight line with a slope of 2 for a wide range of concentrations (Fig. 1). The apparatus is fully automatic, analysing a sample every 5 min[7]. It can be obtained commercially from several manufacturers[8].

The reaction between sulphur dioxide and oxygen atoms is chemiluminescent[16].

$$O^{\cdot} + O^{\cdot} + SO_2 \rightarrow O_2 + SO_2^*$$
$$SO_2^* \rightarrow SO_2 + h\nu \ (\lambda_{max} = 280 \text{ nm})$$

This reaction has been suggested for the determination of sulphur dioxide, and a sensitivity of 0.001 p.p.m. has been reported[17,9]. A primary difficulty encountered in this type of analysis consists in finding a stable oxygen atom source[9].

Ozone

Beams of fast electrons in air generate concentrations of ozone which may be health hazards. In laboratories dealing with such beams, efficient ventilation is thus needed. Efficient control of the ventilation system demands a suitable method of determining ozone. Nederbragt *et al.*[18] have treated this problem and developed a chemiluminescent method by which ozone can be determined in a reaction with ethylene. Light is emitted between 300 and 600 nm, and is believed to arise from an excited aldehyde linkage[19,20]. The intensity is directly proportional to the ozone concentration. Stevens and Hodgeson[7] have further developed this method and constructed monitors for field use. Sensitivity is reported to be 3 p.p.b. The stability of the analyser has been evaluated by continuous recording of ozone in the air around Los Angeles during 60 days. A drift in calibration of less than 2% was reported.

Ozone detectors based on the Nederbragt method are available from several instrument manufacturers[8].

Nitrogen oxides

For the determination of nitrogen oxides different chemiluminescence methods are available. One method employs the reaction between nitric oxide and ozone[7,8,21–23].

$$NO + O_3 \rightarrow NO_2^* + O_2$$
$$NO_2^* \rightarrow NO_2 + h\nu \ (600\text{–}2800 \text{ nm})$$

Linear response is obtained from 1 p.p.b. up to 10,000 p.p.m. of nitric oxide[8]. None of the following substances interfered with the determination of nitric oxide (at concentrations occurring in atmospheric pollutants): NO_2, CO_2, C_2H_4, NH_3, SO_2 and H_2O[21]. Stevens has investigated the use of such a detector in the field. Thus, the proportion of nitric oxide in the atmosphere near St. Louis, Missouri, was recorded continuously for three months with negligible drift in the apparatus[7]. The same instrument has been employed for measuring the concentration of nitrogen dioxide[23]. Here, thermal catalytic conversion of nitrogen dioxide to nitric oxide must precede the actual analysis. There have been difficulties in making this reaction selective enough. Ammonia may also be present in the

atmosphere, and it too can be converted to nitric oxide. This problem has been reported[23] to be solved by using gold wool at 240° as a catalyst; at this temperature, nitrogen dioxide is quantitatively converted to nitric oxide, but ammonia does not react at all. If the temperature is increased to more than 300° both ammonia and nitrogen dioxide are converted to nitric oxide. A nitric oxide detector may thus be used for measuring NO, or $NO+NO_2$ or $NO+NO_2+NH_3$, by changing the conditions of catalysis. A scrubber is described which specifically removes ammonia[22, 23].

Nitrogen oxides can also be measured through reactions with atomic oxygen[7, 8].

$$NO+O^{\cdot} \rightarrow NO_2^{*} \rightarrow NO_2+h\nu \text{ (450–1800 nm)}$$
$$NO_2+O^{\cdot} \rightarrow NO+O_2$$

This second reaction is faster than the reaction between atomic oxygen and nitric oxide. Thus the sum of the NO and NO_2 concentrations is given. Fontijn *et al.*[21] claim that a higher sensitivity can be reached with the NO_x/O detector than with the NO/O_3 detector. For measuring the nitric oxide concentration only, a silica gel scrubber can be used to remove nitrogen dioxide[7].

The problems of finding suitable O-atom sources have hitherto limited the usefulness of this method[9] (*cf.* sulphur compounds). Oxygen atoms are produced when nitrogen dioxide is photolyzed. In subsequent reaction with nitrogen oxide of the type shown above luminescence arises. This photofragmentation technique[24, 25] is of recent origin and its usefulness is at present hard to assess. A limit of detection of about 0.001 p.p.m. has been reported.

Another means of measuring nitric oxide also employs ozone[7]. In this case a steady ozone stream is fed into a reaction chamber and mixed with the sample of air containing nitric oxide. The ozone concentration is continuously registered in a Nederbragt detector (*cf.* section on ozone analysis). The fast gas phase reaction between ozone and nitric oxide reduces the ozone concentration and thus the output from the photomultiplier of the Nederbragt detector. The decrease in output is proportional to the nitric oxide concentration. The method requires a very stable ozone generator.

Finally, the reactions between hydrogen atoms and nitrogen oxides are also accompanied by chemiluminescence[26].

$$H^{\cdot}+NO_2 \rightarrow NO+{}^{\cdot}OH$$
$$H^{\cdot}+NO+M \rightarrow HNO^{*}+M$$
$$HNO^{*} \rightarrow HNO+h\nu \text{ (650–760 nm)}$$

Its usefulness in analytical applications is limited by the rather weak emission of the luminescent species. A sensitivity of 0.1 p.p.m. has been reported.

Several commercial instruments are available for the determination of nitrogen pollutants[8].

Other compounds

At reduced pressures oxygen atoms and carbon monoxide react to form luminescent species, which emit at about 400 nm. The reaction has been used

for determination of carbon monoxide[17] but so far only a very poor sensitivity has been achieved (limit of detection about 100 p.p.m.). The theoretical limit of detection appears to be several orders of magnitude higher[21].

In a hydrogen–air flame, boron compounds produce intense emission from BO_2 at about 550 nm[27]. This fact has been used for the design of a portable instrument which detects pentaborane in concentrations of less than 0.1 p.p.m.[28].

Organic halides, such as chloroform, iodomethane, and carbon tetrachloride luminesce in a hydrogen–air flame and p.p.m. quantities of such compounds have been determined[29]. Chlorine compounds may be detected by means of a specific flame technique[30]. The sample is burned in hydrogen to produce hydrogen chloride, which is allowed to react with indium metal placed above the flame. In a second flame, the indium chloride produced yields a characteristic line emission spectrum with the strongest peak at 360 nm. Chlorine at the p.p.m. level can be determined. It is believed that the limit of sensitivity is set by the purity of the indium metal and that considerably smaller quantities of chlorine compounds could be determined with indium of higher quality.

ANALYSIS IN THE LIQUID PHASE*

Important chemiluminescent systems

For analytical applications in the liquid state, a few different species are of particular importance—the organic substances luminol and lucigenin and inorganic siloxenes. These systems will be described before their analytical applications are presented.

Luminol. The chemiluminescence of luminol (5-amino-2,3-dihydro-1,4-phthalazinedione) was first described by Albrecht in 1928[31]. Many acylhydrazides have since been checked for their ability to chemiluminesce[32a]. All the compounds examined containing the group

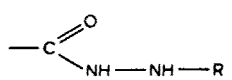

are active. If R is hydrogen, a simple carboxylic acid hydrazide is obtained. A diacylhydrazide results if R consists of another acyl group. Strong chemiluminescence is obtained only from cyclic diacylhydrazides of the same type as luminol. Substitution in the ring structure has a marked influence on the luminescence. Luminol has one of the highest quantum yields. Values between 0.01 and 0.05 have been reported depending on conditions in the solution.

To obtain chemiluminescence from luminol in water, an alkaline solution is needed and also a potent oxidizing agent. For an efficient reaction, other components may also be needed, *e.g.* a metallic catalyst. Despite intensive studies, the mechanism of luminol oxidation in water has not been fully elucidated[32b]. In polar organic solvents such as dimethylsulphoxide, efficient chemiluminescence may be obtained by alkaline oxidation of luminol with oxygen and no other

* Under this heading the very few analyses carried out in or at the solid state are also included.

additives. In this reaction the dianion of 3-aminophthalic acid is obtained in an electronically excited state, yielding a blue light[33,34].

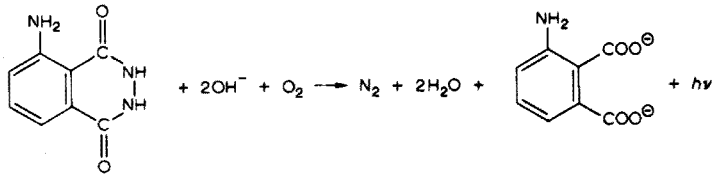

Luminol Dianion of 3-aminophthalic acid

Lucigenin. A blue-green chemiluminescence arises during alkaline oxidation of lucigenin (N,N'-dimethyldiacridinium dinitrate) with hydrogen peroxide[35]. The quantum yield of the process[36] is about 0.01–0.02. The emitting substance is believed to be N-methylacridone[36].

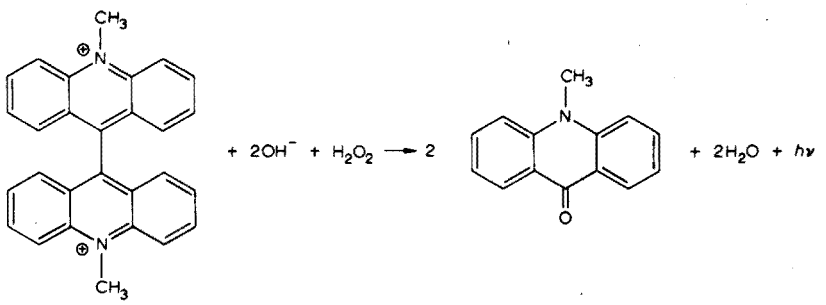

Dication of lucigenin N-Methylacridone

It is considered that the detailed mechanism involves an oxidation step followed by a reduction[32c]. N-Methylacridinium salts react in a similar way[37,38].

The lucigenin reaction is strongly influenced by catalysts and inhibitors. This forms the basis of several analytical applications.

Siloxene. Siloxene and its derivatives are highly polymerized solids[39,40]. They have a permutoid structure, which means that they form a more or less isolated network having a thickness the size of a molecule and where all reacting groups are quantitatively accessible for external agents. The siloxene unit, $Si_6H_6O_3$, consists of a silicon-6-ring. To each silicon atom an oxygen atom is attached, also serving as a bridge to a neighbouring Si-6-ring (Fig. 2).

In siloxene, two bonds are particularly reactive, the Si–H and Si–Si bonds. The six hydrogen atoms of the siloxene unit may be replaced by groups such as halogens, hydroxyl, amino and carboxylic acid esters, without loss of permutoid structure. Siloxene is a potent reducing agent. Si–Si bonds can add oxygen or chlorine or react with water or ammonia, evolving hydrogen.

In very rapid oxidations, *e.g.* by hydrogen peroxide or permanganate in acidic solution, intense chemiluminescence appears. The colour of the light depends on the oxidizing agent, the degree of oxidation and also the colour of the siloxene derivative. The strongest chemiluminescence is not obtained when a particular siloxene derivative is oxidized but with a substance previously called "silicone". This substance was first prepared by Friedrich Wöhler in 1863, using calcium silicide and concentrated hydrochloric acid[41]. Silicone has a variable

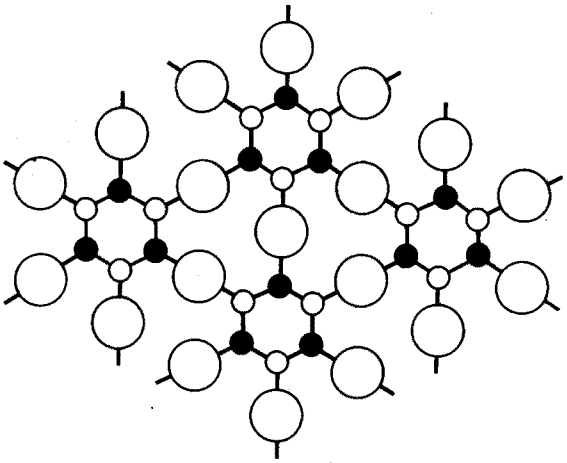

Fig. 2. Schematic figure of a siloxene net. Small circles: silicon; large circles: oxygen. Hydrogen atoms omitted.

composition of siloxene, polyhydroxysiloxene, polychlorosiloxene and different forms of oxidized siloxene where Si–O–Si bonds occur. The relative amounts of these components in the product depend on the method of its preparation. In a well-organized network structure, as in siloxene, it is reasonable to assume that energy can easily be transferred within the network. This energy can become localized to a reactive spot and give rise to various reactions. The presence of hydroxysiloxene in the structure is believed to be responsible for the emission of light. Chemiluminescence could be a result of the liberation of energy in the silicone network when it is oxidized. This energy could be transferred to the unchanged hydroxysiloxene, where light is emitted.

Acid–base titrations

The use of chemiluminescent indicators in acid–base titrations is based on the fact that such indicators only emit light in an alkaline environment. Thus bases as well as acids may be titrated to a point where light is quenched or where light appears. Titration is often carried out by visual end-point detection, but in some cases photoelectric aids have been employed. The advantage of chemiluminescent indicators over conventional dye indicators is that strongly coloured or turbid solutions may be titrated. Examples of such applications are the determination of the acidity of milk, red wine, fruit juice and mustard[42]. The determination of the acid and saponification numbers of dark coloured fats and oils has been reported[43,44]. This latter method of determining acid number has been reported to be as accurate as potentiometric titrations[43]. In measuring colourless solutions, the accuracy and precision have been reported to be the same as with conventional dye indicators[42,45,46]. In chemiluminescent acid–base titrations all indicator systems hitherto employed contain hydrogen peroxide. Such indicators cannot be used with heavy metals as the hydrogen peroxide is decomposed before end-point is reached[42]. The following indicator systems have been used in acid–base titrations: luminol–H_2O_2–catalyst[45,46], lucigenin–H_2O_2[42,47],

luminol–fluorescein–H_2O_2[48], lucigenin–fluorescein–H_2O_2[49] and lophine–H_2O_2–catalyst[42,50].

Redox titrations

Three different luminescent indicators have been found suitable for redox titrations. Usually an oxidizing agent is used as titrant, and titration is carried out to the point where light emission begins. In some cases, it is also possible to use a reducing agent as titrant and carry out the titration until light emission ceases. However, this latter procedure presupposes that the indicator is not destroyed because of reacting too rapidly. Table I presents some indicators and oxidizing agents employed.

TABLE I

INDICATORS AND OXIDIZING AGENTS FOR REDOX TITRATIONS BASED ON RECORDING OF CHEMILUMINESCENCE

Indicator	Luminol	Lucigenin	Siloxene
Oxidizing agents	OCl^-	H_2O_2	Ce^{4+}
	OBr^-		MnO_4^-
			$Cr_2O_7^{2-}$

Luminol as indicator[42,51–53]. In redox titrations, luminol may be used as indicator when hypochlorite or hypobromite is used as titrant in alkaline solution. Luminol is oxidized and luminesces. The hypohalite serves in most cases as the titrant and the titration is carried out until light is emitted. It should be noted that it is not possible to carry out titrations in the presence of ammonia or ammonium salts, as they also react with hypochlorites. A sodium hypobromite solution has been used to titrate the following ions: As^{3+}, Sb^{3+}, SCN^-, CN^-, $S_2O_3^{2-}$, SO_3^{2-}, S^{2-}. Accuracy and precision are high; twelve consecutive titrations of 20 ml of 0.1 *N* arsenic(III) gave an accuracy of -0.05% and a precision of $\pm 0.02\%$. Hypochlorite does not react with all reducing agents as quickly as hypobromite and is therefore often less suited for direct titrations. By carrying out the titration at an elevated temperature (80°) it is possible to determine arsenic(III), antimony(III) and thiosulphate. Hydrazine has been titrated with hypochlorite. Titrations in the opposite direction, *i.e.* with the hypohalite as the titrand, are also possible. In this case it is advisable to dissolve the indicator in the titrant solution, *e.g.* arsenite solution; this avoids the risk of using up the indicator before the end-point.

Chlorates, bromates and chlorites do not interfere even when present in large amounts. For example, the method yields good results in analysing chlorinated lime where 4% of the active chlorine is present in the form of chlorite. The accuracy of the method in analyses of chlorine or bromine water and also detergents containing hypochlorites is better than that obtained by iodometric titration.

Lucigenin as indicator[42,54]. As described above, lucigenin emits light when it is oxidized with hydrogen peroxide in alkaline solution. If, in addition to lucigenin, another substance is present which also reacts with the peroxide, light

emission starts only when peroxide is in excess. Lucigenin may thus be used to indicate the end-point in titrations with hydrogen peroxide, and in this case lucigenin acts reversibly. Potassium hexacyanoferrate(III), arsenic(III) and alkaline hypohalite solutions are good examples of substances which may suitably be titrated in this way. It is, however, necessary to carry out some of these titrations at an elevated temperature (80°). The amount of free halogen in chlorine or bromine water can also be determined very precisely by this method. As lucigenin does not react with any other oxidizing agent but hydrogen peroxide, hypohalites in alkaline solution may also be titrated in the presence of chromates. This makes the method suitable for determination of chromium(III).

Siloxene as indicator[42,55–57]. When siloxene indicator is subjected to a rising potential, as is the case in titrations with an oxidizing agent, a sufficiently high potential causes an emission of light from the indicator. The siloxene indicator has the desired ability to react instantaneously when a small excess of oxidant is present. No catalyst is required. A disadvantage of siloxene is that it is only active in acidic solutions and that the indicator acts irreversibly.

TABLE II

OXIDIZING AGENTS USED AS TITRANTS AND SUBSTANCES ANALYSED IN REDOX TITRATIONS WITH SILOXENE INDICATOR

Titrant	Ce^{4+}	$Cr_2O_7^{2-}$	MnO_4^-	
			Direct analysis	*Indirect analysis*
Test substance	Fe^{2+}	Fe^{2+}		
	As^{3+} [a]		As^{3+}	
			Ti^{3+}	
	Hydroquinone	Hydroquinone		
			Sn^{2+}	
			Mo^{3+}	
	I^-		I^-	
				I_2^- [c]
				IO_3^- [c]
				IO_3^- [d]
				Ag^+ [e]
				V^{5+} [f]
	H_2O_2		H_2O_2	
	$C_2O_4^{2-}$ [b]		$C_2O_4^{2-}$	

[a] The titration must be carried out at 50° and in the presence of iodine monochloride catalyst. [b] OsO_4 as catalyst. [c] After reduction with zinc to iodide. [d] After addition of an excess of iodide solution of known concentration. [e] AgI is precipitated by adding an excess of iodide which is then titrated in the presence of the precipitate. [f] After adding iron(II) in excess.

Kenny and Kurtz[55] found that a potential of about +1.17 V has to be reached before the indicator emits sufficient light to be detected. The siloxene indicator has been very useful in several redox titrations. Table II lists substances which have been determined with siloxene indicator, with various oxidizing agents as titrants. Table III illustrates the accuracy in such titrations.

TABLE III

PERMANGANATE TITRATIONS OF THREE DIFFERENT IONS WITH SILOXENE AS INDICATOR[a]

(n = number of titrations, V = volume of titrand, $\Delta\bar{x}$ = accuracy, σ_x = standard deviation)

Ion	n	V (ml)	$\Delta\bar{x}$ (%)	$\sigma_{\bar{x}}$ (%)
I^-	6	20	+0.12	±0.10
Fe^{2+}	6	20	−0.12	±0.04
Sn^{2+}	6	30	±0.0	±0.03

[a] See ref. 56.

Other types of titrations

Precipitation titrations. If a solution containing lead(II) ions is titrated with potassium chromate solution, a precipitate of lead chromate is formed. The end-point can be observed with the help of the siloxene indicator, which emits light when a small excess of oxidizing agent is present (+1.17 V, see above)[58]. The method has also been used for an indirect determination of sulphate by precipitating lead sulphate and titrating the excess of lead(II)[59].

Several ions, *e.g.* cadmium(II), form precipitates with hexacyanoferrate(III) and can be determined by precipitation techniques[60].

Complexiметric titrations. Complexing the ions of a catalytic heavy metal causes characteristic changes in the chemiluminescence of luminol and lucigenin[61,62]. If a heavy metal ion is titrated with EDTA containing hydrogen peroxide, the end-point may be detected with luminol or lucigenin. When this method is used, direct titration of the following ions is possible: Cu^{2+}, Cd^{2+}, Zn^{2+}, Ni^{2+}, Ca^{2+}, Sr^{2+} and Ba^{2+} [61–63]. In an indirect method[61], lead(II) and mercury(II) are determined by adding EDTA in excess and back-titrating with copper(II) solution. The method is also suitable for micro-titrations[61,63].

Argentometric titration. If an alkaline iodide solution which also contains lucigenin is titrated with silver nitrate solution, lucigenin as a positive ion will be adsorbed on the precipitated silver iodide which is negatively charged with iodide. In this way, lucigenin is prevented from emitting light even when hydrogen peroxide is present. When all iodide has been precipitated, the end-point is reached and the negative surface-charge of the precipitate is eliminated. Lucigenin is then desorbed, and the solution starts to luminesce. It is thus possible to use lucigenin as an adsorption indicator in argentometric titrations of iodide[61]. If the solution is made alkaline with ammonia solution, titration may also be carried out in the presence of chloride and bromide ions, since the corresponding silver salts are soluble in ammonia. In twelve parallel titrations of 20 ml of 0.1 *M* iodide, the standard deviation was ±0.16%. The mean value was the same as the theoretical value.

Titrations in organic solvents. By accident, Dimbat and Harlow[64] found that titrations in other solvents than water are frequently accompanied by weak chemiluminescence, even in the absence of an indicator. At the equivalence point a sharp peak is obtained. The phenomenon has been studied in the case of

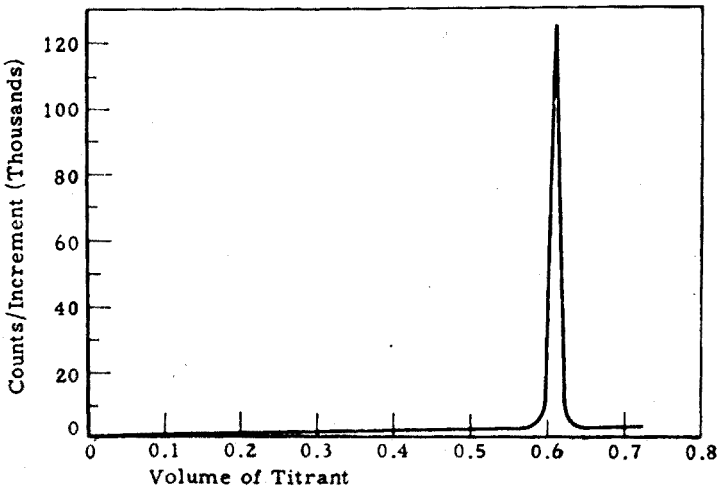

Fig. 3. Luminescent titration of 0.106 meq. hydrochloric acid (1.00 ml of 0.106 *M* HCl (IPA)) in isopropyl alcohol with tetra-n-butyl-ammonium hydroxide (0.175 *N* TBAH (IPA)) (from ref. 64).

acid–base titrations and also titrations of metal alkyls. The results of a titration are shown in Fig. 3 where hydrochloric acid in isopropyl alcohol is titrated with tetrabutylammonium hydroxide. Sulphuric acid in pyridine can also be titrated with tetrabutyl ammonium hydroxide; the result is interesting, because an additional smaller peak was obtained at the position corresponding to the first hydrogen of sulphuric acid, and another considerably stronger maximum was recorded at the equivalence point corresponding to the titration of both hydrogens. No end-point could be detected with aqueous solutions, even at 5 *N*. When metal alkyls, *e.g.* aluminum triisobutyl, are titrated with oxygen in an inert hydrocarbon solvent, a luminescence is observed which is of the same type as that for acid–base titrations; the peak corresponds to the point where one atom of oxygen is taken up by each aluminium atom in the sample. This method for end-point detection in organic solvents is interesting theoretically, but is unlikely to achieve many practical applications[64]. In every case, the mechanism of these luminescence phenomena is essentially unknown.

Determination of inorganic substances based on chemiluminescence measurement

Several metal ions have a pronounced catalytic effect on many chemiluminescent reactions. Frequently, the maximum light intensity is strongly increased and the duration decreases[32d,62]. Optimal conditions for analysis are first determined, *e.g.* pH and concentration of each component in the reagent, and then a calibration curve is prepared by measuring the emission as a function of amount of metal catalyst. Either maximal light intensity or total amount of light may be used as the dependent variable.

Some metal ions have been analysed by recording their inhibiting effect on a chemiluminescent system which is catalysed by some other metal ion. Vanadium, zirconium, cerium and thorium may be determined in this way.

Certain organic substances, *e.g.* a mixture of *o*-phenanthroline and sodium

TABLE IV

DETERMINATION OF METALS BY CHEMILUMINESCENCE

Metal	*Action*	*System*	*Sensitivity*[a] *(μg)*	*Detection*	*Ref.*
V[b]	Inh	Luminol–H_2O_2–$[Co(NH_3)_4(NO_2)_2]Cl$	0.04	Photographic	69
Cr (Cr^{3+})[c]	Cat	Luminol–H_2O_2	0.00003	Photoelectric	66
Mn (MnO_4^-)[d]	Oxidant	Siloxene	0.1	Photographic	70
Mn	Cat	Lucigenin–H_2O_2	1	Photographic	71
Mn	Cat	Lucigenin–H_2O_2–org. amine	0.1	Photographic	72
Mn[e]	Cat	Luminol–H_2O_2–activator	0.00008	Photoelectric	65
Fe[f]	Cat	Luminol–H_2O_2–diethylene-triamine	0.0002	Photoelectric	73
Fe (Fe^{2+})[g]	Cat	Luminol–O_2	0.000005	Photoelectric	74
Co	Cat	Luminol–H_2O_2	0.002	Photographic	75
Co	Cat	Lucigenin–H_2O_2	1		76
Cu[h]	Cat	Luminol–H_2O_2	0.03	Photographic	77
Zr[i]	Inh	Luminol–H_2O_2–Cu^{2+}		Photographic	78
Ag	Cat	Lucigenin–H_2O_2	0.1	Photographic	79
Ce[j]	Inh	Luminol–H_2O_2–Cu^{2+}	0.1	Photographic	80
Os[k]	Cat	Lucigenin–H_2O_2	1		81
Hg	Cat	Luminol–H_2O_2	0.2	Photographic	82
Tl[l]	Cat	Lucigenin–H_2O_2		Photoelectric	83
Pb	Cat	Lucigenin–H_2O_2	0.5	Photographic	84
Bi	Cat	Lucigenin–H_2O_2	5	Photographic	85
Th[m]	Inh	Luminol–H_2O_2–cat	1	Photographic	86

[a] Sensitivity: The minimal amount that can be detected. Authors have defined sensitivity in various ways. The above definition has been chosen in order to allow comparison. Most figures in this column were worked out from the values reported in the original papers. [b] The analysis utilizes the effect of vanadium as a quencher of the system luminol–Co^{3+} complex–H_2O_2. Niobium and tantalum do not quench the luminescence, in contrast to vanadium. [c] Analysis is carried out in a flow system. Interference from other metal ions is eliminated by adding EDTA. The complex Cr^{3+}–EDTA is formed much more slowly than complexes between other metal ions and EDTA. A linear relation between peak height and Cr^{3+} content is obtained up to a Cr^{3+} concentration of 10^{-6} *M*. Samples may be analysed in the field without any other preparation than adding EDTA. Cr^{3+} is active as a catalyst but not Cr^{6+}. As the biological effects of Cr^{3+} and Cr^{6+} differ, the method may be employed for selective determination of chromium ions in water. [d] Light emission results from the reaction between siloxene and permanganate. Mn^{2+} may be determined by oxidation to permanganate with ammonium persulphate in the presence of $AgNO_3$. [e] To increase selectivity and sensitivity, luminol is oxidized in the presence of an activator—a mixture of *o*-phenanthroline and sodium citrate. [f] Diethylenetriamine activates the reaction between luminol and H_2O_2 catalysed by Fe^{3+}. [g] Analysis is carried out in a flow system. It utilizes the fact that Fe^{2+} ions catalyse the reaction between luminol and oxygen. Of the common metal ions, only Fe^{2+} has this ability. Selectivity is therefore high, though excessive quantities of certain ions influence the light reaction. [h] The chemiluminescent determination of copper in high-purity zinc, cadmium and alkali has been described[87,88]. [i] The analysis is based on the quenching effect of zirconium on the reaction between luminol and H_2O_2 catalysed by Cu^{2+} ions. [j] Measurement of reduction in luminescence of the system luminol–H_2O_2–Cu^{2+} in the presence of Ce^{4+} ions. [k] OsO_4 is measured. [l] The method is applicable in determining low concentrations (*ca.* 10^{-5}%) of thallium in indium[83]. [m] Th^{4+} inhibits the light reaction in the system luminol–H_2O_2–catalyst. Cu^{2+} as well as hemin has been employed as catalyst.

citrate, may activate a chemiluminescent reaction catalysed by a metal ion. Thus they increase the sensitivity of the method[65]. The fact that metal ions are active catalysts may also give rise to problems. In a quantitative analysis for a particular cation, other ions may interfere. It is sometimes possible to eliminate such ions with a suitable complexing agent[66].

Table IV lists metals which can be determined in micro-amounts by measuring chemiluminescence.

Chemiluminescent analysis of metals may also be carried out by means of the so-called candoluminescent technique. In this technique light emission is obtained from a radical recombination process in a hydrogen diffusion flame[67]. The metal to be analyzed is fixed in the flame by means of a matrix, usually solid calcium hydroxide. The method is suitable for the determination of bismuth, lead, manganese, antimony and some lanthanides. In a recent communication[68], amounts of bismuth varying from 5 to 1000 μg were determined by monitoring the emission at 399 nm. The future value of this method is at present hard to assess, as the work in the area is rather limited.

Several analyses for inorganic compounds are based on the luminescence accompanying the alkaline oxidation of luminol. Table V describes some of these. Water is the solvent in all cases except in the analysis for oxygen, which is

TABLE V

DETERMINATION OF INORGANIC SUBSTANCES BY CHEMILUMINESCENCE

Substance determined	*Action*	*System*	*Sensitivity[a] (μg)*	*Detection*	*Ref.*
H_2O_2[b]	Oxidant	Luminol–hemin	0.01	Visual	89
	Oxidant	Luminol–Cu^{2+}	0.1	Photographic	77
	Oxidant	Luminol–$[Co(NH_3)_4(NO_2)_2]Cl$	0.002	Photographic	69
Cl_2–ClO^-[c]	Oxidant	Luminol–H_2O_2	0.5	Photographic	90
I_2	Oxidant	Luminol	1	Photographic	91
$K_3Fe(CN)_6$	Oxidant	Luminol	0.3	Photographic	92
CN^-[d]	Inh	Luminol–H_2O_2–Cu^{2+}		Photoelectric	93
S^{2-}	Inh	Luminol–I_2	0.005	Photographic	94
Halides[e]		Luminol–Na_3PO_4–$NaBO_3$			95
O_2[f]	Oxidant	Luminol–$(CH_3)_2SO$–tert-butyl alcohol		Photoelectric	96

[a] Cf. footnote *a* in Table IV. [b] The content of H_2O_2 in industrial brines[97] and water from the river Volga[98] has been determined in this way. [c] Chlorine–hypochlorite in industrial brines[97] and in municipal drinking water[90] has been determined by this method. Chloramine will not influence the light reaction[90]. [d] The luminol oxidation is retarded by cyanide. This leads to an induction period which varies with the CN^--content. The method has been employed for analysing sea water. Cyanide concentrations as low as 3 p.p.m. are determined with a relative error of about 3%. [e] Chloride is electrochemically converted into free chlorine. Chloride concentrations of 10^{-5} g l^{-1} have been determined. Iodides and bromides may also be determined by the method. [f] It has been reported that an oxygen production of 10^{-13} moles s^{-1} can be recorded. Changes in oxygen concentrations of 0.01 p.p.m. in a gas or 10^{-11} *M* in water have been detected.

carried out in a polar organic solvent, dimethylsulphoxide.

Ozone. The determination of ozone in the gas phase has already been discussed (see Analysis in the gas phase, p. 339). The analyses described below depend on reaction in the liquid phase or with the reagent adsorbed on a solid carrier.

Exposure to ozone induces chemiluminescence of rhodamine B. This effect was used by Regener for the determination of ozone, rhodamine B being adsorbed on silica gel[99]. (Luminol was also investigated but was found less suitable[100].) An important disadvantage of the rhodamine B–silica gel system used by Regener is its sensitivity to humidity. Hodgeson *et al.*[101] have however eliminated this problem by treating the gel surface with a hydrophobic agent. Today, this method is the most sensitive one for determining ozone. It is reported that even 1 p.p.b. can be detected. The method is also highly selective. None of the following substances interfere: SO_2, H_2S, NO_2, C_3H_8, H_2O, NH_3, Cl_2 or H_2O_2. Figure 4 shows the vertical distribution of ozone in the atmosphere up to an altitude of 60 km. Analyses are based on the chemiluminescence of rhodamine B measured by a rocket-borne sonde for ozone.

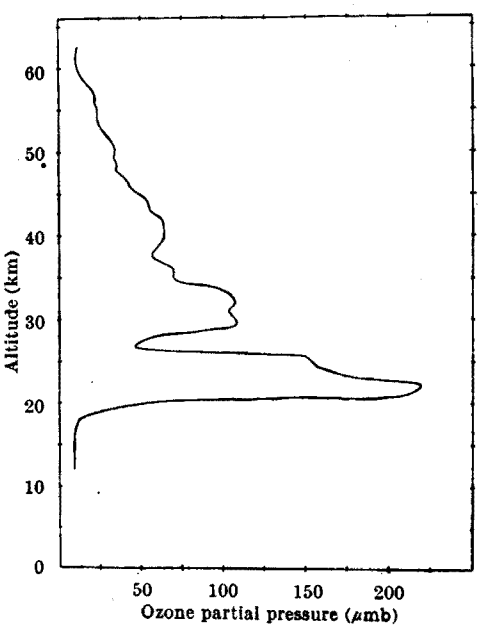

Fig. 4. Vertical distribution of ozone at White Sands Missile Range, New Mexico, on June 15, 1966 (from ref. 102).

Ozone detectors in the liquid phase have also been described, *e.g.* by Bersis and Vassiliou[103]. They used a system consisting of rhodamine B and gallic acid in ethanol. A linear relationship between light emitted and amount of ozone was demonstrated down to 0.0003% (v/v). The above authors say this is probably not the ultimate sensitivity of the method. They report a reproducibility better than $\pm 1\%$.

Determination of organic compounds based on chemiluminescence measurements

Several organic compounds modify chemiluminescent reactions. Table VI compares data on analyses for organic compounds based on such effects. The

TABLE VI

DETERMINATION OF ORGANIC SUBSTANCES BY CHEMILUMINESCENCE

Substance (or group of substances)	*Action*	*System*	*Sensitivity*[a] *(μg)*	*Detection*	*Ref.*
Amino acids	Cat[b]	Luminol–H_2O_2	150 (glycine)	Photoelectric	104
	Inh[b]	Luminol–H_2O_2		Photoelectric	105
Cysteine	Inh	Luminol–I_2	0.01	Photographic	94
Hematin compounds	Cat	Luminol–H_2O_2		Photoelectric	106
Ferritin			2		
Cytochrome c			0.025		
Myoglobin			0.0001		
Hemoglobin			0.0001		
Hematin			0.00006		
Catalase			0.0001		
Organic phosphorus compounds					
Nerve gases, type Sarin		Luminol–sodium perborate–trisodium phosphate	0.5	Photoelectric	107
Insecticides, type Isopestox	Cat	Luminol–H_2O_2	200	Photoelectric	108, 109
Tabun (nerve gas)	Cat	Lucigenin–sodium perborate	100	Photoelectric	110
Isomeric benzene derivatives, containing NO_2, NH_2 and OH groups	Inh	Luminol–H_2O_2 –Cu^{2+}–NH_4OH	400 (phenol)	Photoelectric	111
Naphthols	Inh	Luminol–H_2O_2 –Co^{2+}	20 (1-nitroso--2-naphthol)	Photographic	112

[a] Cf. footnote *a* in Table IV. [b] Amino acids serve as quenchers in the system luminol–H_2O_2–copper amine, enabling their direct determination. However, in the form of a copper complex the amino acids catalyse the luminescence. They can therefore also be analysed in a two-step procedure. First the amino acid reacts with a suitable copper salt to form the copper–amino acid complex, which is then analysed by measuring the light. The direct method is somewhat less sensitive than the two-step method, but the analytical procedure is much simpler.

effect of a compound is named catalytic or inhibiting depending on whether it amplifies or weakens the light reaction. However, in some cases this classification may be incorrect, as it is believed that the compound is consumed in the reaction.

It is notable that very small quantities of different hematin complexes can be determined (see next section). As appears from Fig. 5, a linear relationship between light pulse and amount of substance is obtained for a large number of hematin compounds. According to Neufeldt *et al.*[106] hematin itself is believed to be responsible for the catalytic effect. The iron in hemoglobin, myoglobin and catalase is associated with porphyrin but at the high pH values encountered in the analysis, rapid dissociation takes place and the hematin part is separated from the protein.

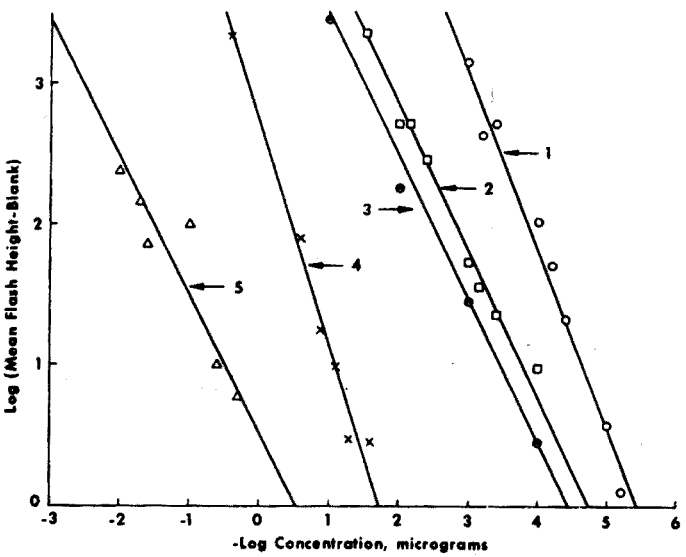

Fig. 5. Effect of concentration of iron-containing compounds on light production: (○) Hematin; (□) catalase; (●) hemoglobin; (×) cytochrome c; (△) ferritin (from ref. 106).

Chemiluminescent techniques for microanalysis of nerve gases were first proposed by Goldenson[107] in 1957 (Table VI). The developer contains sodium perborate, which serves as oxygen-donor and as a buffer to maintain a suitable pH value (pH 9). A blue-green light becomes visible when the nerve gas dissolved in isopropanol is added to the developer. Maximal intensity is obtained after about 15 s and is linearly related to the amount of nerve gas. Free chlorine interferes strongly. In the above system luminol is employed. The possibility of using lucigenin for nerve-gas determination has also been investigated[110], but only Tabun responded positively.

Insecticides of the organophosphorus type can be quantitatively assessed with the help of an alkaline solution of luminol and hydrogen peroxide[108,109]. Isopropanol solutions of the insecticide are used, as they are particularly stable. Essentially a linear relation exists between maximal intensity and the amount of

compound. Minute amounts of insecticides in food such as flour, sugar and rice can be indicated by this method[109]. The insecticides are easily hydrolysed, but this does not influence their toxicological determination. Hydrolyzed phosphoric acid esters are non-toxic and do not activate the luminol chemiluminescence[109].

It has been observed that chemiluminescent reactions are modified by many other organic substances than those mentioned in Table VI. Analytical procedures may thus possibly be developed for these substances, by means of emission measurements. Tentative experiments in this direction have been carried out for aliphatic alcohols[113,114], poly-alcohols[115] and oximes[116], as well as l-ascorbic acid[113], pyridine[113], pyrimidine[113] and acetylcholine[117]. Binary mixtures of aliphatic alcohols may also be analyzed[114]. Figure 6 illustrates typical results of such assays.

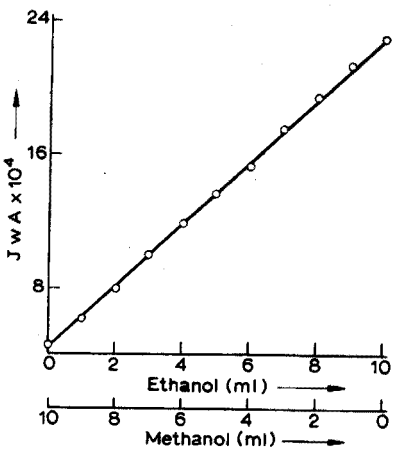

Fig. 6. Effect of mixtures of methanol and ethanol on photoelectric current. Constant volume of alcohol mixture, 10 ml. Chemiluminescent system: alkaline solution of diphenyl-diacridinium-dinitrate and hydrogen peroxide (from ref. 114).

SPECIAL APPLICATIONS

Identification of blood stains (forensic chemistry)

A very sensitive method for the determination of blood stains was first described by Specht[118]. It is based on the way blood catalyses the luminol oxidation; this is due to hemoglobin (see above). Specht employed the system luminol–sodium carbonate–hydrogen peroxide. He discussed the selectivity of the method and found that most substances frequently occurring as contaminants in forensic work do not interfere with the reaction. In particular, he mentioned that no luminescence is caused by rust or other metal oxides, which are known to cause rapid decomposition of hydrogen peroxide.

A disadvantage of Specht's reagent is that it only reacts for dried (denatured) blood. Weber[119] states that this problem may be eliminated by using a different mixture. Sodium hydroxide replaces sodium carbonate, and considerably lower concentrations of hydrogen peroxide and luminol are employed (higher concentrations lead to inhibition). The fact that Weber's reagent also reacts with fresh

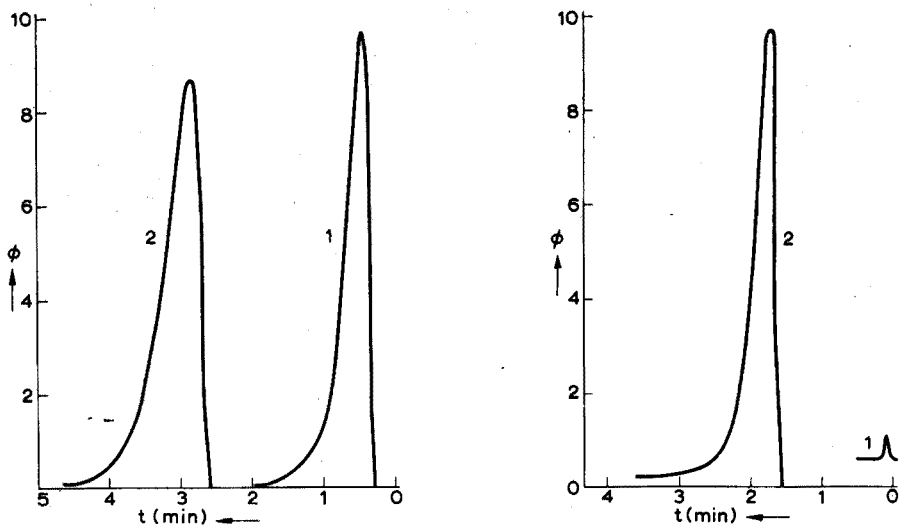

Fig. 7. Intensity–time graphs (ϕ–t) of luminol chemiluminescence after addition of blood solution (1:100,000). (1) Dried blood; (2) fresh blood (from ref. 119).

Fig. 8. Intensity–time graphs (ϕ–t) of luminol chemiluminescence at addition of a solution of dried blood (1:100,000). (1) Specht's reagent; (2) Weber's reagent (from ref. 119).

blood has been explained thus[119]: in strongly alkaline solution containing hydrogen peroxide, there is rapid oxidation to methemoglobin or denaturation to hematin. In contrast to hemoglobin, both of these activate the chemiluminescence of luminol. Figure 7 illustrates that fresh and denatured blood give similar responses. Weber's reagent has other advantages: it is more stable and much more sensitive (Fig. 8). Blood is detectable even when diluted $1:10^7$. Selectivity is high, for few contaminants yield the same strong catalytic effect on the luminol system. However, a relatively large number of substances quench the luminescence. In forensic work, the inhibition caused by urine is particularly important.

Analysis for microorganisms

It is well known that air and water serve as carriers for pathogenic microorganisms. Suitable methods for detecting such organisms are therefore required. Such a method should above all have fast response, high sensitivity and high selectivity. The present authors do not know of any method fully meeting all these requirements.

Oleniacz *et al.*[120,121] found that microorganisms activate the chemiluminescence of luminol in alkaline solution. They employed two different detector systems: one used luminol with sodium perborate; the other used luminol with sodium pyrophosphate peroxide ($Na_4P_2O_7 \cdot 2H_2O_2$). Maximal light intensity was reached within 1 min after the addition of a sample, and complete analysis required about 4 min. The requirement of high sensitivity was satisfactorily met; 10^3–10^5 cells of bacteria per ml of water were easily determined. A linear relationship existed between maximal light intensity and amount of microorganisms for all organisms studied, *e.g. Escherichia coli, Proteus mirabilis* and *Salmonella*

typhimurium. However, it is not possible to determine selectively a certain organism in a mixed population. Another disadvantage of the method is the great sensitivity to chemical contaminants. It has been reported that this difficulty may be overcome in the case of airborne microorganisms; a bacterial filter is used and the sample is analysed before and after being filtered. In the case of waterborne samples this difficulty is more serious. A great number of chemicals (*e.g.* metal ions) activate the luminol chemiluminescence (see above).

Results which indicate that such interference problems can be solved have been reported by Ewetz and Thore[122]. They found that preincubation of the sample and timing of the analysis is of great importance. By using the following procedure, interference from iron and hexacyanoferrate(III) ions can be eliminated: sample and perborate are mixed for 60 s and sodium hydroxide is added; 15 s after addition of alkaline luminol, the light emission is measured. The method has been successfully used for detecting microbiological material in urine. No special treatment of the urine is needed.

Chemiluminescence induced by ozone

Bowman and Alexander[123] observed luminescence from a great many organic compounds on reaction with ozone. It occurs both when the compound is adsorbed on a silica gel surface and when it is dissolved in an organic solvent. The peak height of the emission is linearly related to the amount of organic substance present. Thus quantitative analysis is possible. The limit of detection of many substances lies in the nanogram range or better. Sensitivity is thus comparable to that of many fluoresence methods. The above authors believe that the method is applicable to the analysis of certain chromatograms.

Determination of pore size

Rosenberg and Shombert[124] have indicated a method of determining pore size in an adsorbent by measuring chemiluminescence. A suitable dye is adsorbed on the substance, the pore size of which is to be measured. The dye is excited in a vacuum and its phosphorescence is recorded. When oxygen is suddenly supplied, the decay rate increases, but light emission also starts in another wavelength range. This is due to chemiluminescence of a product formed in the reaction with oxygen. If this light is recorded, the oxygen sensitivity is increased by about two orders of magnitude, compared to recording phosphorescence (system acriflavine–silica gel)[125]. The luminescence decay was found to depend on the rate at which oxygen penetrated the pores of the adsorbent[124]. In two samples identical except for pore size, the decay was more rapid in the gel with larger pores; this was probably because of oxygen penetrating to the dye more rapidly. Rosenberg and Shombert say it should be possible to estimate pore sizes in the range 10–1000 Å from a known relation between pore size and decay curve.

Dosimetry

Hydrogen peroxide is formed when water is exposed to high-energy radiation. It is easy to measure with the help of luminescence from, *e.g.*, the luminol system (see p. 346). In this way, Armstrong and Humphreys[126] constructed a sensitive chemical dosimeter for use in radiation chemistry. Such dosimeters allow the determination of doses below 1000 rads—often the most interesting range of

radiobiology. (The first design of this kind was published in 1955 by Mayneord *et al.*[127], who employed phthalic hydrazide instead of luminol as the chemiluminescent substance.) It is obviously important that the response of the dosimeter depends only on the dose for different types of radiation, *i.e.* it must be independent of linear energy transfer. This demand is often difficult to satisfy in chemical dosimetry, and it is interesting that Armstrong and Humphreys succeeded so well. They obtained direct proportionality between signal (total luminescence) and dose over a range wider than 100–1000 rads when they exposed a system consisting of luminol and copper(II) ions to different types of radiation (*cf.* the G-values in Table VII).

TABLE VII

$G(H_2O_2)$-VALUES OBTAINED BY IRRADIATING WATER WITH BEAMS OF DIFFERENT LINEAR ENERGY TRANSFER[126]

Radiation	*Mean linear energy transfer (eV Å^{-1})*	*$G(H_2O_2)$ (molecules/100 eV)*
^{60}Co γ-ray	0.02	1.22 ± 0.07[a]
250-kVcp X-ray	0.20	1.28 ± 0.09
14-MeV neutron	1.2	1.31 ± 0.04

[a] Standard deviations.

Degradation of polymers

Ashby[128] discovered in 1961 that several polymers, *e.g.* nylon, emit weak light when heated. The phenomenon has been named oxyluminescence as it is caused by oxidative processes and requires the presence of oxygen. At 150° about 10^4 carbonyl groups are formed per emitted photon when polypropylene is oxidized in this way. The presence of an anti-oxidant reduces the emission during a certain initial period. Oxyluminescence may therefore be employed for estimating the stability of a polymer towards oxidative degradation. It may also be used to estimate the ability of a certain chemical to act as an anti-oxidant.

Mechanical treatment, *e.g.* pulverization, of certain polymers in an atmosphere containing oxygen is also accompanied by a weak chemiluminescence[129]. Such polymers are quartz, polyoxymethylene, polystyrene, polyethylene and polymethylmethacrylate. This emission proceeds for about 10–15 min after the treatment; it is believed that the light is caused by recombination of certain radicals. The degree of such mechanical degradation of a polymer can be determined by recording chemiluminescence. The method is said to be 10–100 times more sensitive than ESR or viscosimetry[129]. Special equipment has been constructed for studying luminescent polymers[130,131].

Flows in liquids

Liquid flows can be studied with the help of chemiluminescence as suggested by Friedman[132]. If a solution of luminol and hexacyanoferrate(III) is injected into an alkaline solution containing hydrogen peroxide, the flow boundary is marked by intense luminescence. This is clearly better than following the course

of the flow by injecting a coloured solution. In the latter case, the colour is most intense in the centre of the flow. Applications of Friedman's method are described in a recent paper by Bien *et al.*[133].

CONCLUSION

Measurement of chemiluminescence promises to become an interesting analytical technique. Methods based on it have already achieved wide application. The apparatus is often simple and can easily be modified for field use. Components can be procured and assembled at low cost.

Analysis is rapid and very high sensitivities are often possible. The main difficulty is, particularly in the liquid state, to make the analysis sufficiently selective, *i.e.* to find a system which only reacts with the chemical to be analysed. Most methods have been developed fairly recently and large areas of application are probably still waiting to be investigated.

Permission to reproduce Figs. 1 and 3–8 has been granted. The assistance of the respective authors and editors is gratefully acknowledged.

SUMMARY

Analytical applications based on chemiluminescence are reviewed. Analyses in the gas phase for atmospheric pollutants such as sulphur compounds, ozone and oxides of nitrogen are described. The commonest chemiluminescent systems used in the liquid phase are then discussed. Their applications as indicators in different types of titration are outlined. Determinations of organic and inorganic substances are classified according to their action as oxidant, catalyst or inhibitor. Special applications are described in fields such as forensic science, microbiology, polymer technology, radiation chemistry and flow mechanics.

RÉSUMÉ

On passe en revue les applications analytiques, basées sur la chimiluminescence. On décrit des analyses en phase gazeuse pour le dosage de polluants atmosphériques tels que composés soufrés, ozone, et oxydes d'azote. On examine également les systèmes chimiluminescents les plus courants, en phase liquide, et leurs applications comme indicateurs dans différents types de titrages. Les dosages de substances organiques et inorganiques sont classés suivant leur action comme oxydant, catalyseur ou inhibiteur. Diverses applications dans des domaines spéciaux sont décrites.

ZUSAMMENFASSUNG

Es wird ein Überblick über analytische Anwendungen der Chemilumineszenz gegeben. Analysen in der Gasphase auf atmosphärische Verunreinigungen wie Schwefelverbindungen, Ozon und Stickoxide werden beschrieben. Die am weitesten verbreiteten chemilumineszierenden Systeme, die in der flüssigen Phase angewendet

werden, werden diskutiert. Deren Verwendung als Indikatoren bei verschiedenen Arten von Titrationen wird erläutert. Die Bestimmungen von organischen und anorganischen Substanzen werden nach ihrer Wirkung als Oxydationsmittel, Katalysator oder Inhibitor eingeteilt. Spezielle Anwendungen auf verschiedenen Gebieten werden beschrieben.

REFERENCES

1 B. Radziszewski, *Ber.*, 10 (1877) 70, 321.
2 T. I. Quickenden, *J. New Zealand Inst. Chem.*, 28 (1964) 10.
3 F. McCapra, *Quart. Rev.*, (1966) 485.
4 H. Stork, *Chem.-Ztg.*, 85 (1961) 467.
5 K.-D. Gundermann, *Angew. Chem.*, 77 (1965) 572.
6 K.-D. Gundermann, *Naturwiss.*, 56 (1969) 62.
7 R. K. Stevens and J. A. Hodgeson, New Instrument for Measurement of Gaseous Pollutants, presented at the *Int. Air Pollution Control and Noise Abatement Conf., Jönköping, Sweden, 1971.*
8 R. K. Stevens and J. A. Hodgeson, *Anal. Chem.*, 45 (1973) 443A.
9 J. A. Hodgeson, A Review of Chemiluminescent Techniques for Air Pollution Monitoring, to be published in *Toxicol. Environ. Chem. Rev.*
10 L. S. Bark and P. R. Wood, Photoluminescence and Chemiluminescence in Inorganic Analysis, in *Sel. Annu. Rev. Anal. Sci.*, Vol. 1, The Society for Analytical Chemistry, London, 1971.
11 W. L. Crider, *Anal. Chem.*, 37 (1965) 1770.
12 S. S. Brody and J. E. Chaney, *J. Gas Chromatogr.*, 4 (1966) 42.
13 R. K. Stevens, J. D. Mulik, A. E. O'Keeffe and K. J. Krost, *Anal. Chem.*, 43 (1971) 827.
14 R. K. Stevens, A. E. O'Keeffe and G. C. Ortman, *Environ. Sci. Technol.*, 3 (1969) 652.
15 R. K. Stevens, A. E. O'Keeffe and G. C. Ortman, *ISA Trans.*, 9 (1970) 1.
16 M. F. R. Mulcahy and D. J. Williams, *Chem. Phys. Lett.*, 7 (1970) 455.
17 A. D. Snyder and G. W. Wooten, *Final Report*, Environmental Protection Agency, Research Triangle Park, N.C., Contract No. CPA-22-69-8, NTIS PB-188-103, 1969.
18 G. W. Nederbragt, A. van der Horst and J. van Duijn, *Nature*, 206 (1965) 87.
19 J. A. Hodgeson, B. E. Martin and R. E. Baumgardner, Preprint, Environmental Protection Agency, Research Triangle Park, N.C., *Eastern Analytical Symposium, New York, N.Y., 1970*, Paper No. 77.
20 J. N. Pitts, Jr., W. A. Kummer, R. P. Steer and B. J. Finlayson, *Amer. Chem. Soc. Adv. Chem. Ser.*, 113 (1972) 246.
21 A. Fontijn, A. J. Sabadell and R. J. Ronco, *Anal. Chem.*, 42 (1970) 575.
22 J. A. Hodgeson, K. A. Rehme, B. E. Martin and R. K. Stevens, Measurements for Atmospheric Oxides of Nitrogen and Ammonia by Chemiluminescence, *1972 Air Pollution Control Association Meeting, Miami, Fla., 1972*, Paper No. 72-12.
23 J. A. Hodgeson, J. P. Bell, K. A. Rehme, K. J. Krost and R. K. Stevens, Application of a Chemiluminescence Detector for the Measurements of Total Oxides of Nitrogen and Ammonia in the Atmosphere, *Joint Conference on Sensing of Environmental Pollutants*, American Institute of Aeronautics and Astronautics, New York, N.Y., 1971, Paper No. 71-1067.
24 J. A. Hodgeson and W. A. McClenny, *164th National ACS Meeting, New York City, Aug. 30, 1972*, Paper No. Watr.-61.
25 W. A. McClenny, J. A. Hodgeson and J. P. Bell, *164th National ACS Meeting, New York City, Aug. 30, 1972*, Paper No. Watr.-60.
26 K. J. Krost, J. A. Hodgeson and R. K. Stevens, *Publication Preprint*, Environmental Protection Agency, Research Triangle Park, N.C., 1972.
27 E. J. Sowinsky and I. H. Suffet, *J. Chromatogr. Sci.*, 9 (1971) 632.
28 R. S. Braman and E. S. Gordon, *IEEE Trans.*, Vol. IM-14 (1965) 11.
29 W. L. Crider, *Anal. Chem.*, 41 (1969) 534.
30 P. T. Gilbert, *Anal. Chem.*, 38 (1966) 1920.
31 H. O. Albrecht, *Z. Phys. Chem.*, 136 (1928) 321.

32 K. D. Gundermann, *Chemilumineszenz organischer Verbindungen*, Springer, Berlin–Heidelberg–New York, 1968. (a) p. 65, (b) p. 74, (c) p. 97, (d) p. 77.
33 E. H. White, O. Zafiriou, H. M. Kägi and J. H. M. Hill, *J. Amer. Chem. Soc.*, 86 (1964) 940.
34 E. H. White and M. M. Bursey, *J. Amer. Chem. Soc.*, 86 (1964) 941.
35 K. Gleu and W. Petsch, *Angew. Chem.*, 48 (1935) 57.
36 J. R. Totter, *Photochem. Photobiol.*, 3 (1964) 231.
37 F. McCapra and D. G. Richardson, *Tetrahedron Lett.*, (1964) 3167.
38 F. McCapra, D. G. Richardson and Y. C. Chang, *Photochem. Photobiol.*, 4 (1965) 1111.
39 *Gmelins Handbuch der anorganischen Chemie. Si. Teil B*, 8. Aufl., 1959, p. 591.
40 H. Kautsky, *Kolloid-Z.*, 102 (1943) 2.
41 F. Wöhler, *Ann.*, 127 (1863) 263.
42 L. Erdey, *Ind. Chem.*, 33 (1957) 459, 523, 575.
43 E. Ya. Yarovenko and G. N. Kosheleva, *Zavod. Lab.*, 27 (1961) 407.
44 M. T. Kovats and Z. Paal, *Magy. Kem. Lapja*, 21 (1966) 489.
45 F. Kenny and R. B. Kurtz, *Anal. Chem.*, 23 (1951) 339.
46 F. Kenny and R. B. Kurtz, *Anal. Chem.*, 24 (1952) 1218.
47 L. Erdey, *Acta Chim. Acad. Sci. Hung.*, 3 (1953) 81.
48 L. Erdey, W. F. Pickering and C. L. Wilson, *Talanta*, 9 (1962) 371.
49 L. Erdey, J. Takács and I. Buzás, *Acta Chim. Acad. Sci. Hung.*, 39 (1963) 295.
50 L. Erdey and I. Buzás, *Acta Chim. Acad. Sci. Hung.*, 15 (1956) 322.
51 L. Erdey and I. Buzás, *Acta Chim. Acad. Sci. Hung.*, 6 (1955) 93.
52 L. Erdey and I. Buzás, *Acta Chim. Acad. Sci. Hung.*, 6 (1955) 115.
53 L. Erdey and I. Buzás, *Acta Chim. Acad. Sci. Hung.*, 6 (1955) 123.
54 L. Erdey and I. Buzás, *Acta Chim. Acad. Sci. Hung.*, 6 (1955) 77.
55 F. Kenny and R. B. Kurtz, *Anal. Chem.*, 22 (1950) 693.
56 L. Erdey, I. Buzás and L. Pólos, *Z. Anal. Chem.*, 169 (1959) 187.
57 L. Erdey, I. Buzás and L. Pólos, *Z. Anal. Chem.*, 169 (1959) 263.
58 F. Kenny and R. B. Kurtz, *Anal. Chem.*, 25 (1953) 1550.
59 F. Kenny, R. B. Kurtz, I. Beck and I. Lukosevicius, *Anal. Chem.*, 29 (1957) 543.
60 F. Kenny, B. Russel, R. B. Kurtz, A. C. Vandenoever, C. J. Sanders, C. A. Novarro, L. E. Menzel, R. Kukla and K. M. McKenny, *Anal. Chem.*, 36 (1964) 529.
61 L. Erdey and I. Buzás, *Anal. Chim. Acta*, 22 (1960) 524.
62 L. Erdey, O. Weber and I. Buzás, *Talanta*, 17 (1970) 1221.
63 P. Szarvas, I. Korondán and I. Raisz, *Magy. Kem. Foly.*, 72 (1967) 441.
64 M. Dimbat and G. A. Harlow, *Anal. Chem.*, 34 (1962) 450.
65 I. E. Kalinichenko, *Ukr. Khim. Zh.*, 35 (1969) 755.
66 W. R. Seitz, W. W. Suydam and D. M. Hercules, *Anal. Chem.*, 44 (1972) 957.
67 A. I. Bazhin, V. V. Styrov and V. A. Sokolov, *Russ. J. Phys. Chem.*, 44 (1970) 107.
68 R. Belcher, S. Bogdanski and A. Townshend, *Talanta*, 19 (1972) 1049.
69 A. K. Babko and N. M. Lukovskaya, *J. Anal. Chem. USSR*, 20 (1965) 1153.
70 A. K. Babko, L. I. Dubovenko and L. S. Mikhailova, *Sov. Prog. Chem.*, 32 (1966) 471.
71 L. I. Dubovenko and A. P. Tovmasyan, *J. Anal. Chem. USSR*, 25 (1970) 812.
72 L. I. Dubovenko and A. P. Tovmasyan, *Ukr. Khim. Zh.*, 37 (1971) 943.
73 I. E. Kalinichenko and O. M. Grishchenko, *Ukr. Khim. Zh.*, 36 (1970) 610.
74 W. R. Seitz and D. M. Hercules, *Anal. Chem.*, 44 (1972) 2143.
75 A. K. Babko and N. M. Lukovskaya, *Zavod. Lab.*, 29 (1963) 404.
76 J. Bognar and L. Sipos, *Mikrochim. Ichnoanal. Acta*, 3 (1963) 442.
77 A. K. Babko and N. M. Lukovskaya, *J. Anal. Chem. USSR*, 17 (1962) 47.
78 A. K. Babko, L. I. Dubovenko and L. S. Mikhailova, *Metody Anal. Khim. Reakt. Prep. No. 13*, (1969) 139.
79 A. K. Babko, A. V. Terletskaya and L. I. Dubovenko, *J. Anal. Chem. USSR*, 23 (1968) 809.
80 L. I. Dubovenko and Chan Ti Huu, *Ukr. Khim. Zh.*, 35 (1969) 637.
81 J. Bognar and L. Sipos, *Mikrochim. Ichnoanal. Acta*, 5–6 (1963) 1066.
82 L. I. Dubovenko and T. A. Bogoslovskaya, *Ukr. Khim. Zh.*, 37 (1971) 1057.
83 L. I. Dubovenko and A. P. Tovmasyan, *Ukr. Khim. Zh.*, 37 (1971) 845.
84 L. I. Dubovenko and L. D. Guz, *Ukr. Khim. Zh.*, 36 (1970) 1264.
85 L. I. Dubovenko and E. Ya. Khotinets, *Zh. Anal. Khim.*, 26 (1971) 784.

86 L. I. Dubovenko and Chan Ti Huu, *Ukr. Khim. Zh.*, 35 (1969) 957.
87 A. K. Babko and L. I. Dubovenko, *Zavod. Lab.*, 30 (1964) 1325.
88 L. I. Dubovenko and L. A. Pihpenko, *Visn. Küv. Univ. Ser. Khim.*, 11 (1970) 75.
89 W. Langenbeck and U. Ruge, *Ber.*, 70 (1937) 367.
90 A. K. Babko, A. V. Terletskaya and L. I. Dubovenko, *Ukr. Khim. Zh.*, 32 (1966) 728.
91 A. K. Babko, L. V. Markova and N. M. Lukovskaya, *J. Anal. Chem. USSR*, 23 (1968) 330.
92 A. K. Babko and I. E. Kalinichenko, *Ukr. Khim. Zh.*, 29 (1963) 527.
93 S. Musha, M. Ito, Y. Yamamoto and Y. Inamori, *Nippon Kagaku Zasshi*, 80 (1959) 1285.
94 N. M. Lukovskaya and L. V. Markova, *J. Anal. Chem. USSR*, 24 (1969) 1512.
95 V. N. Kachibaya, I. L. Siamashvili and M. V. Mamukashvili, *J. Anal. Chem. USSR*, 26 (1971) 1654.
96 A. Burr and D. Mayzerall, *Biochim. Biophys. Acta*, 153 (1968) 614.
97 N. M. Lukovskaya, A. V. Terletskaya and N. I. Isaenko, *Zavod. Lab.*, 37 (1971) 897.
98 V. E. Sinelnikov, *Gidrobiol. Zh.*, 7 (1971) 115.
99 V. H. Regener, *J. Geophys. Res.*, 69 (1964) 3795.
100 V. H. Regener, *J. Geophys. Res.*, 65 (1960) 3975.
101 J. A. Hodgeson, K. J. Krost, A. E. O'Keeffe and R. K. Stevens, *Anal. Chem.*, 42 (1970) 1795.
102 J. S. Randhawa, *Nature*, 213 (1967) 53.
103 D. Bersis and E. Vassiliou, *Analyst*, 91 (1966) 499.
104 A. A. Ponomarenko and L. M. Amelina, *J. Gen. Chem. USSR*, 35 (1965) 750.
105 A. A. Ponomarenko and L. M. Amelina, *J. Gen. Chem. USSR*, 35 (1965) 2252.
106 H. A. Neufeld, C. J. Conklin and R. D. Towner, *Anal. Biochem.*, 12 (1965) 303.
107 J. Goldenson, *Anal. Chem.*, 26 (1957) 877.
108 K. Weber, L. Huic and M. Mrazović, *Arh. Hig. Rada*, 9 (1958) 325.
109 K. Weber, J. Matković and M. Bušljeta, *Acta Pharm. Jugosl.*, 19 (1969) 47.
110 K. Weber and J. Matković, *Arch. Toxikol.*, 21 (1965) 38.
111 A. A. Ponomarenko and B. I. Popov, *J. Anal. Chem. USSR*, 19 (1964) 1300.
112 N. M. Lukovskaya and M. I. Gerasimenko, *J. Anal. Chem. USSR*, 26 (1971) 1462.
113 K. Weber, *Z. Phys. Chem.*, B50 (1941) 100.
114 M. Turowska, *Chem. Anal. (Warsaw)*, 6 (1961) 1051.
115 A. A. Ponomarenko, B. I. Popov, L. M. Amelina, L. V. Grishchenko and R. E. Shindel, *J. Gen. Chem. USSR*, 34 (1964) 4179.
116 K. Weber, J. Matković and D. Fleš, *Nature*, 191 (1961) 177.
117 E. Kunec-Vajic and K. Weber, *Experientia*, 23 (1967) 432.
118 W. Specht, *Angew. Chem.*, 50 (1937) 155.
119 K. Weber, *Dtsch. Z. Gesamte Gerichtl. Med.*, 57 (1966) 410.
120 W. S. Oleniacz, M. A. Pisano and M. H. Rosenfeld, *Automation in Analytical Chemistry, Technicon Symposia 1966*, Vol. I, Mediad. Inc., White Plains, N.Y., 1967, p. 523.
121 W. S. Oleniacz, M. A. Pisano, M. H. Rosenfeld and R. L. Elgart, *Environ. Sci. Technol.*, 2 (1968) 1030.
122 L. Ewetz and A. Thore, personal communication.
123 R. L. Bowman and N. Alexander, *Science*, 154 (1966) 1454.
124 J. L. Rosenberg and D. J. Shombert, *J. Phys. Chem.*, 65 (1961) 2103.
125 J. L. Rosenberg and D. J. Shombert, *J. Amer. Chem. Soc.*, 82 (1960) 3257.
126 W. A. Armstrong and W. G. Humphreys, *Can. J. Chem.*, 43 (1965) 2576.
127 W. V. Mayneord, W. Anderson, H. D. Evans and D. Rosen, *Radat. Res.*, 3 (1955) 379.
128 G. E. Ashby, *J. Polymer Sci.*, 50 (1961) 99.
129 M. U. Kislyuk and P. Yu. Butyagin, *Vysokomol. Soedin., Ser. B*, 9 (1967) 612.
130 I. F. Kaimin and Z. Z. Galeis, *Vysokomol. Soedin., Ser. A*, 9 (1967) 245.
131 L. Weissman, E. Schröder and K. Thinius, *Plaste Kautsch.*, 18 (1971) 188.
132 A. S. Friedman, *J. Appl. Phys.*, 27 (1956) 416.
133 F. Bien, W. Davidor and S. S. Penner, *Phys. Fluids*, 14 (1971) 885.

Analytica Chimica Acta, 68 (1974) 363–376
© Elsevier Scientific Publishing Company, Amsterdam – Printed in The Netherlands

THE DOUBLE RADIO-ISOTOPE DERIVATIVE TECHNIQUE FOR THE ASSAY OF DRUGS IN BIOLOGICAL MATERIAL

PART I. THE DETERMINATION OF MAPROTILINE

W. RIESS

Research Department, Pharmaceuticals Division, CIBA–GEIGY AG, Basle (Switzerland)

(Received 13th June 1973)

The double radio-isotope derivative (d.r.i.d.) technique in which one isotope is used to label an internal standard and another to label the reagent is a well established method in biochemistry and physiological chemistry. The assay of steroids[1–3], of catecholamines[4–7] and thyroxine[8] may serve as examples.

Surprisingly, only rudimentary application of this method is to be found in pharmacological chemistry, even though the method makes it possible to administer drugs which have not been radio-labelled and yet to take advantage of radio-tracer analysis. However, the technique requires, first, the radio-synthesis of the internal standard, and, secondly, proper laboratory facilities for handling high specific activities of reagents while keeping the background activity at the lowest possible level. These may be the reasons for the general reluctance to embark on this methodology. Once the necessary facilities have been installed, however, the double radio-isotope derivative technique proves to be a most efficient means of conducting pharmacokinetic studies in animal and man.

THE DOUBLE RADIO-ISOTOPE DERIVATIVE METHOD

The principle of the method

An aliquot of the material to be analysed (blood, plasma, urine, tissue homogenate, etc.) is homogeneously mixed with a definite amount of ^{14}C-labelled compound of the same structure as that to be assayed. By some suitable isolation process (*e.g.* extraction with organic solvents for lipophilic compounds; chromatography for hydrophilic compounds), the compound (^{14}C-standard plus unknown) is separated from the bulk of the biological material and a derivative is prepared with ^{3}H-labelled reagent. For primary and secondary amines as well as alcohols, ^{3}H-labelled acetic anhydride is the reagent of choice; yet any other suitable ^{3}H-labelled reagent can be used provided that its specific activity is sufficiently high to achieve the sensitivity required of the assay. Compounds which do not contain readily reactive groups must be chemically converted before derivatives can be prepared. For instance, tertiary amines can be degraded with bromine cyanide or ethylchlorocarbonate, and then reacted with ^{3}H-acetic anhydride; acids can be converted to the acid chlorides and then reacted with a suitable ^{3}H-labelled amine.

After the preparation of the derivative, an appropriate purification procedure (*e.g.*, extraction or thin-layer chromatography) is applied to separate the wanted ^{3}H-labelled derivative from interfering ^{3}H-labelled by-products of the reaction as well as from excess of ^{3}H-labelled reagent. In order to permit localization of the labelled derivative on the thin-layer plate, microgram amounts of the unlabelled derivative are added as carrier before the purification step.

Each sample emerging from the final purification process is analysed for both ^{3}H-activity and ^{14}C-activity by liquid scintillation counting with the discriminator-ratio method. Appropriately prepared standard samples allow calculation of the overall individual yield of the ^{14}C-internal standard in each sample. By means of the ^{14}C-yield found, the recovered ^{3}H-activity can be corrected to the equivalent of a theoretical 100% yield. The resultant ^{3}H-activity value can be converted to concentration units by the 100% ^{3}H-activity value resulting from an appropriate number of test samples which have been treated in exactly the same way as the unknown and contain a definite, known amount of trial compound.

Composition of sample series

Each series of analytical samples that finally undergoes radiometry should comprise the following sets A and B.

A. Sets of samples that have been taken through the whole purification and derivative preparation:

(*a*) the "unknowns", *e.g.* the blood samples to be assayed, to which internal ^{14}C-standard has been added;

(*b*) "blank" samples to which *only* ^{14}C-internal standard has been added;

(*c*) "blank" samples to which ^{14}C-internal standard plus a known amount of unlabelled standard has been added.

B. Sets of radiometric standards that are merely made up with the same liquid scintillation cocktail as that used for the samples under A:

(*a*) "blank" counting samples so that all other samples can be corrected for background activity;

(*b*) radiometric ^{3}H-standard samples so that the channel ratio of the ^{3}H-activity can be measured at the spectrometer setting chosen. Any suitable ^{3}H-labelled compound can be used for this purpose;

(*c*) radiometric ^{14}C-standard samples made up with the same compound (and preferably the same amount) that is used as the internal ^{14}C-standard in the probes under A.

Data collection and processing

From the sample sets A and B the following data emerge.

The primary known data are:

v (ml) = volume of samples in A (*a*, *b* and *c*) (blood, plasma, urine, etc.)
m(ng) = amount of *internal* ^{14}C-standard added to each probe in A (*a*, *b*, *c*)
n (ng) = amount of radiometric ^{14}C-standard used in each sample of B (*c*)
i (ng ml^{-1}) = unlabelled standard added per ml of samples A (*c*)

The radiometric raw data are:

blank H (c.p.m.) = count rate of blank samples B (*a*) in ^{3}H-channel
blank C (c.p.m.) = count rate of blank samples B (*a*) in ^{14}C-channel

H_1 (c.p.m.) = count rate of radiometric ^{3}H-standard, samples B (b), in ^{3}H-channel
H_2 (c.p.m.) = count rate of radiometric ^{3}H-standard, samples B (b), in ^{14}C-channel
C_1 (c.p.m.) = count rate of radiometric ^{14}C-standard, samples B (c), in ^{3}H-channel
C_2 (c.p.m.) = count rate of radiometric ^{14}C-standard, samples B (c), in ^{14}C-channel
N_1 (c.p.m.) = count rate of derivatized samples, samples A (a, b, c) in ^{3}H-channel
N_2 (c.p.m.) = count rate of derivatized samples, samples A (a, b, c) in ^{14}C-channel

The data which can be calculated are:

H_1^*; H_2^*; C_1^*; C_2^*; N_1^*; N_2^* (c.p.m.)
= radiometric raw data corrected by subtraction of blank count rate of samples B (a) in ^{3}H-channel and ^{14}C-channel, respectively.

$$\mathrm{a} = \frac{H_2^*}{H_1^*} = \text{channel ratio of the radiometric } ^3\text{H-standard samples in B } (b)$$

$$\mathrm{b} = \frac{C_2^*}{C_1^*} = \text{channel ratio of the radiometric } ^{14}\text{C-standard samples in B } (c)$$

$$S_{^{14}\mathrm{C}} = \frac{C_2^*}{n}\,(\text{c.p.m. ng}^{-1}) = \text{specific activity of the radiometric and of the internal } ^{14}\text{C-standard}$$

^{3}H (c.p.m.) = calculated genuine ^{3}H-activity in the samples A (a, b, c)

$$= \frac{b \cdot N_1^* - N_2^*}{b-a} \text{ (for derivation, see ref. 9).}$$

^{14}C (c.p.m.) = calculated genuine ^{14}C-activity in the samples A (a, b, c)

$$= \frac{\mathrm{b}\,(N_2^* - a \cdot N_1^*)}{b-a} \text{ (for derivation, see ref. 9).}$$

$$d\ \% = \frac{100 \cdot {}^{14}\mathrm{C}}{m \cdot S_{^{14}\mathrm{C}}} = \text{overall \% yield of the } ^{14}\text{C-activity of the internal } ^{14}\text{C-standard in the individual samples of A } (a, b, c).$$

d % of recovered ^{14}C-activity is identical theoretically with the % yield of the calculated genuine ^{3}H-activity in the samples A (a, b, c).

Thus we can write:

G (c.p.m.) = $^3\mathrm{H} \cdot 100/d$ = theoretical 100% yield of genuine ^{3}H-activity in the samples A (a, b, c), and

g^0 (c.p.m. ml^{-1}) = G/v = 100% ^{3}H-activity per ml of sample of series A.

If g (c.p.m. ml^{-1}) = g^0 (c.p.m. ml^{-1}) value of ^{3}H-activity from samples A (a),

g' (c.p.m. ml^{-1}) = g^0 (c.p.m. ml^{-1}) value of ^{3}H-activity from samples A (b),

and g'' (c.p.m. ml^{-1}) = g^0 (c.p.m. ml^{-1}) value of ^{3}H-activity from samples A (c),

then $g''-g'$ (c.p.m. ml^{-1}) = 100% ^{3}H-activity resulting from only the added *unlabelled* standard in samples of series A (c).

Thus

E (c.p.m. ng^{-1}) = $(g''-g')/i$ = specific ^{3}H-activity of originally unlabelled standard compound, after ^{3}H-acetylation,

and since

$g-g'$ (c.p.m. ml^{-1}) = 100% ^{3}H-activity resulting only from the unknown quantity of the substance to be analysed in samples of series A (a),

The final result will be:

$x=(g-g')/E$ = found concentration (ng ml^{-1}) of substance in the original "unknowns" of series A (a).

The radiometric raw data are preferably processed on a programmed desk computer. If the Hewlett-Packard computer Model 9100 B is used with an appropriately written program and work sheets such as Tables I–III, the radiometric raw data from the daily out-put of a well organized laboratory can be processed within 30 min.

THE DETERMINATION OF MAPROTILINE

The evaluation of the pharmacokinetic properties of maprotiline (Ciba 34 276-Ba; Ludiomil; 1-(3-methylaminopropyl)-dibenzo[*b*,*e*]bicyclo[2, 2, 2]-octadiene), which has recently been introduced for treatment of depressive illness in man[10], required the development of analytical techniques for assay of the drug in biological fluids. The procedure had to provide high selectivity and sensitivity, as well as sufficient capacity for large sample numbers.

A method has already been described for the determination of desmethylimipramine in biological fluids by single radio-isotope derivative formation[11,12]. This procedure, which ought to be applicable to the assay of any lipophilic primary or secondary amine, consists of the extractive isolation of the free base from the biological sample followed by reaction with ^{3}H-labelled acetic anhydride to form the corresponding radioactive acetamide; after elimination of the excess of reagent, the acetamide is determined by liquid scintillation counting.

An attempt to utilize this method for the assay of maprotiline resulted in unacceptable scatter of results. When the different steps of the procedure were tested by using ^{14}C-labelled maprotiline and unlabelled acetic anhydride, it appeared that the acetylation step was most critical. The yield of the acetyl derivative varied largely and could not be made reproducible within acceptable limits. In addition, when "blank" biological material was taken through the procedure with ^{3}H-labelled acetic anhydride, variable amounts of endogenous compounds and reagent blank interfered in the final stage where only the ^{3}H-acetyl derivative of maprotiline was to be radio-assayed.

Thus, it appeared obvious that if the radio-isotope derivative method was to work, there were two essentials: first a means of correcting for the variability of yields of the expected ^{3}H-acetylderivative, and secondly some means of attaining the necessary selectivity by eliminating the ^{3}H-acetyl products of the "biological

and chemical background". The first was achieved by addition of a known amount of ^{14}C-labelled maprotiline as an internal standard to the biological sample; the second requirement was fulfilled by the addition of unlabelled N-acetyl-maprotiline derivative as carrier and by two-dimensional thin-layer chromatography before the liquid scintillation counting.

Reagents and equipment

^{3}H-Acetic anhydride (500 mCi mmol^{-1}; Radiochemical Centre, Amersham) was diluted with unlabelled acetic anhydride in freshly distilled dried heptane, to give a solution of 50 μCi μmol^{-1} at a concentration of 20 μmol ml^{-1}. This working solution was stored in portions of 1 ml each in fused glass ampoules. Portioning into, and closing of, ampoules must be done with all the precautions necessary to exclude traces of moisture from pipets and ampoules. The charged ampoules were stored at 5°. If properly prepared, the same batch of ampoules can be used for more than one year.

^{14}C-Labelled maprotiline (5 μCi mg^{-1}; I). An aqueous solution containing 400 ng ml^{-1} and a methanolic solution containing 1000 ng ml^{-1} were used.

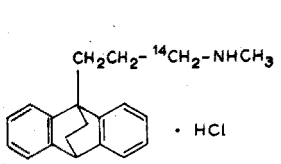

(I)

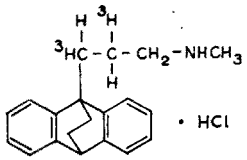

(II)

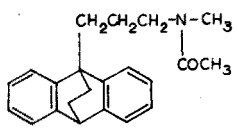

(III)

^{3}H-Labelled maprotiline (10 μCi mg^{-1}; II). A methanolic solution containing 1000 ng ml^{-1} was used, but any other ^{3}H-labelled compound may serve. This solution serves as a radiometric standard to determine the channel ratio of ^{3}H.

Unlabelled N-acetylmaprotiline (III). This was used as carrier.

All the other reagents used were of analytical grade.

For thin-layer chromatography, glass plates (20 × 20 cm) with a *ca.* 0.2–mm layer of silica gel Merck PF_{254} were used. The plates ready for use are commercially available from ANTEC AG, Birsfelden, Switzerland.

Radiometry was performed by means of a Tri-Carb Liquid Scintillation Spectrometer System, Model 3375 (Packard Instrument Co., U.S.A.) and the scintillator used was 2-(4-*tert.*-butylphenyl)-5-(4-biphenyl)-1,3,4-oxidiazole (Scintillator Butyl-PBD, Ciba–Geigy Ltd., Basle, Switzerland) at a concentration of 0.8% in distilled toluene.

Procedure

Extraction. Pipet a 1–3 ml aliquot of blood, or a suitable aliquot of biological fluid, into a conical plastic centrifuge tube, add 500 μl of an aqueous solution (0.4 μg ml^{-1}) of ^{14}C-labelled maprotiline (amount added, 200 ng) and shake for 5 min. Add 3 ml of borate buffer pH 10, and 10 ml of *n*-heptane containing 1% of isoamyl alcohol, shake for 15 min, and then centrifuge for 5 min.

Transfer the heptane phase to a 10-ml glass ampoule, add 1 ml of 0.05 *M* sulfuric acid, close the tube with a polyethylene stopper, shake for 15 min and

centrifuge. Suck off and discard the heptane phase. To the aqueous phase, add 0.5 ml of 1 *M* sodium hydroxide and 5 ml of *n*-heptane, shake for 15 min, and centrifuge. Transfer the heptane phase to a 5-ml glass ampoule, place the ampoule into a thermostated water-bath at 50°, and suck off solvent vapor by means of Pasteur pipets and a water aspirator. Store the ampoules in a desiccator overnight.

Acetylation. (This must be done in the controlled area of a glove box.) To the evaporation residue, add 50 µl of a 0.2% solution of ^{3}H-acetic anhydride in heptane (the amount added is equal to 50 µCi ^{3}H, and 1 µmol of acetic anhydride), followed by 100 µl of dry purified dioxane. Seal the ampoule with a polyethylene cap and heat at 60° in a thermostated metal block for 1 h.

Open the ampoule and evaporate the dioxane by heating to 50° for 15 min and gently sucking off the fumes with a water aspirator. (The aspirated air is passed through two wash bottles containing 5 *M* potassium hydroxide.) Add 2 ml of *n*-heptane and 0.5 ml of 0.1 *M* sodium hydroxide, reseal the ampoule, shake for 5 min, and centrifuge. Transfer the heptane phase carefully to a 2-ml ampoule and evaporate the heptane phase at 50°, sucking off the fumes with a water aspirator.

Chromatography. (This must be done in the controlled area of a fume hood.) To the evaporation residue, add 50 µl of a 0.1% solution of the unlabelled acetyl derivative of maprotiline in chloroform (amount added, 50 µg), and spot this solution on a silica gel thin-layer plate (the excitation wavelength for the fluorescent additive was 254 nm) in such a way as to allow two-dimensional chromatography. For the first dimension develop with (1+1) toluene–acetone to the 10-cm mark; the R_F value of the acetyl compound is *ca.* 0.6. Dry the plate in the fume hood and develop perpendicularly to the first run with (1+1) chloroform–ether, again for a length of 10 cm; the R_F value of the acetyl compound is *ca.* 0.5.

Radiometry. View the plate under the u.v. lamp and mark the spot of the carrier compound with a sharply pointed pin. Cut the plate close to the edge of the carrier spot and scrape the spot into a plastic counting vial containing 0.5 ml of methanol. Add 20 ml of butyl-PBD scintillator (0.8% in toluene) and count together with appropriately prepared standard and test samples (see

TABLE I

EVALUATION OF RADIOMETRIC STANDARDS

Radiometric standards		*Recorded counts*		*Specific activity*	*Ratio* ^{14}*C-channel* / ^{3}*H-channel*
Compound	*ng*	^{3}*H-channel (c.p.m.)*[a]	^{14}*C-channel (c.p.m.)*[a]	*(c.p.m. µg^{-1})*	
^{3}H-labelled maprotiline	500	6075	0.2	$S_{^{3}H} = 12150$	a = 0.000
^{14}C-labelled maprotiline	200	201	1316	$S_{^{14}C} = 6579$	b = 6.559

[a] Average values of four samples each, corrected for radiometric background.

TABLE II

"TWO-POINT CALIBRATION" MODE TO EVALUATE THE SPECIFIC ^{3}H-ACTIVITY OF ORIGINALLY UNLABELLED MAPROTILINE AFTER ^{3}H-ACETYLATION

Maprotiline conc. i(ng ml^{-1})	*Sample volume v (ml)*	*^{14}C-Internal standard added m (ng)*	*Yield of ^{14}C-standard d (%)*	*100% ^{3}H of derivative g (c.p.m. ml^{-1})*	*Mean and standard deviation*
0	3	200	29.1	5253	$\bar{g}' = 5145$
			36.9	5171	
			43.7	5040	$s(\bar{g}') = 41$
			35.1	5135	
166.7	3	200	23.7	17952	$\bar{g}'' = 18221$
			37.4	18600	
			40.9	18447	$s(\bar{g}'') = 178$
			49.0	17884	

Specific ^{3}H-activity $E = (18221 - 5145)/166.7 = 78.45$ (c.p.m. ng^{-1})

Composition of sample series) in the liquid scintillation spectrometer. Use the optimal discriminator setting for simultaneous counting of ^{3}H and ^{14}C.

Data processing. Evaluate the radiometric standards, the specific ^{3}H-activity of the derivative and the final concentrations in the biological samples as outlined in Tables I–III, using the derivations given under Data collection and processing.

Development of optimal conditions

Extraction. The results given in Fig. 1 show that maprotiline can be extracted both from aqueous solution and from blood by heptane above pH 9; it can be

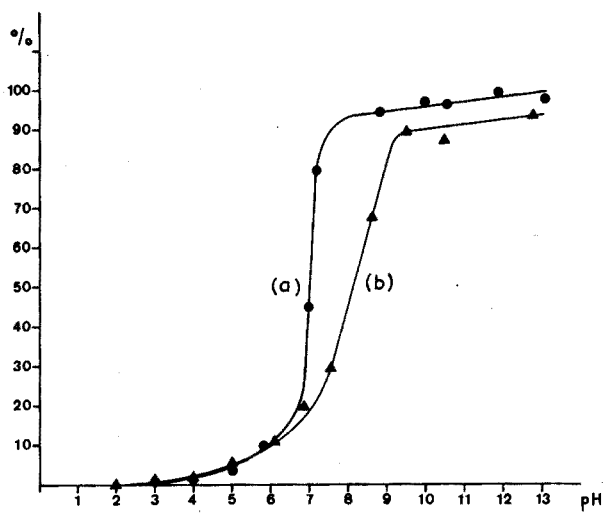

Fig. 1. Variation of extraction of maprotiline with pH: (*a*) from aqueous solution, 6 ml (●), and (*b*) from blood, 3 ml plus buffer 3 ml (▲) by 10 ml of heptane.

TABLE III

TEST ANALYSES OF MAPROTILINE IN HUMAN BLOOD[a]

Conc. given (ng ml^{-1})	*Volume analysed, v (ml)*	*^{14}C-standard added m (ng)*	*Yield of ^{14}C-standard, d (%)*	*100% ^{3}H, g (c.p.m. ml^{-1})*	*Concentration found[b]*	
					x (ng ml^{-1})	*$\bar{x} \pm s(\bar{x})$*
0	3	200	23.8	5032.9	−1.4	−0.1±0.8
			38.2	5320.5	+2.2	
			34.9	5141.1	−0.1	
			37.8	5062.5	−1.1	
5	3	200	24.2	5518.0	4.8	4.6±0.1
			31.4	5511.5	4.7	
			38.0	5522.2	4.8	
			33.7	5476.2	4.2	
10	3	200	30.4	5893.6	9.5	10.2±0.9
			37.4	5822.1	8.6	
			31.3	5902.8	9.7	
			33.9	6149.2	12.8	
20	3	200	35.7	6587.7	18.4	19.1±1.2
			37.4	6903.8	22.4	
			19.3	6475.0	17.0	
			38.2	6609.7	18.7	
40	3	200	42.0	8513.6	42.9	44.3±0.5
			31.8	8619.5	44.3	
			34.2	8709.4	45.4	
			38.8	8629.2	44.4	
60	3	200	36.3	9998.5	61.9	61.2±1.4
			17.3	10225.2	64.8	
			40.9	9760.1	58.8	
			23.7	9779.5	59.1	
80	3	200	29.0	11728.0	83.9	83.4±1.0
			40.9	11786.3	84.7	
			16.3	11451.2	80.4	
			15.8	11769.8	84.4	
100	3	200	37.3	13801.0	110.3	106.6±2.5
			41.4	13858.9	111.1	
			42.5	13351.5	104.6	
			22.7	13016.3	100.3	

[a] Four independent determinations per concentration.
[b] By means of independently determined values $\bar{g}'$ and E of Table II.

reextracted from the heptane phase into aqueous phase at below pH 3. This permits a selective work-up for basic compounds, so that apart from maprotiline only endogenous lipophilic bases can enter the fraction to be processed further.

Acetylation. The acetylation of maprotiline can be carried out with a roughly 10-fold excess of acetic anhydride with dioxane as solvent. When the pure compound was used, the yield of the acetyl product was practically 100%, as demonstrated

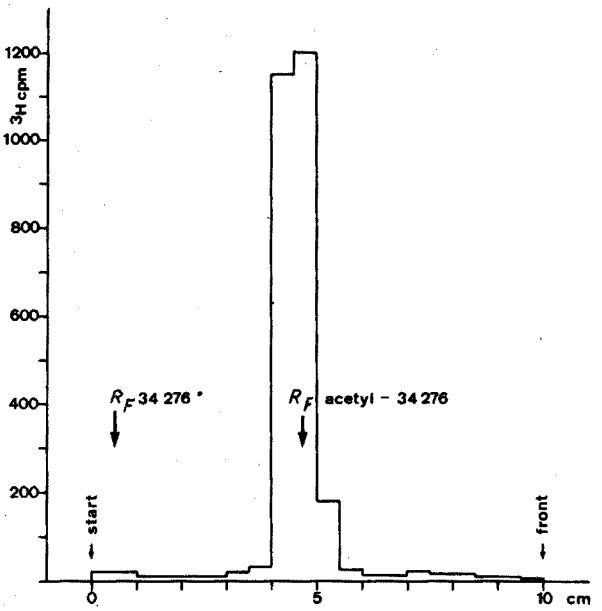

Fig. 2. Radioactivity distribution in thin-layer chromatogram (silica gel, (1+1) toluene–acetone) of the product obtained from acetylation of 500 ng of ^{3}H-labelled maprotiline (Ciba 34 276-Ba) with 10 μg of unlabelled acetic anhydride in 500 μl of dioxane for 1 h at 100°.

by means of acetylation of radioactively labelled maprotiline with unlabelled acetic anhydride followed by thin-layer chromatography (Fig. 2).

In order to test the variability of the overall yield of pure acetyl derivative of maprotiline after extraction from blood and subsequent acetylation the following experiment was set up. From each stock solution containing 200, 300, 400 and 600 ng of ^{3}H-labelled maprotiline per ml of bovine blood, eight 3-ml samples were extracted as described above for bases, and the extracts were subjected to acetylation with 10 μg of unlabelled acetic anhydride in 50 μl of heptane plus 500 μl of purified dioxane at 100° for 1 h. The solvent and excess of acetic anhydride were gently evaporated and the reaction product was taken up in 2 ml of heptane containing 50 μg of the acetyl derivative of ^{14}C-labelled maprotiline which had been prepared before in pure crystalline form. This heptane solution was shaken with 0.5 ml of 0.01 *M* sodium hydroxide and centrifuged, and the heptane phase was separated and evaporated. Part of each residue was spotted on a silica gel plate and developed with (1+1) toluene–acetone. The u.v.–visible spot of the acetyl derivative of maprotiline was scraped off the plate, eluted with 0.5 ml of methanol, and counted for both ^{3}H and ^{14}C activity in the liquid scintillation counter. From the ^{3}H activity recovered, the total yield of pure acetyl derivative of the ^{3}H-labelled maprotiline could be calculated by means of the 100% value of ^{14}C-activity added, and the percentage recovery after chromatography and elution.

As can be seen from Table IV, the overall yields of acetyl product vary between the extreme limits of 38% and 77%. Thus, to arrive at acceptable reproducibility, it is necessary to introduce an internal standard so that the variable overall yield of the acetyl derivative can be corrected for.

TABLE IV

OVERALL YIELDS OF PURE ACETYL DERIVATIVE OF ^{3}H-LABELLED MAPROTILINE AFTER EXTRACTION OF 3 ml OF BOVINE BLOOD AND ACETYLATION

(The actual yields were obtained by addition of acetyl-^{14}C-labelled maprotiline standard after acetylation with unlabelled acetic anhydride, thin-layer chromatography and double isotope assay as specified in the text.)

^{3}H-Maprotiline concentration in bovine blood (ng ml^{-1})	*Overall yield of acetyl derivative (%)*		*^{3}H-Maprotiline concentration in bovine blood (ng ml^{-1})*	*Overall yield of acetyl derivative (%)*	
200	48.7	$n = 8$	400	51.0	$n = 8$
	69.3	$\bar{x} = 55.1\%$		59.0	$\bar{x} = 59.0\%$
	60.7	$s(x) = 11.0\%$		65.7	$s(x) = 4.5\%$
	56.7			59.0	
	49.3			64.3	
	48.7			58.7	
	69.3			57.7	
	38.0			56.7	
300	57.3	$n = 8$	600	75.1	$n = 8$
	41.8	$\bar{x} = 52.0\%$		74.4	$\bar{x} = 70.1\%$
	50.2	$s(x) = 8.0\%$		66.4	$s(x) = 5.5\%$
	52.9			64.7	
	43.6			71.1	
	61.3			61.8	
	45.8			70.9	
	62.7			77.1	

In order to provide a sufficient excess of acetic anhydride, even for larger sample volumes or heavy loads of anhydride-consuming metabolites in the samples, the amount of acetic anhydride was scaled up to 1 μmol (*ca.* 100 μg per sample) in the final method. However, the total ^{3}H-activity used per sample was kept at 50 μCi.

Separation of the ^{3}H-acetyl derivative of maprotiline from the derivatives of metabolites and biogenic compounds. If the extractable bases from 3 ml of "blank" blood or serum are subjected to acetylation with 1 μmol (50 μCi) of ^{3}H-acetic anhydride and processed as described in the Procedure (Acetylation step), as much as 80000 d.p.m. of ^{3}H-activity from reagent background and from ^{3}H-acetyl products of biogenic material may enter the fraction in which ^{3}H-acetyl maprotiline would appear. For this reason, the analytical procedure has to include purification steps which can separate the ^{3}H-acetylmaprotiline from the sample background. The required separation was achieved satisfactorily by two-dimensional thin-layer chromatography as given in Fig. 3, the position of the ^{3}H-acetylmaprotiline being made visible through the unlabelled carrier added before chromatography.

Of the possible metabolites of maprotiline, the N-desmethyl derivative was suspected to interfere with the assay of the parent compound. Thus the chromatographic systems in the two-dimensional t.l.c. were chosen also to separate the ^{3}H-acetyl derivative of the parent compound from that of its N-desmethyl derivative.

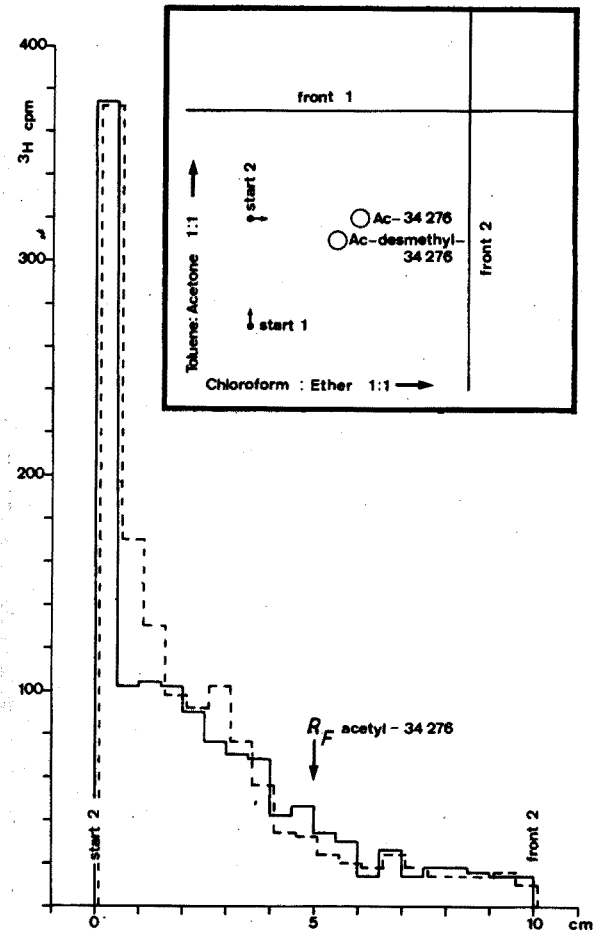

Fig. 3. ^{3}H-radioactivity profile in the track of the second dimension from a two-dimensional t.l.c. of the ^{3}H-acetyl products obtained from the reaction of the extractable base fraction from 3 ml of bovine "blank" blood (——) and from 3 ml of human "blank" serum (– – –). Acetylation with 1 μmol (50 μCi) of ^{3}H-acetic anhydride and subsequent extraction before t.l.c. Box: Two-dimensional chromatographic scheme and locations of the acetyl derivatives of maprotiline and of its N-desmethyl homologue.

Provided that the latter is also available in a ^{14}C-labelled form to serve as internal standard, the proposed configuration of the procedure allows simultaneous determination of maprotiline and its desmethyl metabolite in the same sample.

Correlation between concentration of unlabelled maprotiline in blood and ^{3}H-activity found after extraction, acetylation and purification in the presence of ^{14}C-labelled internal standard

From eight solutions of unlabelled maprotiline in human blood (concentration range between 5 and 600 ng ml^{-1}) as well as from blank blood, multiple analyses were carried out with 3 ml of blood and 200 ng of ^{14}C-labelled maprotiline as the internal standard in each sample. The extraction, acetylation and purification

steps were followed as given in the Procedure. After dual isotope assay of each probe, the ^{3}H-activity was corrected to 100% by means of the percentage of ^{14}C-activity recovered per sample. The numerical data for four independent analyses

TABLE V

CORRELATION BETWEEN ORIGINAL CONCENTRATION OF MAPROTILINE IN HUMAN BLOOD AND 100% YIELD OF ^{3}H-ACTIVITY FOUND IN ^{3}H-ACETYL DERIVATIVE

(Sample volume per analysis, 3 ml of blood. Internal standard per probe, 200 ng of ^{14}C-labelled maprotiline. Four independent analyses per concentration.)

Original concentration in blood (ng ml^{-1})	*Overall yield of internal standard (%)*	*^{3}H-activity of derivative corrected to 100% yield (c.p.m. ml^{-1})*
0	37.6	3957
	39.5	3917
	40.4	3907
	37.2	3991
5	23.5	4347
	20.3	4190
	32.1	4110
	33.4	4148
10	35.8	4533
	35.4	4650
	36.0	4464
	42.1	4503
20	24.4	5144
	36.1	5130
	35.8	5063
	35.1	5163
50	31.5	7081
	32.0	6680
	32.7	7123
	32.3	6946
100	46.3	10547
	33.5	10608
	35.6	10883
	37.0	10541
200	40.3	17508
	47.9	17526
	40.8	18034
	41.2	18074
400	49.0	31458
	48.5	31462
	35.0	31897
	38.5	31488
600	36.4	45661
	39.5	47479
	37.6	46242
	34.7	47265

per concentration are given in Table V. A plot of these data shows a strictly linear correlation. The best fit of the experimental data to a linear regression (least sum of squares of deviations) yields the correlation:

$$^{3}H\ (\text{c.p.m. ml}^{-1}) = 71\ (\text{c.p.m. ng}^{-1}) \cdot C\ (\text{ng ml}^{-1}) + 3682\ (\text{c.p.m. ml}^{-1})$$

The intercept is due to the ^{3}H-activity derived from ^{3}H-acetylation of the ^{14}C-labelled maprotiline internal standard. The slope of 71 (c.p.m. ng^{-1}) is the ^{3}H-specific activity of the originally unlabelled maprotiline after ^{3}H-acetylation.

In order to carry out routine analyses of biological samples, the evaluation of the specific ^{3}H-activity of the acetyl derivative can be reduced to a "two-point calibration" mode manageable within each analytical run. Since the correlation of ^{3}H-activity and original concentration is strictly linear, it is sufficient to determine the intercept of the regression line with the ordinate (^{3}H-activity emerging from blank sample plus ^{14}C-internal standard) and to measure the 100% ^{3}H-activity of reference samples of one defined prefixed concentration of the compound to be assayed as explained under Data collection and in Tables I and II.

Test analyses of maprotiline in human blood

In order to test the precision of the d.r.i.d. method, especially in the low concentration range which would be expected in kinetic studies with single doses of maprotiline, human blood samples containing maprotiline in the range 0–100 ng ml^{-1} were analysed by the proposed procedure. For each concentration four independent analyses were carried out. The specific ^{3}H-activity of the N-acetyl derivative was determined independently by the "two-point calibration" mode (Tables I and II). The results showed that the proposed method has a lower limit of sensitivity of about 2 ng ml^{-1} in a single determination which is sufficient to conduct kinetic studies with single doses in man.

Naturally, the precision of the assay depends on the sample volume, the amount and the specific activity of the ^{14}C-internal standard as well as on the specific activity of the ^{3}H-labelled reagent. Thus the precision can be optimized for each analytical task.

The author is indebted to G. Menge for skilful technical assistance.

SUMMARY

The double radio-isotope technique is described in general, and a sensitive and specific method is presented for the assay of maprotiline (Ciba 34 276-Ba, Ludiomil) in biological materials. The procedure involves the addition of a definite amount of ^{14}C-labelled maprotiline as internal standard, extraction of the free base, and acetylation with ^{3}H-labelled acetic anhydride. The ^{3}H-labelled N-acetyl derivative of maprotiline is then separated by two-dimensional thin-layer chromatography from ^{3}H-active by-products which arise from reagents and biogenic material. Both ^{3}H- and ^{14}C-activities of the purified acetyl derivative are determined simultaneously by liquid scintillation counting. The yield of ^{14}C-activity makes it possible to evaluate the theoretical 100% ^{3}H-activity of the derivative. A convenient method is described to determine the specific ^{3}H-activity of the N-acetyl derivative.

RÉSUMÉ

La technique radioisotopique est décrite et une méthode, sensible et spécifique, est proposée pour le contrôle de la maprotiline (Ciba 34 276-Ba, Ludiomil) dans des substances biologiques. On procède à l'addition d'une quantité déterminée de maprotiline, marquée avec ^{14}C (étalon interne), à l'extraction de la base libre et à une acétylation avec anhydride acétique marqué (^{3}H). Le dérivé N-acétylé, marqué ^{3}H, de la maprotiline est ensuite séparé d'avec des produits secondaires, par chromatographie sur couche mince à deux dimensions. On mesure simultanement les activités ^{3}H et ^{14}C du dérivé acétylé purifié, par comptage à scintillation liquide. Une méthode est décrite pour déterminer l'activité ^{3}H specifique du dérivé N-acétylé.

ZUSAMMENFASSUNG

Das Verfahren der Anwendung zweier Radio-Isotope wird allgemein beschrieben, und es wird eine empfindliche und spezifische Methode für die Bestimmung von Maprotilin (Ciba 34 276-Ba, Ludiomil) in biologischen Proben vorgelegt. Bei dem Verfahren wird der Probe eine definierte Menge von ^{14}C-markiertem Maprotilin als innerer Standard zugefügt, die freie Base durch Extraktion abgetrennt und mit ^{3}H-markiertem Acetanhydrid acetyliert. Das ^{3}H-markierte N-Acetylderivat von Maprotilin wird dann durch zweidimensionale Dünnschichtchromatographie von ^{3}H-aktiven Nebenprodukten abgetrennt, die aus den Reagenzien und biogenen Stoffen entstehen. Die ^{3}H- und ^{14}C-Aktivitäten des gereinigten Acetylderivates werden simultan nach der Flüssig-Scintillations-Methode gemessen. Die gemessene ^{14}C-Aktivität ermöglicht die Berechnung der theoretischen 100%-^{3}H-Aktivität des Derivates. Eine bequeme Methode für die Bestimmung der spezifischen ^{3}H-Aktivität des N-Acetylderivates wird beschrieben.

REFERENCES

1 B. Kliman and R. E. Peterson, *J. Biol. Chem.*, 235 (1960) 1639.
2 T. H. J. Benraad and P. W. C. Kloppenborg, *Clin. Chim. Acta*, 12 (1965) 565.
3 M. A. Rivarola and C. J. Migeon, *Steroids*, 7 (1966) 103.
4 K. Engelman, B. Portnoy and W. Lovenberg, *Amer. J. Med. Sci.*, 255 (1968) 259.
5 K. Engelman and B. Portnoy, *Circ. Res.*, 26 (1970) 53.
6 F. R. Matthias and F. Liemann, *Klin. Wochenschr.*, 48 (1970) 873.
7 L. Rentzhog, *Acta Physiol. Scand., Suppl.*, 377 (1972) 1.
8 G. A. Hagen, L. J. Diuguid, B. Kliman and J. B. Stanburg, *Anal. Biochem.*, 38 (1970) 517.
9 G. T. Okita, J. J. Kabara and G. L. Le Roy, *Nucleon.*, 15 (1957) 111.
10 P. Kielholz, *Depressive Illness, Diagnosis, Assessment, Treatment*, Hans Huber, Bern, 1972.
11 W. M. Hammer and B. B. Brodie, *J. Pharmacol. Exp. Ther.*, 157 (1967) 503.
12 S. R. Harris, L. E. Gaudette, D. H. Efron and A. A. Manian, *Life Sci.*, 9, Part I, (1970) 781.

Analytica Chimica Acta, 68 (1974) 377–385

© Elsevier Scientific Publishing Company, Amsterdam – Printed in The Netherlands

THEORETICAL TEMPERATURE–TIME CURVES FOR ELECTRICALLY HEATED FILAMENT ATOM RESERVOIRS

THEIR SIGNIFICANCE IN ANALYTICAL SPECTROMETRY

M. S. CRESSER and C. E. MULLINS

Department of Soil Science, University of Aberdeen, Aberdeen (Scotland)

(Received 19th July 1973)

The filament atom reservoir is undoubtedly attractive to the analyst as an atom cell with potentially negligible background absorption and emission, and with a capability of atomizing many refractory oxide-forming elements. At present, however, each different filament has shown different condensation and matrix interferences and different absorbance or fluorescence signal *versus* voltage characteristics. Thus each new material or shape of filament has required a lengthy empirical evaluation.

The primary reason for the difficulty in explaining the behaviour of atomic populations produced from electrically heated filaments lies in the transient nature of the atomic vapour cloud. The free atom distribution and lifetime depend not on the filament equilibrium temperature (which is the parameter measured by an optical pyrometer) but on the rate of atomization of the molecular species on the filament. The latter is itself a function of the temperature–time characteristic of the central portion of the filament and of the rate of diffusion of the products of atomization away from the filament. Several workers[1,2] have commented that the duration of the atomic signals are in the range 20–50 ms, and it has been pointed out that some atomization occurs long before the filament reaches its equilibrium temperature[3]. The lifetime of the atomic vapor may be readily monitored directly on a storage oscilloscope[1–6].

The rate at which any given molecular species leaves the filament and the degree of atomization depend on the rate of increase of temperature, at temperatures at which the molecular species exhibits a significant vapor pressure. If the temperature–time curve of the filament can be calculated, it should be possible to extend the basic assumptions made by L'vov for the graphite cuvette[7], to predict the extent of atomization of various elements from the filament. Even if this aspect is not studied in detail, it is clear that high rates of temperature rise can lead to atomization occurring and the atomic vapor disappearing in a time shorter than the response time of a conventional detector-readout system. This fact has been commented on[8] and used to explain why fluorescence or absorption sensitivity tends to reach optimal values at quite low voltages when a slow-response detection system is used[3,8,9], whereas they continue to rise with increasing voltage when fast-response systems are used[2,6]. It also seems likely that the slower the heating rate, the greater is the probability of vaporization with a poor atomization

efficiency. This factor could make a very significant contribution to the final absorbance or fluorescence intensity value.

Condensation interferences have been shown to be the predominant form of interference for filament atom reservoirs[9], and it has been shown that these interferences can be minimized by passing a narrow beam of light at grazing incidence over the filament[2,10]. It seems likely that a similar reduction of condensation interferences could be obtained by increasing the rate of atomization. Thus, both sensitivity and freedom from interferences should be optimized by using the greatest heating rate commensurate with the response time of the detector.

The temperature–time curves for graphite and tungsten filaments of various dimensions have been calculated in this paper to show how, and to what extent, filament dimensions, material, and voltage influence these curves. Filament power consumption has also been calculated, because this will often be a practical limitation. The significance of the results obtained is illustrated by reference to the results published by other workers.

THEORY

The two major sources of energy loss from an electrically heated filament are radiation and conduction along the filament to the end-supports. Since these supports must make good electrical contact with the filament, there must also be a good thermal contact between the two. If the filament is surrounded by a stream of inert gas, an additional energy loss will be incurred, but this is less than 1% of the input power for all filaments discussed here and so can be neglected. Thus the temperature–time characteristics of the filament depend on the applied voltage, filament length and radius; and the density, specific heat, thermal conductivity, resistivity and emissivity of the filament material (V, l, r, γ, C, K, ρ, ε, respectively). Of these, C, K, γ, and ε all show a large temperature-dependence.

The electrical power supplied to the filament, P_{in}, is dissipated by conduction P_{cd} and radiation P_r as well as supplying power to raise the filament temperature P_T, *i.e.*

$$P_{in} = P_{cd} + P_r + P_T \tag{1}$$

Although all these terms are functions of temperature, for a sufficiently small temperature rise ΔT, C, K, ρ, and ε may be assumed to be constant and their value can be taken to be that at $(T+\Delta T/2)$, where T is the temperature of the centre of the filament. However, the temperature of the filament is not uniform along its length.

If electrical energy were converted to heat uniformly along the length of the filament and the thermal conductivity of the filament were likewise uniform, then the temperature profile along the filament would be approximately parabolic below 2,000°K for the filament materials and dimensions considered. In practice, this is not the case and a rigorous treatment would require that the actual temperature profile along the filament should be calculated for each temperature considered and that this profile should be used to integrate each of the power terms in eqn. (1). If a simple temperature profile along the filament is assumed, the above calculation can be greatly simplified at the expense of some accuracy. However, the physical

properties of graphite (particularly its thermal and electrical conductivities and their variation with temperature) are highly variable from one commercial producer to another so that, at least for graphite, there is little to be lost by this approximation.

Consider a filament whose length exposed between the supports at either end is l; in the assumed temperature profile, a central portion kl of the filament is at temperature T, the ends are at room temperature T_R (300°K) and the intermediate portions of total length $(1-k)l$ have a uniform temperature gradient. Equation (1) may then be rewritten as:

$$P_{in} = P_{cd} + P_{r(k)} + P_{r(1-k)} + P_{T(k)} + P_{T(1-k)} + \cdots \tag{2}$$

where suffix k refers to the central region and $(1-k)$ to parts on either side. The various terms in this equation are:

$$P_{in} = \pi r^2 V^2/l\{k\rho_{(T+\Delta T/2)} + (1-k)\rho_{(T')}\} \tag{3}$$

$$P_{cd} = 4K_{(T')}\pi r^2(T+\Delta T/2-T_R)/l(1-k) \tag{4}$$

$$P_{r(k)} = 2kl\pi r\sigma_s\varepsilon_{(T+\Delta T/2)}(T+\Delta T/2-T_R)^4 \tag{5}$$

$$P_{r(1-k)} = 2(1-k)l\pi r\sigma_s\varepsilon_{(T')}(\tfrac{1}{2}(T+\Delta T/2-T_R))^4 \tag{6}$$

$$P_{T(k)} = kl\pi r^2\gamma C_{(T+\Delta T/2)}\Delta T/\Delta t \tag{7}$$

$$P_{T(1-k)} = \tfrac{1}{2}(1-k)l\pi r^2\gamma C_{(T')}\Delta T/\Delta t \tag{8}$$

where γ is the density of the filament material, σ_s is Stefan's constant, Δt is the time taken to raise the centre of the filament from T to $T+\Delta T$, and $T'=\frac{1}{2}(T+T_R+\Delta T/2)$. The bracketed suffices used throughout with ρ, K, ε and C, refer to the temperature values at which these variables should be taken at each stage in the calculation. Again, an approximation is involved in taking some average value of these variables for the sloping part of the temperature profile. Numerical values for these variables were taken from graphs of literature values[11,12] or from regression equations[13]. Temperature–time plots were calculated by repeatedly substituting the values of the above power terms in eqn. (2), with a suitably small value for ΔT.

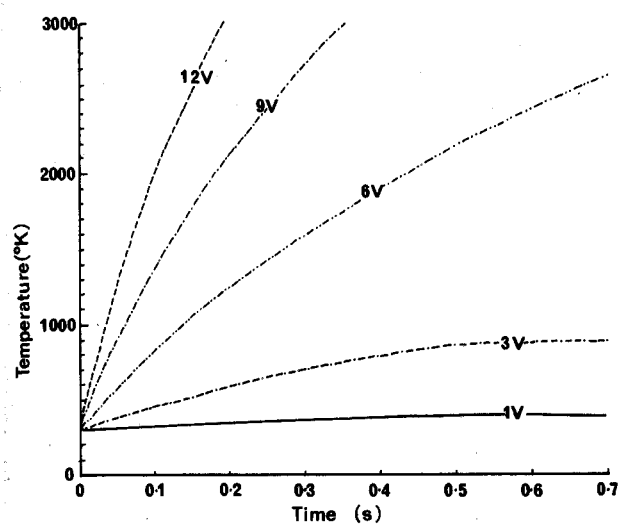

Fig. 1. Effect of filament voltage on heating rate curves for graphite filament, 25 mm long, 1 mm radius.

The choice of a value for k in this approximate calculation is clearly somewhat arbitrary. Values of 0.3 for graphite and 0.5 for tungsten were selected by sketching a parabolic temperature profile and then estimating the perturbation which would be caused by the actual variation of ρ and K along the length of the filament.

RESULTS AND DISCUSSION

By means of the method of calculation already outlined, families of curves were compiled for the following situations:

Plot	*Material*	*Length (mm)*	*Radius (mm)*	*Voltage*	*Figure*
T *vs.* t	Graphite	25	1	1–12	1
T *vs.* t	Graphite	25	0.1–5	6	2
T *vs.* t	Graphite	10–60	1	6	3
T *vs.* t	Tungsten	25	1	1–5	4
P_{in} *vs.* t	Graphite and	25	1	1–12	5
	tungsten	25	1	1–5	5

Curves were not calculated for platinum and tantalum since their physical properties are sufficiently close to those of tungsten to give very similar results.

The effect of voltage on the temperature–time curve of a graphite filament of typical dimensions is shown in Fig. 1. If the assumption made by L'vov[7] that the time taken to atomize a sample is equal to the time necessary for the filament temperature to increase by 100–200° at temperatures around that at which the sample saturated vapor pressure exceeds 0.1 torr, is applied to this situation, then atomization times of 30–60 ms, 13–25 ms, and 8–15 ms are obtained at 6, 9 and 12 V, respectively. These values are in good agreement with the literature values quoted earlier in this paper.

Temperature–time curves for graphite filaments of various radii are shown in Fig. 2. Since input power (P_{in}), power lost by conduction (P_{cd}), and power required to heat the filament (P_T), are all proportional to r^2 (see eqns. 3, 4, 7 and 8), whereas radiation loss is proportional to r, the curves are the same up to the point where radiation loss becomes significant; a smaller radius then becomes disadvantageous.

Because P_{in} decreases while P_T increases with increasing l (see eqns. 3, 7 and 8), the length of filament between the water-cooled supports is a far more critical parameter. This is clearly shown in Fig. 3. It is therefore understandable that Cantle and West[8] found that a reduction in filament length from *ca.* 25 mm to 10 mm caused a substantial increase in the rate of heating. The theoretical rate of temperature rise increases by about six times on reducing the filament length from 25 to 10 mm so that a 10-mm filament operated at 6 V should actually heat up faster than a 25-mm filament operated at 12 V. Power consumption will be less for the former case, and can be further reduced at no loss in heating rate by reducing the radius of the filament.

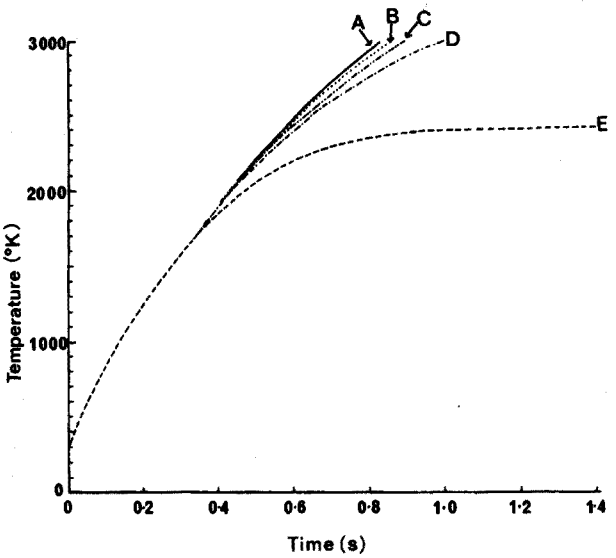

Fig. 2. Effect of filament radius on heating rate curves for 25-mm long graphite filament at 6 V. (A) $r=5$ mm; (B) $r=2$ mm; (C) $r=1$ mm; (D) $r=0.5$ mm; (E) $r=0.1$ mm.

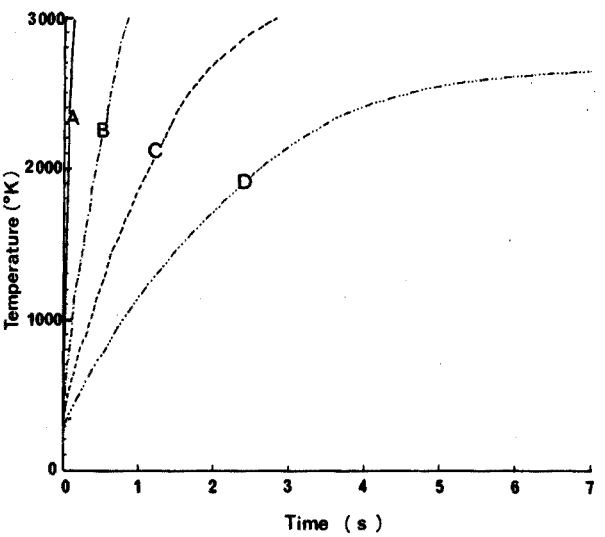

Fig. 3. Effect of filament length on heating rate curves for 1-mm radius graphite filament at 6 V. (A) $l=10$ mmm; (B) $l=25$ mm; (C) $l=40$ mm; (D) $l=60$ mm.

Choice of filament material

A family of temperature–time curves for a tungsten filament of typical dimensions[8] is shown in Fig. 4. The curves are of a shape significantly different from those presented for graphite in Fig. 1. In particular, they initially slope more steeply and then bend over faster than those for graphite. If the electrical power supply to the filament is not capable of an accurately timed short duration

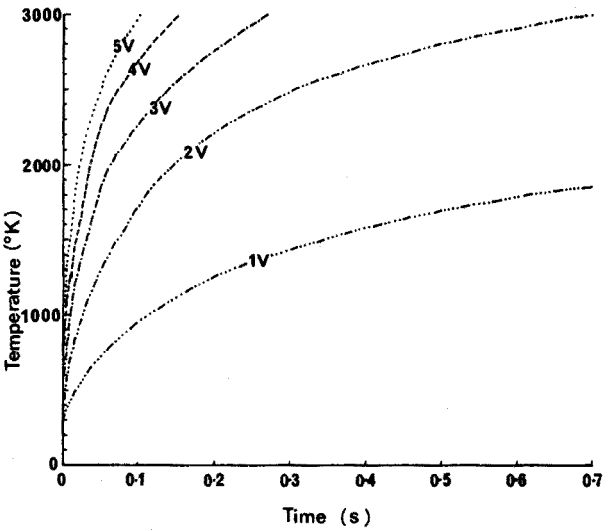

Fig. 4. Effect of filament voltage on heating rate curves for tungsten filament, 1 mm radius, 25 mm long.

(<100 ms) in the atomizing step, then there is a practical limit to the highest voltage and hence heating rate which can be used. This rate must be such that the filament does not sublime (*i.e.* above 3800°K for graphite), melt (tungsten, 3653°K) or undergo severe structural damage. It is clear that if the required heating rate is limited by the above considerations, tungsten is preferable to graphite. For example, if the graphite and tungsten filaments represented by Figs. 1 and 4 are compared, although the tungsten filament takes 1 s to reach 3000°K at 2 V, it reaches 1200°K more rapidly than the graphite filament driven at 12 V, and 2200°K more rapidly than the graphite filament driven at 9 V. Thus for volatile elements in particular, the tungsten filament operated at a low voltage would be expected to give a greater sensitivity and freedom from interferences than a graphite filament of comparable dimensions driven at a much higher voltage. These effects have in fact been observed by Cantle and West[8].

Power requirements

Since resistivity is a function of temperature, the electrical power consumed by a filament depends on its temperature–time curve. Power–time curves (*i.e.* P_{in} *versus* t) are plotted for graphite and tungsten filaments 25 mm long and radius 1 mm for a range of voltages in Fig. 5. These results are plotted for convenience on a log–log scale. For tungsten there is a very marked power surge of about ten times the steady-state power consumption which lasts from 100 ms to 1 s depending on the applied voltage. The fact that even when a steady state is being approached, tungsten still consumes the same power at a lower voltage as graphite is simply an indication of its lower resistivity. Steady-state values of power consumption calculated after a time of a few seconds are comparable to those given by Cantle and West[8] when allowance is made for the greater length of their filaments, although these investigators make no mention of an initial power surge with a tungsten filament.

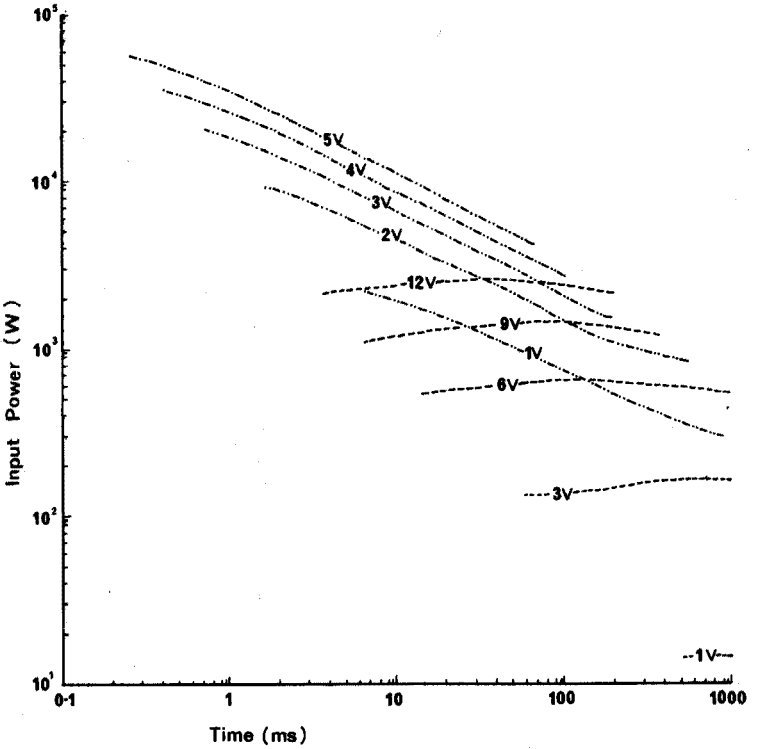

Fig. 5. Input power *vs.* time curves for tungsten (upper series, —·—·—) and graphite (lower series, ---) at various values of voltage. Other parameters as in Figs. 1 and 4.

Lamp modulation and a.c. heating

The original carbon filament atomizer was operated at about 100 A and 5 V (ref. 14); the filament was 22 mm long and 1–2 mm in diameter and was heated to 2000–2500°C within 5 s. As described previously, this will give an atomization period of 40–80 ms. If the light source were modulated at 50 Hz, each light pulse would be 10 ms in duration which is not long compared to the period of atomization. Thus it is clear that the faster rates of atomization which can be produced by operating a graphite filament at a higher voltage or by using a tungsten filament, can be a source of random error unless the light source is modulated at a higher frequency. Alternatively, a d.c. source and detector system may be used[2].

A similar consideration applies to the electrical power which is used to heat the filament. Conventionally, this is derived from the mains via a thyristor control unit and stepdown transformer. The result is that power is fed to the filament in pulses of 10 ms duration. This will have the effect of modulating the temperature–time curve of the filament at 100 Hz as observed by Alder and West[15]. Clearly, one must distinguish here between the rate at which atoms leave the filament and the diffusion processes which occur immediately above its surface. Furthermore, the thermal capacity of the filament will damp down the effect of these modulations. Nevertheless, this potential source of random error should be considered in future

designs. It could be minimized by maintaining a constant phase relationship between the switching on of the filament power supply and the a.c. mains.

Future possibilities

It is apparent that the electrical power consumed by present-day filament atom reservoirs is out of all proportion to the requirements of atomizing a few nanograms of sample. It seems quite feasible to design a filament much smaller than those presently used, yet of sufficient size to atomize the sample adequately in a uniform manner and to be mechanically stable. If, with the appropriate detector electronics, sensitivity can indeed be increased much further by much faster atomization rates, then a reproducible d.c. heating system becomes a necessity. For example, a fixed quantity of charge could be passed through the filament from a large electrolytic capacitor, sufficient to heat it to say 2500°K in a fraction of a millisecond without overheating it. However, filaments of the present dimensions require more energy to heat them than could be provided by a bank of capacitors of practicable dimensions.

The authors are grateful to Dr. A. L. Gelman for useful discussion during the preparation of this manuscript.

SUMMARY

A simple theoretical approach has been used to calculate the temperature and power consumption *versus* time curves for graphite and tungsten filaments 25 mm × 1 mm radius operated at a number of different voltages. Results are also presented to show the effect of filament dimensions. These results suggest that there is scope for improvement in the design of filament atom reservoirs.

RÉSUMÉ

Une approche théorique simple a permis le calcul de courbes température et dépense d'énergie en fonction du temps, pour des filaments graphite et tungstène, opérant à différents voltages. On examine également l'influence des dimensions du filament. Les résultats obtenus montrent qu'il y a des possibilités de perfectionnement des modèles de réservoirs atomiques à filament.

ZUSAMMENFASSUNG

Mit Hilfe einer einfachen theoretischen Annäherung wurden die Temperatur- und Leistungsaufnahme–Zeit-Kurven für Graphit- und Wolfram-Heizfäden 25 × 1 mm Radius berechnet, wobei die Spannungen unterschiedlich gewählt wurden. Es werden auch Ergebnisse vorgelegt, die den Einfluss der Heizfaden-Abmessungen zeigen. Diese Ergebnisse weisen auf Verbesserungsmöglichkeiten beim Entwurf von Heizfaden-Atomreservoiren hin.

REFERENCES

1 A. J. Aggett and T. S. West, *Anal. Chim. Acta*, 57 (1971) 15.

2 D. Alger, R. G. Anderson, I. S. Maines and T. S. West, *Anal. Chim. Acta*, 57 (1971) 271.
3 L. Ebdon, G. F. Kirkbright and T. S. West, *Anal. Chim. Acta*, 58 (1972) 39.
4 J. F. Alder and T. S. West, *Anal. Chim. Acta*, 58 (1972) 331.
5 K. W. Jackson and T. S. West, *Anal. Chim. Acta*, 59 (1972) 187.
6 K. W Jackson, T. S. West and L. Balchin, *Anal. Chim. Acta*, 64 (1973) 363.
7 B. V. L'vov, *Atomic Absorption Spectrochemical Analysis*, Adam Hilger, London, 1970.
8 J. E. Cantle and T. S. West, *Talanta*, 20 (1973) 459.
9 A. J. Aggett and T. S. West, *Anal. Chim. Acta*, 55 (1971) 349.
10 R. G. Anderson, H. N. Johnson and T. S. West, *Anal. Chim. Acta*, 57 (1971) 281.
11 *Handbook of Chemistry and Physics*, 51st Ed., 1970–1971.
12 Ringsdorff manufacturer's data; values used should be typical for RW1V graphite.
13 K. K. Kelly, *U.S. Bur. Mines Bull.*, 584 (1960).
14 T. S. West and X. K. Williams, *Anal. Chim. Acta*, 45 (1969) 27.
15 J. F. Alder and T. S. West, *Anal. Chim. Acta*, 51 (1970) 365.

Analytica Chimica Acta, 68 (1974) 387–394

© Elsevier Scientific Publishing Company, Amsterdam – Printed in The Netherlands

TRACE ANALYSIS FOR SULPHUR AND PHOSPHORUS IN AQUEOUS SOLUTION BY A CARBON FILAMENT ATOM RESERVOIR TECHNIQUE

G. L. EVERETT and T. S. WEST

Department of Chemistry, Imperial College, London SW7 2AY (England)

R. W. WILLIAMS

B.P. Research Centre, Sunbury on Thames, Middlesex (England)

(Received 21st June 1973)

The common analytical techniques of atomic absorption, fluorescence or emission spectrometry are generally not suited to the determination of non-metals, such as sulphur and phosphorus whose most sensitive resonance lines are below 200 nm, unless a separated nitrous oxide–acetylene flame is used in conjunction with a vacuum monochromator.

In hydrogen flames, sulphur and phosphorus give characteristic chemiluminescent emissions from the S_2 and HPO species. These were first utilized analytically by Brody and Chaney[1] who burned the effluent gases from a gas chromatograph in a fuel-rich hydrogen–oxygen flame and thus detected sulphur- and phosphorus-containing insecticides.

The elemental determination of sulphur and phosphorus by this method has been fairly extensively described since then. Dagnall, Thompson and West[2] determined sulphur with air–hydrogen and inert gas-diluted hydrogen diffusion flames; several other workers have described the determination of phosphorus[3–6]. The methods have been applied to the determination of phosphorus in oils[7] and rocks[8] and, with a simple filter photometer, to the determination of sulphur in light hydrocarbon distillates[9].

In the present paper, the emissions of S_2 and HPO excited around a heated carbon filament in a nitrogen–hydrogen diffusion flame are discussed and their measurement is described.

EXPERIMENTAL

Instrumentation

Emission of the S_2 molecular species was excited by a hydrogen–nitrogen diffusion flame burning from the sheathing gas-box of a standard unenclosed Alder and West[10] carbon filament reservoir. To cut down the noise and high background signals involved in using wide slits and unrestricted field viewing, a copper shield tube (11.5×2.5 cm i.d.) was placed horizontally over the filament (see Fig. 1). The tube had two holes (1.8 cm diameter) cut through its centre to make a chimney for the flame gases. One end of the tube was then placed against the entrance slit of the Unicam SP900A monochromator used and the other end was blocked.

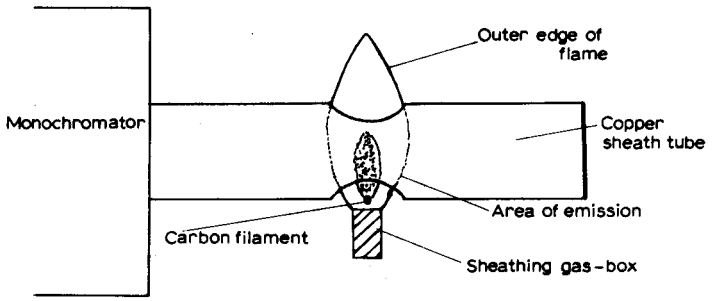

Fig. 1. Schematic diagram of analytical system.

With this system, the emission was confined to the space inside the tube and could easily be viewed by the monochromator with little interference from the continuum emitted by the glowing filament at intermediate temperatures.

The signal from the photomultiplier (EMI 9601B) of the instrument was then fed to a "Type K" amplifier incorporated in a "Telequipment" oscilloscope on which the signal was recorded.

This apparatus has the advantage of being simple and also robust. Quite a large degree of movement of the copper tube can be tolerated before the signal is affected. This is in contrast to atomic absorption or fluorescence methods with resistively heated carbon atomizers where the optical alignment is critical.

The flame

The size of the flame used with this apparatus is governed by the dimensions of the copper tube. It must be small enough to burn entirely in the confines of the tube and must have the correct temperature and gas flow-rates to allow emission to take place within the tube.

It was found that if any hydrogen flow-rate above the minimum on the flow meter (0.6 l min^{-1}) was used, the nitrogen flow-rate required to keep the flame temperature down to the optimum was so high that the flame burnt outside the copper tube and became hazardous to use. The optimal nitrogen flow-rates (2.5 l min^{-1} for HPO and 3 l min^{-1} for S_2 emission) were found by plotting signal *vs.* N_2 flow-rate (Fig. 2). At these flow-rates the flame burned inside the tube with the

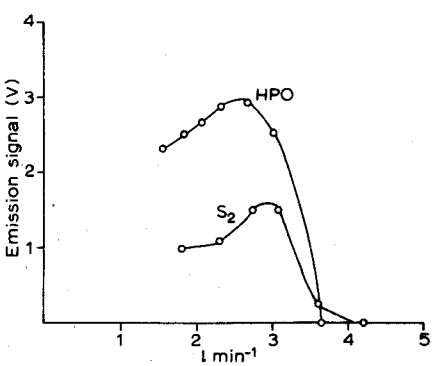

Fig. 2. Optimization of nitrogen flow-rate (H_2 = 0.6 l min^{-1}).

emission in the area desired. These conditions gave a flame that was colourless except for flashes seen when foreign bodies were inadvertently entrained in the flame; this was most noticeable at the top of the flame well away from the emission zone.

A spectral scan of the flame showed it to have very low background in the wavelength regions involved in measurements, *i.e.* 390–400 and 520–530 nm.

Variac voltage

The optimal voltage of "flashing" the sample into the flame was found by plotting signal *vs.* voltage (Fig. 3). For sulphur this was found to be 12 V. For phosphorus the emission peak was not resolved from the continuum at such a high voltage; a compromise was, therefore, made between sensitivity and resolution at 7.2 V.

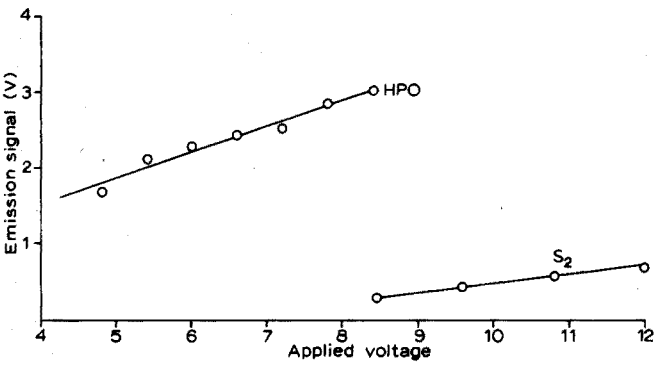

Fig. 3. Optimization of Variac voltage for filament.

Slit-width

For maximal sensitivity a wide slit-width is necessary, but at the wavelengths used this high sensitivity is accompanied by high background noise and curvature of calibration lines. The optimal value was, therefore, taken as that with the highest signal : noise ratio. This was found to be 0.6 mm for S_2 emission and 0.4 mm for HPO. These slit-widths correspond to spectral band-passes of 12 nm and 18 nm, respectively. Operating conditions are summarized in Table I and the optimized sensitivity data in Table II.

TABLE I

OPERATING CONDITIONS

	S_2	HPO
Peak wavelength	394 nm	526 nm
EHT	−1100 V	−1100 V
H_2 flow-rate	0.6 l min^{-1}	0.6 l min^{-1}
N_2 flow-rate	2.8 l min^{-1}	2.6 l min^{-1}
Variac voltage	12 V	7.2 V
Monochromator slit-width	0.6 mm (12 nm)	0.4 mm (18 nm)

TABLE II

DETECTION LIMITS, REPRODUCIBILITY, WORKING RANGES

(The samples used were solutions of sulphuric acid or phosphoric acid)

	S_2	*HPO*
Detection limit	$5 \cdot 10^{-10}$ g	$4 \cdot 10^{-9}$ g
Reproducibility	±7%[a]	±4.7%[a]
Useful range	0–10 p.p.m.	0–100 p.p.m.

[a] Based on 15 results at 20× detection limit.

Sampling sequence

The following sequence was observed for both sulphur and phosphorus.

At $t = 0$ s, the sample (1 μl) of sulphuric or phosphoric acid solution was placed on the filament;

$t = 10$ s, the hydrogen flow was started;

$t = 15$ s, the flame was lit;

$t = 20$ s, the sample was evaporated into the flame and the emission recorded;

$t = 23$ s, the hydrogen flow was stopped.

This was repeated every 60 s.

RESULTS AND DISCUSSION

Calibration curves

Sulphur. According to theory, the emission intensity of S_2 is proportional to the square of the sulphur concentration. As may be seen from Fig. 4, this is so for levels of sulphur up to 10 p.p.m. at least, but above this level, curvature sets in. Greer and Bydalek[11] have attributed this curvature to self-absorption and corrected for it using the expression

$$\log R = \log C + \log (S)^2 - \alpha K (S)^2$$

where R = instrument response, C and K are constants and α is the absorption

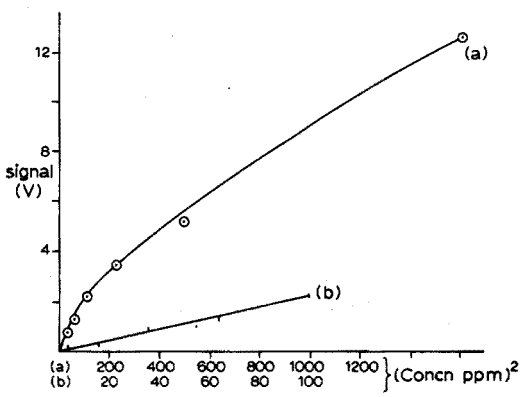

Fig. 4. Calibration curves for sulphur. Signal *vs.* (S) and $(S)^2$ at 394 nm.

coefficient. Firstly, log R *vs.* log $(S)^2$ is plotted and log C calculated from the intercept; αK is then calculated for the points on the calibration line where curvature is observed and a mean value found. A corrected curve $(\log R)_{corr}$ *vs.* log $(S)^2$ is then plotted, where

$$(\log R)_{corr} = \log R + \alpha K(S)^2$$

This should then give a straight line of gradient unity and intercept log C. This treatment was applied to the results obtained. The mean αK value was computed (Table III) from the results for the last four points on the graph (Fig. 5) and the corrected graph was drawn. As may be seen, the graph is linear from 0–40 p.p.m. with a gradient of unity. However, the last three points are well out of line, only the point for 40 p.p.m. being brought back on to the linear portion of the graph. Because the emission process is chemiluminescent, the gross curvature of the last three points is probably due to self-quenching of the luminescence reaction. From this treatment, it can be concluded that between 0–10 p.p.m., the signal intensity is proportional to S^2; the major cause of curvature is self-absorption between 10–40 p.p.m., but self-quenching above 40 p.p.m.

TABLE III

CURVE CORRECTION VALUES FOR αK

c (p.p.m.)	40	60	80	100	
αK ($\cdot 10^{-4}$)	4.75	2.82	1.80	1.34	Mean 2.35

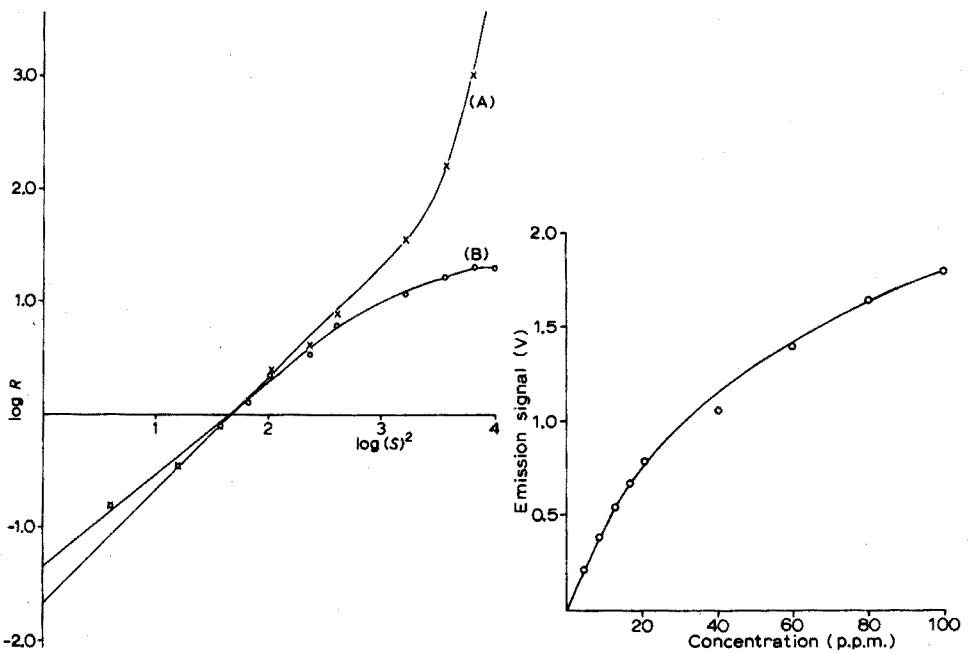

Fig. 5. Curve correction according to Greer and Bydalek. (A) Corrected. (B) Uncorrected.
Fig. 6. Calibration curve for phosphorus. HPO signal *vs.* P at 526 nm.

Phosphorus. The calibration curve for phosphorus is shown in Fig. 6. Since the curvature is gradual over the whole range, it is assumed that only self-absorption occurs; self-quenching would only become significant above the 100-p.p.m. level.

Interferences

The results of cation interference studies are shown in Table IV. For both phosphorus and sulphur, the interference of the series of cations Zn, Na, K, Ca increases with increasing involatility of the metal sulphate or phosphate, thus indicating that the interference is caused by the difficulty in fragmenting these compounds to either S_2 or HPO. This seems to be borne out by the fact that the higher the melting point of the sulphate or phosphate, the higher must be the temperature of the filament before peak emission appears.

TABLE IV

CATION INTERFERENCES

(% Change of peak height. In all cases, the sample solution contained 50 p.p.m. S as sulphuric acid, or 50 p.p.m. P as phosphoric acid)

Interfering ion[a]	*Equal amount*[b]		*10-Fold amount*[b]
	S_2	*HPO*	S_2
Zn	−25	−20	−35
Al	−35	+5	−45
Na	−20	−25	−55
K	−35	−35	−65
Ca	−55	−100	−85
V	0	−40	−20
Cr	−5	−30	−45, +50
Mn	−60, −50	−100	−100
Fe	−5	−100	−80
Co	−40, −35	−100	−70
Ni	−15, −15	−5	−10
Cu	+5	+80	+45
Mo	0	0	+45

[a] Added as chlorides except for V (ammonium vanadate) and Mo (ammonium molybdate).
[b] By weight.

The transition metals show no such trend, but exhibit a peak splitting effect for sulphur emission. This is probably due to the existence of metal–sulphur species in difference metal valency states in the hydrogen diffusion flame. The interferences on sulphur are generally less than those on phosphorus, which is expected as it is easier to break down the sulphates.

Anion interferences were studied for solutions containing 10 p.p.m. of S or P as the free acid, the anions being added as their acids. There was no interference on phosphorus from 10-fold or 100-fold amounts (by weight) of chloride, nitrate, acetate, perchlorate, borate or oxalate. In 10-fold amounts, these anions did not alter the emission of 10 p.p.m. of S, nor did 100-fold amounts of nitrate or acetate; 100-fold amounts of chloride and perchlorate depressed the emission by 15% and

45%, respectively. A 50-fold amount of boric acid or a 32-fold amount of oxalate depressed the sulphur emission by 10% or 15%, respectively.

With regard to mutual interference between sulphur and phosphorus, 10- or 100-fold amounts of phosphate depressed the sulphur signal by 5%; a 10-fold amount of sulphate did not affect the HPO emission, but a 100-fold amount depressed it by 10%. A simultaneous determination of sulphur and phosphorus thus seems possible.

The major interference in this method is the existence of combustible organic fragments in the flame; for example, in 20% acetone the signal from 100 p.p.m. of S or P disappears completely, owing to quenching of the chemiluminescent processes.

Conclusion

If cationic interferences are removed by ion exchange before analysis, this method could provide a useful ultramicro determination for the range 1–100 p.p.m. of sulphur and phosphorus. It is accurate, fast and simple to operate. Replacement of the monochromator by molecular band filters could substantially increase the sensitivity of the analytical procedure.

One of us (G.L.E.) is grateful to the Science Research Council for the award of a CAPS research studentship in conjunction with British Petroleum Research Ltd., Sunbury-on-Thames.

SUMMARY

The chemiluminescent emissions of S_2 and HPO are excited around a resistively heated carbon filament in a hydrogen–nitrogen diffusion flame. Detection limits of $5 \cdot 10^{-10}$ g and $4 \cdot 10^{-9}$ g were obtained, respectively, for sulphur and phosphorus for 1-μl samples of sulphuric and phosphoric acid solutions. Interference effects were studied; there are numerous cationic interferences but few anionic interferences.

RÉSUMÉ

Les émissions chimiluminescentes de S_2 et HPO sont excitées autour d'un filament de carbone chauffé, dans une flamme de diffusion hydrogène–azote. On arrive à des limites de détection de 5.10^{-10} g et 4.10^{-9} g, respectivement pour soufre et phosphore, avec des échantillons de 1 μl de solutions acide sulfurique et acide phosphorique. Les interférences cationiques sont nombreuses, mais pas les interférences anioniques.

ZUSAMMENFASSUNG

Die Chemilumineszenz-Emissionen von S_2 und HPO wurden mit einem Kohlenstoff-Widerstandheizfaden in einer Wasserstoff–Stickstoff-Diffusionsflamme angeregt. Bei 1 μl-Proben von Schwefelsäure- und Phosphorsäurelösungen wurden für Schwefel und Phosphor Nachweisgrenzen von $5 \cdot 10^{-10}$ g bzw. $4 \cdot 10^{-9}$ g erhalten. Störeinflüsse wurden untersucht; zahlreiche Kationen stören, jedoch nur wenige Anionen.

REFERENCES

1 S. S. Brody and J. E. Chaney, *J. Gas Chromatogr.*, 4 (1966) 42.
2 R. M. Dagnall, K. C. Thompson and T. S. West, *Analyst*, 92 (1967) 506.
3 R. M. Dagnall, K. C. Thompson and T. S. West, *Analyst*, 93 (1968) 72.
4 J. D. Kerber, W. B. Barnett and H. L. Kahn, *At. Absorption Newslett.*, 9 (1970) 39.
5 W. B. Barnett, H. L. Kahn and D. O. Manning, *At. Absorption Newslett.*, 8 (1969) 46.
6 A. Syty and J. A. Dean, *Appl. Opt.*, 7 (1968) 1331.
7 W. N. Elliott, C. Heathcote and R. A. Mostyn, *Talanta*, 19 (1972) 359.
8 A. Syty, *At. Absorption Newslett.*, 12 (1973) 1.
9 K. M. Aldous, R. M. Dagnall and T. S. West, *Analyst*, 95 (1970) 417.
10 J. F. Alder and T. S. West, *Anal. Chim. Acta*, 51 (1970) 365.
11 D. G. Greer and T. J. Bydalek, *Environ. Sci. Technol.*, 7 (1973) 153.

Analytica Chimica Acta, 68 (1974) 395–400

© Elsevier Scientific Publishing Company, Amsterdam – Printed in The Netherlands

NUCLEAR MAGNETIC RESONANCE ANALYSIS OF PHARMACEUTICALS*

PART XI. DETERMINATION OF ACETAZOLAMIDE AND ITS SODIUM SALT IN VARIOUS DOSAGE FORMS

JOHN W. TURCZAN

Food and Drug Administration, Department of Health, Education, and Welfare, 850 Third Ave., Brooklyn, N.Y. 11232 (U.S.A.)

(Received 21st May 1973)

Acetazolamide (2-acetylamino-1,3,4-thiadiazole-5-sulfonamide) is an enzyme inhibitor which acts specifically on carbonic anhydrase and is effective in bringing about diuresis. Numerous procedures for the determination of acetazolamide have been discussed in the literature; these include gravimetric[1], titrimetric[2-4], spectrophotometric[5-8], potentiometric[9-10], and polarographic[11] determinations.

There are two methods officially adopted by the USP XVIII[12]. The procedure for acetazolamide in tablets depends on a polarographic reduction at −0.51 V and comparison with a standard. The analysis for the sodium salt of acetazolamide as a sterile powder, which is preserved in containers for sterile solids, is spectrophotometric in nature and uses the absorbance at 265 nm compared to a standard.

The work described here involves quantitative n.m.r. spectroscopy. With this technique, many high dosage pharmaceuticals have been successfully analyzed in this laboratory. It has been shown that very good quantitative results can be obtained, *e.g.* in the case of aminophylline[13], and as a dividend, the n.m.r. spectrum provides for the identification of the active component, thereby contributing significantly to the selectivity of the method.

Different types of samples were studied in this work. The samples of acetazolamide in tablets, sterile solid dosage forms, and in known mixtures were assayed by n.m.r. t-Butanol was chosen as the internal standard in this instance and 25% ammonia solution was selected as the solvent. All of the results were compared to those obtained by the official procedures for acetazolamide. The findings of this study again demonstrate that n.m.r. can provide a simple, accurate and precise method of quantitative analysis.

EXPERIMENTAL

Equipment

Varian A-60 n.m.r. spectrometer equipped with a variable temperature probe

* Other papers in this series:
Part VII. J. W. Turczan, B. A. Goldwitz and J. J. Nelson, *Talanta*, 19 (1972) 1549.
Part VIII. B. A. Goldwitz and J. W. Turczan, *J. Pharm. Sci.*, 62 (1973) 115.
Part IX. J. W. Turczan and B. A. Goldwitz, *J. Ass. Offic. Anal. Chem.*, 56 (1973) 669.
Part X. J. W. Turczan and B. A. Goldwitz, *J. Pharm. Sci.*, 62 (1973) 1705.

(V-6031) having a six-turn insert was used. All spectra were scanned at a probe temperature of 42°.

Materials

The standard used was acetazolamide (Lederle Labs., lot no. 0363-RNXO869) and the internal standard was t-butanol (Matheson, Coleman and Bell, 99+mol%). The samples were obtained from a commercial source. The solvent consisted of 25% (v/v) ammonia liquor in water.

Procedures

For tablets. Weigh and finely powder not less than 20 tablets. Weigh accurately a portion of the powder, equivalent to about 0.5 g of acetazolamide, into a glass-stoppered centrifuge tube. Add about 50 mg of t-butanol, accurately weighed, and 3–4 ml of 25% ammonia solution in water. Stopper, shake for 2 min and then centrifuge. Transfer *ca.* 0.4 ml of the solution to an analytical n.m.r. tube. Place into an n.m.r. spectrometer and obtain the spectrum, adjusting the spin rate so that no spinning side-bands occur between 0.8–1.7 and 1.8–2.8 p.p.m. using the delta scale. All peak field positions are referred to Tiers' salt at 0 p.p.m. Integrate the peaks of interest at least five times.

For vials. Combine the contents of 6 vials containing the equivalent of 500 mg of cryodesiccated acetazolamide as the sodium salt, into a glass-stoppered Erlenmeyer flask with the aid of the 25% ammonia solution. The total volume of solvent should not exceed 12 ml. To this solution add 300 mg of t-butanol, weighed accurately, stopper and shake well. Continue as in the procedure for tablets, beginning with "Transfer *ca.* 0.4 ml of the solution...".

The amount (in mg) of acetazolamide per tablet may be calculated as follows:

$$\text{mg} = \frac{A_a}{A_{tba}} \cdot \frac{EW_a}{EW_{tba}} \cdot \frac{\text{mg}_{tba}}{\text{mg}_{spl}} \cdot \text{avg. tab. wt.}$$

where A_a = integral value of the signal from acetazolamide; A_{tba} = integral value of the signal from t-butanol; $EW_a = 74.08$ (1/3 formula weight); $EW_{tba} = 8.236$ (1/9 formula weight); mg_{spl} = amount of sample taken for analysis.

RESULTS

The choice of solvent and the internal standard is important in any quantitative n.m.r. procedure. In this particular case, since both the drug acetazolamide, and the internal standard t-butanol, are freely soluble in 25% ammonia solution, it is a natural solvent of choice. The solvent introduces no interference with the integration and subsequent determination of acetazolamide, because its protons resonate at 5.0 p.p.m., about 138 Hz from the upfield position where the acetyl protons of acetazolamide resonate. The applicability of t-butanol as an internal standard has been demonstrated previously[13,14]. In this case, it proved to be a suitable internal standard, in that it is very soluble in water and provides a single strong spectral signal at a useful upfield position. The method is rapid, simple to perform and requires no further manipulation once the sample and

internal standard have been dissolved.

The simple uncomplicated spectrum observed for the system under study is shown in Fig. 1. The amount of acetazolamide was determined from the integration of the singlet, which can be ascribed to the 3 acetyl protons of acetazolamide at *ca.* 2.3 p.p.m. (labeled as peak I), and the singlet from the 9 methyl protons of t-butanol (peak II) at *ca.* 1.3 p.p.m. with respect to Tiers' salt (III).

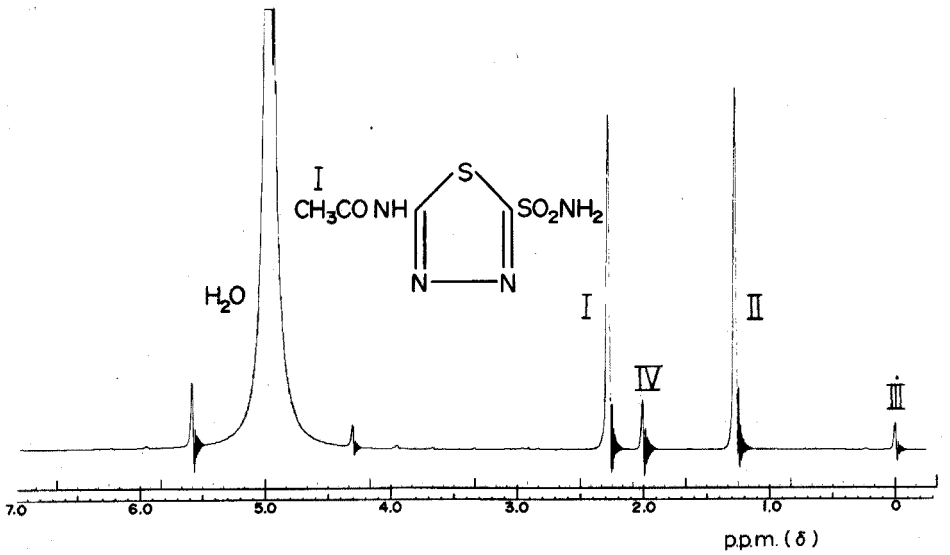

Fig. 1. The n.m.r. spectrum of acetazolamide in 25% ammonia solution. (I) Acetazolamide; (II) t-butanol; (III) Tiers' salt (DSS); (IV) acetate ion.

Table I summarizes the results of the analysis of a group of standard mixtures by n.m.r. The method is accurate and precise with a standard deviation of 0.73%. The proportions of t-butanol to acetazolamide show no significant bearing on the accuracy of the determination for the range of proportions shown in Table I. This n.m.r. procedure was used to analyze 10 commercial preparations of

TABLE I

DETERMINATION OF ACETAZOLAMIDE IN STANDARD MIXTURES BY N.M.R.

Standard mixture	*t-butanol internal standard added (mg)*	*Acetazolamide*		
		Added (mg)	*Found (mg)*	*Recovery (%)*
1	52.0	509.1	504.5	99.1
2	58.1	505.4	499.8	98.9
3	49.6	501.2	502.7	100.3
4	50.1	503.0	500	99.4
5	50.3	251.8	248.8	98.8
6	50.0	749.7	750.5	100.1
7	50.1	500.8	503.8	100.6

TABLE II

DETERMINATION OF ACETAZOLAMIDE IN COMMERCIAL PREPARATIONS

Dosage form	*Declared (mg/unit)*[a]	*Found (n.m.r.)*		*Found (USP XVIII)*	
		(mg/unit)[a]	*(%)*	*(mg/unit)*[a]	*(%)*
Tablets					
1	250	248.3	99.3	255.3	102.1
2	250	248.0	99.2	252.5	101.0
3	500	487.0	97.4	490	98.0
4	500	497.0	99.4	494	98.8
5	125	126.5	101.2	122.3	97.8
6	125	124.3	99.4	123.4	98.7
Injectables					
7	500	496.5	99.3	495.8	99.2
8	500	501.7	100.3	500.1	100.0
9	500	500.6	100.1	499.3	99.9
10	500	498.2	99.6	496.8	99.4

[a] For injection, mg/vial.

acetazolamide. Table II presents a summary of the results for 6 lots of acetazolamide in tablets and 4 lots of the cryodesiccated sodium salt of acetazolamide in vials; for comparative purposes the same lots were analyzed by the corresponding USP XVIII procedures. The agreement between the two analytical approaches in the analysis of tablets is within 2%; however, in the case of the sterile solid, where the sample is a pure material uncomplicated by other formulation components, the agreement is within less than 1%. Thus the data obtained from both procedures are in good agreement; however, the n.m.r. procedure has a distinct advantage over the official USP XVIII method, as is discussed below.

DISCUSSION

The ability of an analytical method to determine the quantity of a drug in the presence of its decomposition products is mandatory. The newly proposed procedure has this capability since it will detect and measure the extent of decomposition of acetazolamide and determine it in the presence of its decomposition products, provided that decomposition in excess of 1% has taken place. The decomposition products of acetazolamide in ammoniacal solution are acetate ion and 2-amino-1,3,4-thiadiazole-5-sulfonamide. Fortunately, the latter decomposition product has no protons other than the 2 amine protons and the 2 amide protons which are easily exchangeable and are part of the signal ascribable to the solvent water, thereby presenting no interference. However, the 3 protons of acetate resonate at 2 p.p.m. or *ca.* 17 Hz upfield (IV, Fig. 1) from the acetyl protons of the intact drug (I). This field position gives adequate separation between the two peaks of interest so that the extent of decomposition of acetazolamide can be measured, and acetazolamide itself can be determined in the presence of its decomposition products.

Neither of the official USP XVIII procedures (polarographic or u.v. spectrophotometric) has this capability. The reason for this is that both USP procedures are based on phenomena involving the 1,3,4-thiadiazole ring moiety which is also part of one of the decomposition products. Although there are some differences between the u.v. spectra and the polarograms of acetazolamide and 2-amino-1,3,4-thiadiazole-5-sulfonamide, these differences are not pronounced and cannot be used as unambiguous quantitative measures of decomposition as can n.m.r. In addition, studies[15] have shown that some tablet excipients such as gelatin and alginic acid suppress the height of the polarographic diffusion current exhibited by the reduction of acetazolamide, producing false low recoveries.

The author expresses his appreciation to Dr. Thomas Medwick, of the Food and Drug Administration, and of Rutgers University, New Brunswick, for his invaluable assistance in the preparation of this paper.

SUMMARY

A simple, accurate and specific n.m.r. procedure is described for the determination of acetazolamide in the pesence of its hydrolysis products in tablets and injection dosage forms. A standard deviation of 0.73% was obtained on 7 synthetic mixtures. The n.m.r. spectrum also provides a very selective means of identification for acetazolamide.

RÉSUMÉ

Une méthode de résonance nuléaire magnétique simple, exacte, et spécifique est décrite pour le dosage d'acétazolamide, en présencé de ses produits d'hydrolyse. Une déviation standard de 0.73% a été obtenue pour 7 mélanges synthétiques. Le spectre r.n.m. constitue également un moyen très sélectif d'identification de l'acétazolamide.

ZUSAMMENFASSUNG

Es wird ein einfaches, genaues und spezifisches n.m.r.-Verfahren beschrieben für die Bestimmung von Acetazolamid in Gegenwart von dessen Hydrolyseprodukten in Tabletten und Injektions-Verabreichungsformen. Bei 7 synthetischen Gemischen wurde eine Standardabweichung von 0.73% erhalten. Das n.m.r.-Spektrum ist auch ein sehr selektives Identifizierungsmittel für Acetazolamid.

REFERENCES

1 A. Mazon and A. Grzeszkiewicz, *Acta Pol. Pharm.*, 17 (1960) 47.
2 P. M. Parikh and S. P. Mukherji, *Indian J. Pharm.*, 20 (1958) 1979.
3 A. Kolusheva and N. Nin'o, *Farmatsiya (Sofia)*, 13 (1963) 21.
4 N. Bellen and M. Szelagowska, *Chem. Anal. (Warsaw)*, 4 (1959) 9.
5 H. Kola, *Pharmazie*, 16 (1961) 297.
6 Contribution in cooperation with Lederle Laboratory, *Drug Standards*, 26 (1958) 63 and 65.
7 H. Kola, *Pharmazie*, 20 (1965) 82.

8 W. Harke, C. Schirren and R. Wehrmann, *Klin. Wochenschr.*, 37 (1959) 1040.
9 K. Weclawska, *Gdansk. Tow. Nauk., Rozpr. Wydz.*, 5 (1968) 211.
10 B. Resibois and B. Picart, *Bull. Soc. Pharm. (Lille)*, 1 (1970) 35.
11 A. F. Summa, *J. Pharm. Sci.*, 51 (1962) 474.
12 *The United States Pharmacopoeia*, Mack Publishing Co., Easton, Pa., 18th Rev., 1970, pp. 14 and 604.
13 J. W. Turczan, B. A. Goldwitz and J. J. Nelson, *Talanta*, 19 (1972) 1549.
14 B. A. Goldwitz and J. W. Turczan, *J. Pharm. Sci.*, 62 (1973) 117.
15 S. Sherken, private communication.

Analytica Chimica Acta, 68 (1974) 401–406
© Elsevier Scientific Publishing Company, Amsterdam – Printed in The Netherlands

BEITRAG ZUM PROBLEM DER BANDENVERSCHIEBUNG IN DEN I.R.-SPEKTREN VON DIALKYLDITHIOCARBAMIDATEN

TEIL III. PYRROLDITHIOCARBOXYLATE. DER BEREICH VON 4000–300 cm^{-1}

R. KELLNER, P. PROKOPOWSKI und H. MALISSA

Institut für Analytische Chemie und Mikrochemie, Technische Hochschule, Wien (Österreich)

(Eingegangen den 29. Juli 1973)

Frühere Arbeiten[1–3] beschäftigten sich u.a. mit dem Problem der Zuordnung der stärksten Absorptionsbande in den I.R.-Spektren von Dialkyldithiocarbamidaten (Strukturmodell I)

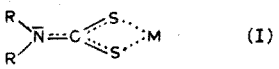

(I)

Aus der Theorie der Entstehung von IR-Spektren ist bekannt, dass die Intensität einer Bande mit dem Betrag der Änderung des Dipolmomentes des schwingenden Moleküls bei der Ausführung einer bestimmten Normalschwingung unmittelbar verknüpft ist.

Daher wurde die stärkste Absorptionsbande (im Bereich 1550–1400 cm^{-1}) einer Valenzschwingung der C–N-Gruppe, der polarsten Gruppe im Molekül I, zugeordnet. Experimentelle Beweise für diese Annahme standen bis heute noch aus. einer Bande mit dem Betrag der Änderung des Dipolmomentes des schwindigenden Moleküls bei der Ausführung einer bestimmten Normalschwingung unmittelbar Es wurde zwar versucht, die I.R.-Spektren von Äthylxanthogenaten (II)

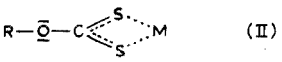

(II)

zum Vergleich mit den I.R.-Spektren der Diäthyldithiocarbamidate heranzuziehen[1,2], doch ist der Vergleich der I.R.-Spektren von I und II nicht ideal.

Die Autoren schlossen aus dem Auftreten einer starken Absorption bei dem Verbindungen des Typs II zwischen 1300 und 1200 cm^{-1} auf das Vorliegen einer reinen C–O-Einfachbindung, während durch das Auftreten der starken Bande um 1500 cm^{-1} bei den Verbindungen (I) der partielle Doppelbindungscharakter bewiesen werden sollte. Der Vergleich der beiden Verbindungstypen I und II erscheint jedoch nicht berechtigt, wenn man die Masseneinflüsse auf die Lage von I.R.-Banden berücksichtigt.

Eine Normalkoordinatenanalyse von Platin–Dithiocarbamidat (III) und dessen deuteriertem Analogen (IV)[4]

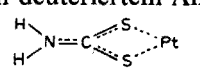

(III)

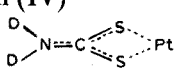

(IV)

ergab z.B. die stark differierenden Werte für die unverkoppelte ν-C–N von 1437 cm^{-1} für (III) und 1474 cm^{-1} für (IV). Für die ν-C–N in einer Verbindung (V)

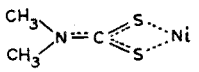

(V)

geben Durgaprasad *et al.*[5] einen berechneten Wert von 1551 cm^{-1} an. Der Einfluss der Liganden am Stickstoff auf die Lage der ν-C–N ist klar erkennbar.

Zur Klärung der Natur der starken Absorptionsbande in den IR-Spektren der Tetramethylendithiocarbamidate boten sich daher nur zwei Wege an:

1. eine Normalkoordinatenanalyse der tatsächlichen Verbindung, was jedoch bei einer 17-atomigen Struktureinheit der Punktgruppe C_{2v} mit einem hohen mathematischen Aufwand verbunden ist,

2. eine Untersuchung der I.R.-Spektren von möglichst masseähnlichen, isostrukturellen Verbindungen, in denen mit Sicherheit eine C–N-Einfachbindung vorliegt.

Verbindungen, die die Forderung 2 erfüllen, sind die Pyrroldithiocarboxylate (VI). Der sich gegenüber den Tetramethylendithiocarbamidaten durch das Fehlen von vier H-Atomen ergebende Massenunterschied ist bei einem Molgewicht von 146 pro Ligand (TMDTC) minimal. Infolge der Aromatizität des Pyrrols wird das freie Elektronenpaar des N daran gehindert, an einer C–N-Doppelbindung wie in III–V teilzunehmen. Das Gleichgewicht (VI) liegt vollständig auf der linken Seite.

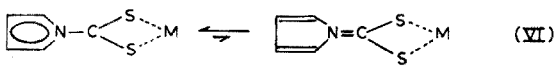

(VI)

Der folgende Bericht beschriebt die Realisation der experimentellen Beweisführung.

EXPERIMENTELLER TEIL

Darstellung von Pyrroldithiocarboxylaten

Während bei sekundären Aminen wie Diäthylamin und Pyrrolidin die Darstellung der N-Dithiocarbamidate leicht durchführbar ist und ein gängiger Weg zur Trennung sekundärer Amine von tertiären ist, waren alle derartigen Versuche mit Pyrrol ergebnislos. Das Nichtzustandekommen dieser elektrophilen Addition von Schwefelkohlenstoff an das aromatische Amin kann aus einem Vergleich der Basizitäten erklärt werden, die für Pyrrolidin 11.3, Diäthylamin 11.1, für Pyrrol aber nur 0.4 bei 20° betragen[6].

Deshalb mussten die Versuche zur Darstellung der Pyrroldithiocarboxylate über die Zwischenstufe des Pyrrolkaliums durchgeführt werden, welches zur Addition des Schwefelkohlenstoffs in Dimethylformamid gelöst wurde.

Da weder das Natrium- noch das Ammoniumsalz der Pyrroldithiocarbonsäure isolierbar waren, wurden die Metallchelate durch Zusatz der jeweiligen löslichen Metallsalze zur Dimethylformamid-Lösung gebildet und durch Zusatz eines vielfachen Überschusses an Waser ausgefällt. Dabei war es notwendig, bei der Bildung von Pyrroldithiocarboxylat die Temperatur der Lösung unter $-5°$ zu halten, um eine Umlagerung des N-Pyrroldithiocarboxylats in 2-Pyrroldithiocarboxylat zu vermeiden.

Die auf diese Art hergestellten Metall–Pyrroldithiocarboxylate wurden zur Reinigung wieder in Dimethylformamid gelöst und mit Wasser ausgefällt, da das Umkristallisieren wegen der geringen Löslichkeit dieser Substanzen in organischen Lösungsmitteln nicht möglich war. Die Elementaranalysen brachten bei den Ni-, Cd- und Pb-Komplexen zufriedenstellende Ergebnisse, während in den anderen Fällen die aus dem schwierigen Herstellungsgang zurückgebliebenen Verunreinigungen nicht vollständig entfernt werden konnten, was sich auf die für diese Arbeit ausgewerteten intensiven Banden nicht auswirkt.

Spektrenaufnahme

Die infrarotspektroskopischen Untersuchungen wurden mit einem I.R.-

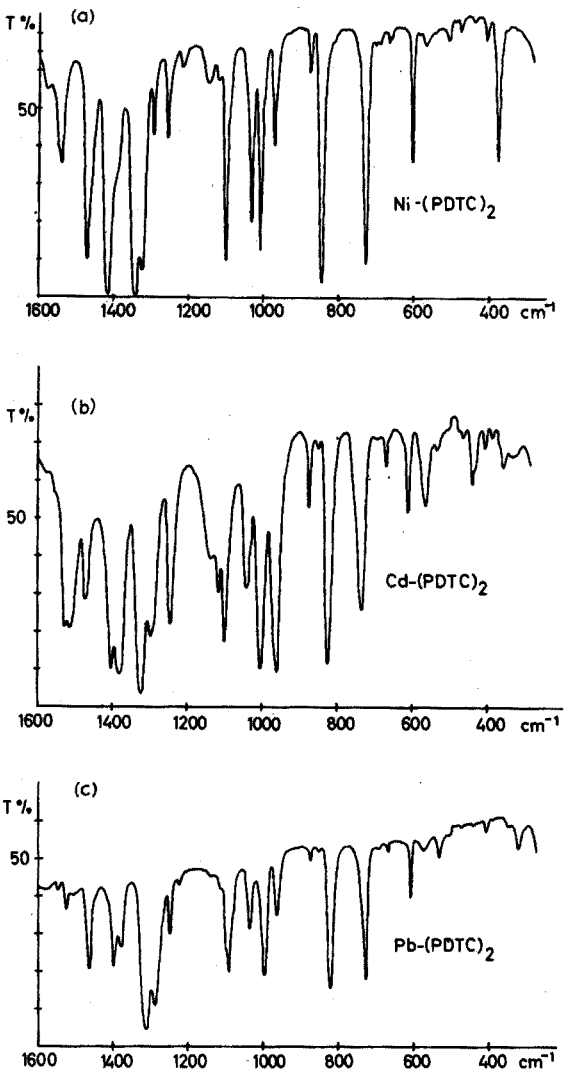

Abb. 1. I.R.-Spektren der untersuchten Substanzen. (a) Ni–$(PDTC)_2$; (b) Cd–$(PDTC)_2$; (c) Pb–$(PDTC)_2$.

Spektrophotometer der Fa. Perkin-Elmer, Typ 180, durchgeführt. Die getrockneten Substanzen wurden mit Kaliumbromid verrieben (0.5 Gew.% Substanz in KBr) und im Wellenzahlenbereich von 4000 bis 200 cm^{-1} aufgenommen.

DISKUSSION

Die Spektren der untersuchten Substanzen zeigen keine Absorption im Bereich der N–H-Bande, was das Vorliegen von N-Dithiocarboxylaten und die Abwesenheit von 2-Dithiocarboxylaten beweist. Man findet schwache C–H-Banden bei 3100 und 2900 cm^{-1}, weiters die durch den Aromaten hervorgerufene Absorption bei 1600–1400 cm^{-1} und 1100 cm^{-1}. Die für die Dithiocarboxylate charakteristischen Banden sind die ν-C–N bei 1300 cm^{-1}, deren Lage sich mit dem Zentralatom des Komplexes ändert, die ν-C–S bei *ca.* 1000 cm^{-1}, die ihre Lage nicht wesentlich ändert, sowie die wichtige Bande der asymmetrischen M–S-Valenzschwingung bei 400–300 cm^{-1} (als Beispiele die Spektren von Ni–, Cd–und Pb–Pyrroldithiocarboxylat in der Abb. 1).

Beim Vergleich der Spektren der von Kellner untersuchten Metall–Tetramethylendithiocarbamidate[3] mit jenen der Metallpyrroldithiocarboxylate fällt auf, dass

1. die Verschiebung der C–N- und der M–S-Banden einen ähnlichen Verlauf zeigen (Abb. 2),

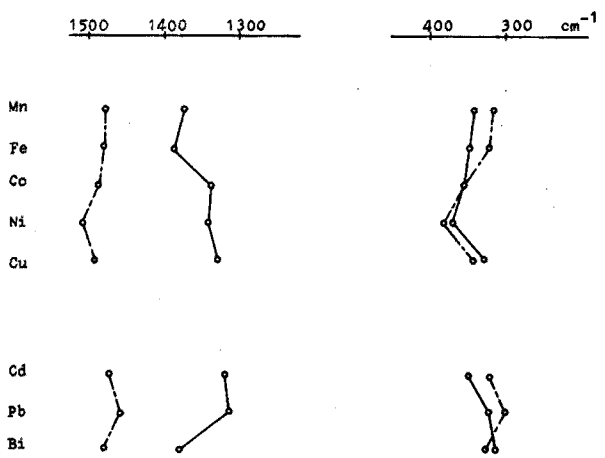

Abb. 2. Lage der ν-C–N und der ν-M–S in Pyrroldithiocarboxylaten und Tetramethylendithiocarbamidaten. (——) Pyrroldithiocarboxylate; (– – – –) Tetramethylendithiocarbamidate.

2. die Lage der ν-C–N bei den Pyrroldithiocarboxylaten um *ca.* 150 cm^{-1} tiefer liegt als jene der Tetramethylendithiocarbamidate, was auf das Vorliegen einer C–N-Einfachbindung wegen der nur schwer polarisierbaren aromatischen Gruppe im Liganden schliessen lässt, und

3. die Metall–Schwefel-Banden bei beiden Verbindungstypen im gleichen Wellenzahlenbereich liegen, wobei die Verschiebungen innerhalb einer Verbindungsgruppe bei den Pyrroldithiocarboxylaten geringer ist als bei den Tetramethylendithiocarbamidaten. Die Ursache dafür ist wieder im Liganden zu suchen, dessen

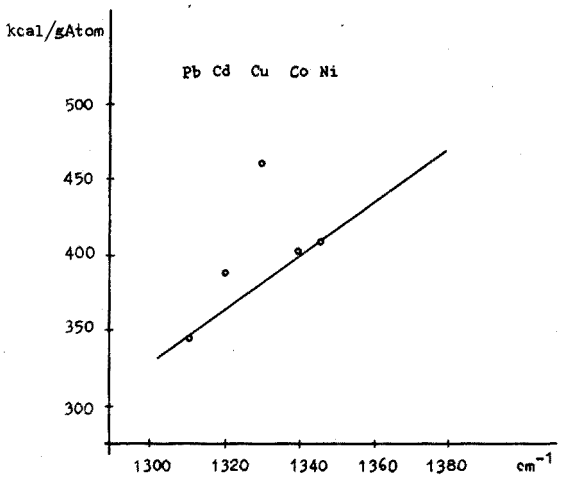

Abb. 3. Abhängigkeit der ν-C–N von Pyrroldithiocarboxylaten vom zweiten Ionisierungspotential der Metalle.

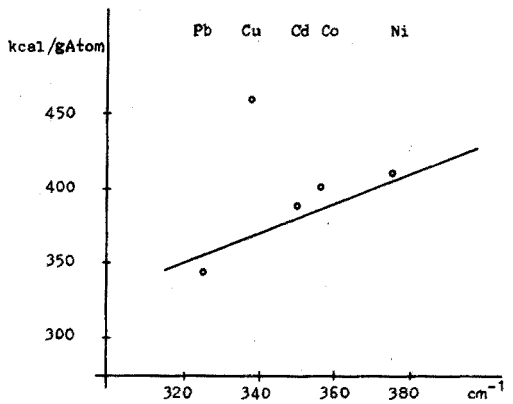

Abb. 4. Abhängigkeit der ν-M–S von Pyrroldithiocarbosylaten vom zweiten Ionisierungspotential der Metalle.

schwer polarisierbarer aromatischer Anteil eine starke Veränderung der Stärke der Metall–Schwefel-Bindung entsprechend den Elektronegativitäten der Metalle nicht zulässt.

Betrachtet man die Spektren der Metall–Pyrroldithiocarboxylate untereinander, so bemerkt man, dass die C–N- und M–S-Banden die grössten Verschiebungen aufweisen. Bringt man die Lage dieser Banden in Korrelation zu den Ionisierungspotentialen der entsprechenden Metalle, so ergibt sich eine annähernd lineare Beziehung (Abb. 3 und 4). Die Abweichung des Kupfer-Komplexes könnte dadurch erklärt werden, dass dieser in anderer Struktur vorliegt.

ZUSAMMENFASSUNG

Das Ziel dieser Arbeit war, Substanzen herzustellen (Pyrroldithiocarboxylate),

die den bereits untersuchten Tetramethylendithiocarbamidaten in Masse und Struktur möglichst ähnlich sind, aber eine C–N-Einfachbindung enthalten und diese Verbindungen infrarotspektroskopisch zu untersuchen. Im I.R.-Spektrum dieser neuen Verbindungen tritt die intensivste Bande im Bereich von 1300 cm^{-1} auf, die auf Grund ihrer Lage einer C–N-Einfachbindung zugeordnet werden kann. Da die entsprechende Bande im Spektrum der Tetramethylendithiocarbamidate um *ca.* 150 cm^{-1} zu höheren Wellenzahlen verschoben auftritt, erscheint die Annahme berechtigt, der C–N-Bindung in den Tetramethylendithiocarbamidaten den Charakter einer partiellen Doppelbindung zuzuordnen.

SUMMARY

An i.r. spectrometric study of specially prepared pyrroledithiocarboxylates is described. These compounds were selected as being very similar in mass and structure to the previously studied tetramethylenedithiocarbamates (TMDTC) except for the presence of a single C–N bond. The i.r. spectra of the new compounds show very intense bands in the region of 1300 cm^{-1}, which can be ascribed to the C–N bond. The corresponding bands in the spectra of the TMDTC compounds are shifted by *ca.* 150 cm^{-1} to higher wavenumbers, hence it seems correct to suggest that the C–N bond in such compounds has the character of a partial double bond.

RÉSUMÉ

Les auteurs ont effectué une étude sur la spectrométrie infra-rouge de pyrroledithiocarboxylates préparés spécialement. Ces composés ont été choisis comme étant très similaires, en masse et structure, aux tétraméthylènedithiocarbamates précédemment examinés (TMDTC), à l'exception d'une liaison simple C–N. Les spectres i.r. des nouveaux composés présentent des raies très intenses dans la région de 1300 cm^{-1} qui peuvent être attribuées à la liaison C–N. La position des bandes correspondantes dans le spectre des composés TMDTC est plus haute par *ca.* 150 cm^{-1}, ainsi on peut supposer que la liaison C–N dans ces composés présente un caractère de double liaison partielle.

LITERATUR

1 J. Chatt, L. A. Duncanson und L. M. Venanzi, *Suom. Kemistilehti*, 29B (1956) 75.
2 A. T. Pilipenko, *Zh. Neorg. Khim.*, 14 (1969) 462.
3 R. Kellner, *Anal. Chim. Acta*, 63 (1973) 277.
4 K. Nakamoto, *J. Chem. Phys.*, 39 (1963) 423.
5 G. Durgaprasad *et al.*, *Can. J. Chem.*, 47 (1969) 631.
6 A. Albert, *Chem. Heterocyclen*, 219 (1962).

Analytica Chimica Acta, 68 (1974) 407–413

© Elsevier Scientific Publishing Company, Amsterdam – Printed in The Netherlands

THE DETERMINATION OF TRACE METALS IN HIGH-PURITY SODIUM CALCIUM SILICATE GLASS, SODIUM BOROSILICATE GLASS, SODIUM CARBONATE AND CALCIUM CARBONATE BY FLAMELESS ATOMIC-ABSORPTION SPECTROMETRY

C. W. FULLER and J. WHITEHEAD

Tioxide International Limited, Billingham, Teesside TS18 2NQ (England)

(Received 25th June 1973)

The levels of trace metal impurities which affect the light-scattering and absorption properties of glasses required for laser communication systems, with fibre optic wave-guides have been outlined previously[1,2]. The determination of these impurities at concentrations down to 0.01 $\mu g\ g^{-1}$ in high-purity glasses and in the materials used for preparing them, presents many problems; the most important being (*a*) the possibility of sample contamination and (*b*) the paucity of suitably sensitive analytical techniques. Experimentally, the ideal technique for this type of work is neutron activation analysis[1], for problems of sample contamination are not relevant. Neutron activation analysis does, however, suffer from lack of sensitivity for some of the important metal impurities and has inherent problems in the high activity caused by the generation of sodium-24.

In these laboratories work has been carried out on improving the procedures available for trace element determinations in high-purity glasses and in the materials required for the production of these glasses. Methods have recently been published for the determination of platinum in glass[3] by an X-ray fluorescence technique and the determination of iron and copper in silica[4] by a flameless atomic-absorption technique. The determination of trace metals in glasses, calcium carbonate and sodium carbonate by flameless atomic-absorption spectrometry, recently reported briefly[5], is described here in detail.

EXPERIMENTAL

Apparatus

A Perkin-Elmer Model 306 atomic-absorption spectrophotometer was used with an HGA-70 Graphite Furnace[6], and a Model 165 recorder. Argon was used to provide the inert atmosphere within the graphite furnace. Grooved graphite tubes were used for all determinations; these were found to remove the problems invariably encountered when the normal graphite tubes are used for the analysis of organic solvents.

Oxford "Sampler" micropipettes fitted with disposable plastic sampling tips were used for introducing solutions into the graphite tube.

Reagents

Standard solutions containing 1000 μg ml^{-1} of the element being determined were prepared as follows.

Copper and nickel. Dissolve the pure metals in the minimal quantity of nitric acid and then dilute appropriately with distilled water.

Manganese and iron. Dissolve their sulphates in the appropriate quantity of distilled water, containing 1 ml of hydrochloric acid per litre.

Cobalt. Dissolve cobalt chloride in the appropriate quantity of distilled water, containing 1 ml of hydrochloric acid per litre.

Chromium. Dissolve potassium dichromate in the appropriate quantity of distilled water.

Composite standard solutions, containing all six elements, required for calibration purposes, were prepared as required by the appropriate dilution of the stock solutions with distilled water.

"Suprapur" hydrofluoric and perchloric acids (E. Merck, Darmstadt) were used for dissolving the samples.

All other reagents used were of analytical-grade quality.

Recommended procedure

All samples were analysed in duplicate where possible and duplicate blank determinations were done simultaneously. Place the glass samples in a platinum dish and heat in a furnace at 800–900° for 0.5–2 min (depending on the size and shape of the sample), then shatter them by dropping a few millilitres of distilled water onto the pieces of glass. Grind the samples to a fine powder with an agate pestle and mortar. Weigh 1.00 g of the sample into a platinum crucible, add 4 ml of hydrofluoric acid and 5 ml of perchloric acid and heat gently to dryness. For carbonates, weigh 1.00 g of sample into a platinum crucible, add 3 ml of perchloric acid to dissolve the sample, and heat gently to dryness.

TABLE I

INSTRUMENTAL CONDITIONS FOR THE DETERMINATION OF IRON, COPPER, NICKEL, COBALT, MANGANESE AND CHROMIUM BY FLAMELESS ATOMIC-ABSORPTION SPECTROMETRY

	Fe	*Cu*	*Ni*	*Co*	*Mn*	*Cr*
Sample aliquot (μl)	20	20	50	50	20	20
Programme setting[a]	6	6	7	7	6	6
Atomization voltage[a]	9½	9½	9½	9½	9½	9½
Drying time (s)	30	30	90	90	30	30
Ashing time (s)	30	30	30	30	30	30
Atomization time (s)	5	5	5	5	5	5
Scale expansion	×2	×2	×10	×5	×1	×2
Calibration range (μg ml^{-1})	0.02–5.00	0.01–0.50	0.02–0.50	0.01–0.50	0.01–0.50	0.01–0.50
Wavelength (nm)	248.3 and 372.0	324.7	232.0	240.7	279.5	357.9

[a] These figures refer to the use of a "grooved" type graphite tube.

Both types of sample are now treated in the same way. Dissolve the residue in a mixture of 0.1 ml of perchloric acid and 4 ml of water and transfer the solution to a 10-ml volumetric flask. Wash out the crucible with 5 ml of a solution containing *ca.* 5% (w/v) sodium diethyldithiocarbamate and 10% (w/v) sodium acetate, buffered at pH 6 and previously purified by extraction with isobutyl methyl ketone. Transfer these washings to the volumetric flask and allow the flask and contents to stand for 15 min. Add 1 ml of isobutyl methyl ketone to the flask and shake thoroughly for 3 min, and then allow the layer of isobutyl methyl ketone to separate in the neck of the flask; this extract is used for all subsequent determinations.

Determine the concentrations of iron, copper, nickel, cobalt, manganese and chromium in each sample by flameless atomic-absorption spectrometry under the instrumental conditions shown in Table I. Establish the concentrations from calibration graphs constructed using aqueous standards solutions and instrumental conditions identical to those used for the samples. Then determine the true sample concentrations by subtracting the blank readings from the sample readings.

RESULTS AND DISCUSSION

The direct analysis of the finely ground glass or carbonate samples by atomic-absorption spectrometry would be highly desirable, for this would ensure the absence of any problems from reagent blanks, and would decrease considerably the possibility of sample contamination. However, as was described in the case of silica[4], the efficient atomization of a refractory matrix is impossible. Moreover, even if complete atomization were possible, it can be shown that the analysis is not feasible. Approximately 0.4 mg of a glass sample will completely fill a graphite cell when atomized at 2,500°; so a glass containing 0.01 μg g^{-1} of impurity would produce in the graphite cell $4 \cdot 10^{-12}$ g of atoms of that impurity. The detection limits, at the present time[7,8], for iron, copper, nickel, cobalt, manganese and chromium with the Perkin-Elmer HGA 70 system are shown in Table II. Thus, even allowing

TABLE II

DETECTION LIMITS BY FLAMELESS ATOMIC-ABSORPTION SPECTROMETRY WITH THE PERKIN-ELMER HGA 70 SYSTEM

(Values in g)

Fe	*Cu*	*Ni*	*Co*	*Mn*	*Cr*
$4 \cdot 10^{-11}$	$1 \cdot 10^{-11}$	$1 \cdot 10^{-10}$	$7 \cdot 10^{-11}$	$1 \cdot 10^{-11}$	$4 \cdot 10^{-11}$

for the approximate nature of the calculations, five of the elements have detection limits an order of magnitude or more higher than that required for the direct analysis to be possible. However, these figures also show that if all the metal impurities in 1 g of glass or carbonate were separated from the matrix and concentrated into a volume of 1 ml, then by taking up to 50-μl aliquots of the extract, the determination of all six elements becomes feasible. The "effective weight of glass" being analysed has been increased by more than two orders of magnitude.

The general extraction of diethyldithiocarbamate–metal complexes into isobutyl methyl ketone was chosen for this work, because considerable information was available on its uses, both in the literature[9,10] and from work previously carried out in these laboratories.

When determinations down to 0.01 $\mu g\ g^{-1}$ are carried out, particular attention must be paid to experimental detail, purity of reagents and the cleanliness of apparatus and the surrounding laboratory conditions. For these reasons the following points are essential:

(*a*) all platinum, plastic and glass ware should initially be thoroughly cleaned and then retained solely for this type of work;

(*b*) reagents of the highest purity available should be used and where possible further purification undertaken if necessary;

(*c*) the absolute minimum of apparatus should be used;

(*d*) the samples should be dissolved under an extraction hood and all work should be carried out in a clean atmosphere, preferably in a clean air cabinet.

The minimal quantity of acids required to dissolve efficiently 1 g of powdered glass was found to be a mixture of 4 ml of hydrofluoric acid and 5 ml of perchloric acid and for the carbonates, 3 ml of perchloric acid. High-purity commercial acids were found to be of sufficient purity to determine down to 0.01 $\mu g\ g^{-1}$. If it is necessary to determine lower levels, then the application of techniques such as sub-boiling point distillation should give considerably purer acids[10]. A mixed sodium acetate–sodium diethyldithiocarbamate solution, buffered at pH 6, was employed, so that both these reagents could be purified before use, by extraction with isobutyl methyl ketone. A platinum crucible and a 10-ml volumetric flask were the only pieces of apparatus used in the chemical separation. These precautions give rise to reproducible and acceptable levels of impurities in the blank solutions (Table III).

TABLE III

NORMAL LEVEL OF IMPURITIES FOUND IN A BLANK DETERMINATION

(Values in μg)

Fe	*Cu*	*Ni*	*Co*	*Mn*	*Cr*
0.10	0.02	0.02	0.01	0.01	<0.005

The level for iron is acceptable at present because the iron content in most glasses is greater than 0.1 $\mu g\ g^{-1}$; if this level is reduced the acids can be further purified as described above, to improve the blank readings. Because the level of iron in some impure samples can be as high as 5 $\mu g\ g^{-1}$ the less sensitive absorption line for iron at 372.0 nm can be used, to avoid the need for sample dilution.

Recoveries of iron, copper, nickel, cobalt, manganese and chromium were demonstrated by analysing samples of sodium carbonate, calcium carbonate and sodium calcium silicate glass to which known additions had been added. The results are shown in Table IV. The recoveries of iron, nickel, cobalt and manganese were excellent in all cases as were the recoveries for copper except in the case of sodium carbonate where they were low but acceptable. Chromium, as expected

TABLE IV

RECOVERIES OF IRON, COPPER, NICKEL, COBALT, MANGANESE AND CHROMIUM ADDITIONS TO A CALCIUM CARBONATE, A SODIUM CARBONATE AND A SODIUM CALCIUM SILICATE GLASS

	Iron ($\mu g\ g^{-1}$)		*Copper ($\mu g\ g^{-1}$)*		*Nickel ($\mu g\ g^{-1}$)*		*Cobalt ($\mu g\ g^{-1}$)*		*Manganese ($\mu g\ g^{-1}$)*		*Chromium ($\mu g\ g^{-1}$)*	
	Found	*Recovered*	*Found*	*Recovered*	*Found*	*Recovered*	*Found*	*Recovered*	*Found*	*Recovered*	*Found*	*Recovered*
$CaCO_3$: Sample	0.19	—	0.05	—	0.21	—	0.02	—	0.02	—	<0.01	—
+0.2 $\mu g\ g^{-1}$	0.37	0.18	0.25	0.20	0.42	0.21	0.24	0.22	0.26	0.24	0.14	0.14
+0.4 $\mu g\ g^{-1}$	0.60	0.41	0.45	0.40	0.61	0.40	0.43	0.41	0.42	0.40	0.27	0.27
Na_2CO_3: Sample	0.23	—	<0.01	—	0.06	—	0.02	—	0.01	—	<0.01	—
+0.2 $\mu g\ g^{-1}$	0.43	0.20	0.16	0.16	0.26	0.20	0.22	0.20	0.21	0.20	0.16	0.16
+0.4 $\mu g\ g^{-1}$	0.63	0.40	0.29	0.29	0.48	0.42	0.42	0.40	0.42	0.41	0.29	0.29
Glass: Sample	0.58	—	0.19	—	0.18	—	0.02	—	0.03	—	<0.01	—
+0.2 $\mu g\ g^{-1}$	0.76	0.18	0.38	0.19	0.37	0.19	0.22	0.20	0.23	0.20	0.06	0.06
+0.4 $\mu g\ g^{-1}$	0.94	0.36	0.59	0.40	0.60	0.42	0.43	0.41	0.42	0.39	0.15	0.15

gave low recoveries, because of losses as chromyl chloride and/or fluoride during the dissolution stages. Despite these poor recoveries for chromium, the method can still give an indication of the chromium levels in the various samples. Relative standard deviations of 5–10% were obtained in all cases at the 0.2 $\mu g\ g^{-1}$ level.

The procedure described here has been in routine use for about nine months and has been used to determine iron, copper, nickel, cobalt and manganese in over one hundred samples.

This work was carried out under a Post Office Research and Development Contract, and is published by permission of the Directors of Tioxide International Limited and of the Senior Director of Development of the Post Office.

SUMMARY

A procedure for the determination of iron, copper, nickel, cobalt, manganese and chromium down to 0.01 $\mu g\ g^{-1}$ in sodium calcium silicate glass, sodium borosilicate glass, sodium carbonate and calcium carbonate is described. The analytical procedure depends on the separation at pH 6 of the metal diethyldithiocarbamates into isobutyl methyl ketone, and their determination by flameless atomic absorption spectrometry, with a Massmann-type graphite furnace. The limiting factors on the detection limits attainable are discussed and related to the purity of the acids used for sample solution, sample contamination during chemical separation and the sensitivity of the analytical technique.

RÉSUMÉ

Une méthode est décrite pour le dosage du fer, du cuivre, du nickel, du cobalt, du manganèse et du chrome en quantités pouvant descendre jusqu'à 0.01 $\mu g\ g^{-1}$, dans du verre au silicate sodicocalcique, du verre au borosilicate de sodium, du carbonate de sodium et du carbonate de calcium. Elle est basée sur la séparation à pH 6 des diéthyldithiocarbamates métalliques dans la méthylisobutylcétone et dosage spectrométrique par absorption atomique sans flamme, avec four de graphite de type Massmann. On examine les limites de détection possibles, la contamination de l'échantillon au cours de la séparation chimique et la sensibilité de la méthode.

ZUSAMMENFASSUNG

Es wird ein Verfahren beschrieben, mit dem Eisen, Kupfer, Nickel, Kobalt, Mangan und Chrom bis zu 0.01 $\mu g\ g^{-1}$ herab in Natrium-Calcium-Silicat-Glas, Natrium-Borosilicat-Glas, Natriumcarbonat und Calciumcarbonat bestimmt werden können. Die Metalle werden durch Extraktion der Diäthyldithiocarbamate bei pH 6 mittels Isobutylmethylketon abgetrennt und durch flammenlose Atomabsorptionsspektrometrie unter Verwendung eines Graphitofens vom Massman-Typ bestimmt. Die die erzielbaren Nachweisgrenzen bestimmenden Faktoren werden diskutiert und mit der Reinheit der für die Probenlösung verwendeten Säuren, mit der Probenverunreinigung während der chemischen Abtrennung und mit der Empfindlichkeit des analytischen Verfahrens in Beziehung gestzt.

REFERENCES

1 C. K. Kim, S. S. Voris and W. G. French, *Glass Technol.*, 12 (1971) 128.
2 D. E. Campbell and P. B. Adams, *Glass Technol.*, 10 (1969) 29.
3 C. W. Fuller, G. Himsworth and J. Whitehead, *Analyst*, 96 (1971) 177.
4 C. W. Fuller, *Anal. Chim. Acta*, 62 (1972) 261.
5 C. W. Fuller, *At. Absorption Newslett.*, 12 (1973) 40.
6 D. C. Manning and F. J. Fernandez, *At. Absorption Newslett.*, 9 (1970) 65.
7 F. J. Fernandez, *At. Absorption Newslett.*, 11 (1972) 123.
8 F. J. Fernandez and D. C. Manning, *At. Absorption Newslett.*, 10 (1971) 65.
9 Yu. A. Chernikhov and B. M. Dobkina, *Zavod. Lab.*, 15 (1949) 1143.
10 J. Nix and T. Goodwin, *At. Absorption Newslett.*, 9 (1970) 119.

Analytica Chimica Acta, 68 (1974) 415–424

© Elsevier Scientific Publishing Company, Amsterdam – Printed in The Netherlands

EXTRACTION OF SOME DICARBOXYLIC ACIDS BY TRI-ISOOCTYLAMINE

A. S. VIEUX, N. RUTAGENGWA, J. B. RULINDA and A. BALIKUNGERI
Laboratoire de Chimie Analytique, Université Nationale du Zaïre, Campus de Kinshasa (Zaïre)
(Received 26th June 1973)

The extraction of mineral acids from aqueous solutions with the aid of long-chain aliphatic amines has been intensively investigated, but, in comparison, little has been published on the extraction of organic acids. In the first published work on amines as extracting agents, Smith and Page[1] did mention the feasibility of extracting organic acids with a 5% solution of methyldioctylamine in chloroform. Subsequently, the extraction of some other organic acids was investigated[2–13].

In the case of dicarboxylic acids, detailed investigations were conducted on the extraction of oxalic[14–17] and malonic[18] acids. These studies were mainly concerned with the determination of the equilibria involved and the nature of the organic compounds formed. However, the conclusions reached, concerning the neutralization of either one or both of the carboxyl groups in the reaction of dicarboxylic acids with long-chain aliphatic amines, are divergent, and it is clear that the equilibria involved remain very much open to question. The present work was carried out to determine some of the parameters characterizing the interaction of the first three dicarboxylic acids in the aliphatic series—oxalic, malonic and succinic—with tri-isooctylamine. To our knowledge, the equilibria involved for succinic acid have not been reported before.

Extractions were made with tri-isooctylamine in various undissociated solvents, such as benzene, xylene, chloroform, 1,2-dichloroethane and *o*-dichlorobenzene. These solvents, which have been used for the extraction of acids and metallic ions by alkylamines, were chosen on the basis of their behavior as described in the literature: benzene and xylene are basic aromatic diluents capable of interacting via their π-electrons with the ammonium cation; chloroform, a polar acidic diluent, provides the possibility of hydrogen bonding to the anion; 1,2-dichloroethane and *o*-dichlorobenzene have relatively high dielectric constants. Carbon tetrachloride, a useful rather inert solvent, was tried, but was not chosen because of the low value of the distribution coefficient in extraction.

In this work, chemical data were obtained by the method of isomolar series, the dependence of the acid content of the organic phase on the acid concentration of the aqueous phase, and the dependence of the distribution coefficient on the concentration of the amine. The solubilities of the oxalic acid salt of tri-isooctylamine in various solvents and the determination of its molecular weight are reported.

EXPERIMENTAL

Reagents

Tri-isooctylamine (R_3N) was used. This tertiary amine is quite basic[19] and

appears to be convenient for such a study. The many published works dealing with the use of this amine, confirm its excellent extractive properties[6, 20–26]. The difficulty in defining the exact structure of this amine comes from its isomeric nature[21]. The commercial product has a purity of 98%; this was confirmed by analysis. The commercial product was purified by vacuum distillation (10 mm Hg, 215°). The molecular weight of the amine determined by potentiometric titration was 353.7.

Redistilled reagent-grade Merck solvents were used. The chloroform (Merck p.a.) used was washed 3–4 times with twice its volume of water to remove the 1% of ethanol.

Oxalic, malonic and succinic acids were of analytical grade. Oxalic acid was purified as described by Kolthoff and Sandell[27]. Malonic acid was purified as described by Hall[28]. Succinic acid was recrystallized twice from water[29].

Freshly prepared solutions were used. Amine solutions in organic diluents as well as aqueous acidic solutions, were prepared by weighing. Aqueous solutions were made up with deionized water. For the method of isomolar series, two total concentrations were used: 0.25 *M* and 0.50 *M*.

Extraction

The acids were extracted at room temperature ($25 \pm 2°$). The tri-isooctylamine solutions were shaken in the extraction tubes for 20 min, with equal volumes of aqueous solutions of the acids; preliminary experiments showed that this time was sufficient for complete equilibration. Except for oxalic acid, neither a third phase nor a variation of volume of the two phases was observed. After centrifuging, suitable aliquots of the aqueous phase and of the organic phase were pipetted for the determination of acid concentrations. First, the distribution of the acids between the organic solvents and the water phase was determined. Correction for this was made when necessary.

Methods of analysis

Amine solutions were titrated with standard perchloric acid solution in a homogeneous water–alcohol phase in the ratio of 10% organic solution, 75% ethanol and 15% water.

The concentrations of the initial aqueous solutions of acids were checked by potentiometric titration against standard alkali, with a pH meter (Radiometer pHM 4c). In order to provide an inert atmosphere in the titration vessel, argon was slowly passed over the solutions. The concentration of aqueous oxalic acid solutions was also checked by permanganate titration.

After the extraction, the acid contents of both the aqueous and the organic phases were determined by potentiometric titration. The acid content of the organic phase was determined in a homogeneous water–alcohol phase in the same ratio as that previously mentioned for amine determination. All determinations of the acid content were performed under an argon atmosphere. When a precipitate was formed, *e.g.* with oxalic acid, the organic phase and the precipitate were placed together in a homogeneous water–alcohol phase, in the ratio already indicated. Sometimes, the acid content of the organic phase was obtained by difference. Good agreement was found between the two methods. Experimental data agreed within $\pm 1\%$; reported results are the average of at least two determinations.

Melting point and molecular-weight determinations of the salt of oxalic acid with tri-isooctylamine

Samples of the precipitate of the alkylammonium salt of oxalic acid were used for the determination of its melting point and its molecular weight, after vacuum-distillation of the diluent and drying in a desiccator. Samples were purified by recrystallization from petroleum ether (b.p. 40°–60°). Two methods were used to determine melting points: microscopic observation, with a Leitz-Wetzelar melting-point apparatus equipped with a platinum heating plate, and the capillary tube method in a concentrated sulfuric acid bath.

The molecular weight was determined by the cryoscopic method with a Beckmann equilibrated thermometer. Nitrobenzene was chosen as cryoscopic liquid.

RESULTS AND DISCUSSIONS

The extraction systems were studied by the method of isomolar series, by the distribution of the acids between the aqueous and organic phases and by consideration of the dependence of the distribution coefficient of the acids on the concentration of the amine.

The method of isomolar series is seldom used in the case of extraction with alkylamines. It has been used in investigating the extraction of nitric acid[30], the interaction of oxalic acid with trioctylamine[15], and the extraction of rhenium in its highest oxidation state between aqueous nitric acid and tris-(2,2,4-trimethyl-pentylamine)[31]. Figure 1 gives the results of the experiments with tri-isooctylamine

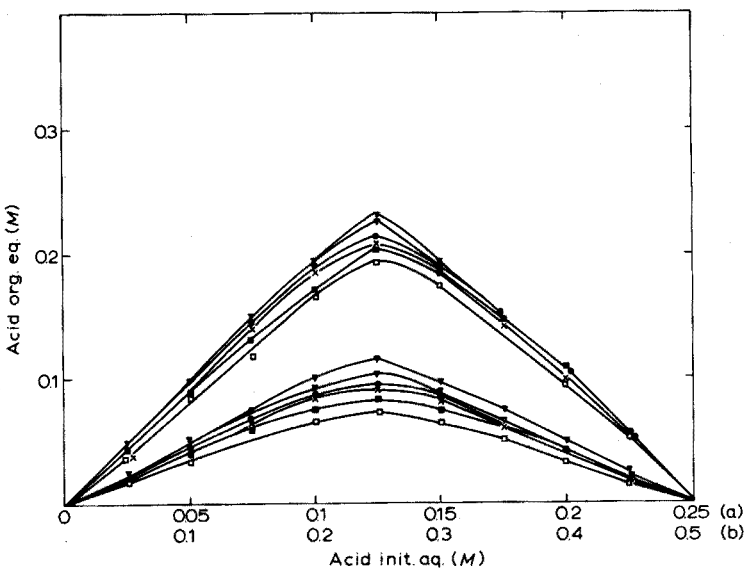

Fig. 1. Relation of acid concentration in the equilibrated organic phase (org. eq.) to the initial acid concentration in the aqueous phase (init. aq.). (a) TIOA + $H_2C_2O_4$ = 0.25 *M* in xylene (■), C_6H_6 (●) and $CHCl_3$ (▽); TIOA + $CH_2(COOH)_2$ = 0.25 *M* in xylene (□), C_6H_6 (×) and $CHCl_3$ (▼); (b) TIOA + $H_2C_2O_4$ = 0.50 *M* in xylene (■), C_6H_6 (●) and $CHCl_3$ (▽); TIOA + $CH_2(COOH)_2$ = 0.50 *M* in xylene (□), C_6H_6 (×) and $CHCl_3$ (▼).

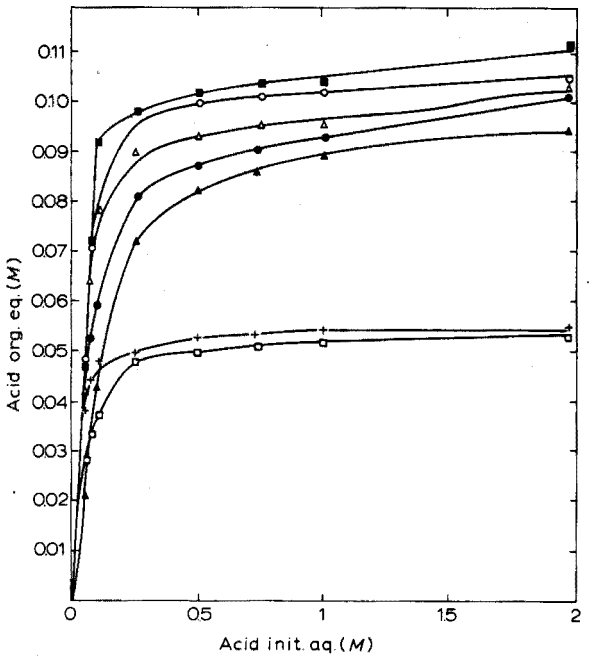

Fig. 2. Distribution of malonic acid between an aqueous solution and a solution of tri-isooctylamine in various solvents. Benzene (□), *o*-dichlorobenzene (+) with $R_3N_{init.}$ equal to 0.05 *M*; xylene (●), benzene (●), *o*-dichlorobenzene (△), chloroform (○) and 1,2-dichloroethane (■) with $R_3N_{init.}$ equal to 0.1 *M*.

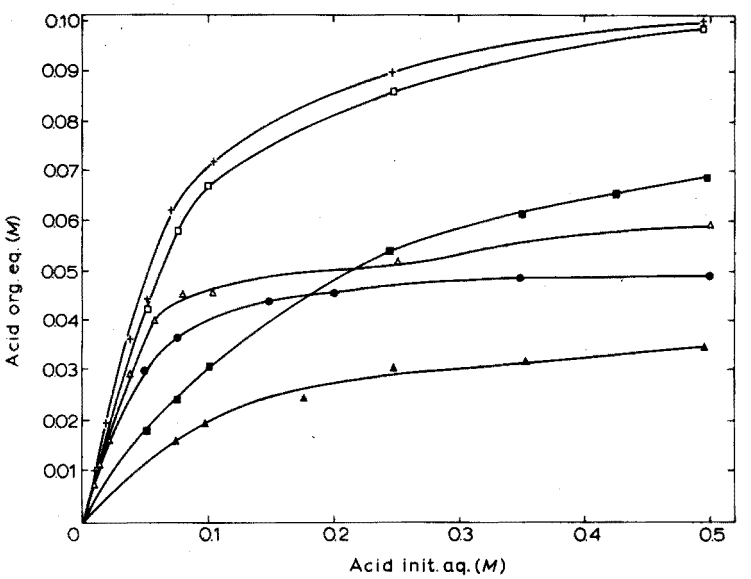

Fig. 3. Distribution of succinic acid between an aqueous solution and a solution of tri-isooctylamine in various solvents. *o*-Dichlorobenzene (▲), 1,2-dichloroethane (●) and chloroform (△) with $R_3N_{init.}$ equal to 0.05 *M*; *o*-dichlorobenzene (■), 1,2-dichloroethane (□) and chloroform (+) with $R_3N_{init.}$ equal to 0.1 *M*.

plus aqueous acid of concentrations 0.5 *M* and 0.25 *M*, for oxalic and malonic acids. From the shape of the curves obtained, it may be assumed that both oxalic and malonic acids interact with tri-isooctylamine (R_3N) to form compounds whose stoichiometric compositions are $R_3N \cdot H_2C_2O_4$ and $R_3N \cdot CH_2(COOH)_2$, respectively.

The data obtained on the distribution of malonic and succinic acids between an aqueous solution and a solution of tri-isooctylamine in various solvents are cited in Figs. 2 and 3. For succinic acid, the rather low solubility of the acid in the aqueous phase limited the range of high concentrations to 0.5 *M*. Malonic acid is highly soluble in water[32]; consequently, quite a wide range of initial aqueous acid concentrations could be investigated. For both acids, the relatively low value of the distribution coefficient limited the range of investigations for an initial high molar ratio of amine to the initial concentration of acid in the aqueous phase. It appears that malonic and succinic acids interact similarly with tri-isooctylamine. However, the distribution coefficient of succinic acid is smaller than that of malonic acid. This could be related to the structure of the acids in aqueous solutions. Substituted succinic acids have been shown to contain internal hydrogen bonds, but this feature is not apparent for malonic acid solutions[33]. From Figs. 2 and 3 it can be seen that with increasing acid concentration in the aqueous phase, the acid concentration in the organic solution increases monotonically to a molar ratio, *i.e.* $(CH_2)_n(COOH)_{2\,org.eq.} : R_3N_{init.} = 1:1$, where $n = 1$ or 2, for malonic and succinic acids, respectively. Any further increase of acid concentration in the organic phase occurs considerably more slowly.

From Figs. 2 and 3 it is evident that there is no point of inflexion on the curves corresponding to the neutralization of the two carboxyl groups. Lipovskii and Kuzina[17] obtained a curve of similar shape and they assumed the formation of the hydrogenoxalate of trioctylamine. The results of Bullock *et al.*[14] also showed that when the oxalic acid concentration is increased, the amine–oxalic acid mole ratio in the organic phase becomes equal to unity, which implies complete formation of the hydrogenoxalate of methyldioctylamine in chloroform. However, according to these authors, at low oxalic acid concentrations in the organic phase, the oxalate species is formed.

After vacuum-distillation of the solvent and drying in a desiccator, samples of different ratios of the amine and acid were paraffin-like. When the ratio of tri-isooctylamine to acid was high, the paraffin-like residue after distillation separated into two phases. The infrared spectra of the two phases showed that one phase corresponded to free tri-isooctylamine, while the other gave indications of acid extraction.

The results of the distribution of acids between the tri-isooctylamine phase and water are presented as logarithmic plots of the acid distribution coefficients *vs.* the amount of amine in the organic phase at equilibrium in Fig. 4. The slope of the relationship is close to unity. It can be estimated that the acid salt of tri-isooctylamine is formed, and that the salt exists as ion pairs.

The different sets of results show agreement between the various chemical methods and lead to the conclusion that only one carboxyl group is neutralized. It can thus be assumed that, in the range of the concentrations considered, the interaction between tri-isooctylamine and the acids, leads to the formation of the

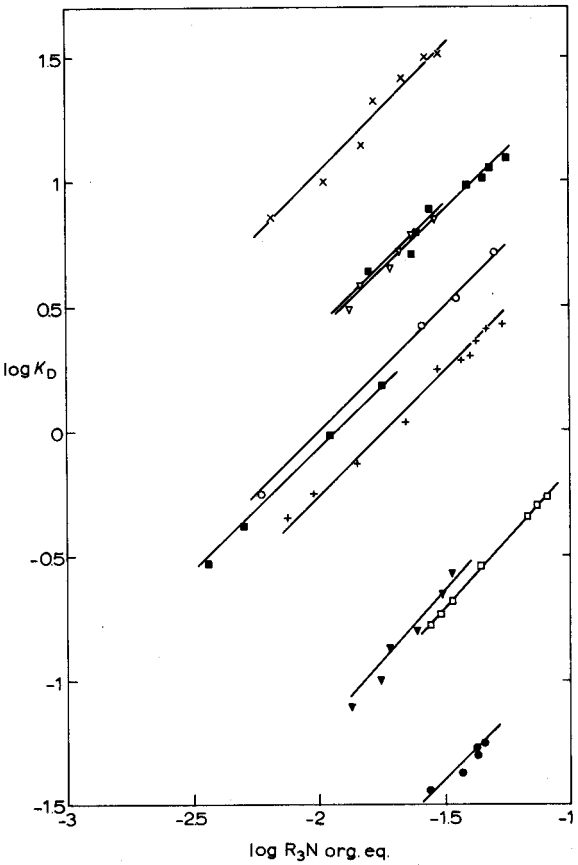

Fig. 4. Logarithmic plots of the distribution coefficients of the organic acid *vs.* the amount of tri-isooctylamine in the organic phase at equilibrium. Oxalic acid in *o*-dichlorobenzene (▽), 1,2-dichloroethane (×) ($R_3N_{init.} = 0.05$ *M*). Malonic acid in benzene (+), *o*-dichlorobenzene (■) ($R_3N_{init.} = 0.1$ *M*). Succinic acid in benzene (●), *o*-dichlorobenzene (▼), 1,2-dichloroethane (■) ($R_3N_{init.} = 0.05$ *M*); *o*-dichlorobenzene (□) and 1,2-dichloroethane (○) ($R_3N_{init.} = 0.1$ *M*).

hydrogenoxalate, the hydrogenmalonate and the hydrogensuccinate of tri-isooctylamine. However, for high molar ratios of amine:organic acid content, the possibility of the formation of neutral salts cannot be excluded.

It has been mentioned in the literature[14,15,17] that a white precipitate is formed between the phases in the extraction of oxalic acid with the aid of alkylamines, the formation of this precipitate depending on the concentration of the acid in the aqueous phase. The same phenomenon was observed with tri-isooctylamine. In benzene, xylene, and *o*-dichlorobenzene, at low aqueous acid concentrations (up to 0.03 *M*), the organic phase remained clear; with increasing aqueous acid concentrations a white suspension appeared in the organic phase, which, on cooling to 5°, crystallized into a white precipitate. For aqueous acid concentrations of 0.08 *M*, a definite white precipitate was formed between the phases. In chloroform and 1,2-dichloroethane, the same observations were made but the formation of the precipitate occurred at much higher aqueous acid concentrations, which

suggests that the nature of the solvent may play an important role in this phenomenon.

It is known that the diluent interacts with both the amine and the quaternary ammonium salt through its functional groups, and with the salt through long-range coulombic effects[34,35]. In general, the higher the dielectric constant of the diluent, the better the extraction. Differences in the magnitude of extraction caused by diluent interactions may become very large, as illustrated in Figs. 2 and 3. For oxalic acid, even though *o*-dichlorobenzene and 1,2-dichloroethane have dielectric constants of the same magnitude[36], better results are obtained with 1,2-dichloroethane. The fact that the solubilities in 1,2-dichloroethane and chloroform are similar, suggests chemical bonding of the diluent with the free ion pair, as noticed in the extraction of acetic acid with triethylamine in chloroform[4].

In all cases, the precipitate is easily dissolved in a water–alcohol phase in the approximate ratio, in volume, of 10% organic phase and precipitate, 75% ethanol and 15% water. Lipovskii and Kuzina[17] noticed the relatively good solubility in chloroform of anhydrous preparations with a trioctylamine:oxalic acid ratio of 1:1 or 1:2, even without the addition of water. The solubility in chloroform could be due to the formation of a hydrogen bond with the ammonium cation in view of the participation of the proton of chloroform in a bond with the other oxygen atom of the carboxylate group. The melting point of the crystalline salt was found to be $76.0 \pm 0.1°$.

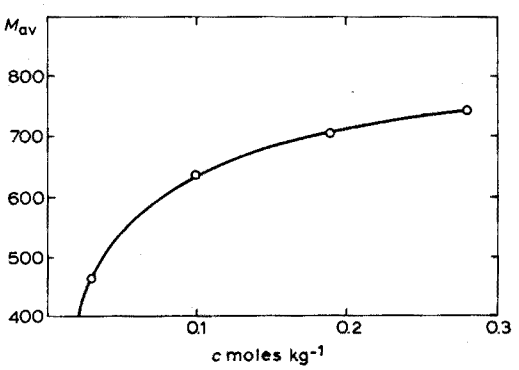

Fig. 5. Dependence of the average molecular weight of tri-isooctylamine hydrogenoxalate on its concentration in nitrobenzene.

The molecular weight was determined from the formula $M = (P_p \cdot K)/(\Delta t \cdot P_s) \cdot 1000$, where P_p and P_s are the weights of the precipitate and diluent, respectively, Δt is the depression of the freezing point, and K is the cryoscopic constant of the diluent (nitrobenzene: $K = 6.89$ according to Lipovskii and Kuzina[17]). Because anhydrous tri-isooctylamine is so slightly soluble in benzene, nitrobenzene was used as a cryoscopic liquid, in order to elucidate whether the anhydrous crystalline hydrogenoxalate has a monomeric or dimeric structure. The data obtained are cited in Fig. 5. Even though the limited solubility of the hydrogenoxalate salt in nitrobenzene does not allow the average molecular weight of the dimer to be reached, it is obvious from the shape of the curve that the crystalline molecule of

the hydrogenoxalate of tri-isooctylamine has a dimeric structure which may be:

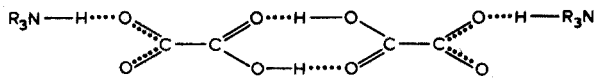

However, as logarithmic plots of the acid distribution coefficient *vs.* the amine concentration in *o*-dichlorobenzene and 1,2-dichloroethane give a straight line, there is evidence of the breakdown of this dimeric structure in solutions in the diluents. The breakdown of the dimeric structure has been observed in the spectra of equimolar mixtures of carboxylic acids with water[37].

These conclusions are in agreement with those of Lipovskii and Kuzina[17] for trioctylamine hydrogenoxalate, the structure of which in chloroform solution was found to be monomeric and for which the following structure has been proposed:

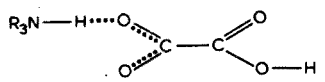

SUMMARY

The extraction of oxalic, malonic and succinic acid with tri-isooctylamine in various organic solvents has been investigated. Chemical data obtained by the method of isomolar series, and studies of the dependence of distribution coefficients on the acid concentration in the aqueous phase and the amine concentration in the organic phase, indicate that the acids interact with tri-isooctylamine to form compounds whose stoichiometric compositions are $R_3N \cdot H_2C_2O_4$, $R_3N \cdot (CH_2)(COOH)_2$ and $R_3N \cdot (CH_2COOH)_2$ for the three acids. The solubility of the salt of oxalic acid in various diluents is discussed. By molecular weight determination, the crystalline salt of hydrogenoxalate of tri-isooctylamine was found to be dimeric; but there was evidence of the breakdown of the dimer in *o*-dichlorobenzene and 1,2-dichloroethane solutions.

RÉSUMÉ

Une étude est effectuée sur l'extraction des acides oxalique, malonique et succinique, au moyen de tri-isooctylamine dans divers solvants organiques. Les valeurs chimiques obtenues indiquent que les trois acides réagissent avec la tri-isooctylamine pour former des composées dont les compositions stoechiométriques sont$R_3N \cdot H_2C_2O_4$,$R_3N \cdot (CH_2)(COOH)_2$ et $R_3N \cdot (CH_2COOH)_2$. On examine la solubilité du sel de l'acide oxalique dans divers diluants. La détermination du poids moléculaire montre que le sel cristallin de l'hydrogénooxalate de tri-isooctylamine est dimère, avec mise en évidence dans l'*o*-dichlorobenzène et le dichloro-1,2-éthane.

ZUSAMMENFASSUNG

Die Extraktion von Oxal- Malon- und Bernsteinsäure mittels Tri-isooctylamin in verschiedenen organischen Lösungsmitteln wurde untersucht. Die nach der Methode der isomolaren Reihen erhaltenen chemischen Ergebnisse und die Untersuchung der Abhängigkeit der Verteilungskoeffizienten von der Säurekonzentration in der wässrigen Phase und der Aminkonzentration in der organischen Phase weisen darauf hin, dass die drei Säuren mit Tri-isooctylamin unter Bildung von Verbindungen der stöchiometrischen Zusammensetzung $R_3N \cdot H_2C_2O_4$ bzw. $R_3N \cdot (CH_2)(COOH)_2$ bzw. $R_3N \cdot (CH_2COOH)_2$ reagieren. Die Löslichkeit des Oxalsäuresalzes in verschiedenen Verdünnungsmitteln wird diskutiert. Nach Molekulargewichtsbestimmungen ist das kristalline Hydrogenoxalat von Tri-isooctylamin dimer; jedoch gab es Hinweise darauf, dass das Dimere in *o*-Dichlorbenzol- und 1,2-Dichloräthan-Lösungen aufgespalten wird.

REFERENCES

1 L. S. Smith and J. E. Page, *J. Soc. Chem. Ind.*, 67 (1948) 49.
2 L. Moore, *Anal. Chem.*, 29 (1957) 16.
3 H. F. Hibbert and D. M. P. Satchell, *J. Chem. Soc. (B)*, 5 (1968) 573.
4 G. M. Barrow and E. A. Yerger, *J. Amer. Chem. Soc.*, 76 (1954) 5211; 77 (1955) 4474.
5 E. A. Yerger and G. M. Barrow, *J. Amer. Chem. Soc.*, 77 (1955) 6206.
6 F. L. Moore, *Anal. Chem.*, 32 (1960) 1075.
7 A. S. Vieux, *Bull. Soc. Chim. Fr.*, (1969) 3364.
8 A. A. Lipovskii and M. G. Kuzina, *Zh. Neorgan. Khim.*, 12 (1967) 236.
9 E. Hogfeldt, F. Fredlund and K. Rasmisson, *Trans. R. Inst. Technol.*, 229 (1964).
10 L. Kuca and E. Hogfeldt, *Acta Chem. Scand.*, 21 (1967) 1017.
11 S. Bruckenstein and A. Saito, *J. Amer. Chem. Soc.*, 87 (1965) 698.
12 G. Fraenkel, R. L. Belford and P. E. Yankwich, *J. Amer. Chem. Soc.*, 76 (1964) 15.
13 N. Zaman, E. Merciny and G. Duyckaerts, *Anal. Chim. Acta*, 56 (1971) 261.
14 J. I. Bullock, S. S. Choi, D. A. Goodrick, D. G. Tuck and E. J. Woodhouse, *J. Phys. Chem.*, 68 (1964) 2687.
15 V. S. Smelov and A. V. Strakhova, *Radiokhim.*, 5 (1963) 509.
16 A. A. Pushkov, V. S. Shmidt and V. N. Shesterikov, *Tr. Mosk. Khim. Tekhnol. In–Ta*, 43 (1963) 12.
17 A. A. Lipovskii and M. G. Kuzina, *Radiokhim.*, 10 (1968) 175.
18 C. Kabwe, *Anal. Chim. Acta*, 54 (1971) 343.
19 A. Rieux, M. Rumeau and B. Tremillon, *Bull. Soc. Chim. Fr.*, (1964) 1053.
20 R. Kollar, V. Plichon and J. Saulnier, *Bull. Soc. Chim. Fr.*, (1969) 2193.
21 F. L. Moore, *Anal. Chem.*, 30 (1958) 908.
22 W. L. Ott, H. R. MacMillan and W. R. Hatch, *Anal. Chem.*, 36 (1964) 363.
23 B. E. McClellan and V. M. Benson, *Anal. Chem.*, 36 (1964) 1965.
24 A. R. Selmer-Olsen, *Anal. Chim. Acta*, 31 (1964) 33.
25 A. S. Vieux, *Bull. Soc. Chim. Fr.*, (1968) 4281.
26 A. S. Vieux, *Bull. Soc. Chim. Fr.*, (1969) 3366.
27 I. M. Kolthoff and E. B. Sandell, *Textbook of Qualitative Inorganic Analysis*, MacMillan, New York, 1952, p. 529.
28 G. A. Hall, *J. Amer. Chem. Soc.*, 71 (1949) 2691.
29 J. Steigman, R. Deiasi, H. Lilenfeld and D. Sussmann, *J. Phys. Chem.*, 72 (1968) 1132.
30 V. V. Fomin, R. N. Maslova and L. L. Zaitseva, *Zh. Neorgan. Khim.*, 5 (1960) 1383.
31 A. S. Kertes and A. Beck, *J. Chem. Soc.*, (1961) 1926.
32 *Handbook of Chemistry and Physics*, 50th Ed., CRC, 18901 Cranwood Parkway, Cleveland, Ohio, 44128 C-359 (1969–1970).
33 D. Chapman, D. R. Llyoyd and R. H. Prince, *J. Chem. Soc.*, (1964) 550.

34 R. M. Diamond, *Solvent Extraction Chemistry*, Amsterdam, 1967, p. 349–361.
35 W. Muller, G. Duyckaerts and J. Fuger, in H. A. C. McKay, T. V. Healy, I. L. Jenkins and A. Naylor, *Solvent Extraction Chemistry of Metals*, MacMillan, London, 1965, p. 233.
36 G. Charlot and B. Tremillon, *Les Réactions Chimiques dans les Solvants et les Sels Fondus*, Gauthier-Villars, Paris, 1963, p. 594.
37 D. Hadzi and N. Sheppard, *Proc. R. Soc.*, A216, no. 1125 (1953) 247.

Analytica Chimica Acta, 68 (1974) 425–434

© Elsevier Scientific Publishing Company, Amsterdam – Printed in The Netherlands

BESTIMMUNG DER BESTÄNDIGKEITSKONSTANTE UND DES MOLAREN EXTINKTIONSKOEFFIZIENTEN VON SCHWACHEN ML-KOMPLEXEN AUS DER JOBSCHEN KURVE

Z. SLOVÁK und J. BORÁK

Forschungsinstitut für reine Chemikalien, Lachema, Brno (Tschechoslowakei)

(Eingegangen den 25. Juni 1973)

Schaeppi und Treadwell[1] benutzten die bekannte Beziehung

$$K = \frac{1-\gamma}{\gamma^2 c} \tag{1}$$

zwischen dem Dissoziationsgrad γ eines Komplexes ML und seiner Gesamtkonzentration c bei vernachlässigbarer Dissoziation für die Berechnung der Stabilitätskonstante K. Sie nahmen dabei an, dass γ einfach experimentell zugänglich ist, nämlich dass $\gamma = d$ (vgl. Definitionsgl. 5 und Abb. 1). Ohne Rücksicht auf die Tatsache, dass Schwarzenbach[2] bereits im Jahre 1949, und später dann Asmus[3] in einer umfassenden Arbeit, die allgemeine Ungültigkeit des angenommenen Ausdruckes

$$K = \frac{1-d}{d^2 c} \tag{2}$$

bewiesen haben, kann man seine Anwendungen bis heute finden (vgl. z.B. Zit. 4).

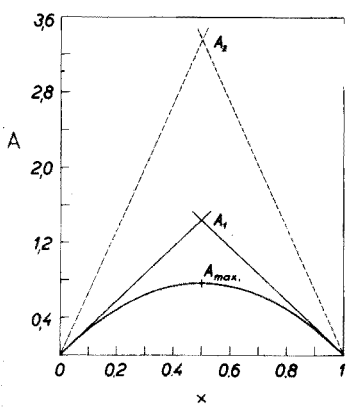

Abb. 1. Jobsche Kurve mit den eingezeichneten Werten A_1, A_2 und $A_{max.}$. Konstruiert für $c_0 = 2.5 \cdot 10^{-4}$ M; $K = 0.3 \cdot 10^4$, $\varepsilon = 2.7 \cdot 10^4$ l mol^{-1} cm^{-1}.

Neben den angeführten Autoren[2,3], haben sich Klausen und Langmyhr[5,6] mit dem theoretischen Verlauf von Jobschen Kurven ausführlich befasst. Die Gleichung einer allgemeinen Jobschen Kurve wurde aus dem Massenwirkungsgesetz

abgeleitet, und die Steigungen ihrer Tangenten für $x \to 1$ bzw. $x \to 0$ wurden berechnet. Für einen Komplex ML gilt[2,3], dass diese Steigungen sich nur durch das Vorzeichen unterscheiden:

$$f_{\substack{x\to 1\\ x\to 0}} = \pm \frac{Kc_0}{Kc_0+1} \tag{3}$$

Bei der Bildung von Komplexen mit einem anderen Verhältnis der stöchiometrischen Koeffizienten als 1:1 ist die Steigung mindestens einer der Tangenten bei $x \to 1$ bzw. $x \to 0$ gleich Null.

Klausen[7] beschrieb eine Methode zur Bestimmung von Stabilitätskonstanten, die auf der Methode der kontinuierlichen Variationen und auf Computer-Auswertung der maximalen Extinktionswerten bei verschiedenen totalen Molkonzentrationen beruht; seine Methode eignet sich auch zum Unterscheiden zwischen den Komplexen ML und M_2L_2.

Bei vielen Untersuchungen der Komplexbildung, besonders beim Studium der analytischen Eigenschaften von verschiedenen Reagenzien, wird oft nur eine Jobsche Kurve gemessen und ausgewertet. Es wurde bisher keine allgemeine kritische Untersuchung der Anwendbarkeit der experimentell sehr bequem erreichbaren Grösse d für die Ermittlung der Beständigkeitskonstante K ausgeführt. Lediglich in einem konkreten Fall der Bildung eines Co-Rhodanokomplexes berechnete Schwarzenbach bereits in der erwähnten Arbeit[2] den richtigen Wert von K aus der Steigung der Tangente der Jobschen Kurve in ihrem Ursprung und aus ihrem maximalen Extinktionswert. Mit Rücksicht auf die mathematisch definierten Werte A_1 (Schnittpunkt der Tangenten für $x \to 1$ und $x \to 0$) und $A_{max.}$ (aus der allgemeinen Gleichung einer Jobschen Kurve) ist es möglich eine Funktion $d = f(Kc_0)$ abzuleiten. Die Ableitung, Diskussion der Anwendbarkeit und ein Applikationsbeispiel dieser Fuktion für den Fall der Bildung eines Komplexes ML waren die Ziele dieser Arbeit.

THEORETISCHER TEIL

Benutzte Symbole und Grundbeziehungen

A Extinktion (Punkt an der Jobschen Kurve)

A_1 Schnittpunkt der Tangenten einer Jobschen Kurve bei $x \to 1$ und $x \to 0$

A_2 A_1 für die Annahme eines unendlich festen Komplexes

$A_{max.}$ Maximalwert von A; für einen ML-Komplex ist $A_{max.}$ dem Wert von A bei $x = 0.5$, d.h. bei $c_L = c_M = c_0/2$ gleich

K Beständigkeitskonstante (scheinbare Stabilitätskonstante) eines Komplexes ML

$$K = [ML]/[M][L] \tag{4}$$

K^x falscher Wert von K (aus Gl. 2 berechneter K-Wert)

d Extinktionsverhältnis nach der Definitionsgl. (5), vgl. auch Abb. 1.

$$d = (A_1 - A_{max.})/A_1 \tag{5}$$

ε molarer Extinktionskoeffizient eines Komplexes ML

$$\varepsilon = 2A_2/c_0 \tag{6}$$

ε_{ef} effektiver molarer Extinktionskoeffizient eines Komplexes ML

$$\varepsilon_{ef} = 2A_1/c_0 \tag{7}$$

c Komplexkonzentration [ML] bei $x=0.5$ und $K\to\infty$ ($c=c_0/2$)
c_L Ligand-Totalkonzentration (molar)
c_M Metall-Totalkonzentration (molar)
c_0 Summe der Ligand- und Metall-Totalkonzentrationen; für die Jobschen Methode der kontinuierlichen Variationen gilt

$$c_M + c_L = c_0 = \text{Konst.} \tag{8}$$

x Molbruch des Metalls oder Liganden
Δ, ∂ Fehler.

In allen Erwägungen werden die Extinktionswerte für eine 1 cm Küvette, gemessen gegen den entsprechenden Blindansatz, angenommen.

Ableitung der Funktion $d=f(Kc_0)$

Aus der allgemeinen Gleichung einer Jobschen Kurve bei der Bildung eines Komplexes ML folgt[2] für A_{max}.

$$A_{max} = \frac{\varepsilon c_0}{2} - \frac{\frac{1}{2}\varepsilon[(1+2Kc_0)^{\frac{1}{2}}-1]}{K} \tag{9}$$

Für die Darstellung der Jobschen Kurve in den Koordinaten A *vs.* c_M bzw. c_L resultiert aus Gl. (3) nach dem Einsetzen aus Gl. (6) und (7):

$$\frac{\varepsilon_{ef}}{\varepsilon} = \frac{Kc_0}{Kc_0+1} \tag{10}$$

Die gesuchte Funktion $d=f(Kc_0)$ erhalten wir nach dem Einsetzen aus Gl. (6), (9) und (10) in die Definitionsgl. (5):

$$d = \frac{1}{(Kc_0)^2}\,[(1+2Kc_0)^{\frac{1}{2}}(1+Kc_0) - Kc_0 - 1] \tag{11}$$

Bemerkungswert ist der Funktionsverlauf für $Kc_0\to 0$:

$$\lim_{Kc_0\to 0} d = \tfrac{1}{2} \tag{12}$$

Bestimmung von Kc_0

In Abb. 2 (Kurve 1) wird die Funktion $d=f[\log(Kc_0)]$ veranschaulicht,

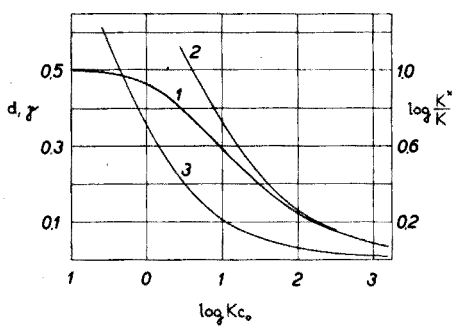

Abb. 2. Graphische Darstellung der Funktionen $d=f(\log Kc_0)$ (Kurve 1) und $\gamma=f(\log Kc_0)$ (Kurve 2) für ML-Komplexe. Abhängigkeit des Verhältnisses K'/K von dem Wert von Kc_0 (Kurve 3).

woraus die Möglichkeit der Ablesung von log Kc_0-Werten aus einem experimentell ermittelten Wert von d etwa für zwei Grössenordnungen von Kc_0 ersichtlich ist.

Der maximale Fehler bei der Bestimmung von d (laut Gl. 5) wird durch Gl. (13) gegeben,

$$\Delta_d = \frac{A_{max.}}{A_1^2}\,\partial A_1 + \frac{1}{A_1}\,\partial A_{max.} \tag{13}$$

wobei $\partial A_{max.}$ und ∂A_1 die Fehler der experimentellen Bestimmung von $A_{max.}$ und A_1 bedeuten. Nach dem Einsetzen für A_1 aus Gl. (5) erhalten wir einen Ausdruck für die Abhängigkeit von Δ_d von den relativen Messfehlern bei der Bestimmung von A_1 und $A_{max.}$:

$$\Delta_d = (1-d)\left(\frac{\partial A_1}{A_1} + \frac{\partial A_{max.}}{A_{max.}}\right) \tag{14}$$

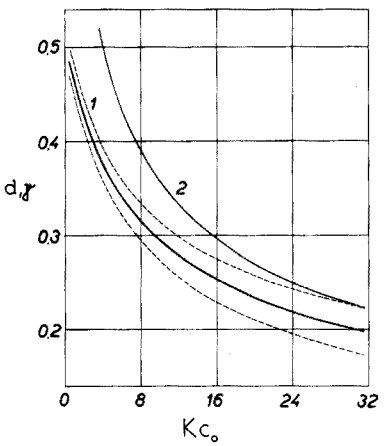

Abb. 3. Graphische Darstellung der Abhängigkeiten $d \pm \Delta_d = f(Kc_0)$ (Kurve 1) und $\gamma = f(Kc_0)$ (Kurve 2).

In Abb. 3 (Kurve 1) wird ein Teil der Funktion $d = f(Kc_0)$ mit den Genauigkeitsgrenzen (gestrichelt) dargestellt. Die Berechnung der Grenzen erfolgte nach Gl. (14) unter einer vereinfachenden Voraussetzung, nämlich dass $A_{max.}$ immer auf $\pm 1\%$ rel. und A_1 auf $\pm 2\%$ rel. genau gemessen werden. Mit Rücksicht auf die Schwierigkeiten bei der Messung von kleinen Extinktionen nahmen wir bei der Bestimmung von A_1 im Vergleich zu $A_{max.}$ einen grösseren Fehler an, obgleich es sich um einen gewogenen Mittelwert, abgeleitet von mehreren Extinktionsmessungen, handelt (zwei Tangenten). Bei bedeutend voneinander abweichenden Absolutwerten der Steigungen beider Tangenten kann die Voraussetzung der ausschliesslichen Bildung eines ML-Komplexes nicht erfüllt sein. Die Richtigkeit der Annahme des Komplextypus, einschliesslich der Unterscheidung zwischen den Komplexen ML und M_2L_2 kann durch die logarithmische Transformation der ganzen Jobschen Kurve erfolgen (vgl. weiter unten). An dieser Stelle wollen wir auf ein in der Praxis oft auftretendes Bestreben, keine echte Tangente einer Jobschen Kurve für $x \to 0$ bzw. $x \to 1$ zu konstruieren, sondern eine Gerade durch die ersten experimentell gemessenen Punkte durchzulegen, hinweisen. Der auf diese Art und Weise entstandene Fehler wurde im Rahmen dieser Mitteilung nicht berücksichtigt. In

Abb. 4 sind (gestrichelt) die maximalen Grenzen des relativen Fehlers einer K-Bestimmung aus den Werten von $d \pm \Delta_d$ gezeichnet. Die Werte von $K\%$ wurden aus den graphisch aus Abb. 3 abgelesenen Kc_0-Werten ausgerechnet.

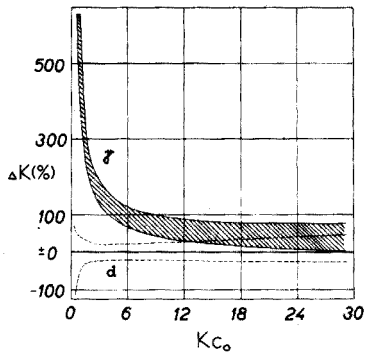

Abb. 4. Relativer Fehler einer K-Bestimmung nach Gl. (11) (d) und nach Gl. (2) (γ).

Bei der Fehleranalyse haben wir eine mögliche Abweichung bei der Angabe von c_0 nicht berücksichtigt, da sie unter der Voraussetzung eines gut definierten Komplexbildners offensichtlich wenig bedeutend ist.

Zum Vergleich wurde in Abb. 2 (Kurve 2) auch die Funktion $\gamma = f(\log Kc_0)$ (nach Gl. 1) dargestellt. Bei der Auswertung der experimentell bestimmten Werten von d mit Hilfe der Gleichung (2), d.h. bei dem Ablesen aus der Kurve 2, Abb. 2, entsteht ein systematischer positiver Fehler. Seine Grösse druckten wir als $\log(K^x/K)$ aus (Abb. 2, Kurve 3). Aus Abb. 3, in der auch die Funktion $\gamma = f(Kc_0)$ dargestellt wurde, ist es ersichtlich, dass der systematische positive Fehler der Bestimmung von Kc_0 nach Gl. (2) unter den oben angeführten Voraussetzungen dem maximalen negativen Wert des zufälligen Fehlers bei der Kc_0-Bestimmung mit Hilfe der Funktion $d = f(Kc_0)$ (Gl. 11) erst bei einem Wert von $Kc_0 = 32$ gleicht. Das bedeutet, dass nur bei $Kc_0 > 32$ ein Teil der durch die Anwendung von Gl. (2) erhaltenen Ergebnissen beim Einsetzen von experimentell bestimmten d-Werten richtig sein kann. Die völlige Ersetzung der Funktion (11) durch die Funktion (2) wäre jedoch unter der Voraussetzung möglich, dass der systematische positive Fehler bei der Bestimmung von Kc_0 aus Gl. (2) gegenüber dem zufälligen aus der experimentellen Anordnung bei dem Festlegen von d folgenden Fehler vernachlässigbar würde. Diese Bedingung wird sogar bei $Kc_0 = 100$ kaum erfüllt; der systematische Fehler der K-Bestimmung aus Gl. (2) beträgt hier noch $+16\%$.

In Abb. 4 sind die Gebiete der maximalen relativen Fehler bei der Bestimmung von K mit Hilfe der Beziehungen (11) und (2) veranschaulicht. Man kann eine Vergrösserung des zufälligen Fehlers bei der K-Bestimmung aus d beiderseits von einem Optimum, das bei etwa $Kc_0 = 7$ ($+24\%$, -19%) liegt, beobachten. Dies befindet sich im Einklang mit dem Verlauf der Funktion $d = f(Kc_0)$ (Abb. 2 und 3) und mit der Grösse des Fehlers Δ_d (Gl. 14) unter den eingeführten Vereinfachungen. Für die praktischen Bestimmungen von K ist das Gebiet $0.43 > d > 0.26$, d.h. $2 < Kc_0 < 15$, zu bevorzugen.

Bestimmung von ε

Aus der bestimmten Werten von Kc_0 und A_1 kann man mit Hilfe von

Gl. (7) und (10) den Wert des molaren Extinktionskoeffizienten ε des Komplexes ML berechnen. Eine graphische Darstellung der Beziehung zwischen dem Verhältnis der Tangentensteigung einer Jobschen Kurve bei $x \to 0$ bzw. $x \to 1$ (ε_{ef}) zu der hypothetischen Steigung bei 100%-iger Reaktion (ε) und dem Wert von Kc_0 befindet sich in Abb. 5. In dem optimalen Gebiet der Bestimmung von Kc_0 aus d ($2 < Kc_0 < 15$) ist die reale Tangentensteigung gegenüber der theoretischen Steigung bei vernachlässigbarer Dissoziation des Komplexes um 34% bis 6% erniedrigt. Der verhältnismässig grosse Fehler bei der Bestimmung von Kc_0 macht sich in dem Bruch $(Kc_0+1)/Kc_0$ nur begrenzt geltend (man benutzt den gleichen Kc_0-Wert sowohl in dem Zähler als auch in dem Nenner). In dem weiter ober diskutierten Optimum der Kc_0-Bestimmung ($Kc_0 = 7$) kann man den Ausdruck $\varepsilon/\varepsilon_{ef}$ mit einer Genauigkeit von +2.9–2.5% erhalten.

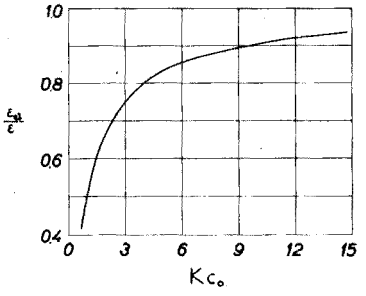

Abb. 5. Abhängigkeit der Verhältnisse von molaren Extinktionskoeffizienten von dem Wert von Kc_0.

Logarithmische Transformation einer Jobschen Kurve

Die Richtigkeit der erhaltenen Werte von K und ε (und der Voraussetzung, dass in dem ganzen Konzentrationsgebiet nur ein einziger dissoziierter ML-Komplex gebildet wird) kann durch Transformation der Jobschen Kurve bewiesen werden. Aus der allgemeinen Gleichung der Stabilitätskonstante K für einen Komplex M_aL_b und aus Gl. (8) folgt nach Einführung der Grössen A und ε:

$$K = \frac{\frac{A}{\varepsilon}}{\left[c_0\left(1-\frac{c_L}{c_0}\right)-a\frac{A}{\varepsilon}\right]^a\left(c_L-b\frac{A}{\varepsilon}\right)^b} \tag{15}$$

Nach einer Umformung und Logarithmieren kann man schreiben:

$$-\log K = \log \frac{\left(c_M - a\frac{A}{\varepsilon}\right)^a \varepsilon}{A} + b \log\left(c_L - b\frac{A}{\varepsilon}\right) \tag{16}$$

In den Koordinaten $\log(\varepsilon c_M - A)/A$ *vs.* $-\log(c_L - A/\varepsilon)$ erscheint also eine richtig interpretierte Jobsche Kurve bei der Bildung eines Komplexes ML als eine Gerade mit der Steigung -1 und dem Ordinatenachseabschnitt gleich $\log K$.

Die ganze Jobsche Kurve kann vor allem bei bedeutend dissoziierten Komplexen transformiert werden, bei welchen die Differenz $(\varepsilon c_M - A)$ gegenüber dem Messfehler von A auch an den pseudolinearen Ästen der Jobschen Kurve bedeutend

ist. Für $Kc_0 > 10$, wo ε_{ef} von ε nur etwa um 10% und weniger abweicht (vgl. Abb. 5), kann man in begrenztem Masse nur den mehr oder weniger kurzen krummen Kurvenabschnitt in der Nähe des Maximums transformieren.

In allen Fällen, wo es experimentell möglich ist, sollte man ε auch direkt bei einem genügenden Überschuss einer der reagierenden Komponenten bestimmen. Aus Gl. (10) folgt, dass ein negativer Fehler von max. 1% $\{(\varepsilon-\varepsilon_{ef})/\varepsilon=0.01\}$ bei $Kc_0 \geqslant 99$ entsteht. Bei den unabhängig bestimmten Werten von ε kann man die logarithmische Transformation zur Bestimmung von K und gleichzeitiger Kontrolle der richtigen Annahme des Komplextypus benutzen.

ANWENDUNGSBEISPIEL

Milligan und Lindstrom[4] befassten sich mit den Problemen der spektralphotometrischen Bestimmung von Kalzium mit Reagenzien aus der Reihe der Derivaten von Glyoxal-bis(2-hydroxyanil). Ein gegenseitiger Vergleich zwischen sieben Reagenzien (Tabelle I) wurde durch die Auwertung von Jobschen Kurven mit Hilfe der Beziehung (2) gezogen. Da in der zitierten Mitteilung[4] die vollen experimentell gemessenen Kurven gezeichnet sind, haben wir uns erlaubt die oben abgeleiteten Beziehungen zur Bestimmung von K und ε aus d und ε_{ef} auf diesen Fall anzuwenden. Bereits beim ersten Blick auf die publizierten Kurven ist es vor allem bei den stärker dissoziierenden Komplexen ersichtlich, dass die Geraden durch die ersten experimentell gemessenen Punkte gelegt wurden und somit von den Tangenten für $x \to 1$ bzw. $x \to 0$ abweichen. Für die Bestimmung von d benutzten wir deshalb immer den höheren Wert jedes ersten gemessenen Punktes (mit Ausnahme des verhältnismässig wenig dissoziierten Komplexes mit dem Reagens 3, Tabelle I, bei welchem der Wert von A_1 direkt von der Abb. 5, Zit. 4, entnommen wurde). Das Nachprüfen des Textes und der Ergebnisse in Zit. 4 ergab, dass die dort angeführten Konzentrationsangaben unter den einzelnen Abbildungen gleich $c_0/2$ sind ($c_0 = 2.50 \cdot 10^{-4}$ M für die Reagenzien 1, 3, 5, 6, 7 und $1.25 \cdot 10^{-4}$ M für die Reagenzien 2 und 4).

Die erhaltenen Werte von K im Vergleich zu K^x (nach Gl. 2 berechnet) und die molaren Extinktionskoeffizienten ε (nach Gl. 10) sind in Tabelle I zusammengestellt. Die publizierten Werte für die Beständigkeitskonstanten (K_h, Zit. 4) liegen den K^x-Werten nahe.

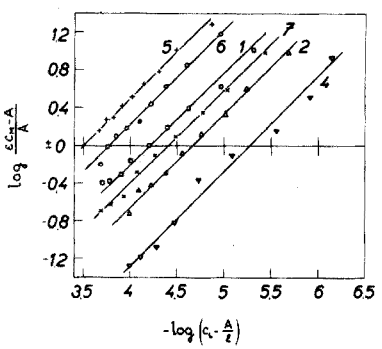

Abb. 6. Transformierte Jobsche Kurven für die Reaktionen von Ca^{2+} mit den Reagenzien 1, 2, 4, 5, 6 und 7 (vgl. Tabelle I).

TABELLE I

ERGEBNISSE DER BESTIMMUNG VON K UND ε

Nr.	*Reagens*	pH^a	λ^a	d	Kc_0	$K \cdot 10^{-4}$	$K^x \cdot 10^{-4}$	$\Delta K\%^b$	$\varepsilon_{ef}{}^c$	ε^c
1	Glyoxal-bis(2-hydroxyanil)	12.3	520	0.380	3.7	1.5	3.4	+129	1.31	1.6
2	Glyoxal-bis(2-hydroxy-4-methylanil)	12.3	520	0.351	5.3	4.2	8.4	+100	1.98	2.3
3	Glyoxal-bis(2-hydroxy-5-methylanil)	12.5	540	0.233	20.3	8.1	11.3	+40	1.045	1.1
4	Glyoxal-bis(2-hydroxy-4,5-dimethylanil)	12.3	540	0.263	14.2	11.4 5	17.0	+49	1.56	1.6
5	Glyoxal-bis(2-hydroxy-5-chloroanil)	12.3	540	0.473	0.75	0.3	1.9	+533	1.16	2.7
6	Glyoxal-bis(2-hydroxy-5-tert-amylanil)	12.5	540	0.441	1.5	0.6	2.5	+317	0.97	1.6
7	Glyoxal-bis(2-hydroxy-5-carbomethoxyanil)	11.8	505	0.350	5.4	2.2	4.2	+91	1.59	1.8

[a] In einem Gemisch Wasser–Methanol 1:1, aus Zit. 4 übernommen.
[b] $\Delta K\% = (K^x - K)/K \cdot 100\%$.
[c] $(1\ mol^{-1}\ cm^{-1}) \cdot 10^{-4}$.

Die Richtigkeit der Werte von K und ε wurde durch logarithmische Transformation der Jobschen Kurven bestätigt, mit Ausnahme des Reagenses 3, wo im Einklang mit der Theorie für die höheren Kc_0 die Streuung der transformierten Punkte zu gross war. Die Resultate der logarithmischen Transformationen sind in Abb. 6 dargestellt; die gezeichneten Punkte wurden nach Gl. (16) für die aus den publizierten Abbildungen der Jobschen Kurven entnommenen Extinktionen berechnet. Die Numerierung der Kurven in Abb. 6 entspricht der Reihenfolge der Komplexbildner in Tabelle I. Die kleinere Genauigkeit der logarithmischen Transformationen bei $Kc_0 > 10$ ist an der Gerade 4, Abb. 6 ($Kc_0 = 14.2$), im Vergleich zu den anderen transformierten Kurven ersichtlich. Da aber für die Transformierbarkeit einer Jobschen Kurve (und gleichzeitig auch für die optimalen Bestimmungsbedingungen von K und ε aus d) die Grösse des Produktes Kc_0 massgebend ist, kann man in der Praxis auch relativ wenig dissoziierte Komplexe bei einer genügend klein gewählten Konzentration c_0 erfolgreich untersuchen, und umgekehrt. Anschaulich wird es am Beispiel der Reaktionen der Reagenzien 3 und 4, Tabelle I.

Der von uns bestimmte Wert von $\varepsilon = 1.66 \cdot 10^4$ l mol^{-1} cm^{-1} für den Kalziumkomplex von Glyoxal-bis(2-hydroxyanil) ist in guter Übereinstimmung mit einer Angabe von Umland und Meckenstock[8] ($1.638 \cdot 10^4$).

SCHLUSSFOLGERUNGEN

Die optimalen Bedingungen für die Bestimmung von K und ε eines Komplexes ML, d.h. von Daten, deren Kenntnis für eine gründliche Untersuchung jeder analytischen spektralphotometrischen Methode unumgänglich ist, durch Auswertung einer einzigen Jobschen Kurve (d, ε_{ef}) liegen bei $2 < Kc_0 < 15$. Bei dem Versuch soll c_0 so gewählt werden, damit der Wert von d möglichst zwischen 0.26 und 0.43 liegt. Das bedeutet, dass die verhältnismässig festeren Komplexe ($K > 10^5$) bei möglichst niedrigen, die bedeutend dissozierten Komplexe ($K < 10^4$) bei möglichst

hohen Konzentrationen c_0 untersucht werden sollten. Die Möglichkeiten der Wahl von c_0 sind bei kleinen Konzentrationen durch die Genauigkeit der Extinktionsmessungen, bei hohen Konzentrationen durch die Löslichkeit und durch die aus erhöhter Ionenstärke folgenden Effekten, begrenzt. Bestimmungen von K mit Hilfe einer spektralphotometrischen Methode mit der Messung einer der Gleichgewichtskonzentration des Komplexes proportionalen Grösse (Extinktion) werden bei $Kc_0 > 50$ problematisch mit Rücksicht auf die steigenden Messfehler. In keinem praktisch bedeutenden Fall kan man sich der einfachen Beziehung (2) bedienen.

Die Richtigkeit der gewonnenen Ergebnisse bei $Kc_0 < 10$ kann man durch die geeignete Transformation der ganzen Jobschen Kurve in logarithmische Koordinaten beweisen.

Bei weniger dissoziierten Komplexen ist es meistens möglich, den Wert von ε direkt bei $Kc_0 \geqslant 100$ zu bestimmen. Die Bestimmung von K kann dann auch aus dem Maximum der Jobschen Kurve $A_{max.}$, die bei einer geeigneten (niedrigen) Konzentration c_0 konstruiert wird, nach der einfachen Gl. (1) erfolgen, wobei für c, $c_0/2$ und für γ

$$\gamma = \frac{\varepsilon \frac{c_0}{2} - A_{max.}}{\varepsilon \frac{c_0}{2}}$$

eingesetzt wird.

ZUSAMMENFASSUNG

Eine Beziehung zur Bestimmung der Beständigkeitskonstante K eines dissoziierten Komplexes ML aus den experimentellen Daten einer einzigen Jobschen Kurve wurde abgeleitet und diskutiert. Die Wahl von c_0 (Summe der Ligand- und Metall-Totalkonzentrationen bei der Jobschen Methode der kontinuierlichen Variationen in isomolaren Lösungen) soll für optimale Resultate die Bedingung $2 < Kc_0 < 15$ erfüllen. Aus den Steigungen der Tangenten einer Jobschen Kurve in ihren Ausgangspunkten und aus dem ermittelten Wert von Kc_0 kann man den Wert des molaren Extinktionskoeffizienten berechnen. Für die Richtigkeitskontrolle der Resultate wurden die ganzen Jobschen Kurven bei $Kc_0 < 10$ durch Transformation in logarithmische Koordinaten linearisiert. Als Anwendungsbeispiele der abgeleiteten Beziehungen wurden die publizierten Angaben über die Untersuchung der Reaktionen von Ca^{2+} mit Glyoxal-bis(2-hydroxyanil) und mit seinen Derivaten interpretiert.

SUMMARY

A relationship for the determination of the stability constant K of a dissociated complex ML from the experimental data of a single Job curve is derived and discussed. For best results, the concentration c_0 (the total ligand + metal concentration for Job's method of continuous variations in isomolar solutions) must be selected so that $2 < Kc_0 < 15$. The value of the molar absorptivity can be calculated from the slopes of the tangents at the start points of the Job curve

and from the established value of Kc_0. In order to check the results, the whole Job curve for $Kc_0 < 10$ is linearized by transformation to logarithmic coordinates. As an example of the treatment, some published results on the reaction of calcium(II) with glyoxal-bis(2-hydroxyanil) and its derivatives are interpreted.

RÉSUMÉ

Une étude est effectuée sur la détermination de constante de stabilité K de complexes faiblement dissociés ML, à l'aide des valeurs expérimentales d'une courbe simple de Job. Pour obtenir les résultats les meilleurs, la concentration c_0 (ligand total + concentration du métal selon la méthode de Job à variations continues, en solutions isomolaires) doit être choisie de façon que $2 < Kc_0 < 15$. L'absorption molaire peut être calculée à partir de l'inclinaison des tangentes aux points de départ de la courbe de Job et à partir de la valeur établie de Kc_0. Afin d'enregister les résultats, la courbe de Job $Kc_0 < 10$ est linéarisée par transformation en logarithmes. La réaction du calcium(II) avec glyoxal-bis(2-hydroxyanil) et ses dérivés est choisie comme exemple.

LITERATUR

1 Y. Schaeppi und W. D. Treadwell, *Helv. Chim. Acta*, 31 (1948) 577.
2 G. Schwarzenbach, *Helv. Chim. Acta*, 32 (1949) 839.
3 E. Asmus, *Z. Anal. Chem.*, 183 (1961) 321.
4 C. W. Milligan und F. Lindstrom, *Anal. Chem.*, 44 (1972) 1822.
5 K. S. Klausen und F. J. Langmyhr, *Anal. Chim. Acta*, 40 (1968) 167.
6 K. S. Klausen und F. J. Langmyhr, *Anal. Chim. Acta*, 28 (1963) 335.
7 K. S. Klausen, *Anal. Chim. Acta*, 44 (1969) 377.
8 F. Umland und K. U. Meckenstock, *Z. Anal. Chem.*, 176 (1960) 96.

Analytica Chimica Acta, 68 (1974) 435–445

© Elsevier Scientific Publishing Company, Amsterdam – Printed in The Netherlands

TITRIMETRIC APPLICATIONS OF MULTIPARAMETRIC CURVE-FITTING

PART 1. POTENTIOMETRIC TITRATIONS OF WEAK BASES WITH STRONG ACIDS AT EXTREME DILUTIONS

DANA M. BARRY and LOUIS MEITES

Department of Chemistry, Clarkson College of Technology, Potsdam, N.Y. 13676 (U.S.A.)

(Received 22nd June 1973)

Titrimetry has long been, and continues to be, among the most frequently applied and most intensively investigated techniques of quantitative analysis. During the thirty years or so since physicochemical ways of following titrations and locating end-points came into general use under the aegis of Kolthoff, Furman, and others, there have been a great many developments in the field and some have achieved great practical importance. The introduction of EDTA and similar reagents not only reawakened interest in complexiметric titrimetry and masking and made possible the development of a large number of practical analytical methods that are now justly deemed indispensable, but also provided the stimulus for much subsequent research in physical and inorganic chemistry. The development of the theory and practice of acid–base titrimetry in non-aqueous solvents made it possible to perform many titrations that are difficult or impossible in water. The possibility of generating reagents electrochemically has led to the development of some methods of extraordinary accuracy and precision, to the use of reagents too unstable to be used in other ways, and to routine applications at levels of concentration once thought to be prohibitively low. New ways of obtaining data during titrations have been devised; in some cases these have led to improvements of accuracy, precision, or sensitivity, while in others they have made it possible to perform titrations that could not have been followed in other ways.

However, there has been much less progress in the fundamental area of end-point location: the development of Gran plots[1–3] has been the most noteworthy advance in the last quarter century.

Titration curves may be considered to fall into two classes: sigmoidal and segmented[4]. Sigmoidal curves are associated with potentiometric titrations, and end-point location based on them generally involves the application of some graphical or numerical technique designed to find the point of maximum slope. Segmented curves are obtained in conductometric, amperometric, spectrophotometric, and other kinds of titrations in which the property plotted along the ordinate axis of the curve is proportional to the concentration of some reactant or product; the Gran plots are transformations of data obtained potentiometrically into forms that yield segmented curves. Sigmoidal curves have the disadvantage that their points of maximum slope cannot coincide exactly with the corresponding

equivalence points for many common kinds of titrations; when exact coincidence is possible it occurs only under unlikely circumstances[5–7]. Fortunately the discrepancy is often negligibly small, but when it is not the systematic error of a titration may be appreciable. Another limitation is that the inflection point becomes less and less well marked as the concentration of the solution titrated and the equilibrium constant of the titration reaction decrease: if either or both is sufficiently small, the inflection may vanish completely, so that end-point location becomes quite impossible. Segmented curves have the advantages that the points of intersection corresponding to the end-points generally coincide exactly with the equivalence points, at least in principle, and that the unfavorable effects of decreasing the concentration of the solution titrated and the equilibrium constant of the reaction can, up to a point, be circumvented by extrapolating the linear segments obtained at some distance on either side of the end-point. However, this expedient too is of limited utility, and titrations of very dilute solutions based on reactions with modest equilibrium constants remain difficult or impossible.

This paper describes a new technique of end-point location and the results obtained by applying it to just such titrations. It employs multiparametric curve-fitting[8] to combine data obtained during the titration with a theoretical equation for the titration curve in such a way as to yield the best estimates of the parameters in that equation. In the case we shall discuss, there are three significant parameters: the concentration of the solution titrated, an equilibrium constant, and an apparent activity coefficient. In an analytical application the appropriate values of the second and third may be known for the conditions employed in the tiration, or they may not. In either event it is the concentration of the solution titrated that is of paramount significance in practical analysis. We shall show that the technique is not only capable of evaluating that concentration more accurately and precisely than it can be evaluated in any other way but also, and much more importantly, capable of evaluating it under conditions so unfavorable that its evaluation in any other way would be highly hazardous if not wholly impossible.

While this work was in progress, Anfalt and Jagner[9] suggested that multiparametric curve-fitting of titration data should yield higher accuracy and precision than any other technique. Partly because of the complexity of the titration system with which they were concerned, they did not implement this suggestion, but they are nevertheless the first to have recognized the possibilities inherent in the technique. Still more recently, Ingman *et al.*[10] employed a related procedure to analyze binary mixtures of formic, acetic, and propionic acids; like the work described below, this would not have been possible had conventional techniques of end-point location been employed.

EXPERIMENTAL

For the present purpose, it seemed best to select a titration system whose behavior was simple and well understood and that was just amenable to conventional techniques of end-point location at one end of a convenient range of experimental conditions but wholly intractable to them at the other. These considerations led to the choice of the potentiometric titration of acetate ion with hydrochloric acid.

Stock solutions, one 0.1 *M* in potassium acetate and the other 1.0 *M* in hydrochloric acid, were prepared from reagent-grade materials, and each was brought to an ionic strength of 3.00 *M* by adding reagent-grade potassium chloride. The solution of hydrochloric acid was standardized against tris(hydroxymethyl)aminomethane[11] and was then used to standardize the solution of potassium acetate by potentiometric titrations made in the ordinary way. More dilute solutions of potassium acetate and hydrochloric acid were made by diluting the stock solutions with 3.00 *M* potassium chloride so that the ionic strength was constant throughout. Calibrated glassware was employed.

For each titration an accurately known volume of an appropriate solution of potassium acetate was placed in a tall-form beaker equipped with a tightly fitting stopper having several holes, of which one was used for the tip of the microburet from which the acid was added; another carried a Corning 39533 coarse-porosity fritted-glass gas-dispersion cylinder, through which a slow stream of nitrogen was passed continuously both before and during the titration to exclude carbon dioxide. The nitrogen was equilibrated with 3 *M* potassium chloride by passage through an efficient gas-washing bottle that preceded the cell. Magnetic stirring was employed; in an early stage of the work drifts of pH were sometimes observed and traced to heating by the stirrer, and a box of filter paper was thereafter placed between the stirrer and the titration cell to obviate this. Measurements of pH were made with a Corning Model 012 glass-electrode pH meter standardized against both 0.05 *M* potassium tetroxalate and a solution of potassium hydrogen tartrate saturated at 25°[12].

Usually about a dozen points were obtained during each titration: the first after 0.4 ml of acid had been added, and the others at successive intervals of *ca.* 0.8 ml until a total of 10 ml had been added. The volume of acetate solution and the ratio of its concentration to that of the acid were always such that the equivalence point was expected to correspond to 8.0 ml of acid. According to this schedule of addition, the two points closest to the equivalence point were at 7.6 and 8.4 ml, each 5% away from it. As the rate of attainment of equilibrium is generally lower near the equivalence point than anywhere else, and as clustering points around the equivalence point would be impossible for an analyst dealing with a titration curve on which the inflection was very poorly defined or altogether absent and would probably offer no substantial advantage if it could be done, this schedule seemed to be a reasonable representation of the data that might be obtained manually or read off a recorded titration curve. In some titrations as many as 20 data points were obtained at 0.5-ml intervals. No significant variation of accuracy or precision could be observed as a result of this variation of the number of points.

The coordinates of the points were transferred to paper tape and combined with the multiparametric curve-fitting program now in general use in our laboratory[13] and an overlay that solved eqns. (2) and (3) (below) to yield the value of the pH at each experimental point corresponding to the values of the parameters furnished by the main body of the program. The computations were performed on a PDP8/I computer (Digital Equipment Corporation, Maynard, Mass.) operating in a 5-user configuration that made 4096 words of core available for this work.

THEORY

By combining an electroneutrality equation with the equation

$$K_a = [H^+][X^-]/[HX] \tag{1}$$

that defines the formal or concentration dissociation constant of the conjugate acid of the base titrated in the titration medium employed, it is easily shown that the concentration of hydrogen ion is given by

$$[H^+]^2 + \left(K_a + \frac{V_b^0 c_b^0 - V_a c_a}{V_b^0 + V_a}\right)[H^+] - \frac{V_a^0 c_a^0 K_a}{V_b^0 + V_a} = 0 \tag{2}$$

at the point where V_a ml of a c_a M solution of a strong monobasic acid has been added to V_b^0 ml of a c_b^0 M solution of a weak monoacidic base X^-. It is assumed that the base is fairly weak and that the very beginning of the titration is ignored; if these two assumptions are satisfied, $[H^+]$ will everywhere be much larger than $[OH^-]$, so that the latter can be ignored in the electroneutrality equation and terms in K_w need not appear in eqn. (2).

To convert the hydrogen-ion concentration obtained by solving eqn. (2) into a pH value that can be compared with the one measured at the same point, one may write

$$pH = -\log_{10}(y_{H^+}[H^+]) \tag{3}$$

where y_{H^+} would be the single-ion molarity activity coefficient of hydrogen ion if the defined pH of a National Bureau of Standards reference buffer solution were equal to the negative logarithm of the activity of hydrogen ion in it, and if the liquid-junction potentials involved in the standardization and measurement were identical. The first of these conditions is probably nearly true but cannot in principle be known to be exactly so; the experimental conditions employed here were such that the same things are true of the second. To disclaim any possible suggestion that the present technique obviates the thermodynamic problems that are involved in single-ion activity coefficients, we shall refer to y_{H^+} as the "apparent activity coefficient of hydrogen ion".

Three cases may arise. The simplest is that in which a base for which the identity and value of K_a in the titration medium employed are known, and in which a value of y_{H^+} is available from prior titrations of the same base or other bases in the same medium. The next more complex is that in which the titration is performed in a medium for which y_{H^+} is known, but in which K_a is unknown either because the identity of the base is unknown or because data on titrations of that base in that medium have not previously been subjected to multiparametric curve-fitting. The third and most complex is that in which both y_{H^+} and K_a are unknown, as will always be true when a new titration medium is employed.

The most important practical effect of the difference among these cases is on the computation time required. The third entails a three-parameter fit to eqns. (2) and (3), since c_b^0, K_a, and y_{H^+} are all unknown. The second entails only a two-parameter fit because the average value of y_{H^+} obtained from prior three-parameter fits to data on the titrations of other bases in the same medium can be inserted into eqn. (3) as a constant, leaving only the values of c_b^0 and K_a to be

adjusted by the program until the best fit is obtained. In the first, which would arise in the routine analysis of a large number of similar samples, prior values of both K_a and y_{H^+} can be inserted into eqns. (2) and (3) so that only the value of c_b^0 has to be adjusted. On a dedicated minicomputer employing a reasonably efficient language such as POLYBASIC (Digital Equipment Corporation Users' Society, Maynard, Mass.) or FORTRAN, execution time in this simplest case averages about a minute per titration.

In practical analysis the numerical values of K_a and y_{H^+} are immaterial, save that the former may be used to identify the base that is titrated if its identity is not already known. That the difference between the values of K_a for, say, acetic and propionic acids can, in principle, be used to distinguish between the titration curves obtained by titrating their anions with a strong acid has been known for a long time. As the present technique furnishes values that are constant within a few thousandths of a pK-unit from one replicate titration to another, it is evident that it offers real possibilities in identification.

However, if the identity of the base is known *a priori*, there will be no use for the values of K_a and y_{H^+} even though they sometimes have to be evaluated in order to find c_b^0, as they do if the titration is performed in a new medium. Nevertheless, an unconditional requirement for the success of this technique is that the values of K_a and y_{H^+} must not change during the titration. It is therefore essential that the titration mixture contain a high and nearly constant concentration of some electrolyte and that its temperature be nearly constant throughout the titration. Variations of electrolyte concentration affect the liquid-junction potential and hence the measured pH values; variations of ionic strength affect not only the activity coefficient of hydrogen ion but also the activity coefficients of the base and its conjugate acid, and thereby alter the value of K_a by virtue of the equation

$$K_a = (y_{HX}/y_{H^+}\, y_{X^-})K_a^0 \qquad (4)$$

that relates this to the thermodynamic dissociation constant K_a^0; variations of temperature affect the liquid-junction potential, the values of the activity coefficients, and the value of K_a^0.

Reasonable precautions suffice. It is appropriate to use a reagent considerably more concentrated than the solution being titrated and to bring both to as nearly as possible the same ionic strength by adding appropriate amounts of an indifferent electrolyte, such as potassium chloride, to them, but variations of a few per cent in the ionic strength are so unlikely to have a detectable effect that great pains need not be taken to avoid them. We have been able to detect small differences among values of K_a obtained from titrations performed at considerably different temperatures, but not to detect errors resulting from ordinary variations of room temperature during a titration. However, it does seem advisable to provide some means of controlling the temperature, perhaps to $\pm 0.5°$, in a titration that must be carried out at a non-ambient temperature.

RESULTS AND DISCUSSION

For want of prior knowledge about the values of K_a and y_{H^+} appropriate to potassium chloride solutions of ionic strength 3 M, the data were initially

TABLE I

VALUES OF THE PARAMETERS IN EQUATIONS (2) AND (3)

(The first line of the Table gives the values and standard deviations of the parameters obtained in titrations of 0.0992 *M* acetate with 1.0574 *M* hydrochloric acid. Each subsequent line corresponds to the multiplication of each of these concentrations by a factor of 0.39961_6. On each line except the first, the "expected" value of c_b^0 is that calculated by multiplying 0.099233 (the average concentration of the stock solution obtained from the results of 18 titrations with $c_b^0 \geq 0.002$ *M*) by the appropriate power of this dilution factor. Quantities given in parentheses are the relative standard deviations of c_b^0 and the absolute standard deviations of pK_a and $\log_{10} y_{H^+}$. All titrations were performed at $23.5 \pm 0.5°$)

c_b^0 (*M*)			pK_a	$\log_{10} y_{H^+}$	*Number of titrations*	*Mean standard error of a single pH value*
Expected	*Found*	*Relative error (%)*				
0.099233	0.099296 (±0.06%)	+0.06	4.888 (±0.003)	0.242 (±0.008)	4	±0.0074
0.039650	0.03965_0 (±0.15%)	−0.01	4.881 (±0.003)	0.241 (±0.001)	5	±0.0038
0.015847	0.01584_9 (±0.02%	+0.01	4.881 (±0.003)	0.244 (±0.001)	3	±0.0024
0.006333	0.006332 (±0.04%)	−0.02	4.885 (±0.002)	0.226 (±0.007)	3	±0.0034
0.002531	0.002529 (±0.07%)	−0.06	4.880 (±0.001)	0.240 (±0.004)	3	±0.0040
0.0010113	0.001017 (±0.20%)	+0.56	4.873 (±0.004)	0.244 (±0.002)	3	±0.0082
0.0004041	0.0004144 (±0.19%)	+2.5	4.841 (±0.005)	0.251 (±0.004)	3	±0.0176
0.0001615	0.0001789 (±3.0%)	+10.8	4.787 (±0.022)	0.252 (±0.005)	4	±0.029
0.00006454	0.0001187 (±2.8%)	+84	4.412 (±0.023)	0.283 (±0.001)	3	±0.055

subjected to three-parameter fits, and the results of these are summarized in Table I.

Four titrations of portions of the stock solution, which was nominally 0.1 *M* in acetate, gave an average value of 0.09930 ± 0.00006 (0.06%) *M* for its concentration. Locating the inflection points of four other titrations, in which the data were thickly clustered around the inflection point as is customary in potentiometric titrations, gave a mean value of 0.09920 ± 0.0002 (0.20%) *M*. The difference between these means is partly due to the fact that the point of maximal slope precedes the equivalence point under these conditions; numerical calculations based on the considerations outlined by Meites and Goldman[5] showed that the error is *ca.* 0.02%. More important, however, is the fact that, as Fig. 1 shows, the inflection is simply not sharp enough to permit really precise location of the point of maximum slope.

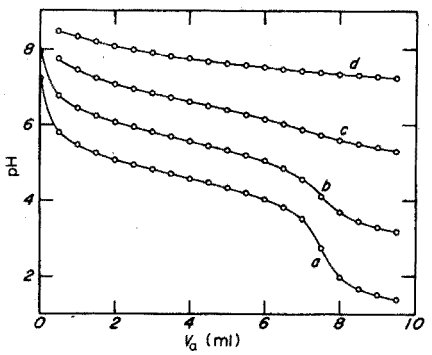

Fig. 1. Titration curves obtained in potentiometric titrations of 79.98 ml of potassium acetate with hydrochloric acid in 3.0 *M* potassium chloride at $23.5 \pm 0.5°$. The concentrations of potassium acetate and hydrochloric acid were, respectively: (a) 0.0992, 1.057; (b) 0.01585, 0.1691; (c) 0.001011, 0.01081; (d) $6.45 \cdot 10^{-5}$, $6.92 \cdot 10^{-4}$ *M*. The ordinate scale is given for curve a; curves b, c, and d are shifted upward, b by 1 unit, c by 2, and d by 3, with reference to this scale.

At this level the curve-fitting procedure gives a mean value indistinguishable from, and a precision half an order of magnitude better than, the conventional procedure. As the concentration of acetate decreases, the quality of the inflection deteriorates rapidly, as is shown by Fig. 1. Few analysts would attempt a precise determination of acetate on the basis of a titration curve as ill-shaped as curve b; even fewer would attempt anything more than a crude guess on the basis of one like curve c. It can be shown that the point of minimum slope and the point of maximum slope coalesce and vanish altogether if the concentration of acetate is below $3.5 \cdot 10^{-4}$ *M* and if the concentration of the strong acid is ten times that of acetate, as was always very nearly true in these titrations. With real data the inflection points are impossible to detect even at higher concentrations: we could not always find one for $1.0 \cdot 10^{-3}$ *M* acetate, and yet the curve-fitting procedure gave results with an accuracy and a precision of 0.5 and 0.2%, respectively, at that concentration.

Results like those in Table I are available if the analyst has no prior knowledge whatever of the system with which he is dealing. As his prior informa-

tion becomes more extensive, the number of degrees of freedom decreases and the certainty with which the concentration of an extremely dilute solution can be evaluated improves. The other extreme is represented by Table II. This gives the results obtained from the same data in one-parameter fits where c_b^0 was the only parameter being evaluated in eqns. (2) and (3). The values of pK_a and $\log_{10} y_{H^+}$ used in these fits were obtained from Table I by averaging all of the values of each computed from the titrations of 0.001–0.1 M acetate except those for $6 \cdot 10^{-3}$ M solutions, for which the values of $\log_{10} y_{H^+}$ unaccountably deviated from the others by about 0.015 unit. At the higher concentrations of acetate the results in Table II

TABLE II

RESULTS OF ONE-PARAMETER FITS TO EVALUATE c_b^0

(The "expected" concentrations of acetate given in the first column are copied from Table I; the concentrations "found" were obtained in one-parameter fits in which pK_a was taken as 4.881_6 ($K_a = 1.313_4 \cdot 10^{-5}$) and $\log_{10} y_{H^+}$ was taken as 0.2420_5 ($y_{H^+} = 1.7460_0$). These numerical values are averages of those in the fourth and fifth columns of Table I for $c_b^0 \geqslant 1 \cdot 10^{-3}$ M, excluding the ones obtained for $6.3 \cdot 10^{-3}$ M acetate)

c_b^0 (M)			*Number of titrations*	*Mean standard error of a single pH value*
Expected	*Found*	*Relative error (%)*		
0.099233	0.099344 (±0.13%)	+0.11	4	±0.0107
0.039650	0.039620 (±0.26%)	−0.08	5	±0.0052
0.015847	0.015809 (±0.02%)	−0.24	3	±0.0036
0.006333	0.006364 (±0.28%)	+0.49	3	±0.0120
0.002531	0.0025215 (±0.19%)	−0.36	3	±0.0048
0.0010113	0.0010080 (±0.18%)	−0.33	3	±0.0090
0.0004041	0.0003963 (±0.28%)	−1.9	3	±0.0254
0.0001615	0.0001593 (±1.1%)	−1.4	4	±0.037
0.00006454	0.00005259 (±1.8%)	−19	3	±0.092

are slightly but definitely inferior to those in Table I: this is because the variations of ionic strength, liquid-junction potential, temperature, and other experimental conditions, though small in all these titrations, could not be eliminated altogether and can affect pK_a and $\log y_{H^+}$ in the three-parameter fit whereas their entire variations must be thrown onto c_b^0 in the one-parameter fit. At the lowest concentrations of acetate, however, the goodness of the fit deteriorates, and adventitious and meaningless errors are introduced into all of the parameters as the three-parameter fit searches for trivially better conformity to the data; here the real variations of the ionic strength and liquid-junction potential are completely negligible, and constraining pK_a and $\log y_{H^+}$ to have the same values as in more concentrated solutions yields values of c_b^0 that conform much more closely to the truth.

As there is nothing whatever in the prior literature to suggest that titrations might still be performed successfully under conditions as extreme as are represented by the highest of these dilutions, extended comment on the results given in Table II would be gratuitous.

There is an intermediate case, in which other titrations previously made in the same supporting electrolyte provide a value of log y_{H^+} but in which pK_a is not known. This may arise because the identity of the base being titrated is unknown or because, even though its identity is known, there have been no prior titrations of it in the same medium. This situation requires two-parameter fits in which it is c_b^0 and pK_a that are evaluated. The results of such fits to the present data are shown in Table III. From a comparison of the values given in Tables II and III, it may be seen that the one-parameter fit is slightly superior when only the concentration of a very dilute solution is needed, but that the two-parameter fit yields results that are highly acceptable. It cannot be too strongly emphasized that all of these procedures are very much superior to any other procedure yet proposed for end-point location, and that this is true over the whole range of concentrations covered in this work.

ABLE III

ESULTS OF TWO-PARAMETER FITS TO EVALUATE c_b^0 AND pK_a

he "expected" concentrations of acetate given in the first column are copied from Table I; the concentrations ound" were obtained in two-parameter fits in which $\log_{10} y_{H^+}$ was taken as 0.2420_5; as in Table II)

(M)			*pK_a*	*Number of titrations*	*Mean standard error of a single pH value*
xpected	*Found*	*Relative error (%)*			
099233	0.099291 (±0.10%)	+0.06	4.883 (±0.010)	4	±0.0077
039650*	0.039630 (±0.28%)	−0.05	4.880 (±0.003)	5	±0.0044
015847	0.015843 (±0.02%)	−0.03	4.878 (±0.002)	3	±0.0026
006333	0.0063524 (±0.11%)	+0.31	4.885 (±0.004)	3	±0.0060
002531	0.0025306 (±0.10%)	±0.00	4.883 (±0.003)	3	±0.0043
0010113	0.0010165 (±0.29%)	+0.51	4.872 (±0.004)	3	±0.0084
0004041	0.0004118 (±0.31%)	+1.9	4.831 (±0.012)	3	±0.018
0001615	0.0001749 (±2.7%)	+8.3	4.783 (±0.030)	4	±0.029
00006454	0.0001080 (±2.1%)	+67	4.387 (±0.024)	3	±0.055

This work was supported in part by grant number GM-16561 from the Institute of General Medical Sciences of the National Institutes of Health and grant number GP-10325 from the National Science Foundation. We are grateful to the National Science Foundation and the Eastman Kodak Company for Departmental grants that made possible the purchase of the computer system employed.

SUMMARY

A multiparametric curve-fitting procedure is described for locating the equivalence point of a potentiometric titration and is applied to data obtained in titrations of acetate ion with hydrochloric acid over a wide range of concentrations (down to $6.5 \cdot 10^{-5}$ *M* acetate). It does not depend on the existence of a point of inflection on the titration curve, and therefore yields useful results in titrations of

this very weak base at concentrations well below that at which the point of maximal slope disappears. Three parameters are involved: the concentration of the base being titrated, the concentration dissociation constant K_a of its conjugate acid in the medium employed, and the apparent activity coefficient y_{H^+} of hydrogen ion in that medium, and all three of these must be evaluated when a new supporting electrolyte is employed. In 3.0 M potassium chloride at 24°, the apparent activity coefficient of hydrogen ion is 1.746_0, and this value permits data obtained in titrations of other or unknown bases in this medium to be interpreted by two-parameter fits. The value of K_a for acetic acid in this medium is $1.313_4 \cdot 10^{-5}$ M; by means of these two numerical values routine titrations of acetate in this medium can be interpreted by one-parameter fits. It is possible to locate the equivalence point with an accuracy and a precision that cannot be approached by other techniques and even to obtain useful and reliable results under conditions so unfavorable that other techniques fail completely.

RÉSUMÉ

Un nouveau procédé est décrit permettant de localiser le point équivalent d'un titrage potentiométrique; il est appliqué au dosage des ions acétates au moyen d'acide chlorhydrique, pour un vaste domaine de concentrations (allant jusqu'à $6.5 \cdot 10^{-5}$ M en acétate). Il ne dépend pas de l'existence d'un point d'inflexion sur la courbe de titrage, et permet par conséquent d'obtenir des résultats valables lors de titrages de cette base très faible, à des concentrations inférieures à celle de la disparition du point d'inflexion. Divers paramètres sont examinés.

ZUSAMMENFASSUNG

Es wird eine Kurvenangleichungsmethode mit mehreren Parametern für die Bestimmung des Äquivalenzpunktes einer potentiometrischen Titration beschrieben. Sie wird auf Ergebnisse angewendet, die bei Titrationen von Acetat-Ionen mit Salzsäure in einem grossen Konzentrationsbereich (bis zu $6.5 \cdot 10^{-5}$ M Acetat herab) erhalten werden. Das Verfahren hängt nicht davon ab, ob in der Titrationskurve ein Wendepunkt vorhanden ist, und ergibt deshalb brauchbare Ergebnisse dieser sehr schwachen Base bei Konzentrationen unterhalb derjenigen, bei der der Punkt maximaler Steigung verschwindet. Drei Parameter werden berücksichtigt: die Konzentration der zu titrierenden Base, die Konzentrations-Dissoziationskonstante K_a der konjugierten Säure in dem betreffenden Medium und der scheinbare Aktivitätskoeffizient y_{H^+} der Wasserstoffionen in diesem Medium; alle drei Parameter müssen ermittelt werden, wenn ein neuer Trägerelektrolyt verwendet wird. In 3.0 M Kaliumchlorid bei 24° ist der scheinbare Aktivitätskoeffizient der Wasserstoffionen 1.746_0, und aufgrund dieses Wertes können die bei Titrationen anderer oder unbekannter Basen in diesem Medium erhaltenen Ergebnisse durch Zwei-Parameter-Anpassungen interpretiert werden. Der K_a-Wert von Essigsäure in diesem Medium ist $1.313_4 \cdot 10^{-5}$ M; mittels dieser zwei Zahlenwerte können Routine-Titrationen von Acetat in diesem Medium durch Ein-Parameter-Anpassungen ausgewertet werden.

REFERENCES

1 G. Gran, *Acta Chem. Scand.*, 4 (1950) 559.
2 G. Gran, *Analyst*, 77 (1952) 661.
3 F. Ingman and E. Still, *Talanta*, 13 (1966) 1431.
4 J. A. Goldman and L. Meites, *Anal. Chim. Acta*, 30 (1964) 280.
5 L. Meites and J. A. Goldman, *Anal. Chim. Acta*, 29 (1963) 472; 31 (1964) 297.
6 L. Meites and J. A. Goldman, *Anal. Chim. Acta*, 30 (1964) 18.
7 L. Meites and T. Meites, *Anal. Chim. Acta*, 37 (1967) 1.
8 T. Meites and L. Meites, *Talanta*, 19 (1972) 1131.
9 T. Anfalt and D. Jagner, *Anal. Chim. Acta*, 57 (1971) 165.
10 F. Ingman, A. Johansson, S. Johansson and R. Karlsson, *Anal. Chim. Acta*, 64 (1973) 113.
11 J. H. Fossum, P. C. Markunas and J. A. Riddick, *Anal. Chem.*, 23 (1951) 491.
12 V. E. Bower and R. G. Bates, *J. Res. Natl. Bur. Stand.*, 59 (1957) 261.
13 L. Meites, *The General Multiparametric Curve-Fitting Program CFT3*, Computing Laboratory, Department of Chemistry, Clarkson College of Technology, Potsdam, N.Y., 1973.

Analytica Chimica Acta, 68 (1974) 447–454

© Elsevier Scientific Publishing Company, Amsterdam – Printed in The Netherlands

AUTOMATIC CATALYTIC TITRATION OF SILVER

T. P. HADJIIOANNOU, E. A. PIPERAKI and D. S. PAPASTATHOPOULOS
Laboratory of Analytical Chemistry, University of Athens, Athens-144 (Greece)
(Received 17th July 1973)

The phenomenon of catalysis has been widely used for the kinetic determination of various elements[1]. The possibility of using catalytic reactions for the indication of end-points was first pointed out by Yatsimirskii and Fedorova[2] in 1962, who coined the term "catalymetric or catalytic titration". In catalytic titrations, the catalyst serves as a titrant for a solution containing a species which reacts stoichiometrically and very quickly with it, as well as reagents for the indicator reaction which is catalyzed by the titrant and whose rate is monitored to locate the end-point of the titration. In a catalytic titration kinetics is not involved in the main stoichiometric titration reaction but only in the indication of the end-point. Since the excess of titrant at the end-point does not react stoichiometrically but catalytically, a small excess of titrant results in large changes in the rate of the indicator reaction and therefore in sharp concentration changes which can easily be detected by various physicochemical methods. Such sharp changes facilitate the location of the end-point and make it more precise. Titrimetric procedures with visual, potentiometric, spectrophotometric and thermometric catalytic end-points have been used for the determination of several cations and anions[3–18].

The Sandell–Kolthoff reaction, in which a trace of iodide acts as catalyst for the reduction of cerium(IV) in the presence of arsenic(III), has been used as an indicator reaction for the titration of silver[2,3,6,10,16]. The present paper describes an automatic method for the determination of silver, in the range 10^{-7}–10^{-3} *M*, based on this indicator reaction. Reaction rates are followed potentiometrically or spectrophotometrically. The control unit of an automatic differential potentiometric titrator coupled with a recording electrometer and a constant-rate burette is used for the automatic iodide titration of silver with a platinum indicator electrode by means of the second derivative technique[19]. It is also possible to determine silver semi-automatically by recording the potentiometric or spectrophotometric titration curve; the end-point is read from the plot after the titration is completed. Working curves are obtained by plotting the end-volumes against the amount of silver.

The automatic procedure can be used even with very dilute samples, down to the 10^{-6} *M* level, and it is accurate, reproducible and simple. The sample is pipetted into the reaction beaker containing fixed amounts of cerium(IV) and arsenic(III), the start button is pressed and the data read off a dial shortly after the start. Microamounts of silver in the range 3–2000 μg were determined with precision and relative errors of about 0.7%. Similar results were obtained with the semi-automatic procedures.

EXPERIMENTAL

Apparatus

For the potentiometric titrations, the titration system described previously[20] was used, except for the following modifications: an indicator platinum electrode (S-30515, E. H. Sargent Co.) and a mercury(I) sulfate reference electrode (Metrohm, Type EA-406) were substituted for the electrodes of the cell unit.

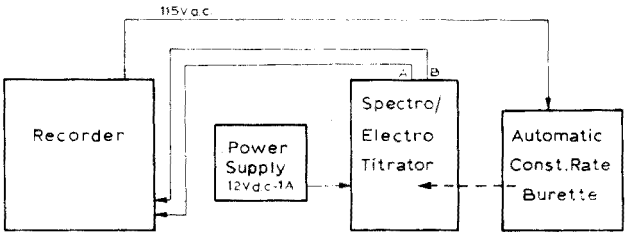

Fig. 1. Block diagram of spectrophotometric titration system.

For the spectrophotometric titrations the system shown in Fig. 1 was used. The Spectro-Electro titration unit of the Sargent–Malmstadt titrator (E. H. Sargent Co., Model SE) was coupled with a potentiometric recorder (E. H. Sargent Co., Model SRL) and a constant-rate burette (E. H. Sargent Co., Model C). The titration unit was modified as follows: the stirrer was actuated from the 117-V a.c. line of the lamp circuit[21] by an appropriate connection. The GE W-90 light bulb, powered by a separate 12 V–1 A regulated power supply[22], was substituted for the GE 64 (6 V) bulb of the instrument. The output signal from the terminals A and B of the terminal board at the rear of the titrator was fed to the recorder for direct recording of the titration curve. The burette was actuated from one of the two 110-V a.c. connectors, marked "Accessories" on the connector block located inside the recorder on the right side under the hinged cover[23]. A narrow third-order transmittance band at 390 nm was selected by dialling the nominal 575-nm second-order interference filter on the Spectro unit and inserting a Corning No. 5970 filter in the auxiliary holder.

Reagents

All solutions were prepared with deionized double-distilled water and reagent-grade substances.

Cerium(IV) solution,0.0155 M. 6.267 g of $Ce(SO_4)_2 \cdot 4\,H_2O$ are dissolved in 1 l of 1 *M* H_2SO_4.

Arsenic(III) solution, 0.336 M. 33.24 g of As_2O_3 are dissolved in 500 ml of 2 *M* NaOH, neutralized with 1 *M* H_2SO_4 and diluted to 1 l.

Dilute standard silver and iodide solutions were prepared from stock 0.01 *M* silver nitrate and 0.06 *M* potassium iodide solutions daily. The very dilute solutions ($< 10^{-6}$ *M*) were prepared just before the measurements. The stock iodide solution was standardized against the primary-standard silver solution.

Procedure

Preparation of equipment. Fill the burette with the appropriate standard iodide solution, depending on the silver concentration of the sample. For automatic

potentiometric titrations, work as previously reported[20], but turn the span switch to the positions 1000, 500 and 200 mV for the ranges 10^{-4}–10^{-3}, 10^{-5}–10^{-4} and 10^{-6}–10^{-5} *M* silver, respectively. For semi-automatic potentiometric titrations, turn the span switch to the positions 500 and 200 mV for the ranges 10^{-5}–10^{-3} and 10^{-7}–10^{-5} *M* silver, respectively. In all cases, turn the lower pH index switch to the appropriate position to bring the pen within scale.

For spectrophotometric titrations, switch the regulated power supply "ON" and the "Spectro-Electro" titrator to the "Spectro" position and throw the polarity switch to position 1. Dial the 575-nm position of the filter wheel and place the Corning No. 5970 filter in the auxiliary holder. Set the pegs in the base to position the 50-ml beakers and connect a stirrer (S-76669-A), a right-angled delivery tip (S-29704) and the burette. Set a range of 100 mV in the recorder and turn the filter switch to position 1.

Semi-automatic titration of silver. Pipet into a 50-ml beaker a 20.00-ml aliquot of the sample, 5.00 ml of 1 *M* sulfuric acid, 1.00 ml of arsenic(III) solution and 1.00 ml of cerium(IV) solution. Lock the burette "ON" and start the stirrer. After the pen on the recording electrometer or the recorder has stabilized (about 5–30 s), turn the function switch to "Record" to obtain the titration curve. For the greatest accuracy, calibrate the recorder for each titration, using the burette reading, because when the chart drive is turned on, a small error in the time axis may be introduced because of play in the motor and gear train of the chart drive system[23].

Automatic titration of silver. The procedure is the same as for the semi-automatic potentiometric titration except that at the beginning the function switch is turned to "Measure" and the titration is started by pushing the "automatic" button and is automatically terminated at the end-point.

RESULTS AND DISCUSSION

The platinum electrode responds rapidly to changes in concentrations of the Ce(IV)–As(III) mixture and with efficient stirring it can be used to follow the indicator reaction with continuous addition of titrant. The reaction can also be followed by monitoring the decrease in absorbance at 390 nm, from the reduction of cerium(IV). During the precipitation titration of silver with iodide, the signal remains practically constant (it may change very slowly because of the uncatalyzed reaction) until the equivalence point is reached, at which point the excess of iodide catalyzes the indicator reaction and a large and sharp change in the signal level occurs.

Ions which react with iodide to form precipitates or strong complexes, *e.g.* Hg(II), Pd(II), etc., should be absent.

There is always a blank because it is necessary to build up a certain iodide concentration, which is a function of titrant concentration, rate of addition of titrant, and experimental conditions such as stirring, electrode geometry, etc. However, all these factors can be kept constant and the blank was very reproducible under a set of experimental conditions, so that reproducible working curves were obtained. The blank was also affected by the concentrations of cerium(IV) and arsenic(III). Concentrations were selected which resulted in sharper end-points, smaller blanks and more reproducible results. The final acidity of the Ce(IV)–As(III) mixture should be larger than 0.2 *M* to prevent precipitation of reduced cerium salts.

The blank in the semi-automatic potentiometric titrations increased from 0.04 ml of titrant to 0.30 ml when the iodide concentration decreased from $6 \cdot 10^{-4}$ to $6 \cdot 10^{-6}$ *M* and it was larger in automatic titrations. In spectrophotometric titrations the blank increased from 0.03 to 0.80 ml when the iodide concentration decreased from $6 \cdot 10^{-3}$ to $6 \cdot 10^{-5}$ *M*. However, the definition of the end-point is so precise that silver can be titrated accurately even with a blank of 0.80 ml.

Recorded curves for the semi-automatic potentiometric and spectrophotometric titration of silver with iodide are shown in Figs. 2 and 3, respectively. The end-point was obtained by extrapolating the linear segments on either side of the equivalence point, since the time (amount of titrant added) required to start the indicator reaction is proportional to the amount of silver present which precipitates iodide and suppresses it from the catalytic cycle.

Working curves were made to read molar concentrations or micrograms of silver in the titrated sample (20 ml). Working curves were prepared for each of four ranges (10^{-3}–10^{-4}, 10^{-4}–10^{-5}, 10^{-5}–10^{-6}, and 10^{-6}–10^{-7} *M* silver) with four iodide standards ($6 \cdot 10^{-3}$, $6 \cdot 10^{-4}$, $6 \cdot 10^{-5}$, and $6 \cdot 10^{-6}$ *M*, respectively). Three standard silver solutions were sufficient for each working curve. These plots were linear for all the concentration ranges tested.

The silver concentration could also be found by direct standardization of the iodide solution against a known amount of silver (proportional method); conditions and especially the silver concentration must then be as similar as possible in both titrations.

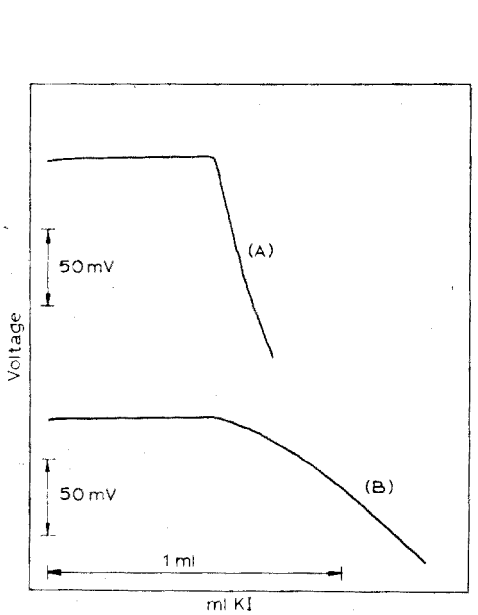

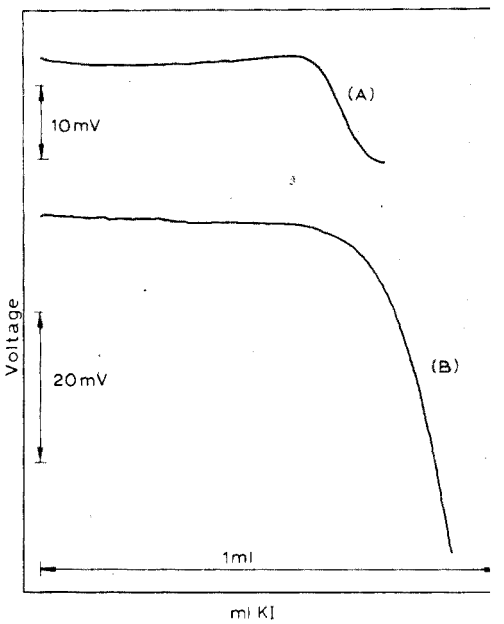

Fig. 2. Recorded curves for the semi-automatic potentiometric titration of silver with iodide. (A) 20 ml of $1.5 \cdot 10^{-5}$ *M* Ag^+ titrated with $6 \cdot 10^{-4}$ *M* KI; (B) 20 ml of $1.5 \cdot 10^{-6}$ *M* Ag^+ titrated with $6 \cdot 10^{-5}$ *M* KI.

Fig. 3. Recorded curves for the semi-automatic spectrophotometric titration of silver with iodide. (A) 20 ml of $1.5 \cdot 10^{-4}$ *M* Ag^+ titrated with $6 \cdot 10^{-3}$ *M* KI; (B) 20 ml of $1.5 \cdot 10^{-5}$ *M* Ag^+ titrated with $6 \cdot 10^{-4}$ *M* KI.

TABLE I

AUTOMATIC POTENTIOMETRIC TITRATION OF SILVER NITRATE WITH POTASSIUM IODIDE

KI titrant (M)	*Ag taken (μg)*	*Ag found (μg)*		*Error (%)*		s_r (%)
		Working curve	*Proportional method*	*Working curve*	*Proportional method*	
$6 \cdot 10^{-5}$	3.24	3.18	3.22	−1.9	−0.6	–
	10.80	10.97	10.71	+1.6	−0.8	1.20($n=4$)
	16.20	16.60	16.27	+2.5	+0.4	–
				Av. 2.0	0.60	
$6 \cdot 10^{-4}$	32.40	32.43	32.40	+0.1	—	–
	53.90	53.60	54.30	−0.6	+0.7	–
	107.9	108.2	108.6	+0.3	+0.6	0.40($n=5$)
	215.7	217.4	218.5	+0.8	+1.3	–
				Av. 0.45	0.65	
$6 \cdot 10^{-3}$	323.6	323.6	322.6	—	−0.3	–
	1079	1089	1080	+0.9	+0.1	0.60($n=4$)
	1618	1637	1633	+1.2	+0.9	–
	2157	2153	2173	−0.2	+0.7	–
				Av. 0.58	0.50	

TABLE II

SEMI-AUTOMATIC POTENTIOMETRIC TITRATION OF SILVER NITRATE WITH POTASSIUM IODIDE

KI titrant (M)	*Ag taken (μg)*	*Ag found (μg)*		*Error (%)*		s_r (%)
		Working curve	*Proportional method*	*Working curve*	*Proportional method*	
$6 \cdot 10^{-6}$	0.324	0.314	0.317	−3.1	−2.2	1.51($n=7$)
	1.080	1.076	1.070	−0.4	−1.0	–
	1.620	1.594	1.605	−1.6	−0.9	–
				Av. 1.70	1.37	
$6 \cdot 10^{-5}$	5.40	5.42	5.39	+0.4	−0.2	–
	10.80	10.80	10.64	—	−1.5	0.97($n=6$)
	16.20	16.28	16.12	+0.5	−0.5	–
	21.60	21.60	22.10	—	+2.3	–
				Av. 0.23	1.12	
$6 \cdot 10^{-4}$	32.40	32.00	32.03	−1.2	−1.1	–
	53.90	54.50	54.20	+1.1	+0.6	–
	107.9	107.5	107.7	−0.4	−0.2	0.76($n=6$)
	215.7	215.3	211.2	−0.2	−2.1	–
				Av. 0.72	1.00	

TABLE III

SEMI-AUTOMATIC SPECTROPHOTOMETRIC TITRATION OF SILVER NITRATE WITH POTASSIUM IODIDE

KI titrant (M)	*Ag taken (μg)*	*Ag found (μg)*		*Error (%)*		s_r (%)
		Working curve	*Proportional method*	*Working curve*	*Proportional method*	
$6 \cdot 10^{-5}$	3.24	3.30	3.26	+1.9	+0.6	–
	10.80	10.77	10.76	−0.3	−0.4	0.55(n=8)
	16.20	15.90	16.28	−1.8	+0.5	–
				Av. 1.33	0.50	
$6 \cdot 10^{-4}$	32.40	32.22	32.13	−0.6	−0.8	–
	53.90	54.22	54.01	+0.6	+0.2	–
	107.9	107.7	108.1	−0.2	+0.2	0.23(n=6)
	215.7	215.7	214.2	—	−0.7	–
				Av. 0.35	0.48	
$6 \cdot 10^{-3}$	323.6	323.0	324.6	−0.2	+0.3	–
	1079	1078	1078	−0.1	−0.1	0.22(n=8)
	1618	1618	1623	—	+0.3	–
	2157	2146	2146	−0.5	−0.5	–
				Av. 0.20	0.30	

Results for aqueous silver solutions of known concentrations are shown in Tables I–III. In the proportional method, the unknown and the control had the same silver concentration. The average errors were about 1.0 and 0.6% in automatic titrations with the working curve and the proportional method, respectively (Table I), 0.9 and 1.2% in semi-automatic potentiometric titrations (Table II), and 0.7 and 0.4% in semi-automatic spectrophotometric titrations (Table III). The results indicate that microamounts of silver in the range 1–2000 μg in a total volume of 27 ml could be determined with relative errors of about 0.7%. In the milligram range the precision and accuracy of the spectrophotometric method (about 0.2%) are comparable to those of other methods more conventionally accepted.

The semi-automatic method provided the best accuracy but took longer than the automatic method; spectrophotometric results were more accurate than the potentiometric ones. Samples in the range 10^{-7}–10^{-6} M silver could only be done semi-automatically.

Work in progress has shown that mercury(II) can be determined in the microgram range (10^{-7}–10^{-3} M) in a similar way. Iodide can also be determined by adding a known excess of standard mercury(II) solution to the sample solution and back-titrating with standard potassium iodide solution. Accuracy and precision for mercury(II) and iodide determinations are about 0.5%.

SUMMARY

An automatic method is described for the catalytic titrimetric determination of microgram amounts of silver. The method is simple and accurate, and is based

on the inhibitory effect of silver ions on the iodide-catalysed Ce(IV)–As(III) reaction. The end-point of titration with iodide is determined either automatically by the second- derivative technique or from the recorded potentiometric or spectrophotometric curves. Microamounts of silver in the range 1–2000 μg were determined with relative errors of about 0.7%.

RÉSUMÉ

Une méthode automatique est décrite pour le dosage titrimétrique catalytique de microquantités d'argent. La méthode est simple et exacte; elle est basée sur l'effect inhibiteur des ions argent sur la réaction catalysée iodure—Ce(IV)/As(III). Le point final du titrage avec l'iodure est déterminé soit automatiquement par la technique à dérivée seconde, soit par des courbes potentiométriques ou spectrophotométriques enregistrées. De microquantités d'argent (de 1 à 2000 μg) ont été déterminées avec des erreurs relatives d'environ 0.7%.

ZUSAMMENFASSUNG

Es wird eine automatische Methode für die katalytische titrimetrische Bestimmung von Mikrogramm-Mengen Silber beschrieben. Die Methode ist einfach und genau; sie beruht auf der Inhibitor-Wirkung von Silberionen auf die jodidkatalysierte Ce(IV)–As(III)-Reaktion. Der Endpunkt der Titration mit Jodid wird entweder automatisch nach dem Verfahren der zweiten Ableitung oder aus den aufgezeichneten potentiometrischen oder spektrophotometrischen Kurven ermittelt. Mikromengen von Silber im Bereich 1–2000 μg wurden mit relativen Fehlern von etwa 0.7% bestimmt.

REFERENCES

1 K. B. Yatsimirskii, *Kinetic Methods of Analysis*, Pergamon Press, Oxford, 1966.
2 K. B. Yatsimirskii and T. I. Fedorova, *Proc. Acad. Sci. USSR*, 143 (1962) 143.
3 K. B. Yatsimirskii and T. I. Fedorova, *Zh. Anal. Khim.*, 18 (1963) 1300.
4 H. Weisz and U. Muschelknautz, *Z. Anal. Chem.*, 215 (1966) 17.
5 H. Weisz and T. Janjić, *Z. Anal. Chem.*, 227 (1967) 1.
6 H. Weisz and D. Klockow, *Z. Anal. Chem.*, 232 (1967) 321; H. Weisz, T. Kiss and D. Klockow, 247 (1969) 248.
7 H. Weisz and T. Kiss, *Z. Anal. Chem.*, 249 (1970) 302.
8 D. Klockow and L. García Beltrán, *Z. Anal. Chem.*, 249 (1970) 304.
9 T. Kiss, *Z. Anal. Chem.*, 252 (1970) 12.
10 H. Weisz, S. Pandel and H. Ludwig, *Z. Anal. Chem.*, 262 (1972) 269; H. Weisz and H. Ludwig, *Anal. Chim. Acta*, 60 (1972) 385.
11 H. Weisz and S. Pandel, *Anal. Chim. Acta*, 62 (1972) 361.
12 H. A. Mottola and H. Freiser, *Anal. Chem.*, 39 (1967) 1294; 40 (1968) 1266.
13 H. A. Mottola, M. S. Haro and H. Freiser, *Anal. Chem.*, 40 (1968) 1263.
14 H. A. Mottola, *Talanta*, 16 (1969) 1267; *Anal. Chem.*, 42 (1970) 630; *Appl. Notes*, 6 (1971) 17.
15 G. L. Heath and H. A. Mottola, *161st Natl. ACS Meet., Los Angeles, U.S.A. 1971.*
16 K. C. Burton and H. M. N. H. Irving, *Anal. Chim. Acta*, 52 (1970) 441.
17 V. J. Vajgand, *Talanta*, 17 (1970) 415.
18 B. E. Reznik, V. T. Chuiko and V. I. Vershinin, *Zh. Anal. Khim.*, 27 (1972) 395.
19 H. V. Malmstadt and E. R. Fett, *Anal. Chem.*, 26 (1954) 1348.

20 T. P. Hadjiioannou and D. S. Papastathopoulos, *Talanta*, 17 (1970) 399.
21 *Instruction Manual, Sargent–Malmstadt Automatic Spectro-Electro Titrator, Model SE*, E. H. Sargent Co., Chicago, Ill., U.S.A.
22 T. P. Hadjiioannou and C. G. Valkana, *Chim. Chron.*, 32A (1967) 89.
23 *Instruction Manual, Sargent Recorder, Model SRL*, E. H. Sargent Co., Chicago, Ill., U.S.A.

Analytica Chimica Acta, 68 (1974) 455–457

© Elsevier Scientific Publishing Company, Amsterdam – Printed in The Netherlands

SHORT COMMUNICATION

Native fluorescence of methaqualone

STEPHEN G. SCHULMAN, J. MICHAEL RUTLEDGE and GEORGE TOROSIAN
College of Pharmacy, University of Florida, Gainesville, Fla. 32610 (U.S.A.)
(Received 21st May 1973)

Methaqualone (2-methyl-3-*o*-tolyl-4(3H)-quinazolinone) is a central nervous system depressant which is similar in its action to the hypnotic barbiturates. Partly as a result of its wide commercial availability, it has recently been labelled as a potential drug of abuse. The analytical chemistry of methaqualone, especially at therapeutic and toxic levels in biological fluids is thus of current interest.

Spot test[1], chromatographic[2,3], absorptiometric[4,5] and fluorimetric[6] methods for the detection and determination of methaqualone have been reported. The spot test for methaqualone[1] is specific only under limited circumstances and lacks sensitivity. The chromatographic and absorptiometric procedures for methaqualone are not inherently sensitive, concentrations of *ca.* $1 \cdot 10^{-5}$ *M* being detectable, and therefore require time-consuming preconcentration and sample preparation. Moreover, the absorption spectra are similar to those of a wide variety of naphthalene derivatives and are therefore suitable for identification only under very carefully defined circumstances.

A fluorimetric procedure devised for methaqualone[6] was based upon reduction, under anhydrous circumstances, with lithium borohydride, to yield the fluorescent dihydromethaqualone (essentially a derivative of anthranilamide). This approach yields a method of analyzing methaqualone at both therapeutic and toxic levels. However, the extraction, drying, dissolution and reduction of methaqualone and the preparation of the reduced sample for measurement are somewhat more time-consuming than is desirable, especially in emergency cases involving comatose patients.

Although it has been reported that methaqualone does not possess native fluorescence[6], such fluorescence can in fact be observed in a variety of solvents such as water, sulfuric acid, methanol and chloroform. At first it was thought that the alleged native fluorescence of methaqualone might result from an impurity in the commercial methaqualone sample employed (William H. Rorer, Inc., Ft. Washington, Pa.). However, the absorption spectra of the commercial sample were identical to those previously reported for methaqualone in dilute acidic and dilute basic aqueous solutions[5]. Absorptiometric pH titration of the sample used yielded a pK_a value of 2.59 ± 0.06. The fluorescence of the sample, at 343 nm in neutral aqueous solutions, was partially quenched and shifted to 339 nm with decreasing pH, yielding the same pK_a value determined absorptiometrically. Moreover, neither the fluorescence spectra nor the fluorimetric titration characte-

ristics of the sample changed with multiple recrystallizations. Consequently, it is believed that the fluorescence at 343 nm arises from the neutral methaqualone molecule while the emission at 339 nm arises from the singly charged cation. That the fluorimetric titration follows the ground state (absorptiometric) titration characteristics indicates that proton exchange is too slow to be detected, during the lifetime of the lowest excited singlet state. As the acid concentration is increased from pH 0.3 to H_0 −10, no appreciable changes occur in the absorption spectrum of methaqualone. However, in concentrated acid the fluorescence maximum shifts to 360 nm yielding a sigmoidal fluorimetric titration curve with an inflection point at H_0 −7.2. This suggests that protonation of the singly charged methaqualone cation has occurred to form the doubly charged cation, during the lifetime of the lowest excited singlet state. The shift to longer wavelengths of the fluorescence spectrum of singly protonated methaqualone, and the fact that no indication of protonation is evident from the absorption spectrum in concentrated acid, indicate that the singly protonated cation is a stronger base in the excited state than in the ground state, the dissociation constant of the doubly charged cation in the excited state (pK_a^*) being −7.2. The shift in the fluorescence spectrum and the pK_a^* of −7.2 can be employed, in conjunction with the Förster cycle[7] to estimate the corresponding ground-state pK_a value. This was found to be −10.8 which is just out of reach of the strongest sulfuric acid solutions available here (H_0 −10.0). The proposed scheme of reactions in the fluorimetric titration sequence of methaqualone is depicted in the following scheme.

The fluorescences of methaqualone and its singly charged cation (at H_0 −1.6) are detectable in aqueous solutions down to about $1 \cdot 10^{-6}$ *M*. However, the ranges of linearity of the fluorescence signals of these species with concentration are limited, extending to about $5 \cdot 10^{-5}$ *M*. Above $1 \cdot 10^{-4}$ *M* the fluorescence intensities of the neutral molecule and singly charged cation decrease with increasing concentration, the emission maxima remaining unchanged. It is likely that the apparent concentration quenching of the neutral species is due, largely, to the low water solubility of methaqualone.

The concentration dependences of the fluorescences of methaqualone in methanol and chloroform are linear from $1 \cdot 10^{-4}$ *M* to $1 \cdot 10^{-6}$ *M*, the lower limit of detection in both bases being about $1 \cdot 10^{-6}$ *M*. At concentrations higher than $1 \cdot 10^{-4}$ *M*, the fluorescence of methaqualone (at 343 nm in both solvents) is rapidly quenched. At $1 \cdot 10^{-3}$ *M* the fluorescence is shifted to 353 nm in methanol and to 355 nm in chloroform. The quantum yields of fluorescence at $1 \cdot 10^{-3}$ *M* are thirteen times lower in methanol and nineteen times lower in chloroform, than at $1 \cdot 10^{-4}$ *M*. At concentrations higher than $1 \cdot 10^{-3}$ *M*, quenching with increasing

concentration is much more gradual than in the interval between $1 \cdot 10^{-4}$ M and $1 \cdot 10^{-3}$ M. The quenching in the latter interval cannot be reconciled with the concentration dependence of the absorption spectrum in this interval and it is therefore suggested that excimer formation or some form of dynamic solute–solute interaction is responsible for this quenching.

The native fluorescene of methaqualone in chloroform extracts of biological fluids should be useful for quantitative analysis, the preparation of the chloroform extract (partial evaporation or dilution) depending upon the suspected dose ingested and the time between ingestion and analysis. Metabolic studies in the literature[2,3] should serve as guide-lines in this regard. Moreover, the acidity dependence of the fluorescence spectrum of methaqualone, reported in this study, should provide a sensitive and selective approach to the reasonably rapid identification of the drug *in situ*.

REFERENCES

1 G. V. Alliston, A. F. F. Bartlett, M. J. deFaubert Maunder and G. F. Philips, *Analyst*, 97 (1972) 263.
2 D. J. Berry, *J. Chromatogr.*, 42 (1969) 39.
3 R. N. Morris, G. A. Gunderson, S. W. Babcock and J. F. Zaroslinski, *Clin. Pharmacol. Ther.*, 13 (1972) 719.
4 A. A. H. Lawson and S. S. Brown, *Scott. Med. J.*, 12 (1967) 63.
5 M. Akagi, Y. Oketani and M. Takeda, *Chem. Pharm. Bull. (Tokyo)*, 11 (1963) 62.
6 S. S. Brown and G. A. Smart, *J. Pharm. Pharmacol.*, 21 (1969) 466.
7 Th. Förster, *Z. Elektrochem.*, 54 (1950) 42.

Analytica Chimica Acta, 68 (1974) 458–461
© Elsevier Scientific Publishing Company, Amsterdam – Printed in The Netherlands

SHORT COMMUNICATION

The fluorimetric determination of sulphide with thiamine

J. HOLZBECHER and D. E. RYAN

Trace Analysis Research Centre, Department of Chemistry, Dalhousie University, Halifax, Nova Scotia (Canada)

(Received 22nd June 1973)

There is interest in sensitive analytical methods for sulphide because of its toxicity. Reported fluorimetric procedures for sulphide either take advantage of ligand-exchange to produce fluorescence[1,2] or of fluorescence quenching[3–6]; enhancement of fluorescence, produced by tying up a quenching agent such as copper(II), has also been used for the determination of sulphide[7].

In a recent study of the use of thiamine for determining phosphate[8], sulphide was found to inhibit the oxidation of thiamine to fluorescent thiochrome; the present paper describes a quenching method based on this principle. The method is comparable in sensitivity to published procedures (ng ml^{-1}), the reproducibility is excellent, and readily available and inexpensive reagents are used.

Experimental

Apparatus and reagents. All fluorimetric measurements were made with an Aminco-Bowman spectrofluorimeter in 1-cm quartz cells with a xenon arc source. The instrument was standardized with a $\mu g\ ml^{-1}$ solution of quinine sulphate; slit widths for all measurements were 1, 4, 5, 5, 4, 3, 5 mm for slits 1–7, respectively.

A stock solution of *ca.* 0.02 *M* permanganate was prepared by dissolving 3.2 g of potassium permanganate in 1 l of twice-distilled water; after three days the manganese dioxide formed was filtered off through a sintered glass crucible, and the permanganate solution was stored in the dark.

Sodium sulphide, $Na_2S \cdot 9\,H_2O$ (J. T. Baker), was chosen as a working standard, as recommended by several authors[5,9], and 0.001 *M* stock solutions were prepared daily from washed and dried crystals; the purity was checked by iodometric titration[10].

The thiamine stock solution was 0.01 *M* thiamine chloride hydrochloride (Aldrich).

The borate buffer (pH *ca.* 7.7) was prepared by mixing 47 ml of 0.1 *M* hydrochloric acid with 53 ml of 0.05 *M* borax.

Procedure. To 2 ml of borate buffer add 1 ml of 10^{-3} *M* thiamine followed by 5 ml or less of an approximately neutral unknown solution containing 0.03–1 μg of sulphide; add 1 ml of 10^{-5} *M* permanganate and make up the volume to 10 ml. After at least 10 min measure the fluorescence intensity at 440 nm with an

excitation wavelength of 375 nm. Determine the concentration from a previously prepared calibration curve.

The blank, which contains all reagents except sulphide, has the highest fluorescence intensity and its reading should be adjusted to a maximum (*ca.* 100) for highest sensitivity.

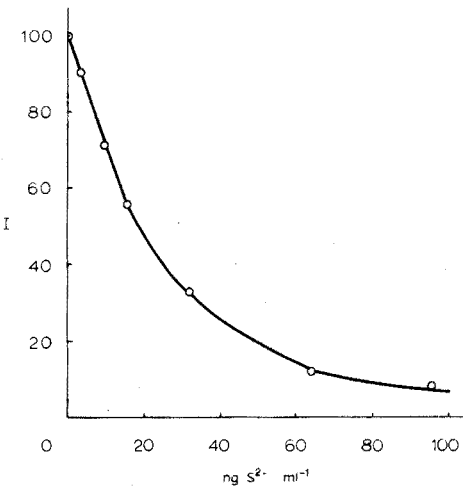

Fig. 1. Calibration curve. Meter multiplier (MM) setting of 0.1 and sensitivity (S) of 9.0 (blank reading was adjusted to read 100.0).

A typical calibration curve is shown in Fig. 1. The curve is linear to 20 ng ml^{-1}; most of the added permanganate has been consumed at sulphide concentrations greater than 20 ng ml^{-1} and the curve levels off. The relative standard deviation of ten determinations of 9.6 ng S^{2-} ml^{-1} was 1.3%.

Effect of anions and cations

Sulphide (9.6 ng ml^{-1}, $3 \cdot 10^{-6}$ mmole) can be determined in the presence of a 10,000-fold molar amount of the sodium or potassium salts of acetate, chloride or fluoride or a 1000-fold amount of bromide, iodide, nitrate, nitrite, perchlorate or sulphate. Results are also satisfactory with a 100-fold amount of phosphate or tartrate and a 10-fold amount of thiocyanate or cyanide. Equimolar concentrations of citrate do not interfere but sulphite and EDTA interfere strongly and must be absent.

Only a 10-fold molar amount of aluminium(III), iron(II) or zinc(II) and equimolar concentrations of iron(III) or nickel(II) can be tolerated. Even equimolar amounts of cadmium(II), cobalt(II), mercury(II) or manganese(II) interfere and must be absent.

Two competing reactions with permanganate, oxidation of thiamine and of sulphide, are involved. Diverse ions can thus interfere by reacting with sulphide, thiamine or permanganate. Since permanganate can undergo a number of reduction steps, interference can occur in any of these steps and to a different degree; the net resulting interference will thus depend upon which processes dominate. Nickel(II) and zinc(II), for example, decrease the fluorescence intensity of both sample and

blank; since the blank contains permanganate and thiamine (but no sulphide), the dominant factor must be interference in the oxidation of thiamine. Phosphate and EDTA, on the other hand, increase both blank and sample intensity and must, therefore, favor the production of thiochrome.

In practical work most interferences are removed by distillation of sulphide as hydrogen sulphide. Sulphite, which is a major interference and which is carried over in the distillation procedure, can be eliminated by using filters impregnated with 5% potassium hydrogencarbonate[11].

Factors affecting fluorescence

Maximal fluorescence intensity is obtained at pH 7.5–8.0. The intensity decreases at both higher and lower pH values and at pH 8.6 and 4.2 there was no difference between blank and sample.

The fluorescence intensity increases with increasing amounts of permanganate. However, when the permanganate concentration is greater than $2 \cdot 10^{-6}$ *M*, solutions become yellow in color owing to the formation of dispersed manganese dioxide. A final permanganate concentration of 10^{-6} *M* was therefore used in the procedure.

A final thiamine concentration of *ca.* 10^{-4} *M* gives maximal fluorescence intensity. At higher concentrations there is a slight decrease in intensity owing to the excessive absorption of either the exciting or emitted light ("inner filter effect").

The fluorescence intensity increases with time but a constant reading is obtained within 10 min and the reading remains stable for at least 1 h. Measurements should be made, therefore, at least 10 min after mixing the reactants.

The fluorescence intensity of the blank does not depend on the order of addition of the reagents (provided that buffer is added first) but the fluorescence of the sample depends on the addition sequence. If sulphide is added last no quenching occurs; if sulphide is added before permanganate, quenching does take place and the fluorescence obtained is independent of the time of thiamine addition.

Although other reagents may be used to oxidize thiamine, permanganate was chosen because of the short reaction time, the high sensitivity and the excellent reproducibility. For example, mercury(II)[12] gave a higher sensitivity but the reproducibility was poor whereas hexacyanoferrate(III) required a higher pH and the reaction was strongly time-dependent.

This work was supported by a grant from the National Research Council of Canada.

REFERENCES

1 L. S. Bark and A. Rixon, *Analyst*, 95 (1970) 786.
2 J. S. Hanker, A. Gelberg and B. Witten, *Anal. Chem.*, 30 (1958) 93.
3 Ya. V. Samoilov, *U.S.S.R. 167, 068*, 1965; *cf. Chem. Abstr.*, 62 (1965) 12446c.
4 A. Grünert, K. Ballschmiter and G. Tölg, *Talanta*, 15 (1968) 451.
5 H. D. Axelrod, J. H. Cary, J. E. Bonelli and J. P. Lodge, Jr., *Anal. Chem.*, 41 (1969) 1856.
6 M. Wronski, *Z. Anal. Chem.*, 180 (1961) 185.
7 F. Vernon and P. Whitham, *Anal. Chim. Acta*, 59 (1972) 155.
8 J. Holzbecher and D. E. Ryan, *Anal. Chim. Acta*, 64 (1973) 147.

9 R. E. Humphrey, W. Hinze and W. M. Jenkines III, *Anal. Chem.*, 43 (1971) 140.
10 P. O. Bethge, *Anal. Chim. Acta*, 10 (1954) 310.
11 J. B. Pate, J. P. Lodge, Jr. and M. P. Neary, *Anal. Chim. Acta*, 28 (1963) 341.
12 J. Holzbecher and D. E. Ryan, *Anal. Chim. Acta*, 64 (1973) 333.

Analytica Chimica Acta, 68 (1974) 462–465
© Elsevier Scientific Publishing Company, Amsterdam – Printed in The Netherlands

SHORT COMMUNICATION

The determination of iodine by atomic absorption and emission spectrometry with a cathode sputtering cell

G. F. KIRKBRIGHT, T. S. WEST and P. J. WILSON
Department of Chemistry, Imperial College, London S.W.7 (England)
(Received 20th July 1973)

The hollow-cathode lamp has been used as the primary background source for analytical atomic absorption spectrometry (a.a.s.) since its introduction by Walsh[1]. Its earlier use in emission spectrometry has been summarized by Tolansky[2]. The use of the sputtering action in the hollow-cathode lamp to produce an atomic vapour in an inert gas discharge suitable for a.a.s. has been reported by Walsh *et al.*[3–5], who determined silver and phosphorus in copper and silicon in aluminium and steel. These sputtering cell assemblies have also been used to determine trace amounts of several elements, with aluminium hollow cathodes[6] and graphite hollow cathodes[7]; Gandrud and Skogerboe[8] used an aluminium disc cathode.

The direct determination of iodine by a.a.s. at the 183.0-nm line corresponding to the transition ($5p^5 \cdot 2P^0_{\frac{1}{2}} - 6s^2 \cdot P_{\frac{1}{2}}$) has been described by L'vov and Khartsysov[9], who used a graphite furnace and a vacuum monochromator, and also by the authors[10], who used a nitrogen-separated premixed nitrous oxide–acetylene flame and a commercial atomic absorption spectrophotometer modified to permit nitrogen purging. In the present communication, the direct determination of iodine with a cathode sputtering cell similar to that proposed by Gandrud and Skogerboe[8] for the determination of the elements Ag, As, Ca, Cd, Hg, Pb, Se and Zn, is reported. The argon-filled sputtering cell is suitable for the direct determination of iodine at its 183.0-nm line by atomic absorption and emission.

Apparatus

A Techtron Model AA4 flame spectrometer was employed. For work at wavelengths below 200 nm, the monochromator was purged with nitrogen via the inlet provided to permit the adjustment of the wavelength calibration. An iodine electrodeless discharge tube fabricated from silica tubing (i.d. 8 mm, wall thickness 1 mm) to form a bulb 270 mm in length, and containing *ca.* 5 mg of elemental iodine was used as the source for a.a.s. studies. This lamp was operated in a $\frac{3}{4}$-wave resonant cavity (Model 210 L, Electromedical Supplies Ltd., Wantage, England) and was powered at 8 W by a 2450-MHz microwave generator (Microtron Mk II, E.M.S., Wantage). The source output was electronically modulated at 285 Hz in phase with the a.c. amplification system of the spectrophotometer. For emission

spectrometry, the radiation from the cell was modulated at 285 Hz by a Techtron mechanical chopper placed between the cell and the monochromator housing. For absorption work, glass tubing fitted with silica end-windows was placed in the light path between the discharge tube source and the sputtering cell, and between the cell and the monochromator; this tubing was purged with nitrogen to provide a transparent path at short wavelengths.

Two cathode sputtering cells were constructed; the early studies were undertaken with a cell constructed exactly as described by Gandrud and Skogerboe[8]. This cell was found to have several disadvantages for iodine, however, and a second cell was constructed as in Fig. 1. The cell length and internal diameter were reduced compared to the cell of Gandrud and Skogerboe, and a demountable anode was employed to allow easier cleaning. A glass rather than Teflon shield was placed around the cathode, as the Teflon tended to overheat after prolonged usage. The cell was fitted with silica end-windows, a gas inlet and an outlet through which it could be evacuated to a level of 0.2 Torr at a rotary vacuum pump. The cell was powered from the mains via a 400-V (225 mA) transformer with a diode rectifier and smoothing capacitors. The voltage input to the transformer was varied with a Variac control. The anode was connected to the power supply through a 4 kΩ resistor and the cathode via a milliammeter. It was also possible to operate the cell from the standard AA4 spectrometer hollow-cathode lamp power supply unit. The absorption and emission signals were recorded with a potentiometric chart recorder (Servoscribe Model R.E.511.20), and the photodetector employed was a 9783A photomultiplier selected for maximum gain (E.M.I. Electronics, Ruislip, England).

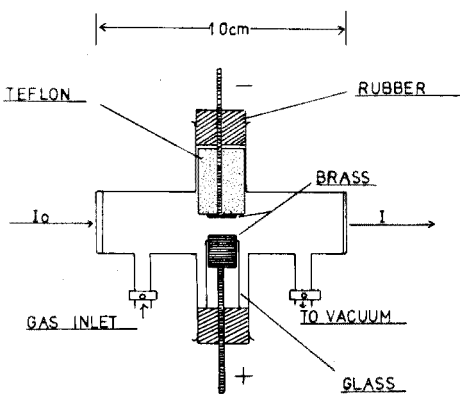

Fig. 1. Redesigned cathode sputtering cell.

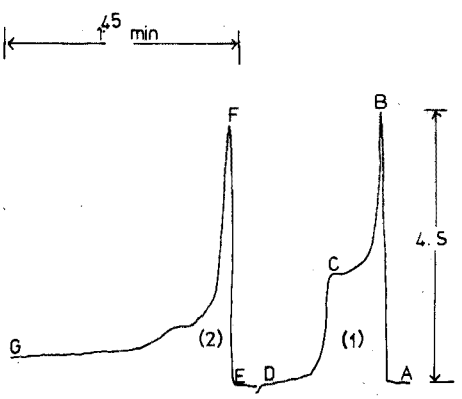

Fig. 2. Absorption signal obtained for 20 μg of iodide. (1) Measurement with sealed system; (2) measurement with continuous flow system. (A, E) Initiation of discharge; (C) cell evacuated; (D, G) discharge off.

Results and discussion

Operating conditions for source and cathode sputtering cell. The optimal conditions required to operate the iodine electrodeless discharge tube with high stability and intensity were obtained when the input to the tube was as low as

possible (5–10 W). The intensity recorded at each of the iodine lines investigated (206.1, 187.6, 184.4 and 183.0 nm) decreased rapidly, and the source noise increased, with increasing power. The use of long discharge tubes (270 mm) was preferred; with shorter bulb lengths, the discharge was difficult to maintain.

For the sputtering cell, optimal conditions for absorption and emission studies were found to be an argon filler gas pressure of 4 Torr and a discharge current of 50 mA. The absorption signal increased gradually over the range 1–6 Torr to a maximum at 6.0 Torr for argon, and then decreased slowly at higher pressures. However, above 5.0 Torr, the discharge became difficult to initiate without a Tesla coil.

The cell employed may be operated either as a continuous flow system or as a sealed system. In the former mode, the flow-rate of argon through the cell was adjusted to maintain a balanced pressure of 4 Torr, whereas in the latter case the cell was evacuated and flushed with argon, and then the pressure within the cell was adjusted to 4 Torr. The signals obtained by operating the cell in these modes are shown in Fig. 2. The sample was introduced into the cell by direct evaporation of 5-μl samples of the analyte on to the brass cathode, and the cell was fitted to an adjustable stand attached to the optical bar of the spectrometer so that the optimal horizontal and vertical positions for absorption and emission studies could be obtained.

Determination of iodine by a.a.s. at 183.0 nm

The limit of detection obtained by a.a.s. under the above optimal operating conditions was 0.03 μg of iodide; the sensitivity (for 1% absorption) was 0.06 μg. With the original cell design of Gandrud and Skogerboe, a limit of detection of 0.15 μg and a sensitivitity of 0.20 μg were obtained. The calibration graph obtained was linear between 0 and 10 μg of iodide; at higher concentrations, the graph showed curvature towards the concentration axis and the absorbance finally became independent of iodine concentration. Aqueous sample solutions containing free iodine, potassium iodide or ammonium iodide were sputtered to yield the same sensitivity (for 1% absorption) under similar operating conditions. When a series of twelve 5-μl samples of 1000-p.p.m. potassium iodide (*i.e.* 5 μg) was sputtered under the optimal conditions of pressure and discharge current, the relative standard deviation was 4%.

Interferences. Interference studies were carried out at two concentration levels; 1 μg of iodide was sputtered in the presence of 5- and 50-fold (weight) amounts of the following ions: chloride, bromide, fluoride, nitrate, sulphate, phosphate, Fe(III), Co(II), Ni(II), Cu(II), Zn(II), Mn(II), Mg(II), Cr(VI), Ta(V), W(VI), Al(III), Ba(II), Sr(II) and Ca(II). The presence of the halides and nitrate had no effect on the absorption signal at 183.0 nm at either level of diverse ion. The presence of 5-fold amounts of the other ions caused a slight suppression of the absorption signal (*ca.* 10%), and considerably greater suppression was observed for 50-fold amounts. These interferences can be compensated by matching sample and standard solutions with respect to the interfering elements or by using the method of standard additions. Alternatively, iodide could be converted to iodine by an amplification procedure, and separated from cations by extraction into an organic solvent such as methyl isobutyl ketone.

Determination of iodine by emission at 183.0 nm

With optimal conditions of discharge current and operating pressure, the limit of detection for iodide measured at 183.0 nm in the emission mode was 0.02 μg (5 × scale expansion). A wavelength scan between 177.0 and 200 nm demonstrated the absence of significant background emission from the cathode material around the 183.0-nm line. The calibration graph obtained was linear to 30 μg. However, the emission signals from day to day were not consistent, the signal intensity depending greatly on operating conditions.

Interferences. The effects of 50-fold (weight) amounts of the diverse ions listed above, on the emission signal of 1 μg of iodide were similar to those observed in absorption. Most of these can be explained by the relatively involatile nature of the iodide sputtered into the discharge, or by spectral interferences; tantalum gave a large positive enhancement.

Conclusion

This study suggests that the inert gas-filled cathode sputtering cell is useful as an atomizing cell for the direct determination of iodine as iodide by both atomic absorption and emission at the 183.0-nm line. In absorption, good reproducibility is obtained; the interferences are not more troublesome than those exhibited in many non-flame cells, and may be compensated for by matching the composition of samples and standards.

An advantage of the cathode sputtering cell compared to other non-flame devices is the longer retention time for the atom cloud in the discharge, so that the absorption peak can be measured with standard equipment. The limits of detection and selectivity obtained would be greatly improved by the use of the Leipert amplification for the oxidation of iodide to iodine and its subsequent extraction into methyl isobutyl ketone, a technique successfully employed in flame work[11]. The sensitivity would also be improved by use of the 178.3-nm line ($5p^5 \cdot {}_2P_{\frac{1}{2}}$–$6s^2 \cdot P_{\frac{1}{2}}$) which has a transition probability 15–20 times[12] greater than the 183.0-nm spin-forbidden line[13], if suitable instrumentation were available.

We are grateful to Beckman Instruments Inc. for the provision of financial support to one of us (P.J.W.).

REFERENCES

1 A. Walsh, *Spectrochim. Acta*, 7 (1955) 108.
2 S. Tolansky, *High Resolution Spectroscopy*, Methuen, London, 1947.
3 B. J. Russell and A. Walsh, *Spectrochim. Acta*, 15 (1959) 883.
4 B. M. Gatehouse and A. Walsh, *Spectrochim. Acta*, 16 (1960) 602.
5 W. G. Jones and A. Walsh, *Spectrochim. Acta*, 16 (1960) 249.
6 J. A. Goleb and J. K. Brody, *Anal. Chim. Acta*, 28 (1963) 457.
7 N. P. Ivanov, M. N. Gusinsky and A. D. Jesikov, *Zh. Anal. Khim.*, 20 (1965) 1133.
8 B. W. Gandrud and R. K. Skogerboe, *Appl. Spectrosc.*, 25 (1971) 243.
9 B. V. L'vov and A. D. Khartsysov, *Zh. Prikl. Spektrosk.*, 11 (1969) 413.
10 G. F. Kirkbright, T. S. West and P. J. Wilson, *At. Absorption Newslett.*, 11 (1972) 53.
11 G. F. Kirkbright, T. S. West and P. J. Wilson, *At. Absorption Newslett.*, 11 (1972) 113.
12 G. M. Lawrence, *Astrophys. J.*, 148 (1967) 266.
13 L. Brewer and J. B. Tellinghuisen, *J. Chem. Phys.*, 54 (1971) 5133.

Analytica Chimica Acta, 68 (1974) 466–469
© Elsevier Scientific Publishing Company, Amsterdam – Printed in The Netherlands

SHORT COMMUNICATION

Spectrophotometric determination of traces of cobalt with 3-hydroxypicolinealdehyde, salicylaldehyde and picolinealdehyde azines

A. GARCIA DE TORRES, M. VALCARCEL and F. PINO-PEREZ
Department of Analytical Chemistry, Faculty of Sciences, University of Sevilla, Sevilla (Spain)
(Received 5th June 1973)

The classical reagents[1] for determining cobalt either offer high sensitivity at an unfavourable wavelength, *e.g.* 1,10-phenanthroline ($\varepsilon = 3.4 \cdot 10^4$ at 270 nm), or suffer from numerous interferences, *e.g.* α-nitroso-β-naphthol ($\varepsilon = 2.6 \cdot 10^4$ at 530 nm), bipyridine ($\varepsilon = 1.6 \cdot 10^4$ at 295 nm), dithizone ($\varepsilon = 5.6 \cdot 10^4$ at 542 nm), oxine ($\varepsilon = 7.8 \cdot 10^3$ at 420 nm), etc. In recent years, numerous spectrophotometric determinations of cobalt have been proposed[2,3] but none of these has entirely solved the problem.

In this communication, some acyclic aromatic azines are proposed as analytical spectrophotometric reagents for cobalt. The synthesis and analytical possibilities of 3-hydroxypicolinealdehyde azine (3-OH-PAA), have already been described[4], and this reagent is compared with salicylaldehyde (SAA) and picolinealdehyde (PAA) azines, to study the influence of the different bonding atoms which participate in the forming of the cobalt chelates.

Experimental

Reagents. Ethanolic or dimethylformamide (DMF) solutions of 3-hydroxypicolinealdehyde, salicylaldehyde and picolinealdehyde azines were used. The syntheses of these reagents have been described[4].

All solvents and reagents were of analytical grade.

Apparatus. Unicam SP 800, Unicam SP 600-s.2, and Beckman DU spectrophotometers with 1.0-cm glass or quartz cells were used, as well as a digital pH meter (Philips, PW 9408) with glass–calomel electrodes.

Procedure with 3-OH-PAA. To the cobalt solution (4–40 μg of Co), add 4 ml of acetate buffer pH 4.5, and 5 ml of 0.02% (w/v) 3-OH-PAA solution in DMF. Heat the samples in a water-bath at 50° for 15 min, transfer to 25-ml flasks, and dilute to volume with water. Measure the absorbance at 545 and 570 nm against distilled water.

Procedure with SAA. To the cobalt solution (75–300 μg of Co) in a 25-ml flask add 10 ml of 0.05% (w/v) SAA solution in DMF, and adjust the pH to 8.0 with sodium hydroxide or hydrochloric acid solutions. Dilute to volume with ethanol–water (3 + 1), and after 15 min measure the absorbance at 530 and 570 nm against a reagent blank solution prepared similarly.

Procedure with PAA. To the cobalt solution (75–300 μg of Co) in a 25-ml flask add 5 ml of 0.1% (w/v) PAA solution in DMF, and adjust the pH to 7.8 with acid or base, as above. Dilute to volume with water, and measure the absorbance at 400 nm after 1 h, against a reagent blank solution prepared similarly.

Reaction of cobalt(III) and 3-OH-PAA

When dilute cobalt(II) and 3-OH-PAA solutions are mixed, the initial yellow colour ($\lambda_{max} = 520$ nm) slowly changes to a strong violet colour ($\lambda_{max} = 545$ nm, shoulder at 570 nm), which becomes stable after 12 h (Fig. 1). The variables which could accelerate the process were studied. Temperature has a notable influence; the stable violet colour is obtained in 10 min on heating at 50–60°.

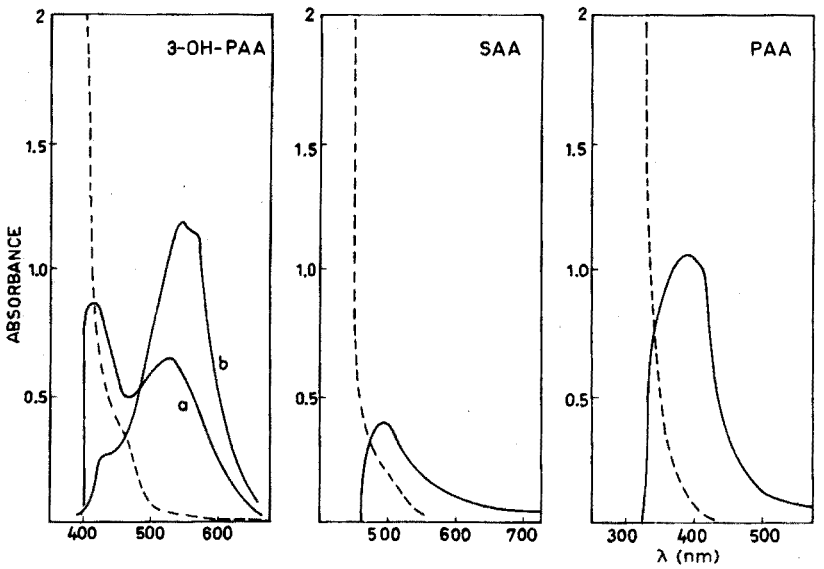

Fig. 1. Absorption spectra of Co(II)–azine complexes (——) against reagent blank (-----). (I) 3-OH-PAA and 2 p.p.m. of Co(II): (a) at 2 min; (b) at 12 h. (II) SAA and 10 p.p.m. of Co(II). (III) PAA and 10 p.p.m. of Co(II).

Oxidants prevent changes in colour, while reducing agents such as ascorbic acid accelerate the change to violet. If an inert atmosphere is used, identical results are obtained. Ultraviolet light does not affect the slow formation of the violet-coloured complex. The optimal pH range is only 4.3–4.6; this coincides with the zone between the pK_1 and pK_2 values of 3-OH-PAA (*i.e.* when the pyridine nitrogens are deprotonated and intermolecular hydrogen-bonding exists). Absorbances drop rapidly with change in pH outside these limits. Beer's law is obeyed between 0.15 and 1.6 p.p.m. of cobalt. The molar absorptivity is $3.04 \cdot 10^4$ l mole^{-1} cm^{-1} at 545 nm and $2.66 \cdot 10^4$ l mole^{-1} cm^{-1} at 570 nm. The metal:ligand stoichiometric ratio is 1:3 (Fig. 2). This forced configuration could be the cause of the slow formation of the complex and of the positive influence of the temperature. The formation constant of the complex is $K_c = 1.7 \cdot 10^{16}$, as calculated from the absorbance

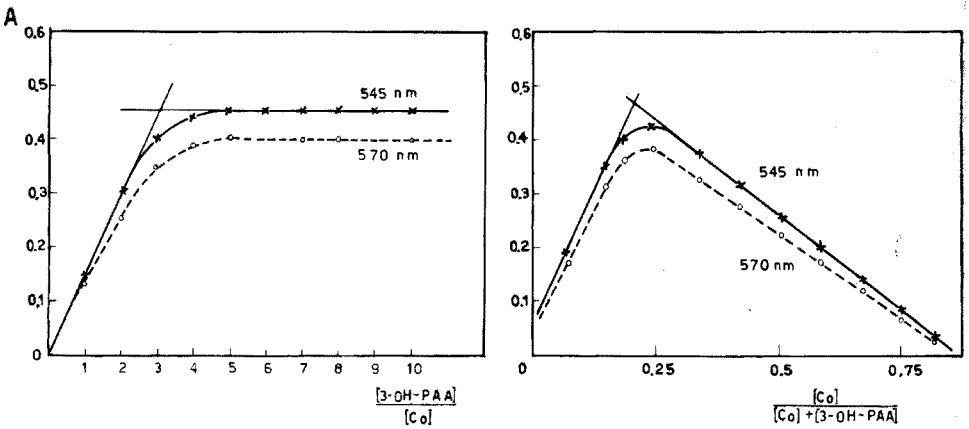

Fig. 2. Composition of the 3-OH-PAA–Co(II) complex, by the molar ratio and continuous variations methods.

measurements in the zone of stoichiometric composition of the curves in Fig. 2. The extraction of the complex was tested for various solvents, but was only successful with benzyl alcohol.

The presence of both pyridine nitrogens and hydroxyl groups probably causes the difference between the $Co(3\text{-}OH\text{-}PAA)_3^{2+}$ complex and the Co(SAA) and $Co(PAA)_2^{2+}$ complexes, with regard to both composition and solution characteristics.

Reaction of cobalt(II) and SAA

When bright yellow solutions of SAA are mixed with dilute solutions of cobalt(II), a yellow-orange complex is obtained; the absorption spectra are shown in Fig. 1. At concentrations above 12 p.p.m., a red precipitate of the complex appears. The optimal pH range is 7.8–8.1. The water:organic solvent ratio must be 1:3 to prevent precipitation of the ligand. Beer's law is obeyed in the concentration range 4–11 p.p.m. of cobalt(II); the molar absorptivity at 530 nm is 1356 l mole^{-1} cm^{-1}. The methods of continuous variations and molar ratio showed a 1:1 cobalt–ligand ratio; the formation constant is $1.7 \cdot 10^5$. The complex is easily extracted with chloroform. The behaviour of the cobalt–SAA complex is entirely parallel to that of cobalt(II) oxinate, $Co(oxine)_2$. SAA is structurally analogous to oxine, with azine nitrogens in place of pyridine. The ease of extraction and the precipitation in aqueous media imply the existence of an uncharged complex. Since the 1:1 complex is developed at basic pH, in which the hydroxyl groups are deprotonated, the structure is probably as follows:

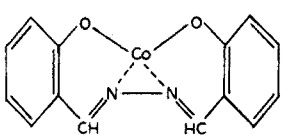

Reaction of cobalt(II) with PAA

When cobalt(II) and PAA solutions are mixed in a partly organic solvent,

a yellow complex is formed (Fig. 1). The optimal pH range for maximal absorbance at 390–410 nm is 7.4–9.5. Beer's law is obeyed between 3 and 11 p.p.m. of cobalt; the molar absorptivity at 400 nm is 3560 l $mole^{-1}$ cm^{-1}. The cobalt(II)–ligand ratio, given by the continuous variations and molar ratio methods is 1:2; the formation constant is *ca.* 10^9. The complex is not extracted into organic solvents. According to Stratton and Busch[5], picolinealdehyde azine behaves as a tridentate ligand in solution and the complex is positively charged, although in the solid state it has another composition. Its behaviour is analogous to that of the cobalt–terpyridine complex ($\lambda_{max} = 450$ nm, optimal pH 7.4–9.8) and differs from those of the 1,10-phenanthroline and the bipyridine complexes, in which the ligand is bidentate.

Spectrophotometric determination of cobalt

The above results show that 3-hydroxypicolinealdehyde azine provides the most favourable analytical reaction with cobalt(II). The maximal absorption wavelength enables water to be used as a photometric blank, the reaction is very sensitive, and the weakly acidic medium used (acetate buffer) reduces interferences. The optimal concentration range evaluated by Ringbom's method is 0.3–1.6 p.p.m. of cobalt; the relative error ($P = 0.05$) of the method is 0.52% at 545 nm and 0.48% at 570 nm. The final absorbance remains constant for several hours.

The ions Pb(II), W(VI), Bi(III), As(III), Mo(VI), Se(IV), Zn, Mn(II), Al, La, Ce(IV), Be, Ca, Sr, Rb, Li, PO_4^{3-}, SCN^-, citrate, tartrate, do not interfere when they are present in concentrations 100 times greater (by weight) than that of cobalt. Cadmium, uranyl and oxalate ions interfere in 60-fold amounts. Ag, Hg(I), Hg(II), Pd, Fe(III), Cu(I), Cu(II), Ni, $S_2O_3^{2-}$ and EDTA interfere when their concentration is six times greater than that of cobalt.

REFERENCES

1 *Spectrophotometric Data for Colorimetric Analysis*, Butterworths, London, 1963, p. 98.
2 D. F. Boltz and M. G. Mellon, *Analytical Chemistry*, 1970; *Anal. Chem.*, 42 (1970) 156 R.
3 D. F. Boltz and M. G. Mellon, *Anal. Chem.*, 44 (1972) 304 R.
4 A. Garcia de Torres, M. Valcarcel and F. Pino, *Talanta*, 20 (1973) 919.
5 W. J. Stratton and D. H. Busch, *J. Amer. Chem. Soc.*, 82 (1960) 4834.

Analytica Chimica Acta, 68 (1974) 470–472
© Elsevier Scientific Publishing Company, Amsterdam – Printed in The Netherlands

SHORT COMMUNICATION

Selective extraction of thallium with N-benzylaniline in chloroform from hydrobromic acid media

M. M. L. KHOSLA
Defence Laboratory, Jodhpur (India)
S. P. RAO
University of Jodhpur, Jodhpur (India)
(Received 4th April 1973)

Many solvent extraction methods for thallium have been reported in the literature. Thallium(III) can be extracted from 1–6 *M* hydrochloric acid[1] or from 0.1–6 *M* hydrobromic acid[2–4] into diethyl ether, but extraction from 1 *M* hydrobromic acid containing some free bromine is usually preferred. At this acidity, gold is extracted nearly completely but gallium and iron(III) are not extracted; elements such as copper, cadmium, cobalt and nickel, can be removed from the ether layer by scrubbing with 1 *M* hydrobromic acid, but arsenic(III), mercury(II) and tin(II, IV) are co-extracted in appreciable quantities.

Thallium(I) can be extracted from ammoniacal citrate–cyanide medium by dithizone[5,6] into chloroform; indium, bismuth, tin(II) and lead accompany thallium. Many other rather inselective reagents can also be used for the extraction of thallium, including 8-hydroxyquinoline[7,8], acetylacetone[9], thenoyltrifluoroacetone[7,10], N-benzyl-N-phenylhydroxylamine[11], tri-n-butylphosphate[12], diethyldithiocarbamate[13], and high molelcular-weight amines[14].

It has already been shown[15] that thallium can be separated from indium(III) by extraction with N-benzylaniline in chloroform from 2 *M* hydrobromic acid. The present communication describes a fuller study of this extraction. Thallium(III) is readily and quantitatively extracted with N-benzylaniline from 0.1–6 *M* hydrobromic acid media, but the extraction is most selective from 2 *M* hydrobromic acid, and the phase separation is then rapid. Thallium(III) is easily stripped from the organic phase with acetate–acetic acid buffer and can be determined by adding a slight excess of EDTA and back-titration with thorium nitrate solution to xylenol orange indicator. Few cations interfere.

Experimental

Reagents. Analytical-grade reagents were used without purification. All standard solutions were prepared in twice-distilled water.

Thallium(III) solution. A 0.05 *M* solution was prepared by dissolving 6.66 g of thallium(I) nitrate (B.D.H. Ltd.) in a minimal quantity of water, followed by three-fold evaporation to dryness with 50 ml, 25 ml and 25 ml of aqua regia. Finally the

TABLE I

PERMISSIBLE AMOUNTS OF VARIOUS IONS IN THE EXTRACTION OF THALLIUM(III)

Foreign ion	*Amount (mg)*	*Foreign ion*	*Amount (mg)*
Hg(II)	50	Mo(VI)	50
Pd(II)	10	W(VI)	10[b]
Pt(IV)	10	V(V)	30[a]
Rh(III)	30	Cr(VI)	30[a]
Cu(II)	30	Ti(IV)	30[a]
Cd(II)	26	Ce(IV)	50[a]
Bi(III)	30	U(VI)	60
Pb(II)	30	Th(IV)	35
Sb(III)	30[b]	Zr(IV)	30
Sn(IV)	100	Sc(III)	25
As(III)	35	Y(III)	30
As(V)	35	Se(IV)	30
Co(II)	58	Te(IV)	30
Ni(II)	58	Ca(II)	100
Zn(II)	30	Sr(II)	100
Mn(II)	30	Mg(II)	100
Fe(III)	30[a]	Phosphate	2000
Al(III)	100	Tartrate	1000
Ga(III)	100	Citrate	1000
In(III)	100	Nitrate	1000
Be(II)	30	Chloride	1000
Nb(V)	14[b]	Sulphate	500
Ta(V)	14[b]	Arsenate	50
		Borate	100

[a] Reduction with sodium sulphite and preferential oxidation of thallium(I) with saturated bromine water.
[b] In the presence of tartrate.

residue was taken up in 120 ml of (1 + 1) nitric acid and the solution was diluted to 500 ml. The solution was standardized as the chromate, after reduction with sulphur dioxide.More dilute solutions were prepared by accurate dilution.

N-Benzylaniline and thorium(IV) solutions were prepared as described previously[15].

General procedure. To an aliquot of solution containing up to 80 mg of thallium, add sufficient saturated bromide water to oxidize thallium(I) to thallium(III); a yellow colour should persist. Boil off excess of bromine (colourless solution). Add enough 40% hydrobromic acid (E. Merck) and water to give 2 *M* acid in a volume of 20 ml. Shake the solution for 1 min with 10 ml of extractant mixture containing 5 ml of N-benzylaniline solution and 5 ml of chloroform. Swirl the separating funnel slightly and separate the chloroform layer. Re-extract the aqueous layer with 10 ml of the extractant mixture. Scrub the combined organic phases with 15 ml of 4.5 *M* hydrobromic acid to remove any co-extracted elements. Strip the thallium(III) from the organic phase by shaking for 1 min with two 35-ml portions of the 0.2 *M* acetate–acetic acid buffer solution, pH 4.5. Transfer the aqueous backextract to a 250-ml conical flask. Add sufficient 0.01 *M* EDTA, and 7 drops of 0.1% (w/v) xylenol orange indicator, and back-titrate the excess of

EDTA with 0.01 *M* thorium nitrate solution to the colour change from yellow to red-violet.

Interference of diverse ions. Thallium(III) could be selectively and quantitatively separated from most of the cations tested (Table I). Bismuth, cadmium, lead and indium were partially extracted, but could be eliminated by scrubbing the organic phase with 4.5 *M* hydrobromic acid. Mercury(II) was co-extracted with thallium(III), but did not interfere in the recommended titration of thallium(III). This element could be completely separated from thallium(III) by twice scrubbing the organic phase with 4.5 *M* hydrobromic acid, but the recovery of thallium decreased to 95%. Vanadium(V), iron(III), chromium(VI), titanium(IV) and cerium(IV) hindered the extraction of thallium, but did not interfere after reduction with sodium sulphite in dilute acid; the solution was boiled to remove sulphur dioxide, and thallium(I) was then selectively oxidized to thallium(III) by gradual addition of saturated bromine water to the hot solution until the precipitate of thallium(I) salt completely dissolved. Palladium(II) was partially extracted but remained in the organic phase. Antimony(V), niobium(V) and tantalum(V) could be kept in solution with tartaric acid.

Common anions such as phosphate, citrate, tartrate, borate, nitrate, chloride, arsenate and sulphate did not interfere.

Effect of acidity and reagent concentration

The concentration of hydrobromic acid was varied from 0.1 *M* to 6 *M* while the concentration of thallium(III) and the extractant were kept constant. The ratio of the aqueous to organic phase was 2.0. Thallium(III) was quantitatively extracted from 0.1–6 *M* hydrobromic acid. The extraction of different amounts of thallium(III) in the range up to 80 mg with a fixed quantity of the extractant as in the General procedure was quantitative, whereas the extraction of 100 mg of thallium with the same quantity of the extractant was 94%.

REFERENCES

1 D. I. Ryabchikov, *Acta Chim. Acad. Sci. Hung.*, 32 (1962) 193.
2 H. M. N. H. Irving and F. J. C. Rossotti, *Analyst*, 77 (1952) 801.
3 I. Wadia and R. Ishi; *Bull. Inst. Phys. Chem. Res. (Tokyo)*, 13 (1934) 262; *Sci. Pap. Inst. Phys. Chem. Res. (Tokyo)*, 34 (1937/38) 787.
4 R. Bock, H. Kusche and E. Bock, *Z. Anal. Chem.*, 138 (1953) 167.
5 J. Minczewski, E. Weiteska and Z. Marczenko, *Chem. Anal. (Warsaw)*, 6 (1961) 515.
6 C. W. Sill and H. E. Peterson, *Anal. Chem.*, 21 (1949) 1268.
7 V. V. Bagreev and Yu. A. Zolotov, *Z. Anal. Khim.*, 17 (1962) 852; 18 (1963) 425.
8 R. M. Dagnall and S. K. Hasanuddin, *Talanta*, 15 (1968) 1025.
9 J. Stary and E. Hladky, *Anal. Chim. Acta*, 28 (1963) 227.
10 F. Hagemann, *J. Amer. Chem. Soc.*, 72 (1950) 768.
11 S. J. Lyle and A. D. Shendrikar, *Anal. Chim. Acta*, 32 (1965) 575.
12 A. K. De and A. K. Sen, *Talanta*, 14 (1967) 629.
13 H. Bode and F. Neuman, *Z. Anal. Chem.*, 172 (1960) 1.
14 T. Suzuki and T. Satobayashi, *Jap. Anal.*, 14 (1965) 414.
15 M. M. L. Khosla and S. P. Rao, *Anal. Chim. Acta*, 58 (1972) 389.

Analytica Chimica Acta, 68 (1974) 473–474

© Elsevier Scientific Publishing Company, Amsterdam – Printed in The Netherlands

SHORT COMMUNICATION

A new procedure for determining the metal content of colourless complexonates

H. M. N. H. IRVING and R. H. AL-JARRAH

Department of Inorganic and Structural Chemistry, University of Leeds, Leeds LS2 9JT (England)

(Received 4th September 1973)

During studies of the liquid–liquid extraction of anionic metal–EDTA complexes by solutions of the long-chain quaternary ion-exchanger Aliquat-336-chloride in 1,2-dichloroethane[1], it was necessary to determine the amount of metal in each phase at levels where titrimetric methods were inapplicable. In the aqueous phase, for example, the metal will be present principally as the anionic complexonate together with an unknown excess of complexing agent, small amounts of dissolved Aliquat-336 and higher concentrations of salts used to adjust the pH and ionic strength. No real problems arise if the complexonate is strongly coloured and can be determined by visual absorptiometry[1,2]. In many cases, atomic absorption spectrometry can be used[1], or the metal can be set free by oxidizing the complexone ligand with hydrogen peroxide[1] before a determination by standard methods. Iron(III) is conveniently measured as the peroxy-complex[1].

The following method was devised for cations such as Hg(II), Cd(II), Pd(II) and V(IV) which form colourless complexes, but it obviously has wider applicability to other metals and to complexonates besides those formed by EDTA. It depends upon their displacement by another cation which forms a more stable complexonate. Zirconium(IV) was selected since it forms very stable complexonates ($\log K_{ZrY} = 29.5$ for the complex with EDTA, H_4Y) and since both the zirconium ion and its EDTA complex are colourless.

On adding zirconium(IV) to an aqueous solution of a metal–EDTA complex, the substitution reaction

$$Zr^{4+} + MY^{n-4} \rightarrow ZrY + M^{n+}$$

proceeds to the right and quantitative displacement of the cation, M^{n+}, can be achieved by using a sufficient excess of zirconium in acidic solution. The displaced cation can then be determined by an appropriate reaction which must, of course, proceed quantitatively in the presence of excess zirconium and its EDTA complex.

The determination of mercury(II) in the presence of excess EDTA

The validity of the new procedure for the determination of mercury in its very stable complex with EDTA ($\log K_{HgY} = 21.8$) was established by treating 5-ml aliquot portions of a mercury(II) salt (1 mg l^{-1}) with (i) 15 ml of 0.5 *M* sulphuric acid, (ii) 10 ml of 0.5 *M* sulphuric acid and 5 ml of zirconium sulphate solution

(20% excess) in 0.5 *M* sulphuric acid, and (iii) 5 ml of EDTA (10% excess) followed by 5 ml of 0.5 *M* sulphuric acid and 5 ml of the zirconium sulphate solution. Acetic acid (2 ml of 6 *M*) and 5 ml of a 0.001% solution of dithizone in chloroform were then added to each solution and after equilibration the absorbances due to mercury(II) dithizonate were measured at 500 nm (1-cm cell) and found to be 0.604, 0.598 and 0.600, respectively. The procedure for other metals was validated in a similar way.

General procedure

Aliquot portions of the aqueous solution of metal–EDTA complex were adjusted to pH $\leqslant$ 1 and a 20% excess of zirconium(IV) sulphate in 0.5 *M* sulphuric acid was added. The displaced metal ion was determined by a standard method, *e.g.* cadmium and mercury(II) by dithizone[3], palladium by *p*-nitrosodimethylaniline[3], and vanadium(IV) as a peroxy complex[3]. Calibration curves were prepared by taking known amounts of metal through the whole procedure. Organic phases were "stripped" by equilibration with concentrated sodium perchlorate or perchloric acid[2].

One of us (R.H. Al-J.) wishes to thank the Ministry of Oil of the Republic of Iraq for financial support.

REFERENCES

1 H. M. N. H. Irving and R. H. Al-Jarrah, *Anal. Chim. Acta*, 65 (1973) 77.
2 H. M. N. H. Irving and R. H. Al-Jarrah, *Anal. Chim. Acta*, 55 (1971) 135; 60 (1972) 345.
3 E. B. Sandell, *Colorimetric Determination of Traces of Metals*, Interscience, New York, 1959, pp. 353, 626, 714 and 929.

Analytica Chimica Acta, 68 (1974) 475–479

© Elsevier Scientific Publishing Company, Amsterdam – Printed in The Netherlands

SHORT COMMUNICATION

Polarographic determination of thallium

J. K. BHADRA, P. BANDYOPADHYAY and B. K. SEN
Inorganic Chemistry Laboratories, University College of Science, Calcutta-9 (India)
(Received 12th June 1973)

Little work has been done on the polarographic study of thallium(III) ion in acidic medium[1–3] and none in alkaline medium. The difficulty lies in the spontaneous and gradual reduction of thallium(III) to thallium(I) in acidic solution ($E^0 \sim 1.252$ V (ref. 4)) in contact with mercury and in the precipitation of hydrated thallium(III) oxide in basic medium. It was found in the work described here that thallium(III) can be so well complexed with triethanolamine that it remains in solution even in decimolar alkali. Its formal potential[5] is a function of pH and is very much reduced in such solutions. This property made it possible to undertake a polarographic study of thallium(III) in alkaline medium in presence of triethanolamine. A typical polarogram is given in Fig. 1: the rise of the first wave overlaps with the anodic dissolution wave of mercury, so that its half-wave potential cannot be determined with certainty; the second reduction occurs at a half-wave potential of -0.52 V *vs.* S.C.E. identical with the Tl(I)/Tl(0) reduction. The current $i_{31}+i_{10}$ (measured with reference to the residual current curve) corresponds to the reduction

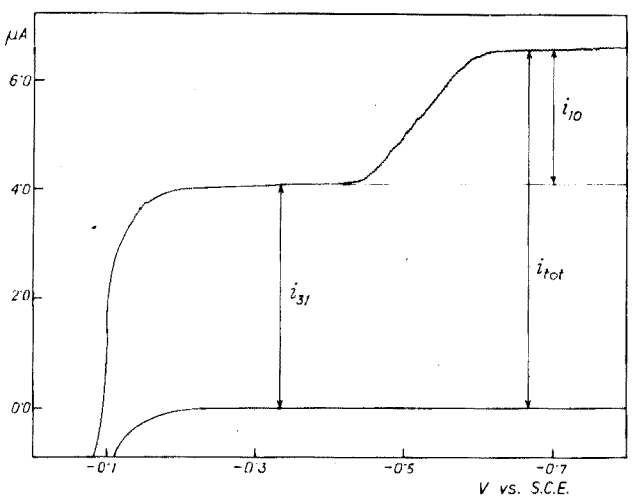

Fig. 1. Polarogram of thallium(III) (10^{-3} *M*) in sodium perchlorate ($\mu=1$) containing 0.3 *M* triethanolamine and 0.1 *M* sodium hydroxide at 25°. High damping was used.

of thallium(III) to thallium(0) and by measuring the two diffusion currents, it is possible to determine thallium(III) and thallium(I) in a mixture. Since chloride ion precipitates thallium(I), sodium perchlorate was used with sodium hydroxide and triethanolamine as the supporting electrolyte; no maximum suppressor was found necessary.

Experimental

Polarograms were recorded at $25 \pm 0.5°$ with a Cambridge pen polarograph; the capillary characteristics were $m = 1.61$ mg s^{-1} and $t = 2.679$ s in a solution at -0.5 V *vs.* S.C.E. A conventional H-type cell was used. In order to avoid any possible chloride contamination, a double bridge of agar–sodium perchlorate (2 *M*) via 2 *M* sodium perchlorate solution was used to connect the test solution with the calomel electrode in saturated sodium chloride. Total cell resistance was negligibly small.

Thallium(I) perchlorate solution was prepared by dissolving thallium(I) carbonate (Merck,, G.R.) in perchloric acid; the solution was standardized gravimetrically as thallium(I) chromate[6]. Thallium(III) perchlorate was prepared by dissolving thallium(III) oxide in perchloric acid; the solution was standardized by weighing as thallium(I) chromate after reduction. Other reagents were of appropriate purity.

In typical experiments 3.6 ml of sodium perchlorate (5 *M*), 5 ml of sodium hydroxide (0.4 *M*), 2 ml of triethanolamine (3 *M*) and varied quantities of thallium(I) perchlorate (2.23 m*M*) were mixed together; various quantities of thallium(III) perchlorate (3.45 m*M*) were added dropwise with vigorous stirring. The volume was then made up to 20 ml by adding distilled water so that the solution was of unit ionic strength and 0.3 *M*, 0.1 *M* and *ca.* 10^{-3} *M* with respect to triethanolamine, sodium hydroxide and thallium, respectively. For experiments with thallium(III), the addition of thallium(I) solution was omitted.

Results and discussion

The limiting currents of the reduction waves were found to be diffusion-controlled, since i_d was found to be proportional to $h^{\frac{1}{2}}$. The diffusion current varied linearly with the concentration of the depolarizer and the value of the diffusion current constant (I), calculated from the Ilkovič equation, was determined from ten different solutions of varying concentrations ranging from 0.1 to 1.0 m*M*. Table I shows several constants (averages of several determinations) for the reduction process at 25°.

TABLE I

POLAROGRAPHIC PARAMETERS FOR THALLIUM(III) REDUCTION ON D.M.E.

System	$i_d h^{-\frac{1}{2}}$ ($\mu A\ cm^{-\frac{1}{2}}$)	I	Q_D[a] (*kcal mole*$^{-1}$)
Tl(III)–Tl(0)	0.93	4.11 ± 0.04	5.8
Tl(III)–Tl(I)	0.58	2.54 ± 0.03	4.6

[a] Q_D is the activation energy of diffusion[7].

The ratio (R) of the diffusion currents for the Tl(III)/Tl(0) and Tl(III)/Tl(I) systems, *i.e.* $(i_{31}+i_{10})/i_{31}$, was constant at a definite temperature, and increased with increasing temperature (Fig. 2). The constancy of R, *viz.* 1.621 ± 0.012 at 25°, could be utilized to determine thallium(I) and thallium(III) in a mixture. Solutions containing a total of one millimole of thallium perchlorate in varying ratios of the two valency forms were polarographed. It is evident that i_{31} and $i_{tot} - R \cdot i_{31}$

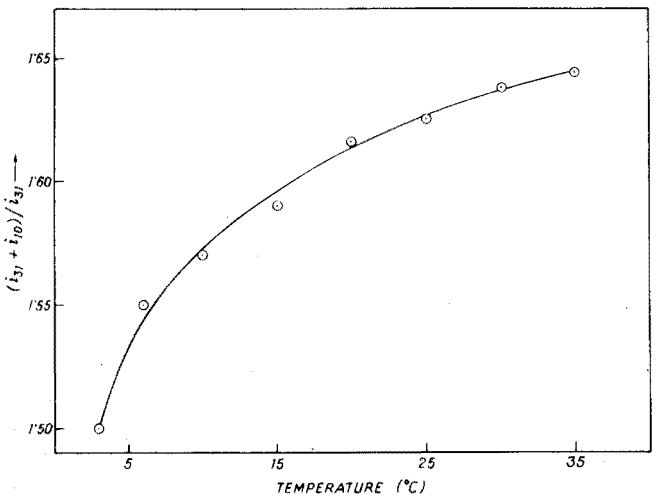

Fig. 2. Dependence of R on temperature.

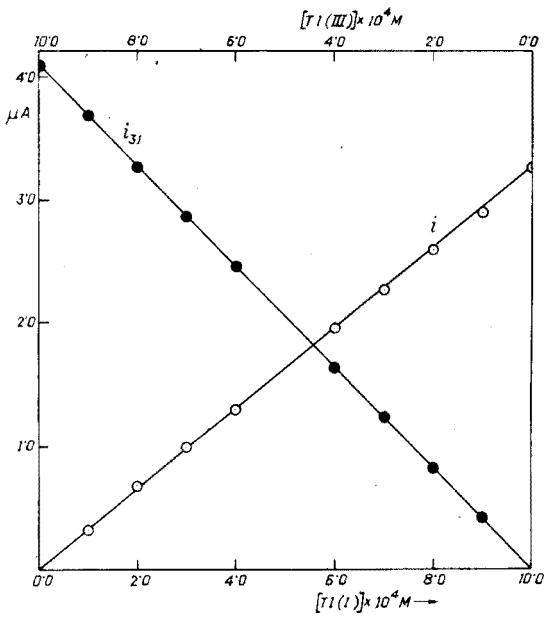

Fig. 3. Plots of diffusion currents of thallium(III) and thallium(I) in a mixture against their concentrations.

(Fig. 1) measure the concentrations of thallium(III) and thallium(I) in the mixture and these are related as follows,

$$i_{31} = k \cdot c_{Tl(III)} \quad \text{and} \quad i = i_{tot} - R \cdot i_{31} = k' \cdot c_{Tl(I)}$$

The plots of i_{31} *vs.* $c_{Tl(III)}$ and i *vs.* $c_{Tl(I)}$ are given in Fig. 3; these can serve as calibration curves for the determination of unknown quantities of thallium(III) and thallium(I) in a mixture. The value of k/k' (1.246), determined from the slope of the curves, is used to establish the Tl(I)/Tl(III) ratios. The ratios taken and those observed experimentally are given in Table II. The determination can be extended down to 0.1 μmole of thallium per ml with a decreased concentration of triethanolamine (0.03 *M*).

TABLE II

POLAROGRAPHIC DETERMINATION OF THALLIUM(III) AND THALLIUM(I) IN A MIXTURE

Concentration $\cdot 10^3$ *M*		i_{31} (μA)	i_{tot} (μA)	$i_{tot} - R \cdot i_{31}$ (μA)	*Tl(I)/Tl(III)*	
Tl(III)	*Tl(I)*				*Taken*	*Observed* $(i_{tot} - R \cdot i_{31})/i_{31}$
0	1.0	—	—	3.26	—	—
0.1	0.9	0.42	3.58	2.90	9.00	8.60
0.2	0.8	0.82	3.92	2.59	4.00	3.93
0.3	0.7	1.23	4.26	2.27	2.33	2.30
0.4	0.6	1.63	4.60	1.96	1.50	1.50
0.6	0.4	2.45	5.27	1.30	0.667	0.661
0.7	0.3	2.86	5.61	0.98	0.428	0.427
0.8	0.2	3.26	5.95	0.67	0.250	0.256
0.9	0.1	3.68	6.28	0.32	0.111	0.108
1.0	0	4.06	6.58	—	—	—

This method of determination is superior to others in acidic solution, because thallium(III) is very stable in alkaline medium in the presence of triethanolamine. A polarographed solution kept for seven days showed no change in the waveheight for either of the two reduction steps. After this period, i_{31} gradually diminished with no change of i_{10}. A similar solution was stable for only 72 h in the presence of mercury, after which period i_{31} diminished and i_{10} increased; this is in agreement with the reported reduction of thallium(III) to thallium(I) on a mercury surface[1] in acidic solution, but the rate was found to be much slower in alkaline medium in the presence of triethanolamine.

Polarographic studies of thallium(III) with other ethanolamines are in progress.

REFERENCES

1 G. W. Smith and F. Nelson, *J. Amer. Chem. Soc.*, 76 (1954) 4714.
2 G. K. Hughes and N. S. Hush, *Aust. J. Sci.*, 10 (1948) 184.
3 O. Farver and G. Nord, *Chem. Commun.*, 15 (1967) 736.

4 W. M. Latimer, *Oxidation Potentials*, Prentice-Hall, New York, 2nd Ed., 1952.
5 To be published.
6 A. I. Vogel, *A Text Book of Quantitative Inorganic Analysis*, E.L.B.S. and Longmans Green, London, 3rd Ed., 1961.
7 A. A. Vlcek, *Collect. Czech. Chem. Commun.*, 24 (1959) 3538.

Analytica Chimica Acta, 68 (1974) 480–483
© Elsevier Scientific Publishing Company, Amsterdam – Printed in The Netherlands

SHORT COMMUNICATION

The rapid determination of sulfur in coal

JACKSON E. HICKS, JAMES E. FLEENOR and HAROLD R. SMITH
Services Analytical Laboratory, Tennessee Eastman Company, Kingsport, Tenn. 37662 (U.S.A.)
(Received 29th April 1973)

The emission of sulfur oxides into the atmosphere from the combustion of fossil fuels is now regulated by both Federal and State legislation; coals are classified not only according to B.T.U. and ash value but also according to the sulfur content. The Eschka method[1] has long been the recognized reference method for the determination of sulfur in coal, but this tedious procedure is unsuitable for routine control. Many combustion techniques have been used to replace the Eschka method; Selvig and Fieldner[2] showed that the bomb-washing and sodium peroxide fusion methods gave results which agreed closely enough with the Eschka method for routine purposes. Laboratories making calorimetric determinations on coal find it convenient to determine sulfur in the washings from the bomb calorimeter; commonly, the time-consuming and error-prone[3] gravimetric barium sulfate determination is applied, and a faster precise analytical finish is needed.

Ross and Frant[4] and Selig[5] have described the determination of sulfate by potentiometric titration with lead perchlorate and a lead ion-selective electrode. This communication discusses the application of this titration to the determination of sulfur in coal, after the sample has been burned in an oxygen bomb. The procedure is more rapid and precise than the standard gravimetric technique.

Experimental

Apparatus. A Metrohm Potentiograph E-436 Recording Titrator equipped with an E-436-D Multi-titration Stand was used. An Orion model 94-82 solid-state lead-selective electrode was used in conjunction with an Orion double-junction reference electrode, model 90–02. The salt bridge compartment of the reference electrode was filled with 1 *M* sodium nitrate. All samples were burned in a Parr 1241 automatic calorimeter with the Parr 1108 stainless steel bomb.

Sodium sulfate, 0.01 M. Dissolve exactly 1.4205 g of analytical reagent-grade sodium sulfate, which has been dried for 2 h at 110°, in distilled water and dilute to 1 l.

Flowers of sulfur (99.9+purity) and *cystine* (N.B.S. Standard Reference Material 143A) were also used.

Procedure. Thoroughly mix the sample of coal and dry for 1 h at 105°. Accurately weigh (±0.1 mg) *ca.* 1 g of dried coal into the metal capsule used

in the Parr bomb. Add 1 ml of distilled water to the bomb. Set up the bomb and pressurize to 25 atmospheres with oxygen. Burn the sample using the normal practices involved in determining the calorific value of coal. Remove the bomb and loosen the pressure release valve to exhaust the gas over a period not to exceed 1 min. Flush the release valve with distilled water and wash the electrodes, capsule and bomb head into the bomb. Wash the contents of the bomb into a 100-ml beaker with about 50 ml of wash water. Add 2 drops of 0.5% (w/v) phenolphthalein in methanol to the combined washings and neutralize with 1 *M* potassium hydroxide solution. Add dilute perchloric acid (15 ml of 85% acid diluted to 1 l) dropwise until the pink color fades, and add one drop in excess. Add 50 ml of reagent-grade 1,4-dioxane and place the electrodes in the beaker. Start the titration with 0.05 *M* lead perchlorate, automatically record the titration curve, and determine the equivalence point. Standardize the titrant against 0.01 *M* sodium sulfate solution.

Results and discussion

Inasmuch as most people who are interested in the sulfur content of coal are also interested in the calorific value, a determination of the bomb washings is attractive. The use of a recording titrator and an ion-selective electrode provides the rapidity and precision desired. It is important that the air should not be flushed from the bomb during pressurization with oxygen. The oxides of nitrogen formed during combustion act as a catalyst in converting sulfur completely to sulfur trioxide and prevent the formation of sulfur dioxide[6].

The lead-selective electrode develops a potential proportional to the logarithm of the activity of the free lead ion in the titrated solution. It is reasonably selective but is poisoned by copper, mercury and silver ions[4]. The following ions interfere[4,5] in the titration of sulfate with lead perchlorate: 50-fold amounts of nitrate or chloride, and 10-fold amounts of hydrogencarbonate at pH 6 (100-fold amounts at pH 4); phosphate must be absent. It was shown that the titration of sodium sulfate in 50 % dioxane was virtually unaffected by pH in the apparent pH range 4–9. The recommended procedure provides a pH of 6–7.

It is important that a double-junction reference electrode be used. The outer chamber is filled with 1 *M* sodium nitrate. With a single-junction electrode, chloride ion from the filling solution may precipitate lead or form lead–chloro complexes. Although the potential of the Orion lead electrode varies with temperature, the only requirement for the present purpose is that the temperature should not change much during the actual titration; calibration of the electrode is not required. The concentration of sulfur in most coal samples is such that no problems were caused by insufficiently fast response of the electrode. The automatic titrator used slowed down the titration rate near the inflection portion of the curve. As recommended by Ross and Frant[4], dioxane was used to reduce the solubility of lead sulfate so that sharp end-points would be obtained; 50 % dioxane was satisfactory whereas more than 70 % caused alkali metal sulfates to precipitate. After combustion of the sample, the sulfur content can be determined in less than 5 min. The potential jump at the end-point of a typical titration curve is *ca.* 150 mV.

The electrode can be stored in air or in a dilute lead solution. After 10–15 titrations, the electrode surface usually requires cleaning with the abrasive

plastic supplied or with Buehler 4/0 Emery polishing paper. The response of the electrode becomes sluggish, reproducibility becomes poor, and the break in the titration curves becomes smaller as the surface of the sensing element becomes coated.

Initially, when the pressure of the bomb was released after combustion, the gas was vented through a tube immersed in water to prevent losses. It was soon found that this step was not required. The most crucial step of the manipulations is the washing of the pressure release valve and bomb electrodes. The pressure release valve especially must be carefully back-flushed into the bomb to prevent losses.

For a series of analyses of sodium sulfate solution, the proposed titrimetric method gave an average value of 0.80 % S with a standard deviation of 0.017 % (10 determinations); the gravimetric determination with barium chloride, which took about 4 h, gave an average value of 0.87% S, with a standard deviation of 0.054 %. Ten determinations of sulfur in a typical coal by the proposed method gave an average value of 0.79 % S with a standard deviation of 0.027 %.

Known amounts of sulfur as flowers of sulfur or cystine were added to samples of coal and activated carbon which were then analyzed by the proposed method. Sample mixtures were usually prepared in a ball mill for 5–6 h, but

TABLE 1

RECOVERY OF FLOWERS OF SULFUR AND CYSTINE ADDED TO COAL OR ACTIVATED CARBON

Original % S	*% S added*	*% S total*	*% S found*	*Error*
Flowers of sulfur added to coal				
0.62	0	0.62	0.62	0
0.62	0.10	0.72	0.70	−0.02
0.62	0.24	0.86	0.87	+0.01
0.62	0.41	1.03	0.99	−0.04
0.62	0.61	1.23	1.15	−0.08
Flowers of sulfur added to carbon				
0.14	0.23	0.37	0.36	−0.01
0.14	0.54	0.68	0.68	0
0.14	0.88	1.02	0.98	−0.04
0.14	1.05	1.19	1.32	+0.13
0.14	1.81	1.95	1.85	−0.10
	0.14 2.13	2.27	2.27	0
Cystine added to carbon				
0.14	0.58	0.72	0.80	+0.08
0.14	0.83	0.97	1.05	+0.08
0.14	1.32	1.46	1.41	−0.05
0.14	2.05	2.19	2.32	+0.13
0.14	2.12	2.26	2.26	0
0.14	2.17	2.31	2.16	−0.15
0.14	5.40	5.54	5.32	−0.22

cystine did not mix well and so was weighed directly into the bomb capsule. Table I shows the results obtained, which indicate a satisfactory recovery of sulfur over the range 0.36–5.54% sulfur.

The sulfur contents of three standard coal samples (N.B.S., S.R.M. 1631) were determined by the proposed method. The results (Table II) agreed quite closely, though sample B consistently gave results lower than the certified value, possibly because of its higher ash content. Some insoluble sulfate may have formed during combustion resulting in slightly lower values.

TABLE II

DETERMINATION OF SULFUR IN COAL (NBS STANDARD REFERENCE MATERIAL 1631)

	Percent by weight		
Coal sample	*Sulfur by titration*[a]	*Sulfur*	*Ash*
		Certified values[b]	
A	0.549	0.546 ± 0.003	5.00 ± 0.02
B	1.92	2.016 ± 0.014	14.59 ± 0.09
C	2.99	3.020 ± 0.008	6.17 ± 0.02

[a] Average of 12 determinations.
[b] For these each participating laboratory reported the average of 12 determinations.

The data reported here indicate that the determination of sulfur in coal by combustion, followed by automatic titration of the bomb-washings with lead perchlorate solution and a lead-selective electrode is satisfactory. As previously stated[2], the bomb-washing approach provides a satisfactory recovery of sulfur from coal samples. With respect to speed, precision, recovery and ease of operation the proposed method is excellent.

The authors are grateful to Ruth S. Jessee who prepared most of the sulfur, coal and carbon mixtures.

REFERENCES

1 ASTM D-271, *Sampling and Analyses of Coal and Coke*, Sections 21 to 24, 1971.
2 W. A. Selvig and A. C. Fieldner, *Ind. Eng. Chem.*, 19 (1927) 729.
3 I. M. Kolthoff, E. B. Sandell, E. J. Meehan and S. Bruckenstein, *Quantitative Chemical Analysis*, MacMillan, New York, 4th Ed., 1969, pp. 603–610.
4 J. W. Ross, Jr. and M. S. Frant, *Anal. Chem.*, 41 (1969) 967.
5 W. Selig, *Mikrochim. Acta*, (1970) 168.
6 S. H. Regester, *Ind. Eng. Chem.*, 6 (1914) 812.

Analytica Chimica Acta, 68 (1974) 484–487
© Elsevier Scientific Publishing Company, Amsterdam – Printed in The Netherlands

SHORT COMMUNICATION

Détermination des naphtènes contenus dans des fractions d'essence de pétrole

F. S. ABO-LEMON
Division du Pétrole, Centre National des Recherches, Le Caire (Egypte)
N. GUICHARD
Division de Chromatographie, Institut Français du Pétrole, Paris (France)
(Reçu le 19 juin 1973)

Il est très important, dans l'industrie du pétrole, de disposer d'une méthode sûre et quantitative pour la séparation et le dosage des naphtènes et des paraffines. De nombreux travaux ont été effectués dans ce but.

Landsberg et Kasanova[1] ont identifié paraffines et naphtènes dans les fractions à point d'ébullition $>125°$–$130°$. Un fractionnement préliminaire a été réalisé, suivi d'une chromatographie sur gel de silice séparant les aromatiques; les cycles à 6 atomes de carbone ont été transformés en dérivés aromatiques par déshydrogénation sur platine à 300°.

Creanga[2] a étendu la méthode ci-dessus aux hydrocarbures à point d'ébullition compris entre 50° et 150°. Les hydrocarbures aromatiques (benzène, toluène, xylènes) sont séparés par chromatographie sur gel de silice (fraction A_1); l'ensemble paraffines + naphtènes constitue la fraction $P+N_{5+6}$. Celle-ci est déshydrogénée pour être convertie en aromatiques. Le produit obtenu est à nouveau fractionné par chromatographie sur gel de silice en aromatiques (A_2) et paraffines + cyclopentanes ($P+N_5$). Ces fractions sont finalement analysées par spectrographie raman.

Une autre technique de déshydrogénation est mentionnée par Rampton[3] utilisant un micro-appareil; celui-ci a servi à Brunnock et Luke[4] pour distinguer cyclopentanes et cyclohexanes. Moisegkov[5] a identifié les naphtènes en C_6 dans la fraction de gasoline de Turkménie par déshydrogénation, selon Musaev et Gal'Peris[6].

Le but de ce travail est l'estimation des naphtènes, du type alkylcyclohexane, dans les fractions pétrolières, par déshydrogénation.

Partie expérimentale

Les essais ont surtout porté sur la détermination des cycloparaffines, par déshydrogénation catalytique, en tête du chromatographe. Après désaromatisation sur gel de silice, deux échantillons ont été examinés par les diverses méthodes: déshydrogénation et analyse chromatographique simultanée, spectrométrie de masse et chromatographie gazeuse pour l'analyse individuelle des constituants ou par groupe.

Appareil. L'appareil utilisé est constitué d'un tube métallique séparé en deux

parties: la partie supérieure, utilisée comme vaporiseur et la partie inférieure comme micro-réacteur. Le micro-réacteur est relié à une colonne chromatographique (tube d'acier inoxydable de 2 nm de diamètre intérieur) remplie de Chromosorb (0.16 0.18 mm) imprégné à 15% de Carbowax. L'azote ou l'hydrogène sont utilisés comme gaz porteur; on contrôle le débit et la pression, au moyen de deux régulateurs à aiguilles. Le chromatographe est équipé d'un détecteur à ionisation de flamme et la température du réacteur est contrôlée par un rhéostat. On a ainsi la possibilité de modifier température du réacteur, débit et pression des gaz.

Catalyseurs. Trois catalyseurs ont été préparés. Le premier est constitué de platine (15%) sur charbon préparé à partir d'acide chloroplatinique, 'analytique'[3]. On régénère le catalyseur actif en le portant à la température de 300° durant 10 h. Les deux autres catalyseurs sont l'un à 0.5% de platine sur alumine et l'autre à 2% de platine sur une alumine à 13% de silice.

Résultats et discussion

Ces trois catalyseurs ont été essayés, sans aucune dilution par support inactif, avec un remplissage complet de l'espace du catalyseur. Les poids des catalyseurs Pt/C, Pt/Al et Pt/Si–Al sont respectivement 0.91 g, 1.4539 g et 1.4950 g. En présence du catalyseur Pt/C, en utilisant l'hydrogène comme gaz porteur, à une température comprise entre 300°–400°, la déshydrogénation du cyclohexane en benzène est faible (10% et 25% respectivement à 300° et 400°); l'opération s'est effectuée comme une hydrogénation. D'autre part, en utilisant l'azote comme gaz porteur, à 385°, on a obtenu déshydrogénation non spécifique des hydrocarbures. Par example, n-heptane, méthylcyclohexane et iso-heptane sont complétement déshydrogénés en toluène; et n-hexane, méthyl-2-pentane, méthylcyclopentane sont transformés en benzène.

Si l'on n'utilise que le tiers ou la moitié du catalyseur, en le diluant avec une substance inerte (firebrick), on arrive à une déshydrogénation non sélective. Tandis que si l'on utilise le tiers du catalyseur, avec un mélange azote–hydrogène comme gaz porteur, on obtient des résultats beaucoup plus satisfaisants.

D'autre part, les catalyseurs Pt/Al et Pt/Si–Al n'ont pas donné de résultats encourageants pour la conversion totale du cyclohexane, utilisé comme témoin. Les conditions optima du catalyseur Pt/C, pour obtenir une déshydrogénation sélective des naphtènes à cycle hexagonal sont: température, 385°; débit total, 69.8 $cm^3\ min^{-1}$; pression d'hydrogène, voisine de 1.9 atm; pression d'azote, voisine de 0.5 atm.

Les paraffines et les naphtènes du type alkylcyclopentane n'ont pas été affectés par les conditions de déshydrogénation utilisées. Cette méthode a été appliquée à deux fractions pétrolières: l'une à point d'ébullition de 99° à 125° et l'autre de 125° à 150°; elles ont été désaromatisées par gel de silice, selon la méthode standard UOP. Le dosage s'est fait avec étalon interne. L'analyse s'effectue à l'aide d'une colonne capillaire de squalane. Les pourcentages en poids correspondent aux pourcentages des surfaces; le chromatogramme est enregistré sur bande magnétique, puis restitué et intégré (Infotronics CRS 40-CRSII MSB). Les résultats sont présentés dans le Tableau I: cycloparaffines totales = 54.5% en poids. En utilisant le spectrométre de masse, on trouve 51.4% en volume (Tableau II). Les résultats obtenus par la méthode de déshydrogénation sont présentés dans le Tableau III.

TABLEAU 1

ANALYSE DES ÉCHANTILLONS DÉSAROMATISÉS[a]

(Résultats exprimés en % poids)

	Fraction 99–125°	*Fraction 125–150°*
Méthyl-2-hexane	0.19	
Diméthyl-2,3-pentane + diméthyl-1,1-cyclopentane	0.05	
Méthyl-3-hexane	0.13	
Diméthyl-1-*trans*-3-cyclopentane	0.28	
Diméthyl-1-*cis*-3-cyclopentane	0.26	
Diméthyl-1-*trans*-2-cyclopentane	0.12	
n-Heptane	1.76	
Diméthyl-2,2-hexane	0.1	
Diméthyl-1-*cis*-2-cyclopentane	1.1	
Triméthyl-1,1,3-cyclopentane	1.2	
Méthylcyclohexane + diméthyl-2,5-hexane	7.4	
Diméthyl-2,4-hexane	1.7	
Éthylcyclopentane	3.8	
Triméthyl-1-*trans*-2-*cis*-4-cyclopentane	3.4	
Triméthyl-1-*trans*-2-*cis*-4-cyclopentane	1.7	
Triméthyl-2,3,4-pentane	0.07	
Diméthyl-2,3-pentane	1.5	
Méthyl-2-heptane	9.2	1.0
Méthyl-4-heptane + triméthyl-1,1,2-cyclopentane	2.8	0.4
Diméthyl-3,4-hexane + méthyl-3-heptane + éthyl-3-hexane	9.6	1.6
Triméthyl-1-*cis*-2-*trans*-4-cyclopentane	1.3	0.1
Méthyl-3-éthyl-3-pentane	1.2	0.2
Cycloheptane	2.0	0.3
Diméthyl-1,1-cyclohexane + diméthyl-*cis*-1,3-(ou *trans*-1,4-)-cyclohexane	8.2	2.1
Méthyl-1-éthyl-*trans*-3-cyclopentane	5.4	1.5
Méthyl-1-méthyl-*cis*-3,1-éthyl-*trans*-2-cyclopentane	6.8	2.1
Méthyl-1-éthyl-1-cyclopentane	0.7	0.2
n-Octane + triméthyl-1-*cis*-3-cyclopentane	7.8	5.1
Diméthyl-1-*trans*-2-cyclohexane	3.0	1.7
Diméthyl-1-*trans*-3,1-*cis*-4-cyclohexane	4.6	2.7
Triméthyl-2,3,5-hexane + isopropylcyclopentane	0.4	0.7
Diméthyl-2,2-heptane	1.0	1.0
Propylcyclopentane	0.1	0.2
Diméthyl-2,4-heptane	0.4	1.2
Méthyl-1-éthyl-*cis*-2-cyclopentane	1.1	1.3
Diméthyl-2,6-heptane + diméthyl-4,4-heptane	0.7	2.3
Diméthyl-3,5-heptane + n-propylcyclopentane + diméthyl-1-*cis*-2-cyclohexane + diméthyl-2,5-heptane	3.1	7.2
Éthylcyclohexane	2.1	4.4
Triméthyl-1,1,3-cyclohexane	0.2	1.0
Diméthyl-2,3-heptane	0.1	1.7
Diméthyl-3,4-heptane + éthyl-4-heptane	0.1	1.9
Méthyl-4-octane	0.6	7.6
Méthyl-2-octane	0.3	5.8
Éthyl-3-heptane	0.1	2.5
Méthyl-3-octane	0.2	6.1
n-Nonane		5.2

[a] Conditions opératoires: colonne capillaire de squalane, longeur 60 m, ∅ interieur 0.25 mm, température 60°, pression azote 0.8 kgf cm^{-2}.

TABLEAU II

ANALYSE PAR SPECTROMÉTRIE DE MASSE

(Résultats exprimés en % volume)

	Fraction 99–125°	*Fraction 125–150°*
Hydrocarbures paraffiniques	40.9	44.8
Hydrocarbures monocycloparaffiniques	49.1	46.1
Hydrocarbures dicycloparaffiniques	2.3	—
Hydrocarbures aromatiques	7.6	8.5

TABLEAU III

COMPARAISON DES RÉSULTATS D'ANALYSES DES CYCLOHEXANES PAR CHROMATOGRAPHIE EN PHASE GAZEUSE ET PAR LA MÉTHODE DE DÉSHYDROGÉNATION[a]

(Résultats exprimés en % poids)

	Chromatographie sur colonne capillaire[b]		*Déshydrogénation*	
	99–125°	*125–150°*	*99–125°C*	*125–150°C*
Monosubstitués				
Méthylcyclohexane + diméthyl-2,5-hexane	7.4	—	5.6	—
Éthylcyclohexane	2.1	4.4	—	1.9
Disubstitués				
Diméthyl-1,1-cyclohexane + diméthyl-1-*cis*-3 et 1-*trans*-4-cyclohexane	8.2	2.1	16.7	6.5
Diméthyl-1-*trans*-2-cyclohexane	3.0	1.7	16.7	6.5
Diméthyl-1-*trans*-3 et 1-*cis*-4-cyclohexane	4.6	2.7	16.7	6.5

[a] Total des cycloparaffines (C_5 et C_6), 54.5%.
[b] *Cf.* Tableau I.

Les auteurs remercient la direction de l'Institut Français du Pétrole qui leur a permis d'effectuer ce travail, et tout spécialement Monsieur Buzon pour ses intéressantes discussions et conseils.

BIBLIOGRAPHIE

1 G. S. Landsberg et B. A. Kasanskii, *Izv. Akad. Nauk SSR, Otd. Khim. Nauk*, 2 (1951) 100.
2 C. Creanga, *Analele Stiint. Univ. 'A.I. Cuza' Iasi, Sect. IC.*, 13 (1967) 191, 201; *Proc. Colloq. Spectrosc. Int.*, 14 (1967) 1335.
3 H. C. Rampton, *Anal. Chem.*, 21 (1949) 377.
4 I. V. Brunnock et C. A. Luke, *Anal. Chem.*, 40 (1968) 2158.
5 Moisegkov, *Neftepererab. Neftekhim. (Moscow)*, 10 (1964) 23.
6 I. A. Musaev et G. D. Gal'Peris, *Dokl. Akad. Nauk SSSR*, 88 (1953) 1.

Analytica Chimica Acta, 68 (1974) 488
© Elsevier Scientific Publishing Company, Amsterdam – Printed in The Netherlands

Announcement

Electrochemical Society Summer Fellowship Awards

The Electrochemical Society will offer three fellowship awards for qualified graduate students for the summer of 1974. Each award will have a stipend of $ 1000, and its purpose is to assist the student to continue his graduate work during the summer months in a field of interest to The Electrochemical Society. These awards are to be known as The Edward Weston Fellowship Award, The Colin Garfield Fink Fellowship Award, and The Joseph W. Richard Fellowship Award.

Candidates' qualifications: "Each award shall be made without regard to sex, citizenship, race or financial need. They shall be made to graduate students pursuing work between the degrees of B.S. and Ph.D. in a college or university in the United States or Canada, and who will continue their studies after the summer period. A previous holder of an award is eligible for reappointment."

Qualified graduate students are invited to apply for these fellowship awards. Applicants must complete an application form and supply the following information:

1. A brief statement of educational objectives.
2. A brief statement of the thesis research problem including objectives, work already accomplished, and work planned for the summer of 1974.
3. A transcript of undergraduate and graduate academic work.
4. Two letters of recommendation, one of which should be from his research adviser.
5. Successful recipients of Fellowships shall agree not to hold other appointments or other fellowships during the summer of 1974.

Application forms are available from the Chairman of the Fellowship Awards Subcommittee, to whom all correspondence should be addressed: Professor G. M. Schmid, Department of Chemistry, University of Florida, Gainesville, Fla. 32611.

Deadline for receipt of completed applications will be March 2, 1974; award winners will be announced on May 1, 1974.

ANALYTICA CHIMICA ACTA, VOL. 68 (1974)

AUTHOR INDEX

ANALYTICA CHIMICA ACTA, VOL. 68 (1974)

SUBJECT INDEX

(Continued from page 4 of covor)

CONTENTS

(continued on inside page of cover)

29 CAN. 2517